Translation Control by Phosphorylation of Ribosomal Proteins

Katharina Maria Brünger

München 2012

Dissertation zur Erlangung des Doktorgrades an der Fakultät für
Chemie und Pharmazie der Ludwig-Maximilians-Universität München

Translation Control by Phosphorylation of Ribosomal Proteins

Katharina Maria Brünger
aus
Bad Mergentheim, Deutschland

2012

Erklärung

Diese Dissertation wurde im Sinne von § 7 Promotionsordnung vom 28. November 2011 von Frau Dr. Katja Sträßer betreut.

Eidesstattliche Versicherung

Diese Dissertation wurde eigenständig und ohne unerlaubte Hilfe erarbeitet.

München, den 27. September 2012

Katharina Brünger

Dissertation eingereicht am 27. September 2012

Erstgutachterin: Dr. Katja Sträßer

Zweitgutachter: Professor Dr. Roland Beckmann

Mündliche Prüfung am 16. November 2012

Publications

Parts of the presented thesis are submitted for publication:

Katharina M. Brünger, Juliane Horenk, Jesper V. Olsen, Matthias Mann and Katja Sträßer. Phosphorylation of ribosomal proteins Rps5 and Rps12 functions in translation initiation (submitted).

During this thesis I contributed to the following publications:

Susanne Röther*, Cornelia Burkert*, **Katharina M. Brünger***, Andreas Mayer*, Anja Kieser and Katja Sträßer (2010) Nucleocytoplasmic shuttling of the La motif-containing protein Sro9 might link its nuclear and cytoplasmic functions, *RNA 16* (7).
* These authors contributed equally.

Britta Coordes, **Katharina M. Brünger**, Kasper Burger, Boumediene Soufi, Juliane Horenk, Dirk Eick, Jesper V. Olsen and Katja Sträßer. Ctk1 function is crucial for efficient translation initiation (submitted).

Summary

Eukaryotic protein synthesis is a sophisticated multistep process, which requires an extensive biological machinery and several control mechanisms. Translation regulation mainly occurs at the level of initiation. One of the key control mechanisms is the phosphorylation of translation initiation factors. Although phosphorylation of ribosomes has been known for decades, there is still very limited knowledge on translation regulation by phosphorylation of the translation machinery itself, the ribosome.

In this study a large-scale phosphoproteomic survey of *Saccharomyces cerevisiae* ribosomal proteins resulted in the identification of 279 ribosomal phosphorylation sites. In a second quantitative phosphoproteomics approach, Stable Isotope Labelling with Amino Acids in Cell Culture (SILAC) was used to assess changes in the phosphorylation pattern in response to a stress-induced shut-down of translation and to – hopefully – identify functional relevant phosphorylation sites. Here, changes in the phosphorylation pattern of 17 ribosomal phosphosites were determined.

Subsequently, a mutational analysis of selected ribosomal phosphorylation sites was performed to assess their function in protein synthesis. Out of the 25 phospho-deficient alanine mutations analyzed so far, twelve showed an altered translation activity in *in vitro* translation active extracts. Interestingly, two phosphorylation sites on proteins of the small ribosomal subunit, Rps5 T38 and Rps12 T23, play a role in translation initiation. The phospho-deficient alanine mutants of these two phosphorylation sites showed a defect in canonical translation initiation. Specifically, Rps5 T38 phosphorylation is important for efficient 48S initiation complex formation and context dependent start codon recognition whereas the phosphorylation of Rps12 T23 functions in initiation complex formation and scanning processivity. Moreover, the two mutations affect growth under specific conditions demonstrating a physiological relevance of these phosphorylation sites.

Taken together, eukaryotic ribosomes are highly phosphorylated and change their phosphorylation pattern in response to stress. In this study the first two ribosomal phosphorylation sites are reported to be important for translation initiation suggesting that many ribosomal phosphosites might function in translation.

Contents

1 Introduction

1.1 Posttranslational Modifications

The biological complexity of eukaryotic cells cannot simply be explained by the number of protein encoding genes, but is regulated by a number of multilayer and interconnected mechanisms. The transcription of DNA into RNA by RNA polymerase II (Svejstrup, 2004) and the cotranscriptional splicing of the mRNA takes place in the nucleus (Black, 2003; Chen and Manley, 2009). After export of the mature mRNAs to the cytoplasm (Kohler and Hurt, 2007), mRNAs are translated into proteins that can be further modified by a diversity of posttranslational modifications (Walsh et al., 2006). Both mechanisms, alternative splicing and posttranslational modifications, enable the cell to expand the coding capacity to generate a much more complex and diverse proteome.

Besides covalent cleavage of the protein backbone by protein proteases or autocatalytic cleavage and covalent alkylation, there exists an extensive array of highly dynamic and reversible posttranslational modification (PTMs). The current literature reports more than 200 different PTMs (Mann and Jensen, 2003). Some PTMs like disulfide bridge formation or glycosylation are relatively stable and crucial for protein folding and maturation of nascent proteins. In contrast, PTMs including protein phosphorylation, ubiquitylation and acylation are readily reversed and thus suitable for regulatory functions and intracellular signaling (Deribe et al., 2010). Proteins cannot only be modified by different types of PTMs or at multiple sites with the same PTM but also in a sophisticated manner separated in time and occurring sequentially. PTMs alter the properties of a protein. The coupling of PTMs with corresponding recognition motifs of interacting partners creates a decoding mechanism for relaying and reacting to changing environmental conditions, thereby initiating signaling pathways and other feedback regulatory mechanisms, e.g. in transcription and translation

(Hunter, 2000; Sims and Reinberg, 2008; Avraham and Yarden, 2011).

1.2 Phosphorylation as Posttranslational Modification in Cellular Pathways

Protein phosphorylation is one of the key PTM in regulatory mechanisms and was one of the first PTMs being described (Fischer and Krebs, 1955; Walsh et al., 1968). Most processes in living cells including the cell cycle, receptor mediated signal transduction, differentiation, proliferation and the metabolism of the cell are regulated by phosphorylation (Hunter, 2000). The interplay of two enzyme classes, protein kinases transferring the γ-phosphate of ATP to hydroxyamino acids (mainly S, T and Y in eukaryotes) and phosphatases removing the phosphate, continuously regulate substrate modification (Krebs and Beavo, 1979). Kinases represent one of the largest families of genes in eukaryotes, for instance, 1.7 % of the human genome encode kinases (Manning et al., 2002). Furthermore, about 30 % of all cellular proteins were estimated to be phosphorylated on at least one residue and 50 % to possess at least one potential phosphorylation site (Cohen, 2000). Actually, Olsen et al. showed that in HeLa S3 cells 70 % of the cellular proteins are phosphorylated (Olsen et al., 2010).

The addition of a phosphoryl group to an amino acid residue confers properties which can have profound effects on protein conformation and function. Under physiological conditions, the phosphate is double-negatively charged and can form extensive hydrogen-bond networks. These properties play an important role in inter- and intramolecular interactions of phosphorylated residues with other amino acids resulting in attractive or repulsive electrostatic effects. However, there is no universal response that allows to predict a general mechanism for regulation by phosphorylation, but a range of different responses to posttranslational modifications (Johnson and Lewis, 2001).

The binding affinity of a protein towards potential interaction partners can be altered drastically by reversible phosphorylation. For instance, the binding of the epidermal growth factor (EGF) to the EGF receptor (EGFR), which is a protein tyrosine kinase, induces a multisite autophosphorylation at the cytoplasmic domains of the EGFR, thereby

recruiting key regulatory proteins via their SH2 (Src homology 2) domain to the activated homodimer (Jorissen et al., 2003). In the EGFR signal transduction cascade these downstream signaling proteins initiate diverse cellular answers by activating signaling pathways such as MAPK (Mitogen-activated protein kinase), PI3K (Phosphatidylinositol 3-kinases) or mTOR (mammalian target of rapamycin). Thereby, the mTOR pathway is the major nutrient sensing pathway (Martin and Hall, 2005; Wullschleger et al., 2006). The EGF signaling pathway is only one impressive example of the crucial role of phosphorylation in biological processes.

1.3 Mass Spectrometry Based Phosphoproteomics

Analysis of protein phosphorylation is still a very challenging task, although breakthrough developments of the past decade now enable the identification and relative quantification of thousands of phosphorylation sites from complex biological samples. Considering that the phosphorylation of proteins is not only a very common, but also a reversible and dynamic process, the dynamic range of the phosphoproteome is similar to that of the proteome itself. However, phosphoproteomics based on mass spectrometry is a powerful tool to analyze and quantify cellular protein phosphorylation events at a global level (Ong and Mann, 2005; Nita-Lazar et al., 2008; Macek et al., 2009).

In the first large scale analysis of the yeast *Saccharomyces cerevisiae* in 2002, a total of 216 peptide sequences defining 282 phosphorylation sites were identified from whole cell lysate in a single experiment (Ficarro et al., 2003). Some of the identified phosphoproteins were ribosomal proteins of the large and the small ribosomal subunits (Rpl12a, Rpl24a, Rpl25, Rpl3, Rpl7a/b, Rps31 and Rps6a).

More recent phosphoproteomic studies have not only the objective to determine phosphorylation sites, but also to profile levels of phosphorylation in different cellular states. The two most frequently used methods for quantitative phosphoproteomics are based on stable isotope labeling: (i) the metabolic labeling by SILAC (Stable Isotope Labeling with Amino Acids in Cell Culture) in which two populations of cells are cultivated in media containing either the normal amino acids or amino acids labeled with

stable (non-radioactive) heavy isotopes (Ong et al., 2002) and (ii) the chemical labeling method iTRAQ (isobaric Tag for Relative and Absolute Quantitation) which is based on the covalent labeling of the N-terminus and side chain amines of peptides with tags of varying mass (Ross et al., 2004).

Gruhler and co-workers combined SILAC with phosphoproteomic methods to investigate and quantify pheromone-induced changes in protein phosphorylation in yeast. They identified more than 700 unique phosphorylation sites in about 500 different yeast proteins that are pheromone regulated (Gruhler et al., 2005). Another study applied SILAC and phosphoenrichment to quantify global phosphorylation changes and site-specific phosphorylation dynamics in EGF stimulated HeLa cells (Olsen et al., 2006). The application of high end mass spectrometry in combination with phosphotyrosine immunoprecipitation and SILAC enabled the time-dependent analysis of the tyrosine phosphorylation cascade in the insulin signaling pathway (Krüger et al., 2008). Thus, quantitative phosphoproteomics provide new insights into protein-kinase mediated signaling networks (Choudhary and Mann, 2010; Kosako and Nagano, 2011).

In summary, these applications demonstrate the impressive capabilities of phosphoproteomics to identify phosphorylation sites, to elucidate dynamic signaling pathways, and due to its unbiased nature, to reveal new biological connections.

1.4 Translation and Its Regulation

Protein synthesis is the last step of gene expression and one of the most important processes in all living cells. Translation of an mRNA into a protein can be subdivided into four stages: initiation, elongation, termination and recycling. In eukaryotes initiation is a highly sophisticated and dynamic process that results in an elongation competent 80S ribosomal complex with the initiator tRNA (Met-tRNAi) for the first amino acid residue positioned at the start codon (AUG) of the mRNA. During elongation the ribosomes assemble in large complexes termed polysomes and the polypeptide chain encoded by the open reading frame (ORF) of the mRNA emerges from the ribosomes. As soon as the ribosomes encounter a stop codon translation is terminated and the polypeptide chain released. After recycling of the ribosomal subunits a new cycle of translation can begin (Fig. 1.1, adapted from

Melnikov et al. (2012)).

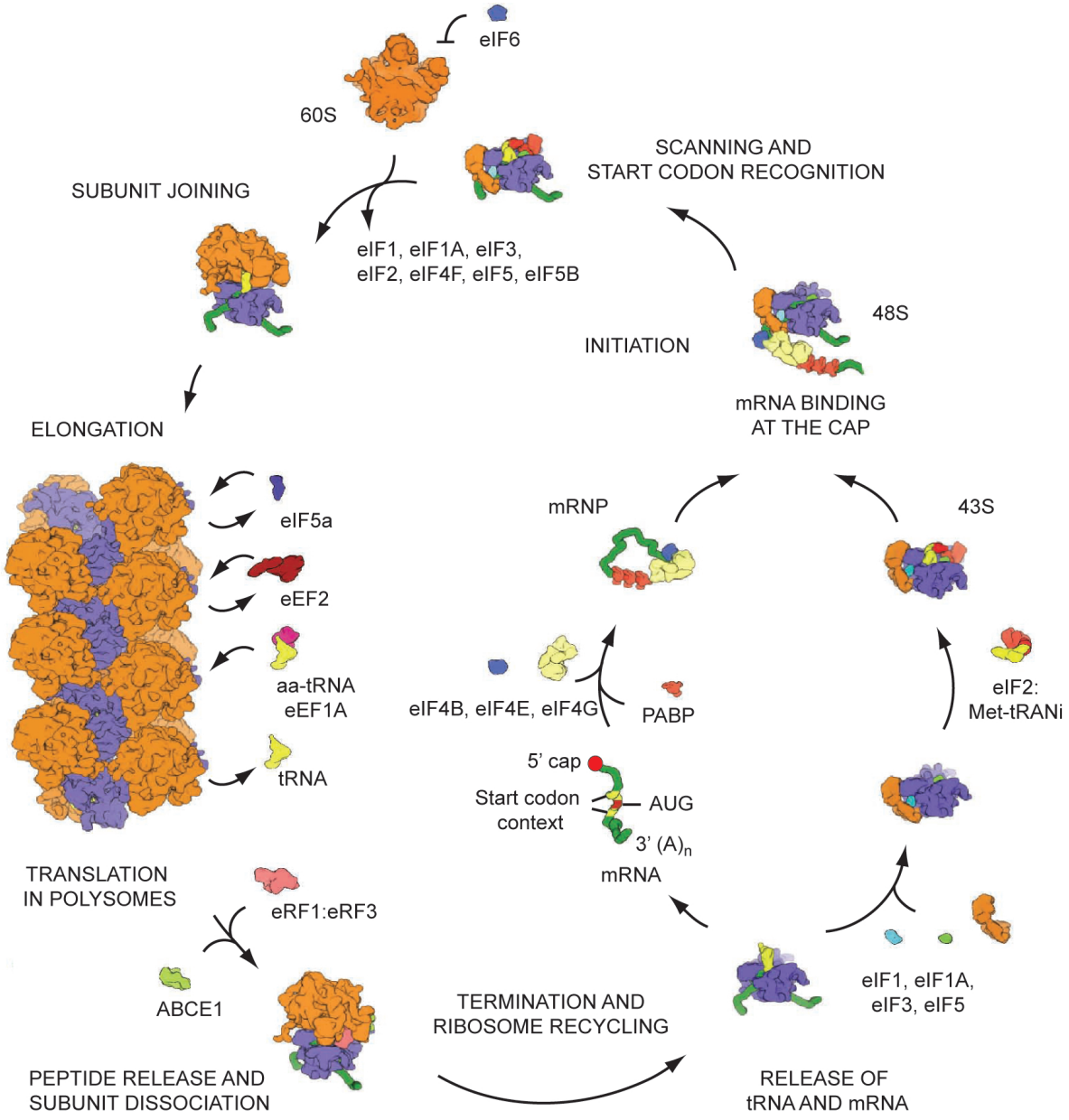

Figure 1.1: The translation cycle (adapted from Melnikov et al. (2012)). Translation can be divided into translation initiation, elongation, termination and ribosome recycling. Each step is assisted by certain factors – initiation factors (eIFs), elongation factors (eEFs), release factors (eRFs) and recycling factors. During the multistep process of translation initiation an elongation competent 80S complex is loaded onto the mRNA and positioned at the start codon. In elongation, the ribosomes assemble in large complexes termed polysomes and the nascent polypeptide chain emerges from the polysomes. Termination occurs when the ribosomes encounter a stop codon and the polypeptide chain is released. During recycling the ribosomes are split into their subunits and the tRNA and mRNA are released. 40S and 60S are depicted as blue and orange silhouettes; translation factors are labeled.

1.4.1 Eukaryotic Translation Initiation

Translation initiation is a complex process in eukaryotes requiring the ribosomal subunits to act in concert with the 12 eukaryotic translation initiation factors. Thereby, an elongation competent 80S complex with the Met-tRNAi in the peptidyl (P-)site of the ribosome is positioned at the correct start codon of the mRNA. Translation initiation starts with the assembly of the 43S pre-initiation complex (PIC) with the ternary complex (TC) containing eIF2, GTP and Met-tRNAi bound to the 40S P-site. 43S PIC formation is assisted by the initiation factors eIF1, 1A, 3 and 5. In yeast eIF1, 3 and 5 together with the TC form a multifactor complex (MFC) which is then recruited to the 40S subunit (Asano et al., 2000). Subsequently, the 43S PIC is recruited to the 5' end of the capped mRNA by the eIF4F complex consisting of the cap-binding eIF4E, the scaffold protein eIF4G, the helicase eIF4A with its auxiliary factor eIF4B and the poly(A) binding protein (Pab1). The 43S complex scans along the 5' UTR of the mRNA until it recognizes the start codon by perfect complementarity of the Met-tRNAi anticodon with the AUG in the P-site of the 40S subunit. Release of eIF1 and hydrolysis of GTP bound to eIF2 assisted by the GTPase-activating protein eIF5 results in a stable 48S PIC. After release of eIF2-GDP and eIF3, the 60S subunit joins mediated by eIF5B to form an 80S initiation complex (IC). Hydrolysis of eIF5B-bound GTP and displacement of the remaining initiation factors leave an elongation competent 80S ribosome on the mRNA. Subsequently, eIF2B catalyzes the GDP exchange on eIF2 to recycle eIF2 for a new round of translation initiation (Lorsch and Dever, 2010; Hinnebusch, 2011; Aitken and Lorsch, 2012). The process of eukaryotic translation initiation is illustrated in Fig. 1.2 (adapted from Hinnebusch (2011)).

Although the scanning model was proposed by Kozak three decades ago, the details of the scanning mechanism remain fragmentary (Kozak, 1978). Scanning is a complex process comprising the unwinding of structured mRNA, ribosomal movement along the mRNA, rejection of mismatches between noncognate codons and the Met-tRNAi anticodon and finally selection of the right start codon in the ribosomal P-site. Generally, the first AUG is the site for translation initiation ('First AUG rule'). But the sequence context surrounding the start codon has a drastic influence on start site selection, to the point that ribosomes bypass the first AUG, so called leaky scanning (Kozak, 1986). In yeast, the consensus

sequence is biased for As with a strong preference for the -3 position upstream of the AUG (Shabalina et al., 2004). Substitution of the -3 A has substantial effects on translation rates (Martin-Marcos et al., 2011).

eIF1 and eIF1A bind cooperatively to the 40S subunit and are crucial for a scanning competent 43S PIC (Maag et al., 2006, 2005; Mitchell and Lorsch, 2008). eIF1 and eIF1A act synergistically in promoting an open scanning competent conformation of the 43S initiation complex (Passmore et al., 2007). Upon start codon recognition a conformational change (closed state) is induced moving eIF1 and eIF1A apart from each other and triggering the release of eIF1 (Maag et al., 2005). eIF1 and eIF1A have opposing effects on start codon recognition. eIF1 promotes scanning and impedes the tight binding of the Met-tRNAi to the P-site at non-AUG codons by stabilizing the open-scanning competent conformation of the 40S subunit. Although the C-terminus of eIF1A acts together with eIF1 to stabilize the open conformation of the mRNA channel with the TC in a mode that prevents full accommodation of the Met-tRNAi in the P-site (Passmore et al., 2007), its N-terminus promotes the closed conformation by releasing eIF1 and full binding of the tRNA in the P-site (Fekete et al., 2007). The release of eIF1 is crucial for start codon selection as in the scanning competent conformation the codons entering the P-site are controlled for perfect base pairing with the Met-tRNAi anticodon without tight binding. Upon perfect matching triggering the conformational change and eIF1 release the mRNA is locked in the closed conformation. eIF1 release is stimulated by eIF5, which competes for its binding site on the 40S (Nanda et al., 2009) and stabilizes the closed conformation of the 40S subunit (Maag et al., 2006). Since eIF2 delivers the Met-tRNAi to the 40S subunit and the hydrolysis of GTP and dissociation of eIF2-GDP releases the initiator tRNA into the P-site, eIF2 is a key player in start site selection (Hinnebusch, 2011). Its α subunit is supposed to be directly involved in start codon context selection as was crosslinked to the important -3 position upstream of the AUG codon (Pisarev et al., 2006). eIF3 as scaffold for initiation factors stimulates many steps in translation initiation and therefore is also involved in scanning and start codon recognition (Hinnebusch, 2006, 2011).

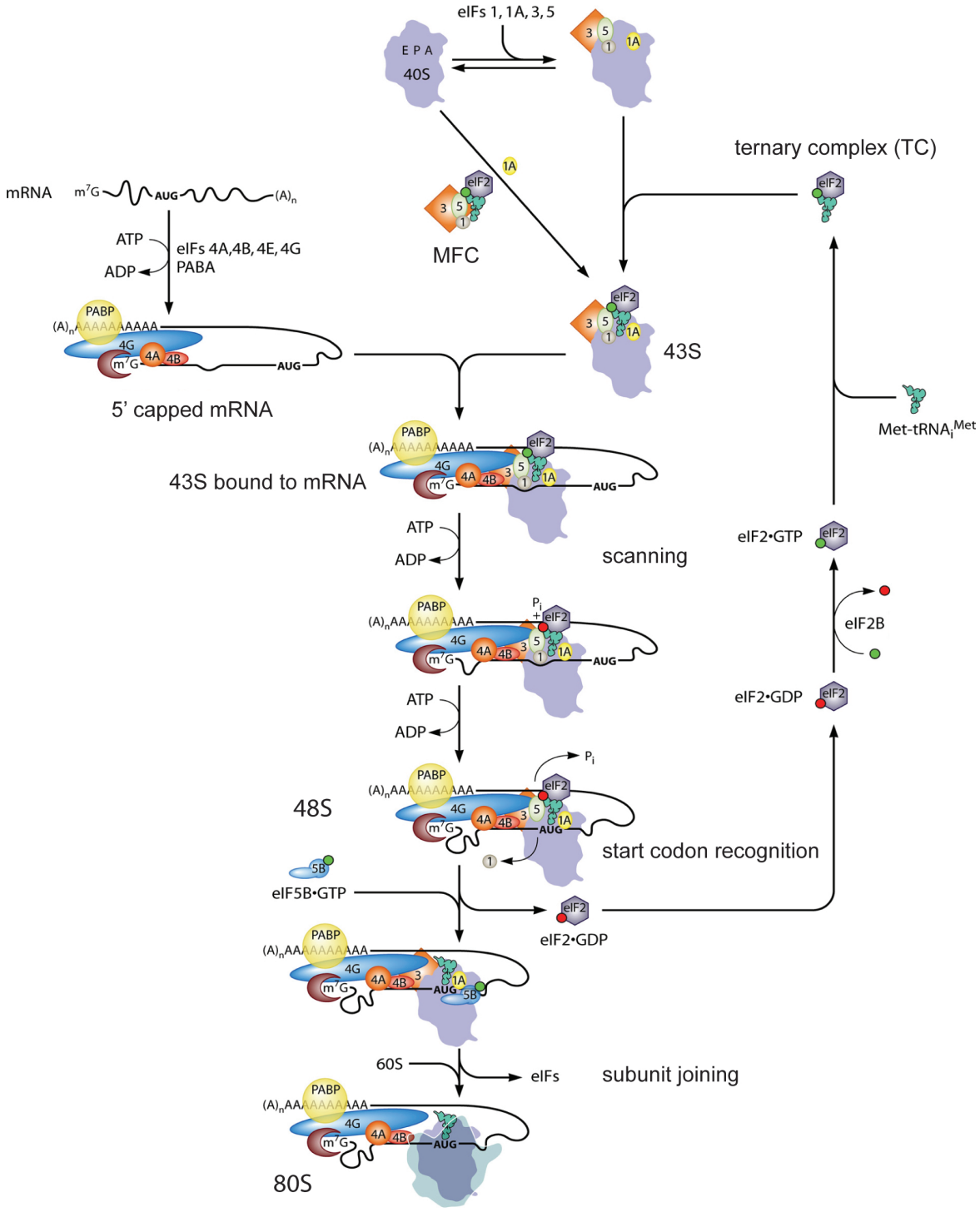

Figure 1.2: The mechanism of cap-dependent eukaryotic translation initiation (adapted from Hinnebusch (2011)). Initiation starts with the assembly of the 43S PIC comprising the 40S and the MFC components followed by the recognition and recruitment of the 5' capped mRNA, the process of 5' UTR scanning and 60S subunit joining and resulting in the formation of an elongation competent 80S ribosome at the start codon. For details see text. 80S ribosome and 40S subunit are depicted as blue silhouettes with location of aminoacyl-tRNA (A), peptidyl (P) and exit (E) site labeled in the 40S subunit; initiation factors (eIFs) are labeled by number; GTP and GDP are depicted as green or red balls, respectively; MFC: pre-assembled multifactor complex.

1.4.2 Eukaryotic Elongation, Termination and Ribosome Recycling

After translation initiation, the Met-tRNAi is positioned at the P-site of the ribosome with the A-site open for the next aminoacyl-tRNA (aa-tRNA) encoded by the mRNA. Translation elongation comprises three steps (i) positioning of the correct aa-tRNA in the A-site, (ii) peptide bond formation leading to a transfer of the peptide from the tRNA in the P-site to the aa-tRNA in the A-site and (iii) translocating the mRNA and tRNAs one position further on the ribosome into the E-site and P-site clearing the A-site for the next aa-tRNA. Translation elongation is assisted by the elongation factors eEF1 (eEF1A and B), eEF2 and the fungi specific eEF3. eEF1A recruits the aa-tRNA in the A-site in a GTP-dependent manner. eEF1B recycles eEF1A-GDP for a new round of elongation. After peptide bond formation, eEF2-GTP catalyzes the translocation step (Fig. 1.1) (Dever et al., 2007).

Termination occurs when the ribosome encounters a stop codon in the A-site. The t-RNA mimicry release factor eRF1 recognizes the stop codon with the help of Dbp5 and Gle1 (Baierlein and Krebber, 2010). After GTP-hydrolysis by eRF3 and its subsequent dissociation ABCE1 (ATP-binding cassette, sub-family E, member 1) binds to the ribosome. eRF1 catalyzes the hydrolysis of the peptidyl-tRNA bond and the release of the polypeptide from the ribosome. Subsequently, ABCE1 triggers the ATP-dependent ribosome splitting into subunits (Pisarev et al., 2010; Becker et al., 2012). Ribosome recycling is coupled with re-initiation when initiation factors such as eIF3, eIF1 and eIF1A bind to the small ribosomal subunit after ribosome recycling (Pisarev et al., 2007). eIF3 might be recruited to the 80S ribosome directly via ABCE1 even before recycling is completed (Jackson et al., 2010).

1.4.3 Translation Regulation by Phosphorylation of Translation Factors

Regulation of such an intricate, multistep process as translation can occur at many steps. Global translation regulation mainly occurs by modification of translation factors – initiation and elongation factors – whereas mRNA specific regulation is mediated by protein complexes that recognize particular elements of the mRNA or by small microRNAs that

hybridize to the mRNA (Gebauer and Hentze, 2004). Most regulation is exerted at the level of initiation.

One key mechanism to regulate translation initiation is the phosphorylation of the α subunit of eIF2 on serine S51. Phosphorylated eIF2α acts as competitive inhibitor of eIF2B, the recycling factor of eIF2-GDP to eIF2-GTP (Sonenberg and Hinnebusch, 2007). eIF2Bϵ, the catalytic subunit of eIF2B, is also a phosphoprotein. Phosphorylation of eIF2Bϵ increases or decreases eIF2B activity depending on the site of phosphorylation (Dever, 2002). A second regulated step in translation initiation is 5' cap recognition by the eIF4F complex. The assembly of eIF4F is suppressed by the eIF4E-binding proteins (4E-BPs). Upon phosphorylation of 4E-BPs, their interaction with eIF4E is disrupted and eIF4E is released to bind the cap and activate the mRNA during translation initiation. Phosphorylation of eIF4B, the auxiliary factor of the RNA helicase eIF4A, results in a better interaction with eIF3, and thus together with phosphorylation of 4E-BPs increases translation initiation (Pierrat et al., 2007).

During elongation, the eukaryotic elongation factor eEF1A and subunits of eEF1B are targets of phosphorylation. However, the effects of these phosphorylation events on translation still have to be shown. Phosphorylation of elongation factor eEF2 impairs interaction with the ribosome, and thus inactivates translation (Proud, 2007).

The two major pathways signaling to the translation machinery in response to stress, starvation or mitogen and growth factor stimulation, are the PI3K/Akt/mTOR1 and Ras-MAPK2 signaling pathways (Proud, 2007; Sonenberg and Hinnebusch, 2009). The serine-threonine kinase mTOR directly phosphorylates the 4E-BPs and the S6 kinases (S6Ks) which in turn phosphorylate eIF4B and the eEF2 kinase. eIF4E and eIF4B are phosphorylated in a Ras-MAPK pathway dependent manner. eIF2α is phosphorylated by a number of kinases, which are activated under different conditions such as stress or starvation, including HRI (Heme-regulated eIF2α kinase), PKR (Protein kinase R), or PERK (PKR-like ER-localized eIF2α kinase) (Dever, 2002). In yeast, Gcn2 (general control non derepressable 2) is the only eIF2α phosphorylating kinase (Hinnebusch, 2005). The major signaling pathways that control the phosphorylation and activity of translation initiation factors are depicted in Fig. 1.3 (adapted from Sonenberg and Hinnebusch (2007)).

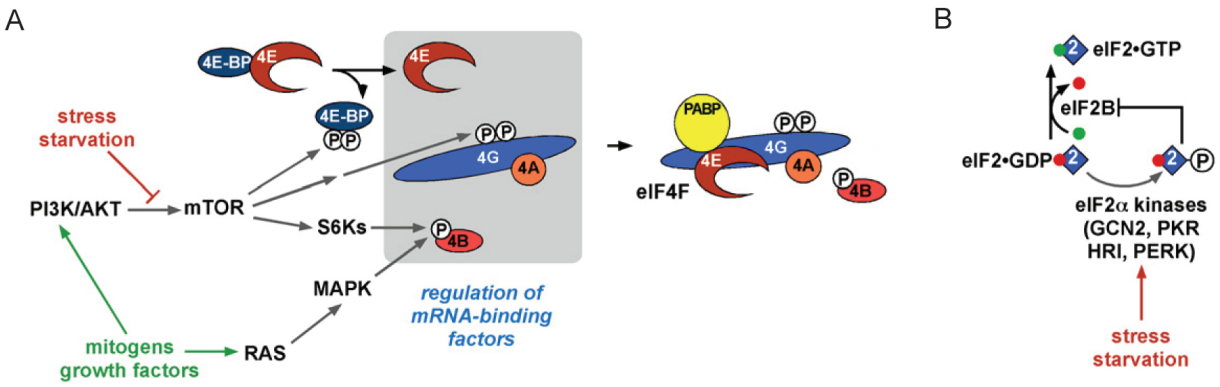

Figure 1.3: The major signaling pathways that control the phosphorylation and activity of translation initiation factors (adapted from Sonenberg and Hinnebusch (2007)). (A) The PI3K/Akt/mTOR and the Ras-MAPK signaling pathways regulate 5' cap recognition by eIF4F. mTOR directly phosphorylates the 4E-BPs and S6 kinases (S6Ks), and indirectly eIF4B and eIF4G. The Ras-MAPK pathway is responsible for the phosphorylation of eIF4E and eIF4B. (B) Under stress or starvation conditions the eIF2α kinases HRI, PKR, PERK3 or Gcn2 phosphorylate S51 of eIF2α thus inhibiting eIF2B. eIFs are labeled by number; GTP and GDP are depicted as green or red balls, respectively; red arrows are repressing, green activating influences.

1.5 The Ribosome and Its Phosphorylation

Decoding of the message and formation of the polypeptide chain is catalyzed by large macromolecular ribonucleoprotein complexes, the ribosomes. Ribosomes consist of two subunits, designated as the small (40S) and the large (60S) ribosomal subunit together forming the 80S ribosome. In *Saccharomyces cerevisiae*, the small subunit consists of an 18S rRNA and 33 proteins, whereas the large subunit is composed of three rRNAs (5S, 5.8S and 28S rRNA) and 46 proteins. The small subunit decodes the information encoded in the ORF of the mRNA, thus controlling the correct base pairing of tRNAs with each mRNA codon. The formation of peptide bonds is catalyzed by the large ribosomal subunit in the so called peptidyl-transferase center. The interplay of ribosomal proteins and rRNA is crucial for the optimal function of the translation machinery. Although the ribosome is considered as a ribozyme (Cech, 2000), ribosomal proteins not only support the structure of the ribosome, but are also involved in mRNA and tRNA recognition, helicase activity, decoding, formation of binding sites for translation factors, peptidyl-transferase activity and formation of the peptide exit tunnel (Kramer et al., 2009; Dresios et al., 2000; Meskauskas and Dinman, 2007; Pisarev et al., 2008; Takyar et al., 2005). However,

the function of ribosomal proteins and their role in translation regulation remains to be elucidated.

Surprisingly little is known about translation regulation and ribosome function by PTMs, in particular by phosphorylation of eukaryotic ribosomal proteins. In earlier studies, proteins of the large and the small ribosomal subunit were reported to be phosphorylated in yeast (Hebert et al., 1977; Kruiswijk et al., 1978; Campos et al., 1990). Ribosomal proteins Rpl3, Rpl11 and Rpl14 from *Saccharomyces cerevisiae* were phosphorylated *in vitro* by a ribosome associated kinase. Furthermore, *in vivo* phosphorylation of the small ribosomal proteins Rps2 and Rps6 and the large ribosomal proteins Rpl3, Rpl9, Rpl11, Rpl24, Rpl30, Rpl44 and Rpl45 have been shown. In two recent studies, an inventory of phosphorylation sites of ribosomes form *Escherichia coli* and mammalian mitochondria was generated by different mass spectrometry methods (Soung et al., 2009; Miller et al., 2009). It was also shown that mammalian mitochondrial ribosomes have a decreased translation rate after *in vitro* phosphorylation with different kinases, thereby hypothesizing that phosphorylation events have a regulatory function in translation.

The most prominent ribosomal phosphoprotein is Rps6 being phosphorylated at two sites in yeast and at least five sites in vertebrates. Several stimuli like heat shock and starvation have been reported to affect the phosphorylation status of Rps6 and lead to a reduction in the phosphorylation level (Ruvinsky and Meyuhas, 2006). However, the phosphorylation of Rps6 seems to have no effect on growth in yeast as shown by mutational analysis (Johnson and Warner, 1987). Thus, the molecular function of Rps6 phosphorylation in translation still remains to be elucidated. Moreover, the ribosomal stalk proteins Rpp0, Rpp1 and Rpp2 are highly phosphorylated in eukaryotes. The stalk is a protuberance of the large ribosomal subunit which directly interacts with cytoplasmic proteins, such as translation elongation factors. Changes in the stalk composition and phosphorylation state affect the capacity of the ribosome to translate a specific subset of mRNAs (Ballesta et al., 1999). Recently, our group revealed that the small ribosomal protein Rps2 is phosphorylated on S238 by the kinase Ctk1. Rps2 is positioned at the mRNA entry tunnel and it is known to be crucial for translation accuracy (Stansfield et al., 1998). We could demonstrate that phosphorylation of Rps2 is important for translational fidelity (Rother and Strasser, 2007).

1.6 Aim of the Study

Translation is an intricate and highly regulated step in gene expression. Translation regulation mostly occurs at the level of initiation. One of the key control mechanisms is the phosphorylation of initiation factors. Although phosphorylation of ribosomes has been known for decades, there is still very limited knowledge on translation regulation by phosphorylation of the translation machinery itself. The aim of this study was to generate a comprehensive catalogue of ribosomal phosphorylation sites and to elucidate the function of selected sites in translation.

Initially, a large-scale phosphoproteomics survey of the yeast *Saccharomyces cerevisiae* ribosome resulted in the identification of new phosphorylation sites in the ribosome. In a second approach, Stable Isotope Labelling with Amino Acids in Cell Culture (SILAC) was used to assess changes in the ribosomal phosphorylation pattern upon stress-induced shut-down of translation and to identify functionally significant phosphorylation sites. With the comprehensive survey of *Saccharomyces cerevisiae* ribosomal phosphorylation sites and the quantification of changes in the ribosomal phosphorylation levels in response to stress the challenge of this study was to determine which of the identified sites are individually or collectively important for translation. To this end, selected phosphorylated residues (S, T or Y) of ribosomal proteins were mutated to either the phospho-deficient A or the phospho-mimicry D residues and subsequently assessed for their translation activity *in vitro*. Twelve of the analyzed ribosomal phospho-mutants showed an effect in the *in vitro* translation assay.

For two of the identified ribosomal phosphorylation sites on the small ribosomal subunit, namely Rps5 T38 and Rps12 T23, the aim was to unravel their function in translation initiation in more detail. This was accomplished by a combination of different *in vitro* and *in vivo* translation assays for different steps of translation initiation ranging from initiation complex formation through scanning processivity to context dependent start codon recognition. Moreover, the physiological relevance of these two phosphorylation sites was addressed by investigating the growth under different conditions.

Taken together, the aim of this study was to show that phosphorylation sites in heavily phosphorylated ribosomes function in distinct steps of translation.

2 Results

2.1 Phosphoproteomic Analysis of Ribosomal Phosphorylation Sites

2.1.1 Identification of Ribosomal Phosphorylation Sites

Phosphorylation of proteins is one of the major regulatory mechanisms used by the cell to control almost all cellular processes, thus also translation. Since 50% of the proteins are supposed to possess at least one phosphorylation site (Cohen, 2000) numerous ribosomal proteins should be phosphorylated. To address the question which ribosomal proteins are phosphorylated and how ribosomal phosphorylation sites are involved in translation, ribosomal phosphorylation sites of the yeast *Saccharomyces cerevisiae* were mapped at steady-state.

To this end, subsequent centrifugation steps with a sucrose density gradient as a final purification step were used to isolate 40S and 60S ribosomal subunits, 80S ribosomes, and polysomes from yeast whole cell extracts (WCEs) under phosphorylation conserving conditions. A high salt wash removed more loosely associated proteins to obtain pure ribosomes. Fractions of the sucrose gradients containing 40S, 60S, and 80S ribosomes or polysomes, which were stabilized by cycloheximide, were pooled. The phosphoproteomic analysis of purified ribosomes was done by Jesper V. Olsen. After in solution digestion of proteins with the endoproteinases Trypsin and LysC the phosphopeptides were enriched using TiO_2 column and analyzed by nanoflow LC-MS/MS on an LTQ Orbitrap instrument (Fig. 2.1). All peptides were sequenced by collision-induced dissociation with multi-stage activation enabled for neutral loss of phosphoric acid. The resulting raw LC-MS files were processed and analyzed with the MaxQuant software suite (www.maxquant.org) and yeast

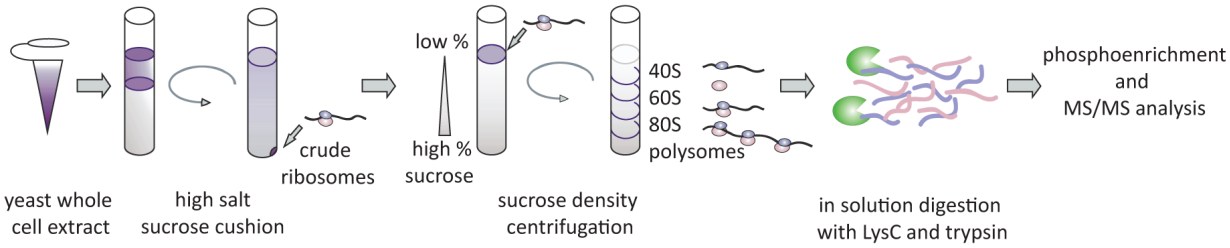

Figure 2.1: Purification of *Saccharomyces cerevisiae* ribosomes for phosphoproteomics analysis using subsequent centrifugation steps with a sucrose density centrifugation as final purification step.

phosphopeptides identified by the Mascot search engine (www.matrixscience.com) at a fixed false discovery rate of $FDR > 0.01$. (Olsen et al., 2006).

In total 66 of the 79 ribosomal proteins of *Saccharomyces cerevisiae* were found to be phosphorylated on at least one phosphorylation site corresponding to 84 % of the ribosomal proteins. This is a larger proportion than the commonly cited 30 % of the proteome (Cohen, 2000) and even higher than the 70 % found in an in-depth study of HeLa S3 cellular proteins over the cell cycle (Olsen et al., 2010). 279 ribosomal phosphorylation sites mainly on S (195) and T (80) and only rarely on Tyr (4) were identified – 117 on the small ribosomal subunit, 144 on the large subunit and 18 on the ribosomal stalk proteins (Table 2.1). On average each ribosomal protein is phosphorylated on 4.6 residues ranging from one to 15 sites. 42 % of the phosphorylated amino acids are conserved in human and mouse suggesting that their function – if any (see Section 2.3 and Section 2.4) – might also be conserved. Based on the available structures (Rabl et al., 2011; Ben-Shem et al., 2011) the majority of sites is located at the surface of the small or large ribosomal subunit including the interface, where they are accessible to kinases and phosphatases (Fig. 3.1).

Table 2.1: Phosphorylation sites in ribosomal proteins identified in this study.

Protein	Phosphosites
Rps0	T103, T112, S114, T219, T220
Rps1	S236, S245, T254
Rps2	S2, S181
Rps3	S104, T207, S221, T231
Rps4	S120, S247
Rps5	S2, T21, T38, S47, S206, T207, S208

Continued on next page

Table 2.1 (continued)

Protein	Phosphosites
Rps6	T15, T163, T180, S232, S233
Rps7	S30, S31, S103, T105, S106, S115, T117, T119, S187, T189
Rps8	S45, T132, S154, S155, S158, S161
Rps9	S13, T14, T161, S162, S184
Rps10	S48, T98
Rps11	S2, T3, T6, S9, T44, S52
Rps12	S2, T19, T23,
Rps13	S12, S13, S14, S19, S30, S147
Rps14	S2, S11, S12, S125, T126, S126, T127
Rps15	S2, S29, T30
Rps16	S2, S6, S15, T17, S34
Rps17	S70, S89, S94, S96, T106, S107, S120, S125
Rps18	S107
Rps19	S5, S117, T139
Rps20	S38, S39
Rps21	S84, Y85, S86
Rps23	S40
Rps24	S2, S14, S56
Rps25	S74, S93
Rps26	S54, S57, Y59, S110
Rps27	T11, S14
Rps28	S3, T5, T8, T19, S37
Rps29	S25
Rpl1	T5, S6, S7, S79, S86
Rpl2	S95, S195, S249
Rpl3	S24, S65, S101, T103, T296, S297, T301, S355
Rpl4	S53, T60, S61, S64, S85, S270, S278, S282, T283, S284, T287, S292, S293, S297, T306
Rpl5	S9, S235
Rpl6	S12, S88, S164,
Rpl7	T8, S11, T16, S113, T115, S228
Rpl8	S29, T30, S126, Y130, S216
Rpl10	S205
Rpl11	T44, S161
Rpl12	S38

Continued on next page

Table 2.1 (continued)

Protein	Phosphosites
Rpl13	T144, T152, S165
Rpl14	T3, S5
Rpl15	T165, T167, T196
Rpl16	S2, S163, S178, S179, S180, S181, T184, S185, S187, S188
Rpl17	S65, S66, S141, S142, S144
Rpl18	S63, S65, S167, T168
Rpl19	S13, T29, S30, S37, T56, S59, S91
Rpl20	T16, S18, S60, S169, T170
Rpl21	S70, S142, T143
Rpl22	S20, S21, T23, T111
Rpl24	S7, S9, S26, S83, S86, S95, T153, S154
Rpl25	T28, S29, T31, S69, T71
Rpl26	T21, S24, S25, S62, S72, S94
Rpl27	S33, S94, T97, T98, S105
Rpl30	S6
Rpl32	S40, S51, S67, S69
Rpl33	S15, S97
Rpl34	T64, S66
Rpl35	S19, S40, S98
Rpl36	T18, S19, T21, S64, S79, T81, S97
Rpl37	T5, S7, T80, S82, S84
Rpp0	Y273, T281, S302
Rpp1A	S62, S96
Rpp1B	S58, S73, S96
Rpp2A	S43, S49, S71, S79, S96
Rpp2B	T65, T68, S72, S73, S100

The presented inventory of yeast ribosomal phosphorylation sites was compared to two phosphorylation databases: PHOSIDA (www.phosida.com) (Gnad et al., 2007) and PhosphoPep (www.phosphopep.org) (Bodenmiller et al., 2007). PHOSIDA and PhosphoPep contain only 9.0 % and 36.6 % of the phosphosites identified by us as well as 2.2 % and 36.6 % additional sites, respectively. Moreover, comparing the presented inventory with UniProt (www.uniprot.org) revealed that 96 sites are reported there in addition to 98 sites not found in this study. Taken together, the most comprehensive

catalogue of ribosomal phosphosites in *Saccharomyces cerevisiae* to date is presented here including 122 novel ones.

2.1.2 Stress-Induced Changes in the Phosphorylation Pattern of Ribosomal Proteins Using SILAC

In a natural environment cells are exposed to a large variety of different stresses and in order to survive they need to react and adapt to the environmental conditions. One response to environmental stress like heat shock or nutrient deprivation is the shut-down of global translation indicated by the accumulation of free 80S ribosomes. For instance, this is mediated by the phosphorylation of initiation factor eIF2α leading to a decrease in TC formation, thus inhibiting translation initiation (see Section 1.4.3). Since phosphorylation of proteins is a broadly used control mechanism of the cell to immediately adapt to changes in the environment, the question whether there are changes in the ribosomal phosphorylation pattern in response to stress-induced shut-down of translation was addressed in this study. To this end, a quantitative phosphoproteomics approach was used to investigate stress-induced changes in the phosphorylation status of ribosomal proteins by Stable Isotope Labeling by Amino Acids in Cell Culture (SILAC) in combination with phosphoenrichment and LC-MS/MS. A shut-down of translation was induced by heat shock and glucose deprivation leading to a loss of heavily translating polysomes and accumulation of free 80S ribosomes on gradient profiles (Fig. 2.2 A-C).

In the SILAC experiment two cultures were grown either in media containing light lysine or heavy lysine and one of the two cultures was treated with either heat shock (10 min at 42°C) or glucose deprivation (5 min in medium lacking glucose). After cell lysis, the extracts of the two cultures were combined for further purification of ribosomes, thereby reducing unspecific variations in the phosphorylation patterns of treated and untreated cells caused by differences in the preparation. Ribosomal subunits and 80S ribosomes were purified and digested with the endoproteinase LysC since only Lys was used for labeling. The phosphopeptides were enriched and analyzed by LC-MS/MS. The amino acids with a different phosphorylation level were determined and the phosphorylation ratio between stressed and untreated samples calculated (Fig. 2.2 D) (Olsen et al., 2006).

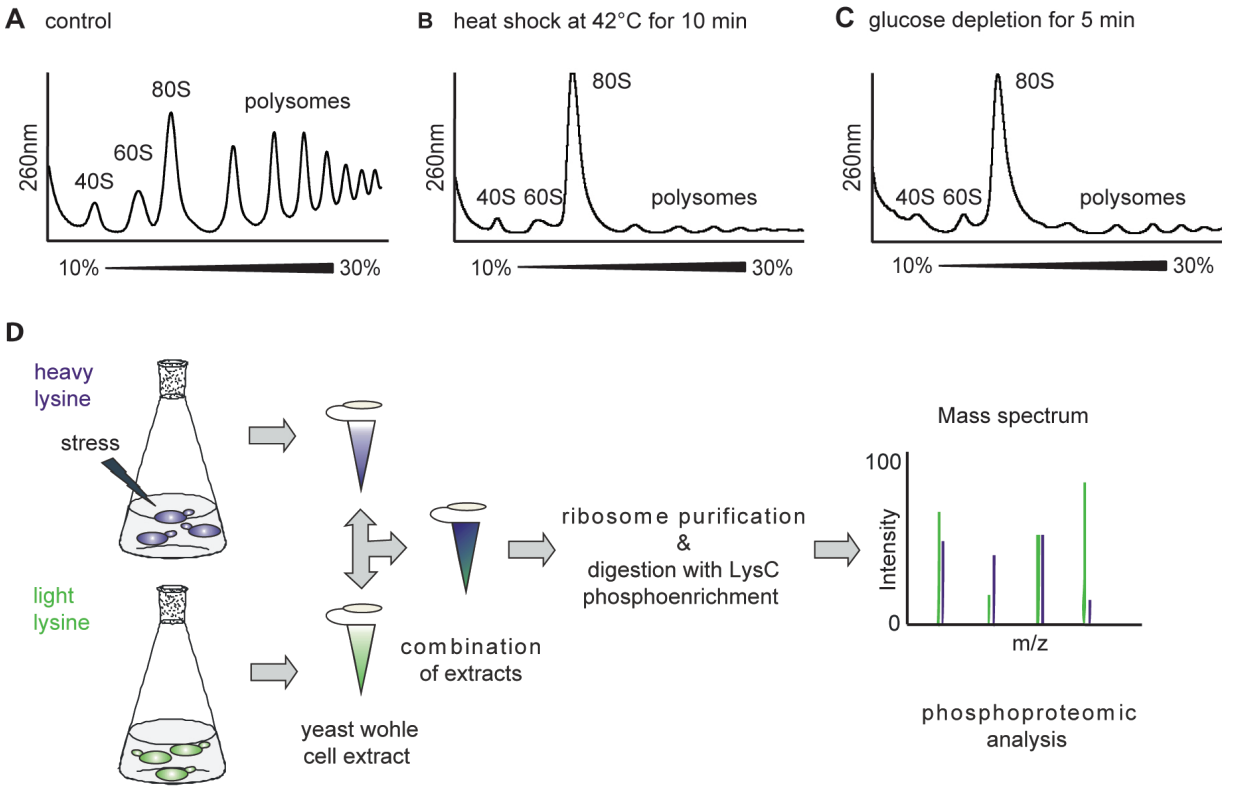

Figure 2.2: Stable Isotope Labelling with Amino Acids in Cell Culture (SILAC) to investigate changes in the phosphorylation pattern of yeast ribosomes. (A-C) Sucrose density gradient profiles of control (A), heat shocked (B) or glucose deprivated cells (C). WCEs were separated on 10-30 % sucrose gradients and absorption was measured at 260 nm. 40S, 60S, 80S and polysome peaks are indicated. (D) Flow scheme of SILAC experiment.

The large majority of identified phosphorylation sites remained unchanged under heat shock and glucose deprivation (Table A.2). Interestingly, eleven and nine ribosomal phosphorylation sites changed their phosphorylation status in response to heat shock and glucose deprivation, respectively (Table 2.2 Table 2.3). Importantly, the two known Rps6 sites S232 and S233 were identified with a reduction in their phosphorylation levels to 30 % in response to heat shock as well as glucose deprivation. Besides the decreased Rps6 phosphorylation, two more sites Rpl24 S86 and Rpl12 S38 showed a reduced phosphorylation status upon heat shock or glucose deprivation (Table 2.2 and Table 2.3). Heat shock induced an increase in the phosphorylation levels of three sites on large ribosomal proteins (Rpl12 S38, Rpl6 S12 and Rpl7 T8), two sites on the ribosomal stalk (RPP2A T43 and T49) and two sites on small ribosomal proteins (Rps2 S2 and Rps3 T207 and S221). In response to glucose deprivation the phosphorylation sites on the large

ribosomal subunit Rpl16 S2 and Rpl24 S9 and on the small subunit Rps7 S10 and T14, Rps15 S2 and Rps16 S15 were increased.

Table 2.2: Phosphosites in ribosomal proteins that change in response to heat shock.

Protein	Phosphosites	Phosphoylation compared to normal growth
Rps2	S2	1.6 ± 0.52
Rps3	T207	1.27 ± 0.14
Rps3	S221	1.22 ± 0.16
Rps6A	S232	0.32 ± 0.24
Rps6A	S233	0.32 ± 0.24
RpL6A	S12	1.43 ± 0.07
RpL7A	T8	1.18 ± 0.2
RpL12A	S38	1.91 ± 0.4
RpL24A	S86	0.59 ± 0.15
Rpp2A	T43	1.22 ± 0.06
Rpp2A	T49	1.22 ± 0.24

Table 2.3: Phosphosites in ribosomal proteins that change in response to glucose depletion.

Protein	Phosphosites	Phosphoylation compared to normal growth
Rps6A	S232	0.33 ± 0.05
Rps6A	S233	0.33 ± 0.05
Rps7B	S10	1.20 ± 0.17
Rps7B	S14	1.20 ± 0.17
Rps15	S2	1.48 ± 0.29
Rps16A	S15	1.40 ±0.41
Rpl12A	S38	0.83 ± 0.09
Rpl16B	S2	1.18 ± 0.13
Rpl24A	S9	1.23 ±0.15

Thus, it could be demonstrated that ribosomal phosphorylation sites change in response to a stress-induced shut-down of translation suggesting that phosphorylation of ribosomes at these sites might be involved in the translational response to stress.

2.2 Mutational Analysis of Selected Ribosomal Phosphorylation Sites

Having identified new ribosomal phosphorylation sites as well as sites that change significantly in response to translational impairment by stress, the aim of this study was to demonstrate the biological significance of some of the identified phosphorylation sites and elucidate the underlying molecular mechanism of their regulation. Therefore, phosphorylation sites identified in the initial phosphoproteomic analysis as well as sites that changed in the SILAC experiments were chosen for mutational analysis. Since the sites identified in the SILAC experiments already showed a response to translational impairment, they most probably are involved in translation regulation – at least in stress-induced control mechanisms. In addition, sites identified in the general phosphoproteomic survey of yeast ribosomes were chosen according to their reproducibility in the different preparations, their intensity of their MS-signal, their position on the ribosome and their conservation in higher eukaryotes.

The phosphorylatable amino acids (S, T and Y) of the selected phosphorylation sites were mutated to the phospho-deficient A and subsequently to the phospho-mimicry D residues (in the case the A mutation showed an influence on translation). The corresponding deletion strains, either a single deletion for single copy ribosomal proteins or the double deletion for two copy ribosomal proteins were supplemented with a wild-type or mutant gene copy on a shuffle plasmid. Subsequently, the translation activity of mutated ribosomal proteins was assessed using translation active extracts of yeast cells to translate either a capped or a Cricket Paralysis Virus (CrPV) IRES containing luciferase mRNA *in vitro* (Fig. 2.3). The capped luciferase mRNA contained the common eukaryotic 5' UTR structure with a 5' m^7GpppG cap and the full set of initiation factors is needed for efficient translation initiation. In contrast, the CrPV 5' UTR contains a so-called Internal Ribosome Entry Site (IRES). Translation of the CrPV IRES differs from canonical cap-dependent initiation in the direct recruitment of 80S ribosomes to the start codon by a distinct secondary structure in the 5' UTR without the help of any translation initiation factors (Wilson et al., 2000; Pestova and Hellen, 2003). First, the phospho-deficient A mutants were assessed in the *in vitro* translation assay to translate the 5' capped luciferase mRNA

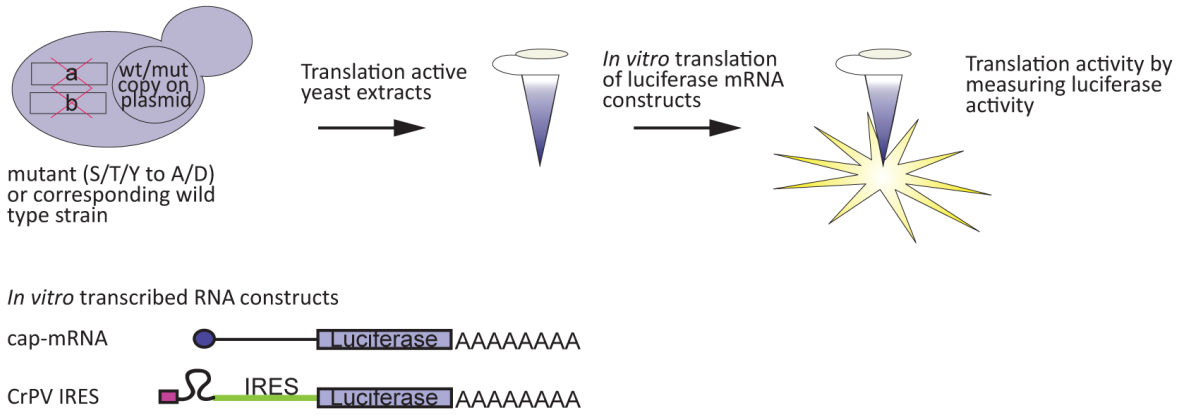

Figure 2.3: Schematic representation of the mutational analysis using an *in vitro* translation assay with *in vitro* transcribed luciferase mRNAs.

compared to the corresponding wild-type. In the case the A mutant and wild-type extracts differed in their translation activity *in vitro*, cap-independent translation activity and the translation activity of the corresponding phospho-mimicry D mutant was assessed.

So far, the *in vitro* translation activity of 25 phospho-deficient A mutants was analyzed (data not shown). Thereof, twelve A mutants showed different translation activity compared to wild-type extracts in cap-dependent translation – the majority of the analyzed phospho-deficient A mutants showed an increase and few sites a decrease in cap-dependent translation activity. The phospho-mimicry D mutants of these phosphorylation sites either possessed translation activity comparable to wild-type indicating that the phosphorylation mimicry corresponds to the wild-type situation in the cell or a decrease indicating that the phosphorylation status might change during the translation cycle or the phospho-mimicry failed.

Intriguingly, phosphorylation sites were identified that seem to be involved in cap-dependent translation indicated by a defect in translating the capped, but not the CrPV IRES containing mRNA, as well as sites that influence cap-independent translation as the mutant affects the translation activity of both constructs. Moreover, the loss of phosphorylation of some sites leads to increased while the loss of other phosphorylations to a decreased translation activity indicating a specific function in translation. Two phosphorylation sites, Rps5 T38 and Rps12 T23, showed a defect in cap-dependent translation when mutated to the phospho-deficient A and their function in translation

initiation was analyzed in more detail.

2.3 Function of Rps5 T38 Phosphorylation in Start Codon Selection

The small ribosomal protein Rps5 forms part of the mRNA exit channel (Fig. 3.3 A). Rps5 belongs to a family of highly conserved ribosomal proteins also containing the prokaryotic Rps7, archeal Rps7 and eukaryotic Rps5. Despite a conserved central core domain and C-terminus, Rps5 proteins contain a variable N-terminus that differs in length between the different species (Fig. 3.3 B). Recently, this N-terminus was reported to be important for 40S subunit function in translation and for efficient translation initiation (Galkin et al., 2007; Lumsden et al., 2009). In this study, two ribosomal phosphorylation sites on the N-terminal part of Rps5 were identified, namely Rps5 T21 and T38. Both sites were analyzed for translation activity using the *in vitro* translation assay system described above (Section 2.2). In contrast to the phospho-deficient *rps5-T21A* mutation that had no effect on the translation activity *in vitro* the phosphorylation of Rps5 T38 is important for translation.

2.3.1 The *rps5-T38A* Mutation Causes a Cap-Dependent Translation Defect

The translation activity of phospho-deficient *rps5-T38A* mutant extracts to translate the capped mRNA was reduced to around 53 % (± 11 %) of the corresponding wild-type extracts. However, the ability to translate the CrPV IRES containing luciferase mRNA was not affected in the *rps5-T38A* mutant translation active extracts compared to *RPS5* wt extracts (Fig. 2.4 A) indicating that the *rps5-T38A* mutation causes a cap-dependent translation defect *in vitro*. In contrast, the phospho-mimicry *rps5-T38D* mutant showed a reduced translation activity for both capped and CrPV IRES containing mRNA reporters to 38 % (± 10 %) of the wild-type activity (Fig. 2.4 A). Thus, the *rps5-T38D* mutation causes a cap-independent translation defect *in vitro*.

In order to rule out that the translation defect is specific for the two exogenous mRNA

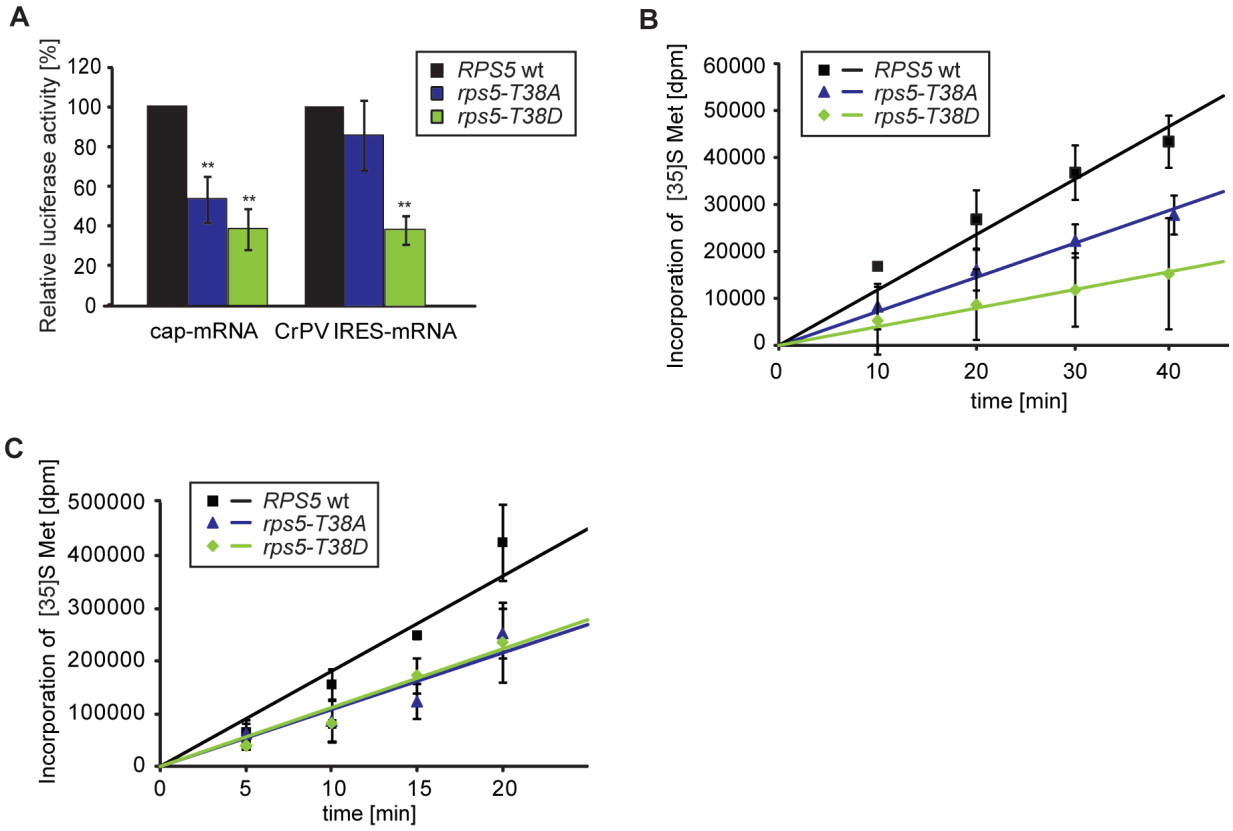

Figure 2.4: The *RPS5* phospho-mutants cause a cap-dependent translation defect. (A) Translation activity of translation active extracts from *RPS5* wild-type, *rps5-T38A*, and *rps5-T38D* mutant cells for the capped and CrPV IRES luciferase mRNA reporters was analyzed by luciferase measurement. For both RNA constructs the activity of the *RPS5* wild-type extracts was set to 100 % (mean ± SD; $n = 4$; ** $p < 0.001$; * $p < 0.05$). (B) Translation activity of *in vitro* translation active extracts to translate endogenous mRNAs was assessed using [35S] methionine to label synthesized proteins in translation active extracts of *rps5-T38A*, *rps5-T38D* and *RPS5* cells. Samples were taken at the indicated time points and incorporated [35S] Met measured by scintillation counting (mean ± SD; $n = 3$; $p < 0.05$ for $t \geq 20$ min). (C) Both Rps5 phospho-mutants cause a decrease in *de novo* protein synthesis compared to wild-type cells measured by incorporation of [35S] Met into newly synthesized proteins. Samples were taken at the indicated time points and [35S] Met incorporation measured by scintillation counting (mean ± SD; $n = 4$; $p < 0.05$ for $t \geq 10$ min).

reporters, the activity to translate endogenous mRNA was assessed using [35S] methionine to measure time-dependent protein synthesis in *in vitro* translation active extracts. In the *rps5-T38A* mutant extracts the translation activity for endogenous mRNAs was around 60 % of the wild-type activity (Fig. 2.4 B). The *rps5-T38D* mutant showed a stronger reduction in the activity to translate endogenous mRNAs to 30 % of the wild-type (Fig. 2.4 B). The translation defect of both *RPS5* phospho-mutants is not dependent on

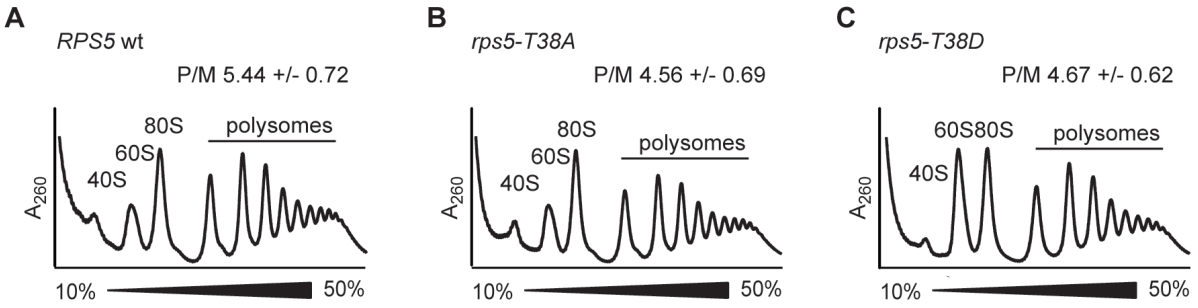

Figure 2.5: In *rps5-T38A* mutant cells the P/M ratio is decreased. (A-C) For polysome profiles of *RPS5* wt (A), *rps5-T38A* (B) and *rps5-T38D* (C) strains, WCEs were separated on 10-50 % sucrose gradients and the absorption at 260 nm was measured. The polysome (P) / monosome (80S;M) ratio was calculated by integrating the area under the respective peaks after substraction of the baseline (mean ± SD; $n = 4$).

the mRNA used to asses the translation activity *in vitro*.

To corroborate the *in vitro* translation defect of both phospho-mutants *in vivo* the incorporation of [35S] methionine into *de novo* synthesized proteins was assessed. After the addition of [35S] methionine to the *rps5-T38A*, *rps5-T38D* and *RPS5* wt cells, samples were taken at the indicated time points and [35S] incorporation was analyzed by scintillation counting of TCA precipitated proteins. For all three strains a linear increase in [35S] incorporation was observed, but *rps5-T38A* and *rps5-T38D* mutant cells showed a reduced translation activity to 60 % of the wild-type level for time points later than 10 min (Fig. 2.4 C). Thus, both phospho-mutants cause a translation defect *in vivo*.

A defect in translation initiation results in an accumulation of free 80S ribosomes (monosomes) and a decrease in heavily translating polysomes indicated by a reduced polysome to monosome (P/M) ratio in polysome gradient profiles. Consistent with the cap-dependent translation defect observed *in vitro* the P/M ratio in polysome gradient profiles of the *rps5-T38A* mutant cells was reduced by 15 % compared to wild-type profiles (Fig. 2.5 A, B). Interestingly, in addition to a reduced P/M ratio the *rps5-T38D* mutation causes an increased 60S peak in polysome gradient profiles that might result from reduced amount of 40S subunits (Fig. 2.5 A, C).

Taken together, both Rps5 T38 phospho-mutations cause a translation defect *in vitro* as well as *in vivo*. Specifically, the *rps5-T38A* mutant showed a cap-dependent, most likely translation initiation defect, whereas the *rps5-T38D* mutant has a cap-independent reduction in translation activity.

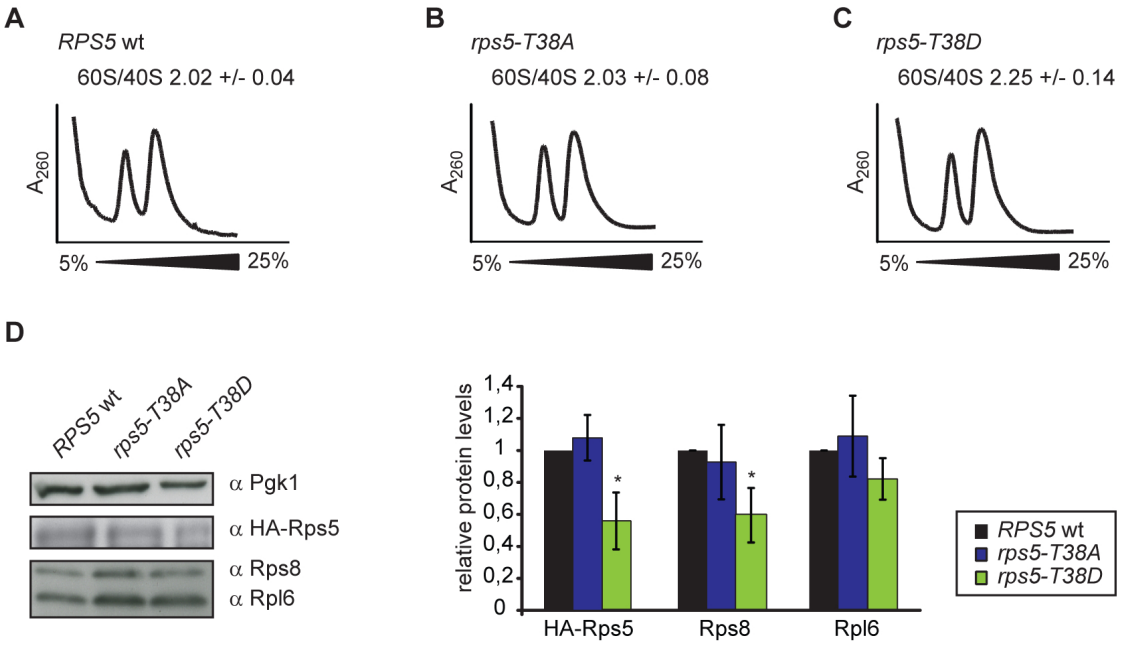

Figure 2.6: *rps5-T38D* mutation leads to lower levels of small ribosomal proteins. (A-C) Ribosomes were split into subunits by omitting Mg^{2+} ions. WCEs of *RPS5* wt (A), *rps5-T38A* (B) and *rps5-T38D* (C) strains were separated on a 5-25 % sucrose gradient. The 60S/40S ratio was calculated as for the P/M ratio. (D) WCEs of either *RPS5* wt, *rps5-T38A* or *rps5-T38D* (as N-terminal 3HA fusions) were analyzed by Western blot using antibodies against Pgk1, HA, Rpl6 and Rps8. HA, Rpl6 and Rps8 signals were normalized to the corresponding Pgk1 signals and protein levels calculated relative to wild-type (mean ± SD; $n = 4$).

2.3.2 In *rps5-T38D* Mutant Cells 40S Subunits Are Decreased

To investigate in more detail the elevated 60S peak in the polysome gradient profiles of *rps5-T38D* mutant cells (Fig. 2.5 C), ribosomes where split into their subunits to determine the levels of 40S and 60S subunits in the cell. To this end, WCEs and sucrose density centrifugation were performed ommiting Mg^{2+} ions. The 60S/40S ratio of the *rps5-T38A* mutant cells equaled *RPS5* wt cells (Fig. 2.6 A, B). However, the increased 60S peak in the *rps5-T38D* mutant is caused by the reduced amount of 40S compared to 60S subunits indicated by the increased 60S/40S ratio (Fig. 2.6 A, C).

This finding was corroborated using Western blot analysis to determine the levels of HA-tagged Rps5 (wt and mutant), the small ribosomal protein Rps8 and the large ribosomal protein Rpl6 relative to Pgk1 (Fig. 2.6 D). For the *rps5-T38A* mutant cells the protein levels were similar to wild-type levels, whereas in the *rps5-T38D* mutant cells the

HA-Rps5 and the Rps8 level was reduced to around 60 % of the wild-type while Rpl6 was almost unaffected (Fig. 2.6). These results suggest that the *rps5-T38D* mutation causes a ribosome biogenesis defect or affects the stability of the small ribosomal subunit whereas the defect observed with the *rps5-T38A* mutation is not caused by an impaired ribosome biogenesis or 40S stability.

2.3.3 Rps5 Phospho-Mutants Do Not Affect Translation Elongation

So far, the obtained results suggest that the *rps5-T38A* mutant causes a translation initiation defect, while the *rps5-T38D* mutant has a cap-independent translation defect caused by a defect in 40S ribosome synthesis or stability. To study elongation independent of initiation a poly(U) assay was performed by Viter Marquez. This assay allows peptide synthesis independent of canonical translation initiation using poly(U) homopolymers as mRNA templates in *in vitro* translation active extracts (Leibowitz et al., 1991). The elongation rate is determined by measuring the time-dependent incorporation of [14C] phenylalanine into poly-F peptides (Fig. 2.7 A, left arrow). In parallel translation fidelity can be assessed by measuring the incorporation of near-cognate [3H] leucine (Fig. 2.7 A, right arrow). Neither *rps5-T38A* nor *rps5-T38D* mutant extracts showed an elongation or translation fidelity defect *in vitro* compared to wild-type extracts (Fig. 2.7 B-E).

In order to assess whether translation fidelity is affected *in vivo*, different dual luciferase reporters developed by Dinman and Bedwell were used (Hager and Dinman, 2003; Salas-Marco and Bedwell, 2005). These reporter plasmids encode Renilla luciferase, a linker, and firefly luciferase mRNA (Fig. 2.8A). The linker containing the L-A (-1) or the Ty1 ($+1$) frameshifting signal (Fig. 2.8 Ai) only enables Firefly translation when the ribosomes fail to maintain the correct reading frame and shift $\pm$ 1 nucleotide. The second dual luciferase set contains point mutations of H245 to Q, R and D (Fig. 2.8 Aii) resulting in an inactive Firefly luciferase. Only when the not cognate amino acid His is incorporated, the Firefly is active. The readthrough frequency of stop codons can be measured with the dual luciferase reporters containing one of the three stop codons in their linker (Fig. 2.8 Aiii). Overall, the *rps5-T38A* and *rps5-T38D* mutations did not severely affect translation fidelity *in vivo*. The *rps5-T38A* mutant showed a slightly increased $+1$ frameshifting

(Fig. 2.8 B) and readthrough frequency (Fig. 2.8 D) compared to wild-type but the observed effect was to small to explain the translation defect observed in the previous experiments. The same is true for the *rps5-T38D* mutant that also showed a minor increase in +1 frameshifting, miscoding for H245D and readthrough of TGA and TAA stop codons (Fig. 2.8 B-D).

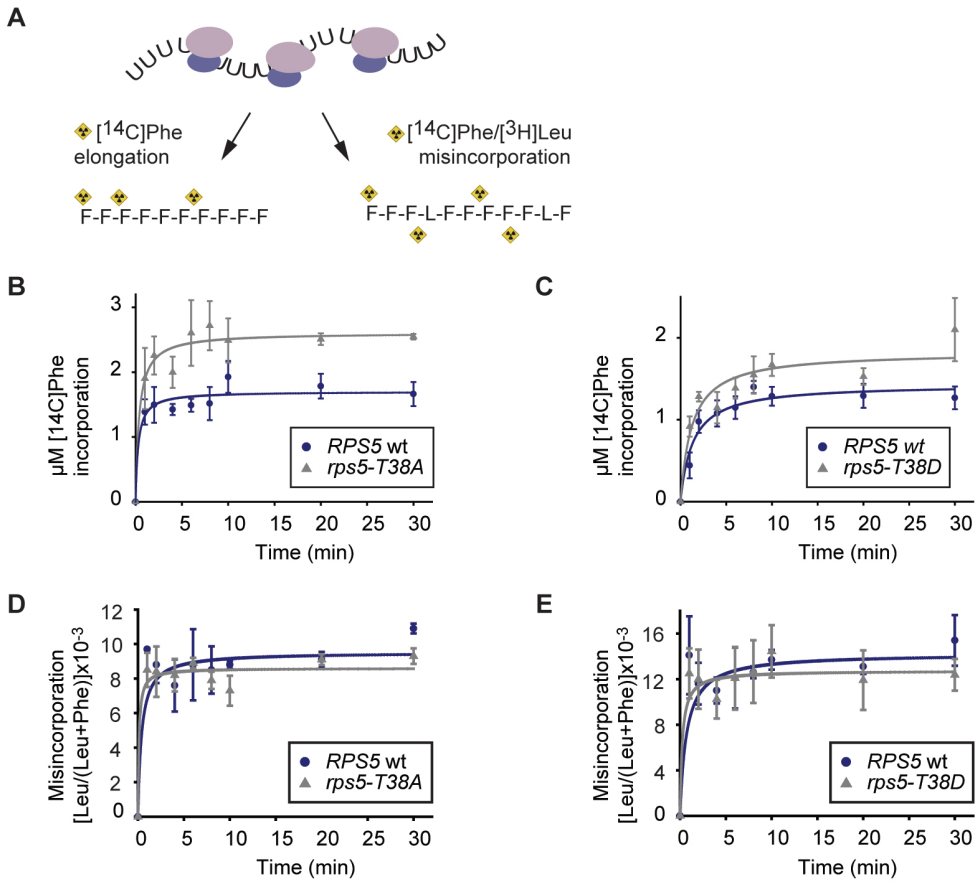

Figure 2.7: *RPS5* phospho-mutants have no elongation defect *in vitro*. (A) Schematic representation of the poly(U) assay. Translation elongation efficiency and fidelity was determined by measuring the incorporation of [14C] phenylalanine (F) and misincorporation of near cognate amino acids by [3H] leucine (L), respectively. (B+C) Both *RPS5* phospho-mutants do not show an elongation defect. The time dependent incorporation of [14C] F into polypeptides in *rps5-T38A* (B) and *rps5-T38D* (C) and *RPS5* wt translation active extracts was determined by scintillation counting (mean ± SD; $n = 3$). (D+E) The translation defect of *RPS5* phospo-mutants does not influence translation fidelity. In translation active extracts of *rps5-T38A* (D) and *rps5-T38D* (E) mutants and *RPS5* wt the incorporation of near-cognate L relative to F incorporation was determined at the indicated timepoints (mean ± SD; $n = 3$).

Taken together, both *RPS5* phospho-mutants do not affect translation elongation indicating that the observed translation defect of the *rps5-T38A* mutant is indeed a

translation initiation dependent defect. Since the *rps5-T38D* mutation has a translation defect caused by impaired ribosome biogenesis or stability and the aim of this study was to elucidate the function of phosphorylation sites in translation and not ribosome biogenesis, only the *rps5-T38A* mutant was further analyzed in more detail.

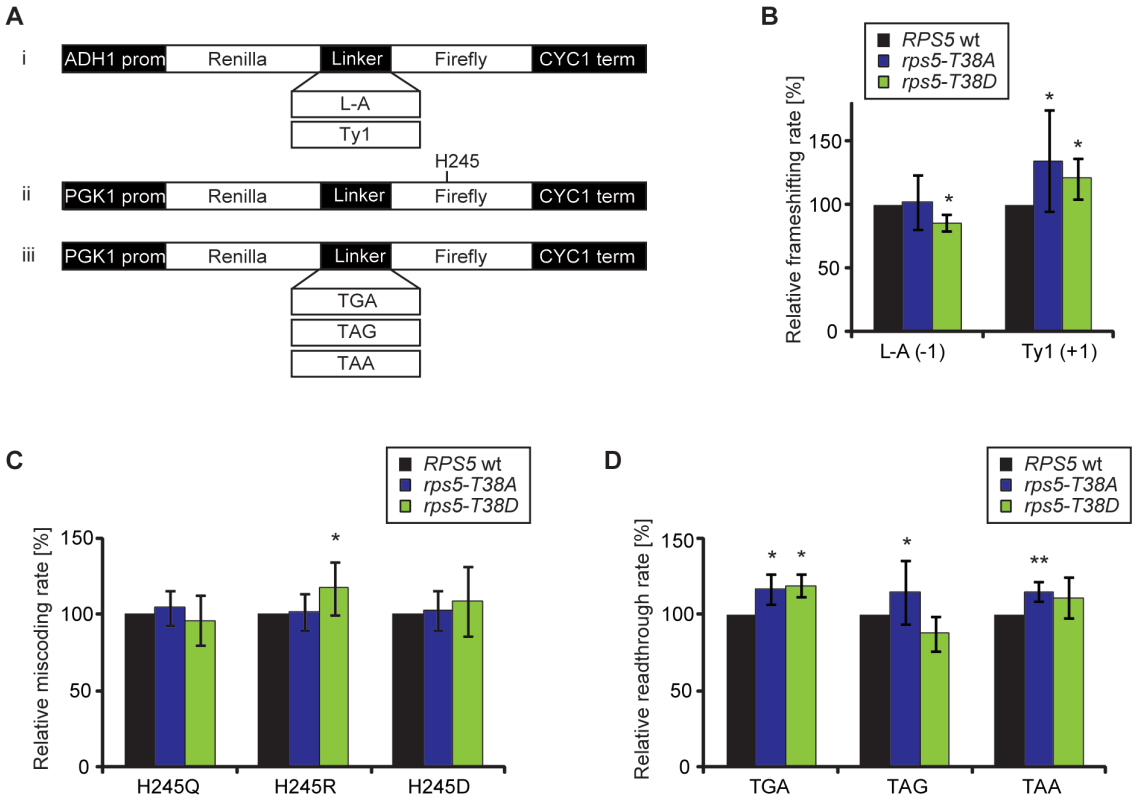

Figure 2.8: Elongation fidelity is unaffected in *RPS5* phospho-mutant cells in *in vivo*. (A) Schematic illustration of different dual luciferase reporters encoding Renilla luciferase, a linker and Firefly luciferase. The linker contains a ±1 frameshifting signal (i) or one of the tree stop codons (iii). In (ii) Firefly H245 is mutated to H245Q, H245R or H245D resulting in an inactive luciferase to measure miscoding of near cognate amino acids. (B-D) *RPS5* wt, *rps5-T38A* and *rps5-T38D* strains harboring the frameshifting (i; B), miscoding (ii; C) and readthrough (iii, D) plasmids were assessed for miscoding events by dual luciferase assay. The Firefly signal was normalized to the Renilla activity and the corresponding ratios of the different reporters normalized to the ratio of a dual luciferase reporter with a readthrough linker and active Firefly. Finally, the resulting ratios were normalized to wild-type (mean ± SD; $n = 6$; ** $p < 0.001$; * $p < 0.05$)

2.3.4 Formation of 48S PICs Is Reduced in the *rps5-T38A* Mutant

To further elucidate the function of Rps5 T38 phosphorylation in translation initiation an *in vitro* translation initiation assay was adapted from Beckmann et al. (2005). In

this assay the incorporation of *in vitro* transcribed [32P] labeled *RPL38* mRNA into translation initiation complexes in translation active extracts was analyzed. The initiation complexes were separated by sucrose density centrifugation followed by scintillation counting of gradient fractions to determine the distribution of the radioactively labeled mRNA. To block elongation the translation initiation reaction was incubated in the presence of cycloheximide. GMP-PNP, a non-hydrolizable GTP analog, was added as indicated preventing the GTP hydrolysis during 60S subunit joining and thus accumulating 48S initiation complexes at the start codon. When only elongation was inhibited by cycloheximide, free mRNPs were accumulating and the 80S peak was significantly reduced in *rps5-T38A* mutant extracts to 84 % of the wild-type extracts (Fig. 2.9 A). In the presence of GMP-PNP, when subunit joining is blocked, the formation of 48S initiation complexes in the *rps5-T38A* mutant extracts was reduced to 77 % of the wild-type while free mRNPs accumulated (Fig. 2.9 B).

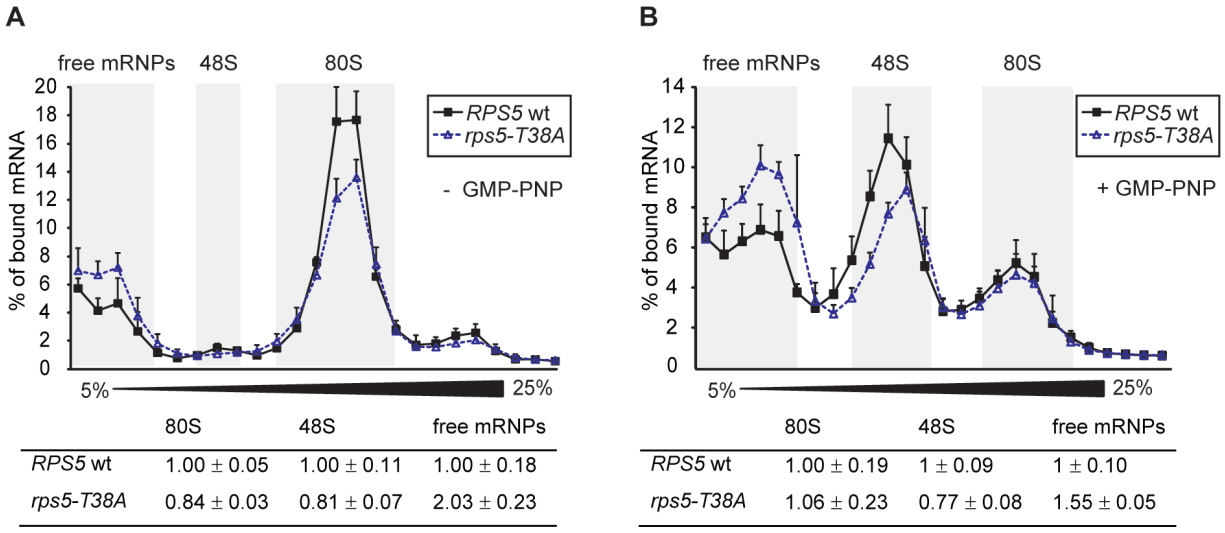

	80S	48S	free mRNPs
RPS5 wt	1.00 ± 0.05	1.00 ± 0.11	1.00 ± 0.18
rps5-T38A	0.84 ± 0.03	0.81 ± 0.07	2.03 ± 0.23

	80S	48S	free mRNPs
RPS5 wt	1.00 ± 0.19	1 ± 0.09	1 ± 0.10
rps5-T38A	1.06 ± 0.23	0.77 ± 0.08	1.55 ± 0.05

Figure 2.9: The *rps5-T38A* mutation causes a decreased 48S PIC formation. (A+B) Incorporation of [32]P labeled *RPL38* mRNA into initiation complexes was analyzed in initiation reactions of translation active extracts. (A) Incorporation of *RPL38* mRNA into initiation complex in the presence of cycloheximide was assessed by sucrose density centrifugation and scintillation counting of gradient fractions. (B) Translation initiation reaction was done in the presence GMP-PNP to accumulate 48S complexes. The fractions containing mRNPs, 48S, and 80S complexes are indicated and the amount of mRNA in each fraction was calculated relative to wild-type (table below; mean ± SD; $n = 3$).

Subsequently, the formation of initiation complexes was assessed *in vivo*. To this end,

the amount of two endogenous mRNAs, *RPL38* and *RPL41A*, associated with native 48S initiation complexes in *rps5-T38A* mutant versus *RPS5* wild-type cells was compared. These two ribosomal mRNAs were chosen due to their high abundance and their relatively short length allowing a good separation of initiation complexes. The cells were treated with cycloheximide to block elongation and initiation complexes were separated by sucrose density centrifugation. The amount of *RPL38* mRNA, *RPL41A* mRNA, and 18S rRNA in each gradient fraction was determined by quantitative reverse transcription real-time PCR (qRT-PCR). In *rps5-T38A* mutant cell the ratio of *RPL38* and *RPL41A* mRNA levels to 18S rRNA was significantly reduced to 50 % (± 16 %) and 52 % (± 21 %), respectively, compared to wild-type cells. Moreover, the pool of free *RPL38* and *RPL41A* mRNA in the mutant was dramatically increased (Fig. 2.10).

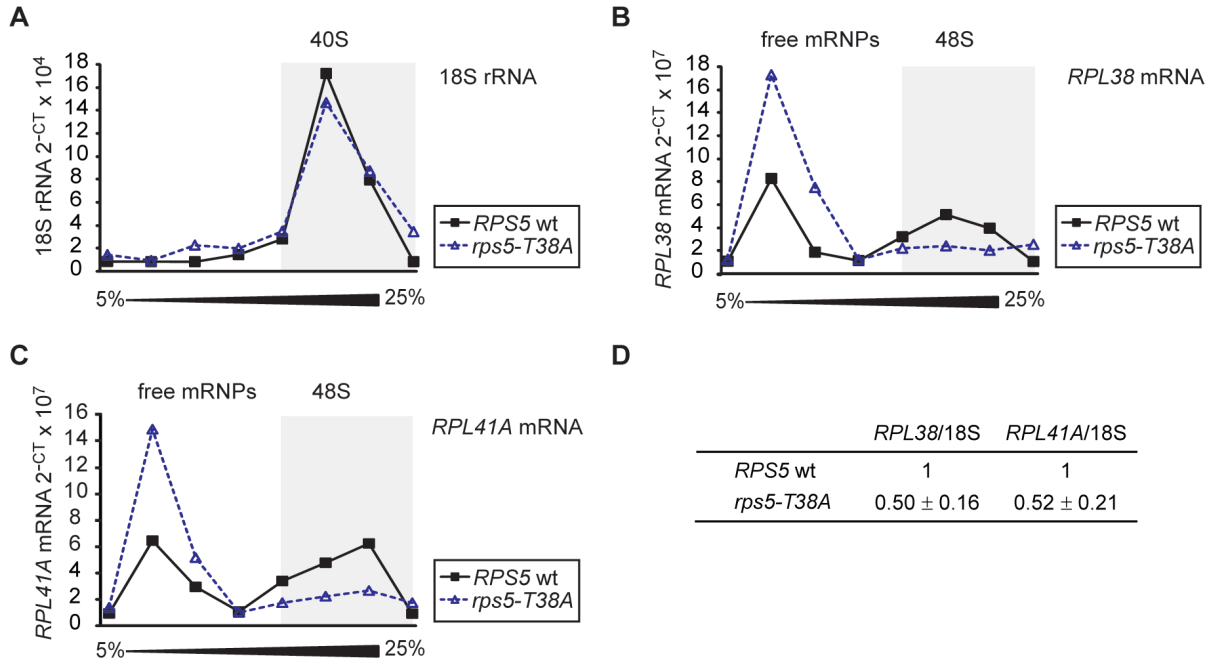

	RPL38/18S	*RPL41A*/18S
RPS5 wt	1	1
rps5-T38A	0.50 ± 0.16	0.52 ± 0.21

Figure 2.10: In *rps5-T38A* mutant cells the association of *RPL38* and *RPL41A* mRNA with 48S PICs is decreased. WCEs of *RPS5* wt and *rps5-T38A* mutant cells were separated by sucrose density centrifugation and total RNA was isolated from each gradient fraction. The amount of 18S rRNA (A), *RPL38* (B) and *RPL41A* (C) mRNA was determined by qRT-PCR using the CT method. One representative example is shown out of four independent experiments. (D) The amount of each mRNA associated with 48S PICs was calculated relative to the 18S rRNA in the indicated fractions an normalized to wt (mean ± SD; $n = 4$).

The 48S PIC is formed during initiation by the recruitment of the mRNA to the pre-assembled 43S complex – 40S subunit associated with eIF1A and the MFC containing

eIF1, eIF3, eIF5 and the ternary complex (TC) – with the help of the cap-binding complex eIF4F (see Section 1.4.1). To assess whether the interplay of all these different translation initiation factors is affected by the loss of Rps5 T38 phosphorylation, the association of several initiation factors with the 40S subunit and 80S/polysomes was investigated. Whole cell extracts form *RPS5* wt and *rps5-T38A* mutant cells were sedimented through sucrose density gradients. To block elongation and stabilize ribosomes bound to mRNAs cycloheximide was added prior to harvesting. The gradient fractions were subjected to Western blot analysis using antibodies against initiation factors and ribosomal proteins as indicated. The signal of each eIF in the 40S or 80S/polysome fractions was normalized to the corresponding Rps8 levels and calculated relative to wild-type (Fig. 2.11). Interestingly, all analyzed translation initiation factors showed an increased and prolonged association with the initiating *rps5-T38A* mutant ribosomes compared to wild-type ribosomes. In the *rps5-T38A* mutant the proper release of initiation factors seems to be impeded during translation initiation. Thus, the phosphorylation of Rps5 T38 seems to be needed for an efficient 48S PIC formation, either directly or indirectly via one or more initiation factors.

2.3.5 Context Dependent Start Codon Recognition Is Impaired in the *rps5-T38A* Mutant

After recruitment of the 43S PIC to the 5' cap of the mRNA, the 43S complex scans along the 5' UTR until it encounters a start codon in the ribosomal P-site. Here, not only the discrimination against non-AUG codons but also the sequence context of the AUG are crucial for efficient start codon selection (see Section 1.4.1).

First, the discrimination between AUG and non-AUG start codons was addressed using the dual luciferase reporter pRaugFFuug encoding AUG-Renilla and UUG-Firefly luciferase reporter mRNAs (Cheung et al., 2007). This reporter plasmid allows to assess in parallel the initiation from AUG and UUG start codons at steady state *in vivo* by dual luciferase measurement. The absolute expression levels of AUG-Renilla and UUG-Firefly luciferase reporter were both reduced in *rps5-T38A* mutant cells compared to *RPS5* wild-type. Interestingly, the effect of the *rps5-T38A* mutation was much stronger on the AUG-Renilla ($33 \pm 11\,\%$) than on the UUG-Firefly reporter ($54 \pm 15\,\%$), thus increasing the UUG vs.

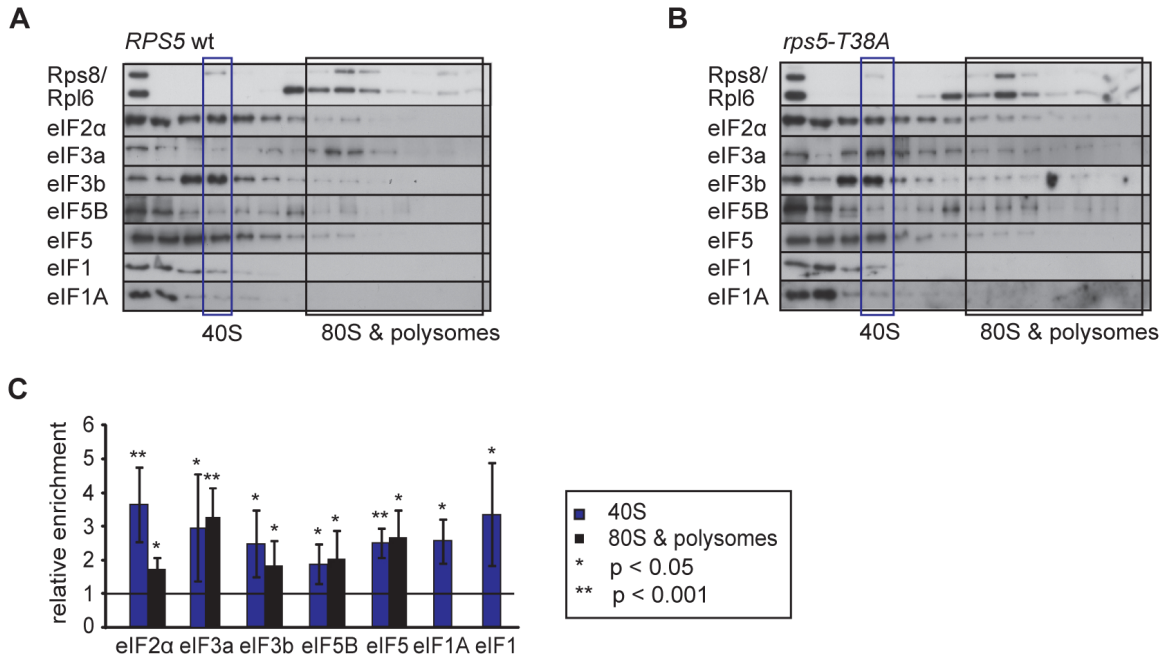

Figure 2.11: The *rps5-T38A* mutation alters the association of initiation factors. (A+B) *RPS5* wt (A) and *rps5-T38A* (B) mutant cells were treated with cycloheximide prior to harvesting. WCEs were separated by sucrose density gradient centrifugation, and gradient fractions were subjected to Western blot analysis using antibodies against the indicated initiation factors and ribosomal proteins. The signal of each eIF in the 40S or 80S/polysomes fractions (boxed) was normalized to the corresponding Rps8 signals. (C) The relative levels of *rps5-T38A* to wild-type were calculated and plotted (mean ± SD; $n = 3$).

AUG ratio almost twofold (Fig. 2.12A). This finding suggests that the *rps5-T38A* mutation impairs start codon recognition *in vivo*.

To assess the discrimination against different start codon consensus sequences *SUI1*-lacZ fusion reporters were used in *rps5-T38A* mutant and *RPS5* wild-type cells (Martin-Marcos et al., 2011). The native poor initiation context of the *SUI1* gene with $_{-3}$CGU-AUG is reported to be unfavorable and to control Sui1 expression via its own function in start codon selection (Ivanov et al., 2010). The poor *SUI1* context was modified to perfectly match the yeast optimal consensus context of $_{-3}$AAA-AUG (*SUI1-opt*-lacZ) and to exacerbate the poor *SUI1* context by introducing $_{-3}$UUU-AUG (*SUI1-UUU*-lacZ) as an even more unfavorable initiation codon context (Fig. 2.13 A) (Shabalina et al., 2004). Since the different reporters encode lacZ fusions the context dependent initiation can be measured by β-galactosidase assay *in vivo* (Miller, 1972). As expected in *RPS5* wild-type cells the *SUI1-opt*-lacZ fusion was expressed more than twice as much as the wild-type *SUI1*-lacZ fusion, whereas the

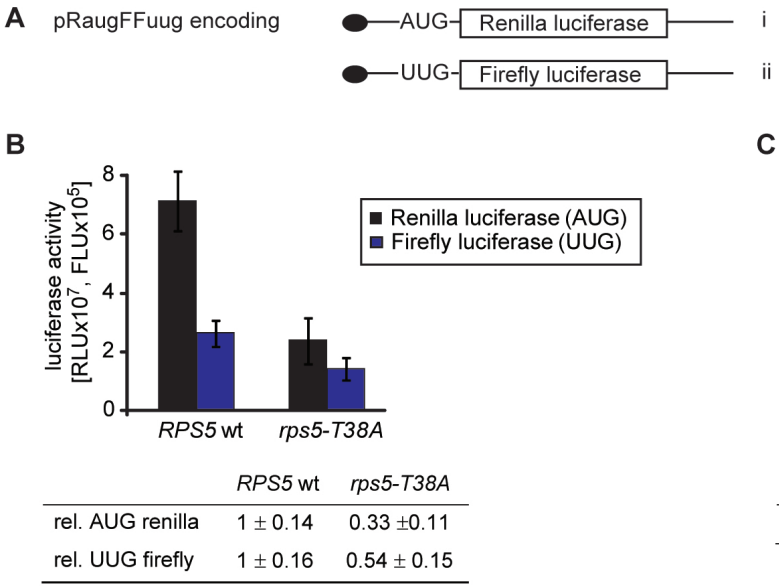

	RPS5 wt	*rps5-T38A*
rel. AUG renilla	1 ± 0.14	0.33 ±0.11
rel. UUG firefly	1 ± 0.16	0.54 ± 0.15

	RPS5 wt	*rps5-T38A*
rel. UUG/AUG	1 ± 0.13	1.91 ± 0.30

Figure 2.12: The *rps5-T38A* mutation leads to increased initiation from non-AUG start codons. (A) Schematic illustration of the dual luciferase reporter pRaugFFuug encoding AUG-Renilla (i) and UUG-Firefly (ii) luciferase. (B) *RPS5* wt and *rps5-T38A* mutant strains harboring the pRaugFFuug plasmid were analyzed by dual luciferase assay. Absolute expression levels of AUG-Renilla [RLU] and UUG-Firefly [FLU] in *RPS5* wt and *rps5-T38A* mutant cells were plotted (graph) and normalized to wild-type (table below; mean ± SD; $n = 4$). (C) Ratios of expression levels of UUG vs. AUG reporter were calculated (graph) and normalized to wild-type levels (table below).

SUI1-UUU-lacZ was expressed at a level 4.4 times below the *SUI1-opt*-lacZ (Fig. 2.12 B). Intriguingly, these differences in the expression level between optimal, poor and highly unfavorable start codon context in *SUI1-opt-*, *SUI1-* and *SUI1-UUU*-lacZ, respectively, was completely lost by the *rps5-T38A* mutation (Fig. 2.12 B). Thus, phosphorylation of Rps5 at T38 is needed for the discrimination between good and poor start codon context.

A powerful assay to investigate scanning processivity was developed by Berthelot et al. using a series of Firefly luciferase encoding constructs with 5' UTRs that range in their length between the 5'cap and the start codon from 43 to 607 nucleotides (Fig. 2.14 A) (Berthelot et al., 2004). The *in vitro* transcribed mRNAs were translated in extracts of *RPS5* wt and *rps5-T38A* mutant cells. The time 40S subunits need to locate the start codon was estimated by comparing the time courses of protein synthesis observed with the mRNAs carrying the different length of 5' UTR. Considering the different delay times

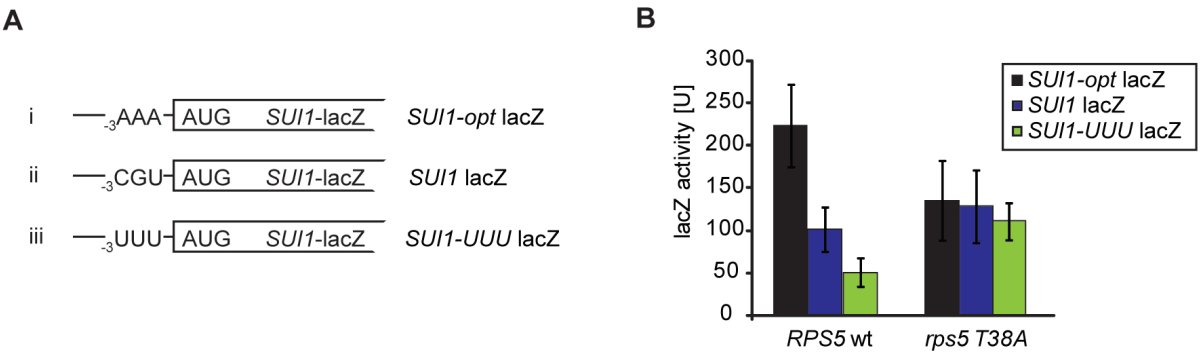

	RPS5 wt	*rps5-T38A*
SUI1-opt lacZ/ *SUI1*-lacZ	2.22	1.06
SUI1-opt lacZ/ *SUI1-UUU* lacZ	4.41	1.22

Figure 2.13: The *rps5-T38A* mutation eliminates discrimination between different AUG context sequences in *SUI1*-lacZ reporters. (A) Representation of different *SUI1*-lacZ reporter plasmids: (i) wild-type *SUI1* context; (ii) optimal consensus sequence *SUI1-opt*-lacZ and (iii) highly unfavorable context *SUI1-UUU*-lacZ. (B) Expression of different *SUI1*-lacZ reporter plasmids depicted in (A) in *RPS5* wt and *rps5-T38A* mutant cells was measured by β-galactosidase activity (miller units U). Ratios of *SUI1-opt*-lacZ/ *SUI1*-lacZ or *SUI1-opt*-lacZ/ *SUI1-UUU*-lacZ were calculated (table below; mean $\pm$ SD; $n = 4$).

for different length eliminated the contribution of the early, undefined phase of loading and activation of scanning competent 40S subunits (Lorsch and Herschlag, 1999). The comparison between the time courses of luciferase synthesis in *RPS5* wt and *rps5-T38A* mutant translation active extracts showed that the *rps5-T38A* mutant ribosomes need almost one minute longer to pass the early, undefined phase (Fig. 2.14 B). However, the *rps5-T38A* mutant ribosomes have the same *in vitro* scanning rate as *RPS5* wild-type ribosomes of approximately 9 nucleotides per second (Fig. 2.14 B). Thus, the *rps5-T38A* mutation does not confer a scanning processivity defect.

Taken together, the *rps5-T38A* mutation impairs context dependent start codon recognition and increases initiation from non-AUG codons *in vivo*.

2.3.6 The *rps5-T38A* Mutation Influences Growth under Different Conditions

Protein phosphorylation is one of the most important posttranslational modifications and allows rapid adaptation to changing environmental conditions. To elucidate the

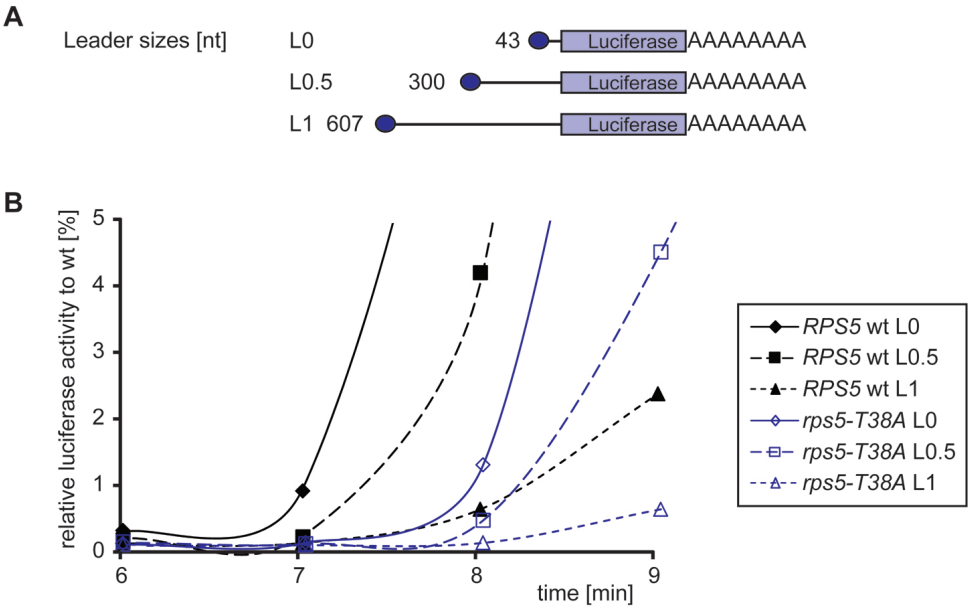

C

	leader	time [min]	scanning rate [nt/sec]
RPS5 wt	L0	6.1	9.7 ± 4.9
	L0.5	6.6	
	L1	7.1	
rps5-T38A	L0	7	9.2 ± 1.2
	L0.5	7.5	
	L1	8	

Figure 2.14: In *rps5-T38A* mutant cells scanning processivity is unaffected. (A) Illustration of *in vitro* transcribed 5' UTR leader luciferase mRNA reporters of various lengths L0, L0.5 and L1 with respective length in nucleotides given. (B) Time dependent analysis of luciferase generation in *in vitro* translation active extracts of *RPS5* wt and *rps5-T38A* mutant cells. The *in vitro* transcribed capped luciferase mRNAs depicted in (A) were translated and luciferase activity measured at the indicated time points (5 to 9 min). One representative example out of three independent experiments is shown. (C) Estimates of delay time of different length 5' UTRs and the resulting scanning rate for *RPS5* wt and *rps5-T38A* mutant extracts are shown (mean ± SD; $n = 3$).

physiological relevance of the Rps5 T38 phosphorylation, the growth of *rps5-T38A* and *RPS5* wt cells was analyzed using microcultivation in liquid cultures in a Bioscreen C Analyzer. The optical density was recorded every 20 min over two days. The obtained growth curves were corrected for non-linearity at stationary phase growth and doubling times were calculated as described by Warringer and Blomberg (2003). Under the majority of tested growth conditions like high salinity, osmotic stress, heat and cold, unfolded protein

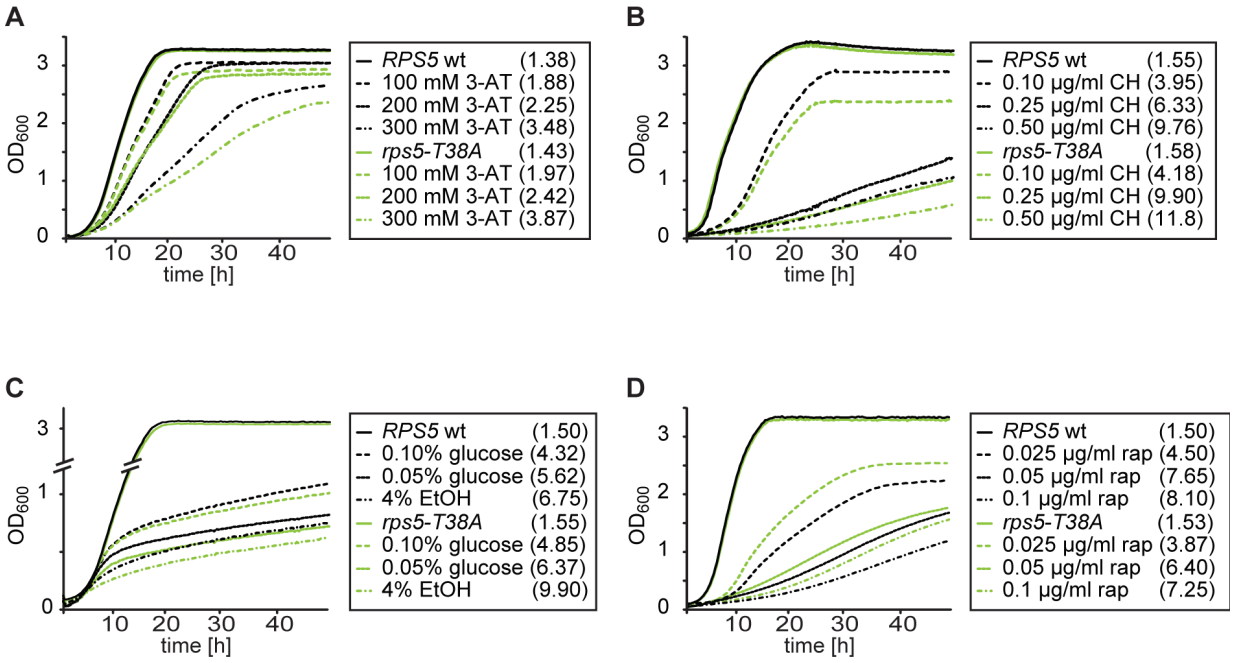

Figure 2.15: In *rps5-T38A* mutant cells growth is affected under different conditions. Growth of *rps5-T38A* and *RPS5* wt cells was recorded for two days in a Bioscreen Analyzer C under different conditions: (A) 3-aminotriazol (3-AT; 100, 200, and 300 mM), (B) cycloheximide (CH; 0.1, 0.25, and 0.5 µg/ml), (C) 0.1 and 0.05 % glucose or 4 % ethanol (in SC without glucose), (D) rapamycin (rap; 0.025, 0.05, and 0.1 µg/ml). Doubling times in hours are given in brackets. All experiments were carried out using two independent spores in triplicates. The observed OD values were corrected for the non-linearity at higher cell densities and doubling times were calculated according to Warringer and Blomberg (2003) (see Section 4.2.13).

response and several translation inhibitors, *rps5-T38A* and *RPS5* wt cells showed the same growth pattern. Interestingly, the *rps5-T38A* mutant cells showed a slightly increased sensitivity to the drug 3-aminotriazole (3-AT) compared to *RPS5* wt cells (Fig. 2.15 A). 3-AT inhibits the synthesis of the amino acid histidine thus starving the cells for this amino acid.

In addition, the *rps5-T38A* mutation causes an increased sensitivity to the translation inhibitor cycloheximide (CH) which inhibits translation elongation by binding to the ribosomal E-site and blocking the translocation step (Fig. 2.15 B) (Loewith and Hall, 2011). Moreover, growth under reduced glucose concentrations or ethanol as carbon source was slightly impaired in the *rps5-T38A* mutant cells compared to *RPS5* wt (Fig. 2.15 C). Surprisingly, the *rps5-T38A* mutant cells were less sensitive to the drug rapamycin (Fig. 2.15 D). Rapamycin is an inhibitor of the conserved Ser/Thr kinase TOR which

regulates cell growth and metabolism in response to environmental causes (Wullschleger et al., 2006; Altmann and Linder, 2010). TOR regulates translation via the kinase S6K and the 4E-BPs. Phosphorylation of 4E-BPs by TOR leads to their dissociation from eIF4E thus promoting cap-dependent translation initiation (see Section 1.4.3).
The *rps5-T38A* mutation causes a growth defect under specific conditions like reduced availability of energy sources and amino acids or in the presence of cycloheximide blocking translation elongation, growth is impaired compared to wild-type. In contrast, the *rps5-T38A* mutant cells are more resistant to rapamycin. Concluding, the loss of Rps5 T38 phosphorylation has an influence on the growth and fitness under specific conditions, thus providing a physiological relevance of this phosphorylation site.

2.4 Rps12 T23 Phosphorylation Affects Scanning

In the general phosphoproteomic survey of *Saccharomyces cerevisiae* ribosomal proteins two sites on the small ribosomal protein Rps12 were identified, namely Rps12 T19 and T23. So far, nothing is reported in the literature about Rps12 except its localization at the mRNA entry channel determined recently by crystallography ((Rabl et al., 2011; Ben-Shem et al., 2011), see also Fig. 3.4). Both phospho-deficient A mutants were assessed for their translation activity *in vitro*. However, only the *rps12-T23A* mutation caused a translation defect.

2.4.1 In *rps12-T23A* Mutant Cells Cap-Dependent Translation Is Impaired

The translation activity of the phospho-deficient *rps12-T23A* mutant extracts to translate the capped mRNA was reduced to 56 % (± 13 %) of the corresponding *RPS12* wild-type cells. In contrast, the translation activity of the *rps12-T23A* mutant extracts to translate the CrPV IRES containing mRNA resembled wild-type levels indicating that only cap-dependent translation is affected (Fig. 2.16 A).
There was no difference in the translation activity of the phospho-mimicry *rps12-T23D* mutant extracts to translate the capped and the CrPV IRES containing mRNA compared

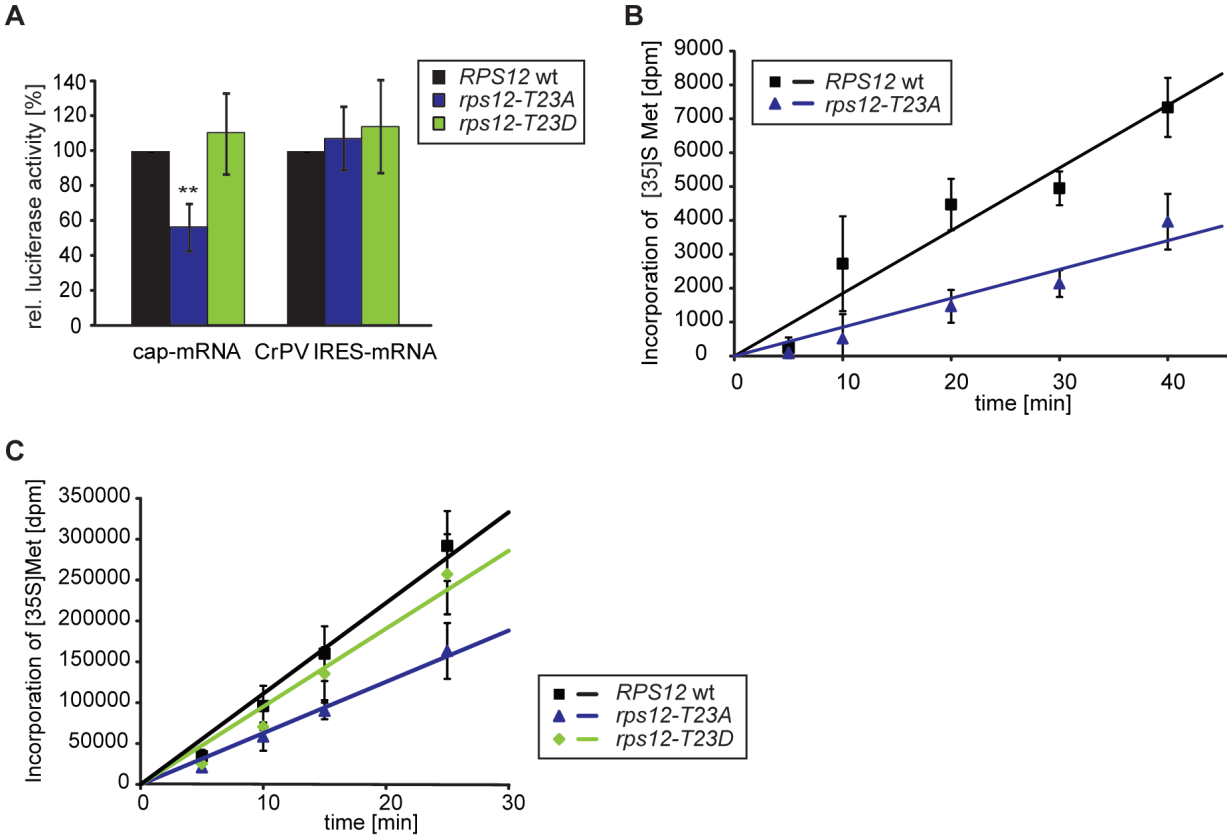

Figure 2.16: The *rps12-T23A* mutation causes a cap-dependent translation defect. (A) Translation activity of translation active extracts from *RPS12* wt, *rps12-T23A* and *rps12-T23D* mutant cells for the capped and CrPV IRES luciferase mRNA reporters was analyzed by luciferase measurement as in Fig. 2.4 A. (B) Translation activity of translation active extracts of *RPS12* wt and *rps12-T23A* mutant cells to translate endogenous mRNAs was assessed *in vitro* using [35S] Met to label synthesized proteins. Experiment performed as in Fig. 2.4 B. (C) The *rps12-T23A* mutation caused a decrease in *de novo* protein synthesis compared to wild-type cells measured by incorporation of [35S] Met into newly synthesized proteins. Experiment performed as in Fig. 2.4 C.

to *RPS12* wt extracts (Fig. 2.16 A). In addition to the two exogenous mRNA reporters, the translation activity of *in vitro* translation active extracts to translate endogenous mRNAs was analyzed in time-dependent protein synthesis using [35S] methionine. In *rps12-T23A* mutant extracts the activity to translate endogenous mRNAs was reduced to 70 % of the wild-type activity (Fig. 2.16 B). Thus, the translation defect of the *rps12-T23A* mutant is not dependent on the mRNA used to asses the translation activity *in vitro*.

Using [35S] methionine labeling to measure *de novo* protein synthesis the *rps12-T23A* mutation caused a reduced translation activity *in vivo* to 70 % of the wild-type whereas the phospho-mimicry *rps12-T23D* showed almost wild-type levels (Fig. 2.16 C).

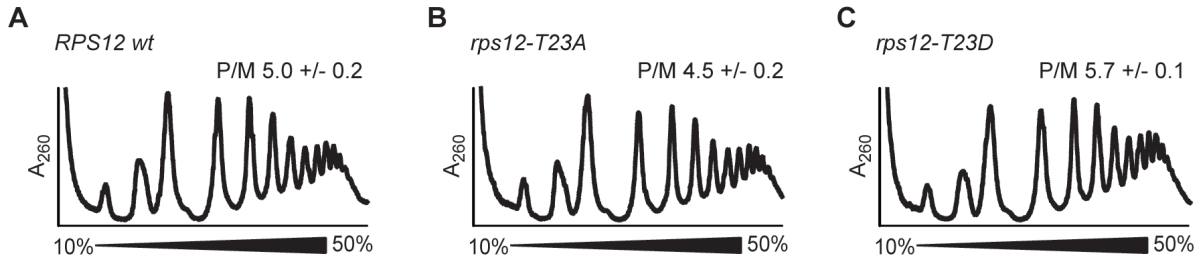

Figure 2.17: The *rps12-T23A* mutation causes decreased P/M ratio. (A-C) WCEs of *RPS12* wt (A), *rps12-T23A* (B) and *rps12-T23D* (C) strains were separated on 10-50 % sucrose gradients and the absorption at 260 nm was measured. The P/M ratio was calculated by integrating the area under the respective peaks after substraction of the baseline (mean ± SD; $n = 4$).

As expected, the decreased cap-dependent translation activity of the *rps12-T23A* mutant resulted in a slight reduction of the P/M ratio in polysome gradient profiles compared to wild-type whereas the *rps12-T23D* mutant showed an even slightly increased P/M ratio (Fig. 2.17). Importantly, the observed translation initiation defect in *rps12-T23A* cells was not caused by lower levels of Rps12 itself or ribosomal subunits as was shown by Western blot analysis of WCEs of *RPS12* wt, *rps12-T23A* and *rps12-T23D* mutant cells using the indicated antibodies (Fig. 2.18).

In summary, Rps12 T23 phosphorylation is needed for efficient translation initiation.

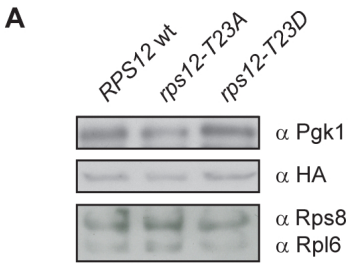

B

rel. levels	*RPS12* wt	*rps12-T23A*	*rps12-T23D*
HA-Rps12	1	1.05± 0.19	0.92± 0.17
Rpl6	1	1.17± 0.14	1.16± 0.20
Rps8	1	1.23± 0.24	1.08± 0.21

Figure 2.18: Both *RPS12* phospho-mutants do not affect ribosomal protein levels. WCEs of either *RPS12* wt, *rps12-T23A* or *rps12-T23D* (as N-terminal 3HA fusions) were analyzed by Western blot using antibodies against Pgk1, HA, Rpl6 and Rps8. HA, Rpl6 and Rps8 signals were normalized to the corresponding Pgk1 signals and protein levels calculated relative to wild-type (mean ± SD; $n = 4$).

2.4.2 The *rps12-T23A* Mutation Does Not Influence Translation Fidelity

Although the obtained data suggests that the *rps12-T23A* mutation causes a translation initiation defect, elongation was assessed independent of initiation using the poly(U) assay (performed by Viter Marquez). The elongation rate was determined by measuring the time-dependent incorporation of [14C] phenylalanine into poly-F peptides, while the translation fidelity was assessed by measuring the incorporation of near-cognate [3H] leucine. There was no elongation or translation fidelity defect detectable for the *rps12-T23A* mutant compared to wild-type cells *in vitro* (Fig. 2.19).

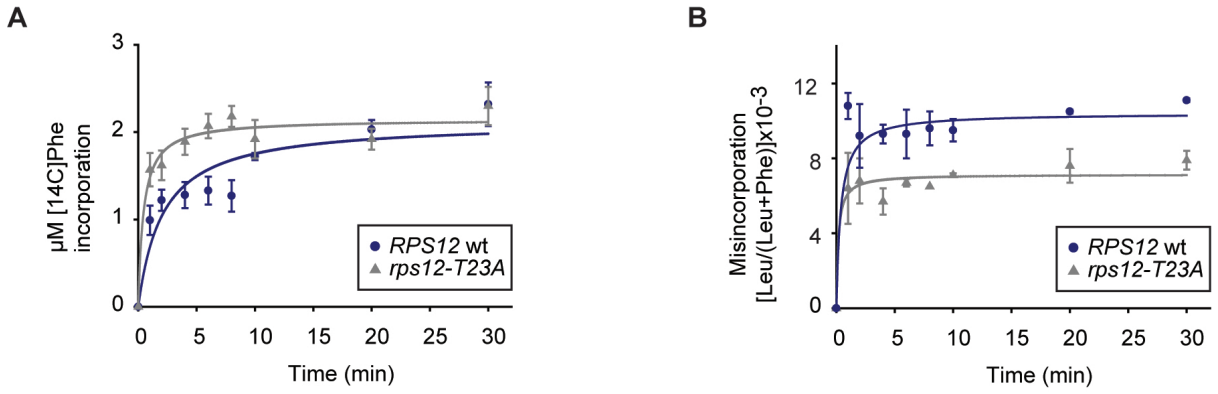

Figure 2.19: The *rps12-T23A* mutant cells have no translation fidelity defect *in vitro*. (A) The time dependent incorporation of [14C] F into polypeptides in *RPS12* wt and *rps12-T23A* mutant translation active extracts was determined by scintillation counting (mean ± SD; $n = 3$). (B) In translation active extracts of *RPS12* wt and *rps12-T23A* mutant cells the incorporation of near-cognate [3H] L relative to F incorporation was determined at the indicated time points (mean ± SD; $n = 3$).

In order to assess translation fidelity of the *rps12-T23A* mutant cells *in vivo*, different dual luciferase reporters (see Section 2.3.3 and Fig. 2.8 A) were used to measure frameshifting, readthrough and misincorporation rates. The *rps12-T23A* mutant did not affect frameshifting and readthrough of stop codons compared to wild-type (Fig. 2.20 A, B). Only misincorporation of near-cognate amino acids was slightly affected – with the H245Q mutation reporter *rps12-T23A* cells showing a hyperacurate phenotype while the H245D mutation caused an increased misincorporation (Fig. 2.20 C). However, the observed effect was to small to explain the translation defect observed in the previous experiments. Thus, the translation defect of the *rps12-T23A* mutant cells must be caused by a different step

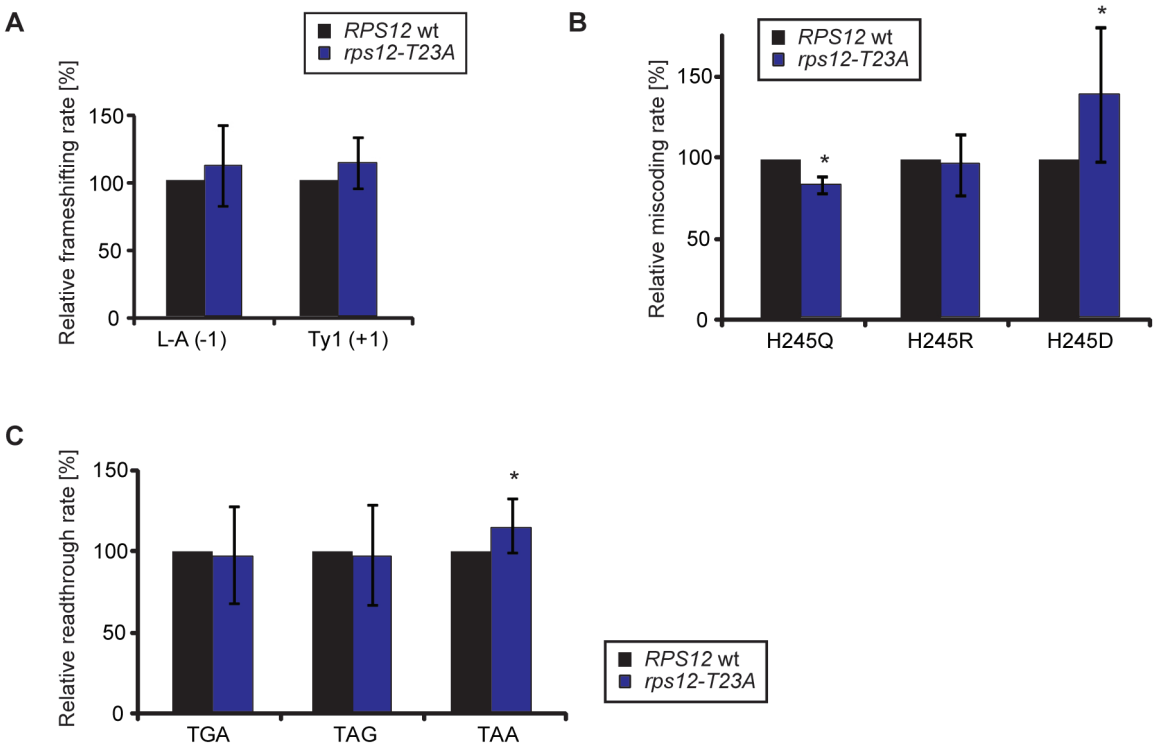

Figure 2.20: Translation fidelity is unaffected in *rps12-T23A* mutant cells in *in vivo*. (A-C) *RPS12* wt and *rps12-T23A* mutant strains harboring the frameshifting (A), miscoding (B) and readthrough (C) plasmids depicted in Fig. 2.8 A were assessed for miscoding events by dual luciferase assay. The different miscoding rates were calculated as in Fig. 2.8 (mean ± SD; $n = 6$; * $p < 0.05$).

in translation, most likely during translation initiation.

2.4.3 The *rps12-T23A* Mutation Causes Decreased Initiation Complex Formation

Having first indications that Rps12 T23 phosphorylation is needed for efficient canonical translation initiation, the step of translation initiation Rps12 T23 phosphorylation functions in should be elucidated. To this end, the incorporation of *in vitro* transcribed [32P] labeled *RPL38* mRNA into initiation complexes of *rps12-T23A* mutant and *RPS12* wt translation active extracts was analyzed as described in Section 2.3.4. When elongation was blocked by the addition of cycloheximide 80S initiation complexes were decreased in extracts of the *rps12-T23A* mutant to 87 % (±7 %) of *RPS12* wt extracts (Fig. 2.21 A). Moreover, a reduction of 80S initiation complexes in the *rps12-T23A* mutant extracts to

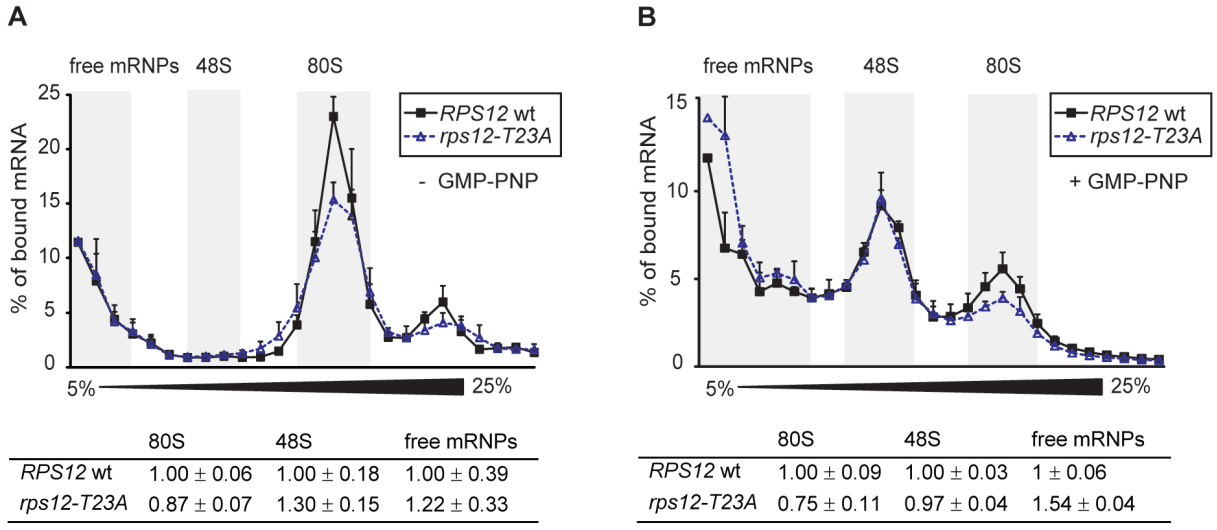

	80S	48S	free mRNPs
RPS12 wt	1.00 ± 0.06	1.00 ± 0.18	1.00 ± 0.39
rps12-T23A	0.87 ± 0.07	1.30 ± 0.15	1.22 ± 0.33

	80S	48S	free mRNPs
RPS12 wt	1.00 ± 0.09	1.00 ± 0.03	1 ± 0.06
rps12-T23A	0.75 ± 0.11	0.97 ± 0.04	1.54 ± 0.04

Figure 2.21: In *rps12-T23A* mutant cells the formation of 80S initiation complexes is affected. (A+B) Translation initiation assays of *RPS12* wild-type and *rps12-T23A* mutant translation active extracts was performed in the presence of cycloheximide (A) and additional GMP-PNP (B) as described in Fig. 2.9.

75 % (±11 %) was also observed in the presence of GMP-PNP blocking 60S subunit joining. 48S PIC formation was not affected, but free mRNPs accumulated (Fig. 2.21 B). This result suggests that the formation of 80S initiation complexes is affected in *rps12-T23A* mutant translation active extracts *in vitro*.

Interestingly, *in vivo* the 48S PIC formation is affected by the *rps12-T23A* mutation. The ratio of *RPL38* and *RPL41A* mRNA to 18S rRNA was significantly reduced to 35 % (±22 %) and 45 % (±34 %), respectively, comparing *rps12-T23A* mutant to wild-type cells (Fig. 2.22, also see Section 2.3.4). Moreover, *rps12-T23A* and wild-type cells differed in their distribution of *RPL38* and *RPL41A* mRNA – in the mutant the amount of mRNAs incorporated into 48S initiation complexes was diminished while free mRNPs were increased. This difference between the *in vitro* initiation assay with reduced 80S formation and the *in vivo* observed reduction of 48S PIC might be due to the stability of (scanning) 43S complexes on the mRNA. It is generally believed that 43S complexes scanning along the mRNA are only stably bound to the mRNA after start codon recognition (see Section 1.4.1). In the *in vivo* experiment, the 48S complexes could fall apart during extract preparation whereas they are formed *de novo* in the *in vitro* assay. Alternatively, the *rps12-T23A* mutation leads to a defect in 48S complex formation that is not detectable in the *in vitro* initiation assay or causes two independent defects in 48S as well as 80S

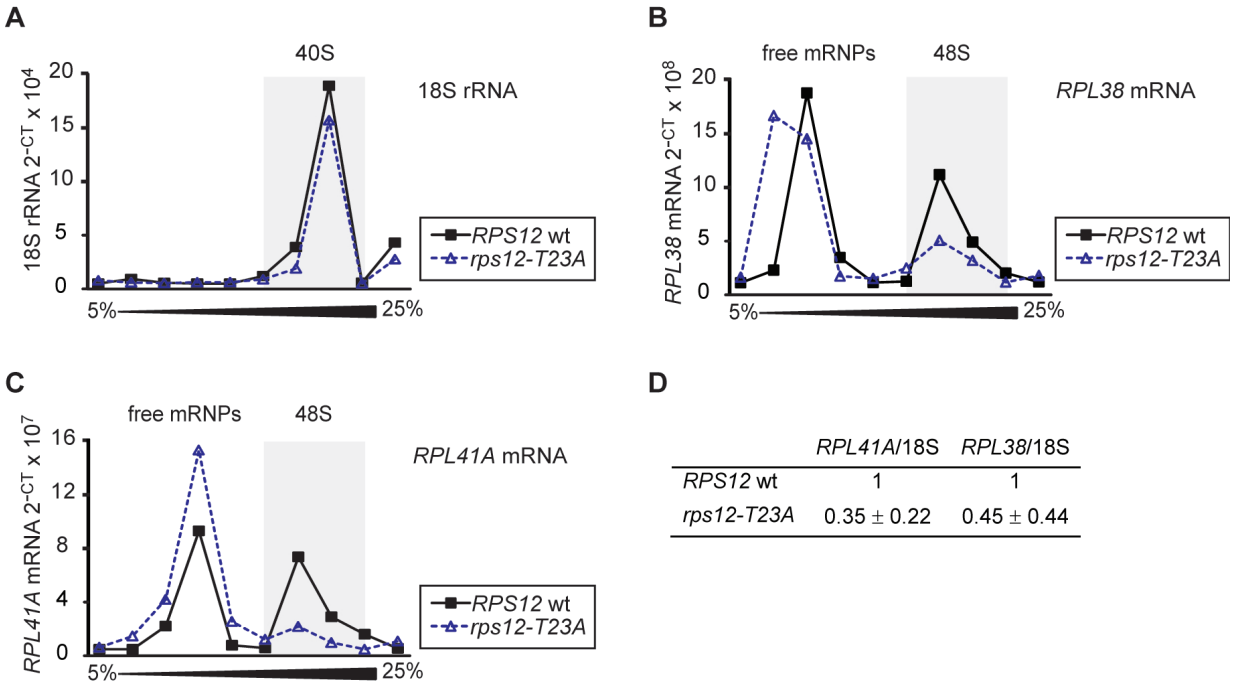

Figure 2.22: The *rps12-T23A* mutation causes a decrease in 48S PIC formation *in vivo*. In *RPS12* wt and *rps12-T23A* mutant WCEs 18S rRNA (A), *RPL38* (B) and *RPL41A* (C) mRNA was determined by qRT-PCR. Experiment as in Fig. 2.10 (mean ± SD; $n = 4$).

formation that are detected in either assay.

In addition, an alteration in the association and release of translation initiation factors from *rps12-T23A* mutant ribosomes compared to *RPS12* wt ribosomes was observed using Western blot analysis of gradient fractions and antibodies against several initiation factors (Fig. 2.23). Components of eIF1, eIF1A, eIF3, and eIF5B are more tightly associated with the *rps12-T23A* mutant 40S subunit compared to wild-type. Furthermore, eIF2α, eIF3, eIF5 and eIF5B remain associated longer with the initiating and elongating mutant 80S ribosomes. Thus, the *rps12-T23A* mutation impairs the proper release of initiation factors during translation initiation and the formation and/or stability of translation initiation complexes.

2.4.4 Scanning Processivity Is Reduced in *rps12-T23A* Mutant Cells

The decreased formation of translation initiation complexes might be due to a reduced processivity and stability of scanning 43S complexes on the mRNA. To assess the scanning

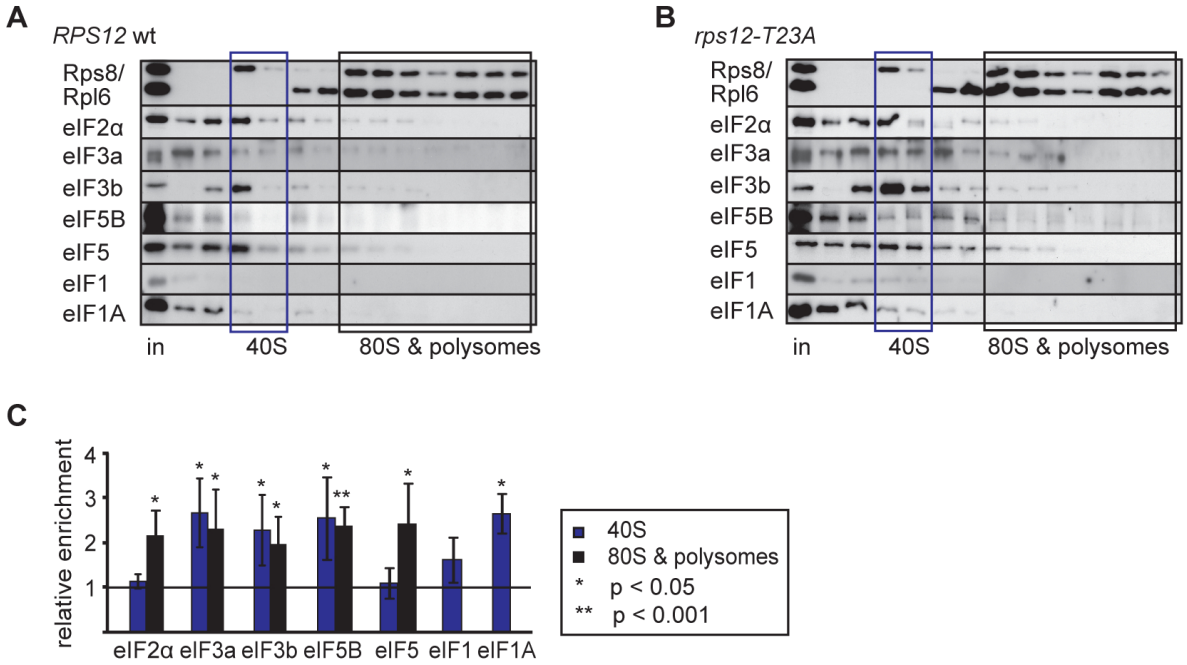

Figure 2.23: In *rps12-T23A* mutant cells the association of initiation factors is altered. (A+B) Gradient fractions of *RPS12* wt (A) and *rps12-T23A* mutant (B) were subjected to Western blot analysis using antibodies against the indicated initiation factors and ribosomal proteins. Experiment as in Fig. 2.11. (C) The relative levels of *rps12-T23A* to *RPS12* wt were calculated and plotted (mean ± SD; $n = 3$).

rate in *rps12-T23A* mutant cells, the scanning processivity assay described by Berthelot et al. (see Section 2.3.5) was used to determine the rate of scanning *in vitro*. The different *in vitro* transcribed luciferase mRNA constructs were translated in either wild-type or *rps12-T23A* mutant translation active extracts and the scanning rates of wild-type and mutant ribosomes were estimated (Fig. 2.24). For the wild-type a delay of about 30 to 40 seconds for 300 nt was observed indicating that wild-type ribosomes have an average scanning rate of approximately 8.6 nt per second. The *rps12-T23A* mutant ribosomes need roughly one minute for 300 nt resulting in a scanning rate of around 4.7 nt per second. Thus, the initial delay time differs between the wild-type and *rps12-T23A* mutant extracts from 5.5 min to 6 min which is not only due to the slower scanning of the mutant but might also be the result of problems in assembling and activating the scanning competent 48S complex (Lorsch and Herschlag, 1999). In translation active extracts the phospho-deficient *rps12-T23A* mutant ribosomes have a decreased scanning processivity compared to wild-type ribosomes.

A

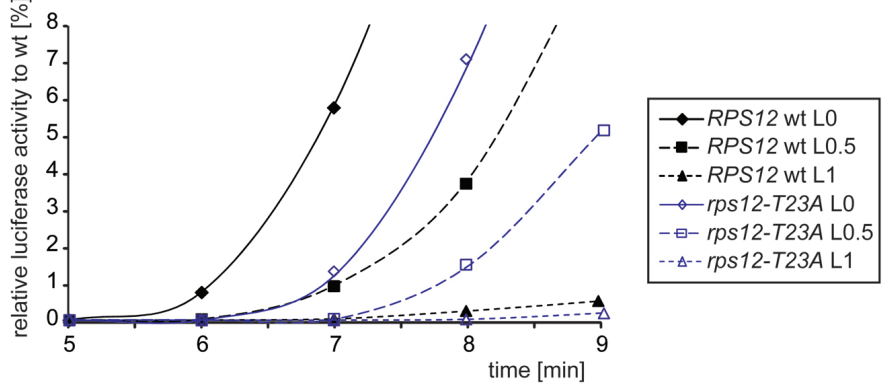

B

	leader	time [min]	scanning rate [nt/sec]
RPS12 wt	L0	5.5	8.6 ± 0.1
	L0.5	6	
	L1	6.7	
rps12-TA23	L0	6	4.7 ± 0.3
	L0.5	7	
	L1	8	

Figure 2.24: In translation active extracts of the *rps12-T23A* mutant scanning processivity is reduced. (A) Time dependent analysis of luciferase generation in *in vitro* translation active extracts of *RPS12* wt and *rps12-T23A* mutant cells. The *in vitro* transcribed capped luciferase mRNAs depicted in Fig. 2.14A were translated and luciferase activity measured at the indicated time points (5 to 9 minutes). One representative example out of four independent experiments is shown. (B) Estimates of delay time of different length of 5' UTRs and the resulting scanning rate for *RPS12* wt and *rps12-T23A* mutant extracts are shown (mean ± SD; $n = 4$).

In order to assess other steps in translation initiation that might be affected in the *rps12-T23A* mutant strain the ratio of UUG vs. AUG start codon translation was measured using the dual luciferase reporter pRaugFFuug. The *rps12-T23A* mutation does not increase the initiation from UUG start codons compared to wild-type (Fig. 2.25 A). Furthermore, *rps12-T23A* mutant ribosomes were also capable to discriminate against poor AUG context sequences in the *SUI1*-lacZ constructs like wild-type cells (Fig. 2.25 B). Taken together, the inability to phosphorylate Rps12 on T23 leads to a reduced processivity of the scanning 43S complex on the mRNA, resulting in a reduction of initiation complexes

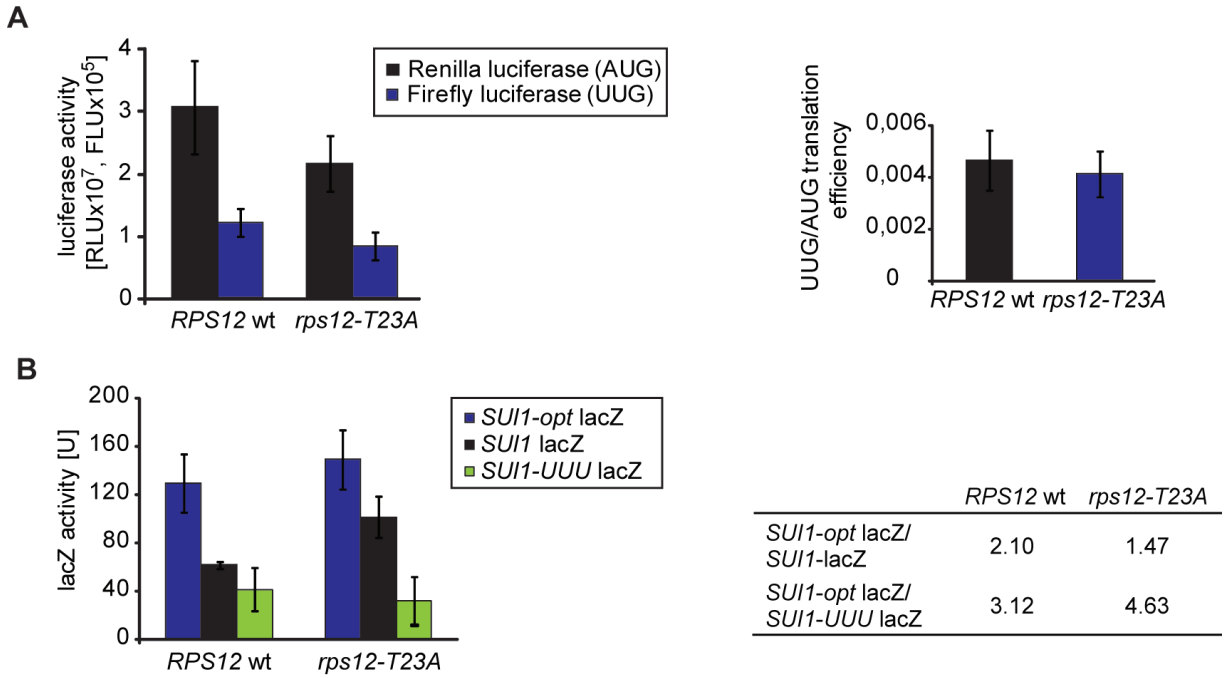

	RPS12 wt	*rps12-T23A*
SUI1-opt lacZ/ *SUI1*-lacZ	2.10	1.47
SUI1-opt lacZ/ *SUI1-UUU* lacZ	3.12	4.63

Figure 2.25: The *rps12-T23A* mutation has no effect on start codon recognition. (A) *rps12-T23A* mutant and *RPS12* wt cells have the same UUG/AUG ratio. *RPS12* wt and *rps12-T23A* mutant strains harboring the pRaugFFuug plasmid were assessed by dual luciferase assay as in Fig. 2.12. (left) Absolute expression levels of AUG-Renilla and UUG-Firefly in the *RPS12* wt and *rps12-T23A* cells were plotted (mean ± SD; $n = 4$). (right) Ratios of expression of UUG versus AUG reporter were calculated. (B) *rps12-T23A* mutation discriminates between different AUG context sequences in *SUI1*-lacZ reporters. Expression of reporter plasmids in *RPS12* wt and *rps12-T23A* mutant cells was measured by β-galactosidase assay as in Fig. 2.13 (mean ± SD; $n = 4$).

like 48S and 80S initiation complexes that are formed at a later stage of translation initiation.

2.4.5 In *rps12-T23A* Mutant Cells the Growth Is Impaired under Specific Conditions

To investigate the physiological role of Rps12 T23 phosphorylation the growth of *rps12-T23A* and *RPS12* wt cells under different conditions was measured using microcultivation in a Bioscreen C Analyzer. The *rps12-T23A* mutant cells grew like *RPS12* wt cells under normal growth conditions. However, the *rps12-T23A* mutant cells showed a slightly increased sensitivity to the elongation inhibitor cycloheximide and the inhibitor of the TOR signaling pathway rapamycin (Fig. 2.26 A+B). Moreover,

the *rps12-T23A* mutant cells could not metabolize ethanol as the only carbon source as well as *RPS12* wt cells (Fig. 2.26 C). In the presence of tunicamycin, the growth of the *rps12-T23A* mutant cells was more reduced in comparison to *RPS12* wt cells (Fig. 2.26 D). Tunicamycin, a mixture of homologous nucleoside antibiotics, inhibits the N-linked glycosylation of nascent proteins in the endoplasmic reticulum (ER) causing protein misfolding and activation of the unfolded protein response (UPR). Taken together, the growth of *rps12-T23A* mutant cells is more severely affected than the growth of *RPS12* wt cells under specific conditions, thus indicating that the phosphorylation of Rps12 T23 is important under specific circumstances.

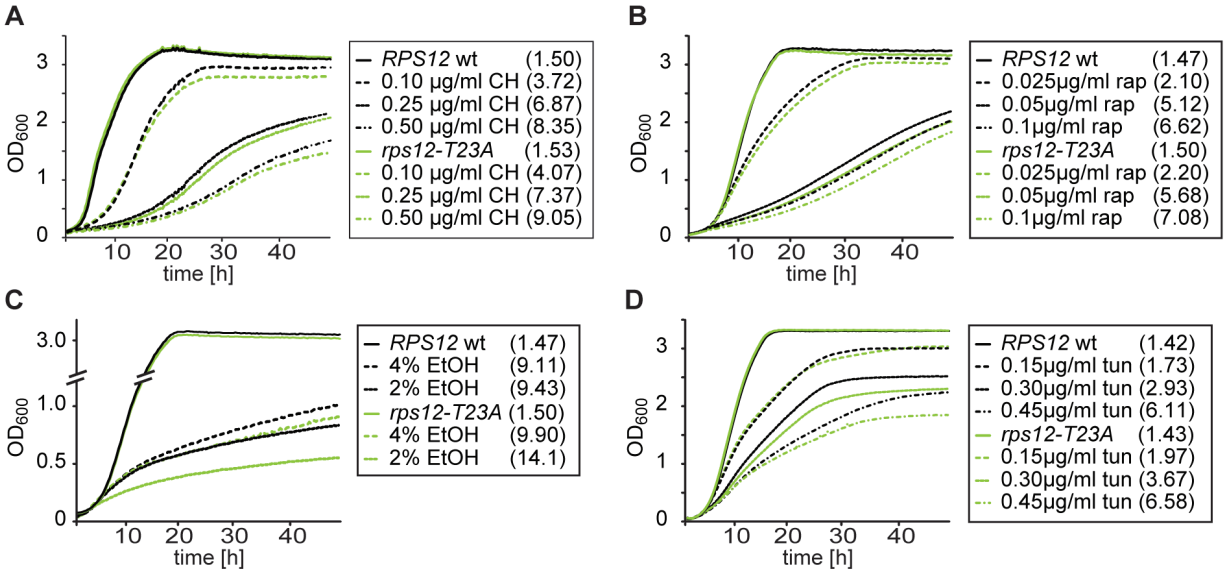

Figure 2.26: The *rps12-T23A* mutation influences growth under different conditions. Growth of *rps12-T23A* and *RPS12* wt cells was measured under the following conditions: (A) cycloheximide (CH; 0.1, 0.25, and 0.5 µg/ml), (B) rapamycin (rap; 0.025, 0.05, and 0.1 µg/ml), (C) ethanol (2 and 4 % in SC without glucose), (D) tunicamycin (tun; 0.15, 0.3, and 0.45 µg/ml). Doubling times in hours are given in brackets. Experiment as in Fig. 2.15.

3 Discussion

3.1 Phosphorylation of Ribosomal Proteins

Protein phosphorylation is one of the most important posttranslational modifications and allows for rapid adaptation to changing environmental conditions. Almost all cellular processes including translation are regulated by phosphorylation. However, very little is known about the phosphorylation of ribosomal proteins and its function in translation. Therefore it is of major interest to gain an overview of ribosomal phosphorylation and a deeper understanding of its function in translation.

In this study, subsequent centrifugation steps under phosphorylation conserving conditions in combination with phosphoenrichment and LC-MS/MS were used to generate a comprehensive inventory of *Saccharomyces cerevisiae* ribosomal phosphorylation sites. As expected, the majority of ribosomal proteins are phosphorylated at steady-state *in vivo*. In total 279 phosphorylation sites were identified – importantly, 122 novel ones. Eukaryotic ribosomes are highly phosphorylated with 84 % of the ribosomal proteins possessing at least one phosphorylation site compared to 70 % of proteins being phosphorylated in Hela S3 cells (Olsen et al., 2010). The phosphorylation sites identified in two previous phosphoproteomic studies, summarized in the databases PHOSIDA and PhosphoPep, are partially overlapping with the set of phosphosites identified in this study, but contain less ribosomal phosphosites. This is most likely due to the fact that here ribosomal proteins were enriched whereas both other approaches aimed to identify phosphosites on all cellular proteins of yeast cell extracts (Gnad et al., 2007, 2009; Bodenmiller et al., 2007, 2008). Moreover, Bodenmiller et al. used different peptide preparation and enrichment techniques, thus making it possible to detect different phosphorylation sites. Since the number of identifiable phosphosites depends on the enrichment technique and peptide preparation, most likely even more ribosomal

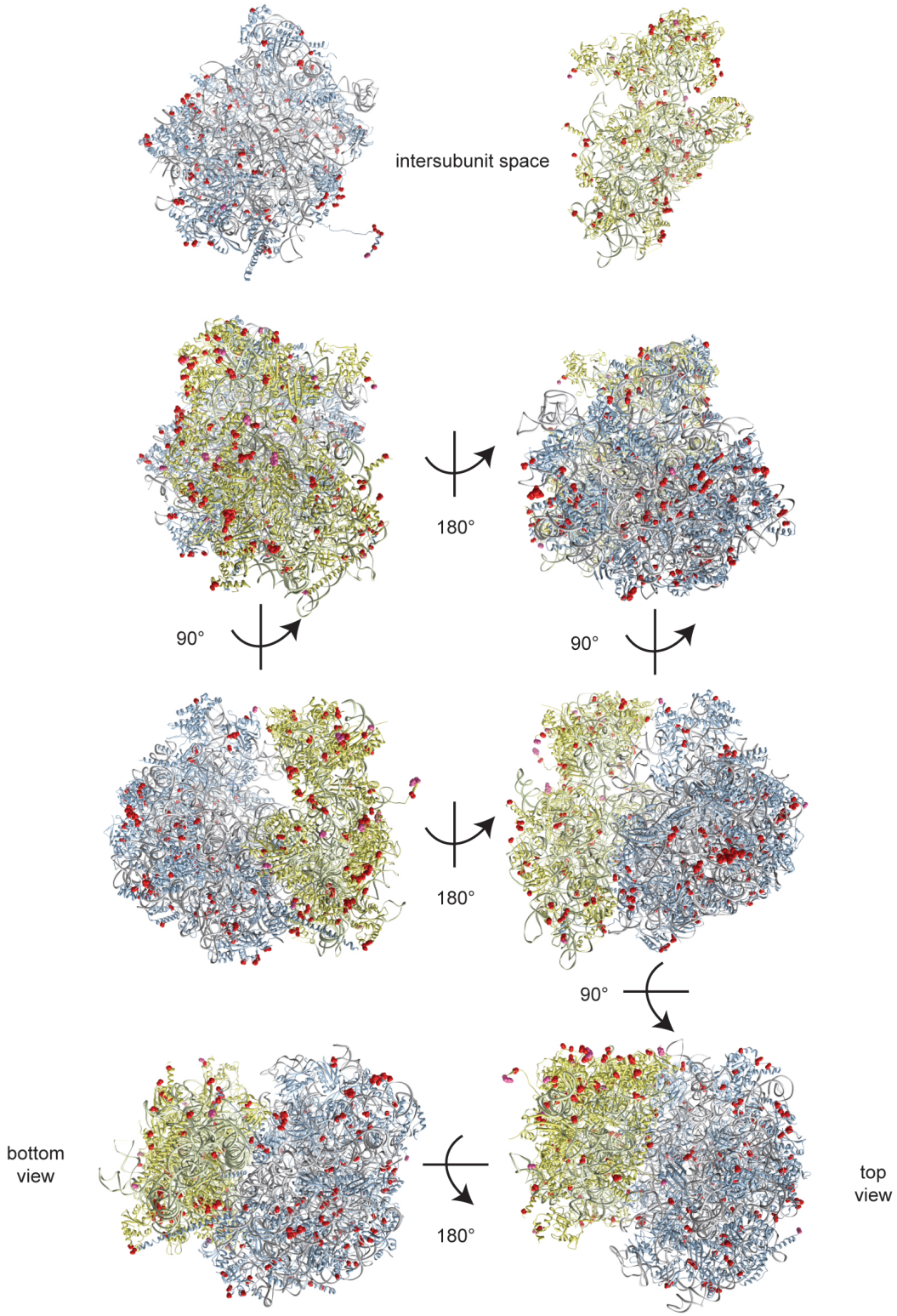

Figure 3.1: Localization of ribosomal phosphorylation sites on the 80S structure. Phosphorylated amino acids are depicted as red spheres and in the case they are not localized the last amino acid is shown as pink sphere. Large ribosomal proteins are colored in blue, small ribosomal proteins in yellow and rRNA in gray. The structure was taken from Ben-Shem et al. (2011).

phosphosites remain to be discovered. Nevertheless, it could be shown that eukaryotic ribosomes are highly phosphorylated.

The identified phosphorylation sites are located mainly on the surface of the ribosome and/or in the intersubunit space making them accessible for potential kinases and phosphatases during the translation cycle (Fig. 3.1). Although many of the identified phosphorylation sites are accessible on the surface, the question arises how they might influence ribosome function as several of them are localized on the surface and at the back of the ribosome quite distant to the active center of the ribosome. However, there are two possibilities: phosphorylation of a ribosomal protein might either (i) directly influence translation by inducing conformational changes or (ii) indirectly via recruitment of translation factors. Those phosphorylation sites identified on parts of ribosomal proteins that are buried in the inside of the ribosome might be accessible during ribosome biogenesis or have a more constitutive function in stabilizing the ribosome structure or be important for ribosome biogenesis. For instance, Rps3 phosphorylation by Hrr25 and subsequent dephosphorylation was shown to be important for efficient assembly of pre-40S subunits (Schäfer et al., 2006) and phosphorylation of Rpl18 is required for folding and binding to the 5S rRNA (Bloemink and Moore, 1999).

Taken together, a comprehensive survey of *Saccharomyces cerevisiae* ribosomal phosphorylation sites is presented identifying 122 novel phosphorylation sites. Thus, eukaryotic ribosomes are heavily phosphorylated at steady-state *in vivo*.

3.2 Stress-Induced Changes in the Phosphorylation Pattern of Ribosomal Proteins

Using an unbiased quantitative SILAC approach, numerous phosphorylation sites on ribosomal proteins were identified that change their phosphorylation status upon heat shock and/or glucose depletion (Table 2.2 and Table 2.3). Importantly, in this study the loss of Rps6 phosphorylation upon stress was reproduced. Hence, the applied stress conditions indeed induce a stress response leading to specific phosphorylation and dephosphorylation events. A second indication that the cells shut-down translation was

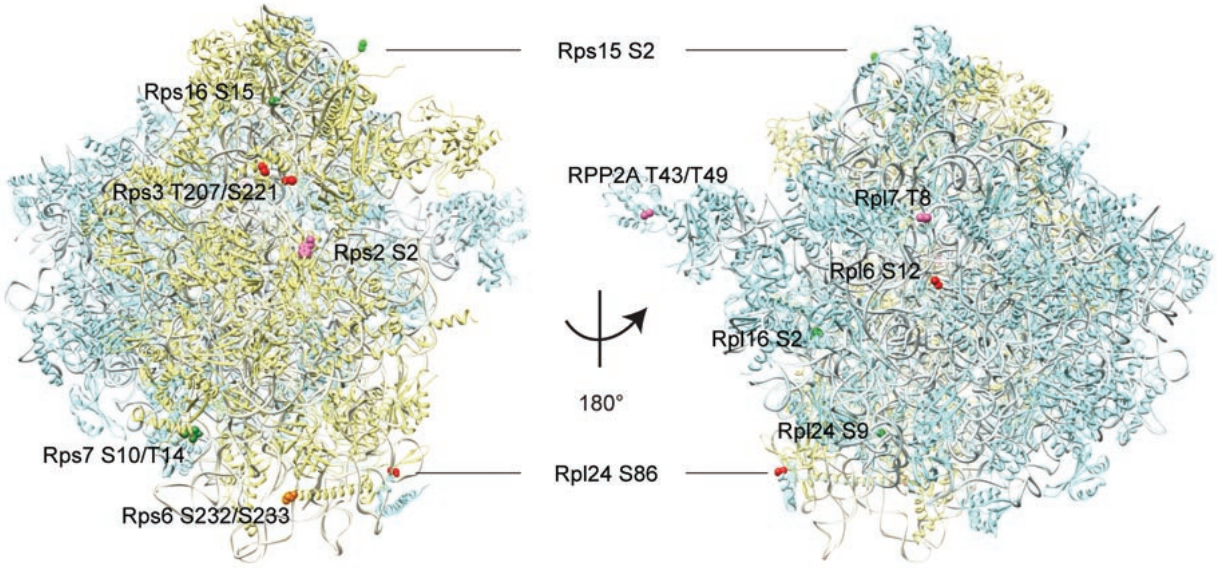

Figure 3.2: Localization of ribosomal phosphorylation sites on the 80S structure changing upon stress. Phosphorylated amino acids are depicted as red/dark green spheres and in the case they are not localized the last amino acid is shown as pink/light green/orange sphere. In red/pink and dark/light green the phosphorylation sites that change upon heat shock and glucose depletion, respectively, are shown. In orange is the last amino acid of the C-term of Rps6 colored in which the two phosphorylation sites are located that responded to both stresses. Large ribosomal proteins are colored in blue, small ribosomal proteins in yellow and rRNA in gray. The structure was taken from Ben-Shem et al. (2011).

the increased 80S peak and loss of polysomes in gradient profiles comparing heat shocked or glucose depleted cells to untreated control cells (Fig. 2.2 C+D). Interestingly, only four sites, Rps6 S232/S233, Rpl24 S86 (heat shock), and Rpl12 S38 (glucose depletion), are less phosphorylated after heat shock or glucose depletion, whereas the majority of sites showed an increased phosphorylation. In a recent study mammalian mitochondrial ribosomes were *in vitro* hyperphosphorylated by different kinases and subsequently showed decreased translation activity *in vitro* (Miller et al., 2009). Therefore, it is tempting to speculate that an increased phosphorylation of ribosomal proteins leads to decreased translation activity as it is expected after a shut-down of translation by stress. Moreover, one of the identified sites, Rpl12 S38, was more phosphorylated upon heat shock and less phosphorylated upon glucose depletion, making it an especially interesting site responding differently to diverse stresses.

In this study, the cultures in the SILAC experiment were only labeled with heavy and

light Lys and therefore, the peptides were digested solely with LysC. For this reason, relatively large peptides were generated and thus giving a possible explanation why only so few and different sites were identified – 97 phosphosites compared to 279 in the general phosphoproteomics analysis (Table A.2 and Table 2.1). Most likely there will be more stress-induced changes in the ribosomal phosphorylation pattern which could be identified using double labeling with heavy Lys and Arg in combination with different peptide preparation methods (see Section 3.1).

The ribosomal proteins that change in their phosphorylation status upon stress are located on different sites mainly on the back of the ribosome and do not cluster at any specific region – expect for the two Rps3 sites which are in close proximity (Fig. 3.2). It is therefore rather unlikely that one kinase and phosphatase phosphorylates and dephosphorylates, respectively, more than one site at a time suggesting that (i) different signaling pathways might be involved, (ii) sequential phosphorylation/dephosphorylation takes place or (iii) several kinases of the same pathway are binding to different positions on the ribosome.

3.3 Phosphorylation Sites Have Different Effects on Translation

The challenge of the presented project was the identification of ribosomal phosphorylation events that are important for translation. To this end, phosphorylation sites were selected for mutational analysis based on (i) the intensity of their MS signal, (ii) their reproducibility in the different preparations, (iii) their accessibility on the ribosome, (iv) their conservation in higher eukaryotes and (v) whether their phosphorylation status changes upon stress indicating a role in translation, specificlly in stress dependent translation control. However, it is not possible to draw conclusions from the signal intensity for the abundance of the phosphorylation in the cell due to the characteristics of the generated peptides for MS analysis (size, charge *etc.*). One attempt to assess the abundance of ribosomal phosphorylation was to resolve ribosomal proteins on 2D gels and stain phosphorylated proteins, unfortunately this was not conclusive and was not pursued further (data not shown).

Translation active extracts of phospho-deficient A and phospho-mimicry D mutant strains were assessed for their activity to translate a 5' capped and a CrPV IRES containing mRNA *in vitro*. Out of the 25 phosphorylation sites analyzed so far twelve showed different translation activity *in vitro* compared to the corresponding wild-type (data not shown). Interestingly, there are phospho-mutants that have an increased or decreased activity and mutants that influence cap-dependent and cap-independent translation. Thus, phosphorylation of ribosomal proteins might be used in diverse steps of the translation cycle. In the future, it will be fascinating to unravel for all of these functional phosphorylation sites the step in translation they are important for and to demonstrate their physiological relevance.

3.4 Rps5 T38 Phosphorylation Functions in Context Dependent Start Codon Recognition

In this study strong evidence is provided that Rps5 T38 phosphorylation is important for efficient canonical translation initiation. The phospho-deficient *rps5-T38A* mutation causes a cap-dependent translation defect *in vitro* and a defect in *de novo* protein synthesis *in vivo* (Fig. 2.4). Specifically, the formation of 48S initiation complexes is decreased in *rps5-T38A* mutant cells compared to *RPS5* wt cells (Fig. 2.9 and Fig. 2.10). Moreover, the *rps5-T38A* mutation causes increased initiation from non-AUG start codons (Fig. 2.12). In addition, the discrimination against good and poor start codon context is eliminated in the *rps5-T38A* mutant cells (Fig. 2.13), indicating that Rps5 T38 phosphorylation functions in context dependent start codon recognition.

During translation initiation first the MFC (eIF1, 3, 5 and the TC) and eIF1A bind to the 40S subunit forming the 43S PIC. The pre-assembled 43S PIC is recruited to the 5' cap of the mRNA and subsequently starts to scan the 5' UTR for a start codon in a suitable consensus context (see Section 1.4.1). The recognition of the AUG by perfect complementarity with the Met-tRNAi anticodon in the ribosomal P-site completes scanning followed by the release of eIF1 (Maag et al., 2005) and the hydrolysis of eIF2-bound GTP

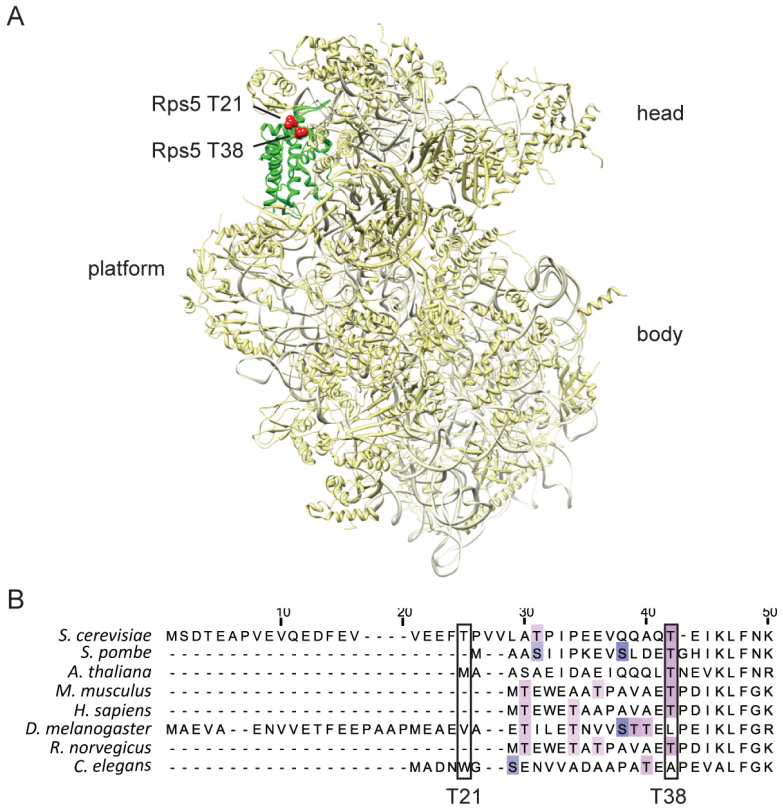

Figure 3.3: Localization of Rps5 T21 and T38 on the ribosome and protein sequence conservation of the N-terminus of Rps5. (A) Phosphorylated amino acids are depicted as red spheres, Rps5 protein in green and all other small ribosomal proteins in yellow and rRNA in gray. The 40S structure was taken form Ben-Shem et al. (2011). (B) Multiple sequence alignment of Rps5 protein sequence (UniProt, www.uniprot.org). Colors used are purple for S and pink for T; light - weakly, dark - highly conserved; boxed are the two sites T21 and T38.

(Huang et al., 1997; Algire et al., 2005). The recognition of the start codon and base pairing of the Met-tRNAi anticodon with the start codon is crucial for stable 48S PIC formation (Maag et al., 2005). Thus, the inability of *rps5-T38A* mutant cells to efficiently recognize the start codon might also cause the decreased formation of 48S PICs observed *in vitro* and *in vivo*.

Although it remains to be elucidated how the *rps5-T38A* mutation impedes start codon selection, initiation factors might be involved since the *rps5-T38A* mutant ribosomes are able to translate the CrPV IRES containing mRNA which does not need any initiation factors. In addition, the release of several initiation factors is altered in *rps5-T38A* mutant ribosomes (Fig. 2.11). Possible candidates are eIF1, 1A, 2, 3 and 5 since mutations in these factors lead to a so called suppressor of initiation codon mutation (Sui$^-$) phenotype that

confer an increased initiation from UUG codons as observed for the *rps5-T38A* mutant cells (Castilho-Valavicius et al., 1990; Fekete et al., 2007; Saini et al., 2010; Pestova and Kolupaeva, 2002; Valasek et al., 2004; Huang et al., 1997). Moreover, the T38 phosphorylation site lies in the variable N-terminus of Rps5 and forms a part of the mRNA exit channel (Fig. 3.3). The yeast Rps5 N-terminus is 21 aa longer than the human Rps5 N-terminus. Replacing yeast Rps5 with its human homologue altered translation fidelity and affected the recruitment of specific mRNAs to the ribosome (Galkin et al., 2007). Using different truncated Rps5 variants Lumsden et al. (2009) showed that the first 24 aa only play a minor role whereas deletion of aa 1-30 and 1-46 impairs translation initiation by affecting the association with eIF2 and eIF3. In addition, both Rps5 and eIF2α were crosslinked to -3 thioU upstream of the AUG start codon on mRNAs in mammalian 48S PICs (Pisarev et al., 2006, 2008), and also eIF3 locates in close proximity being crosslinked to nucleotides -8 to -17 upstream of the AUG codon (Pisarev et al., 2008), supporting eIF2 and eIF3 as possible candidates.

In contrast, Rps5 might also be directly involved in start codon selection. First, it crosslinked specificlly to the -3 position which is crucial for optimal AUG sequence context in yeast (Pisarev et al., 2006) explaining the loss of discrimination against poor AUG context in the *rps5-T38A* mutant. Additionally, -3 thioU also cross-linked specificlly to the prokaryotic homologue rpS7 in prokaryotic ribosomal initiation complexes indicating a conserved function of rps5/rps7 (La Teana et al., 1995). Second, Rps5 T38 phosphorylation might influence the structure or conformation of initiation complexes. During start codon recognition the 43S PIC rearranges from an open, scanning permissive to a closed conformation mediated by eIF1 and eIF1A (Passmore et al., 2007). It is tempting to speculate that Rps5 T38 phosphorylation might influence the transition from the open, scanning competent conformation to the closed after start codon recognition either directly or via interaction of initiation factors with the mRNA and the 43S during translation initiation.

The fact that the *rps5-T38D* mutation causes a ribosome biogenesis or stability defect suggests that the phosphorylation of Rsp5 T38 needs to be reversible. Provided that the phospho-mimicry D mutation indeed resembles the phosphorylation of Rps5 at T38, the permanently phosphorylated state causes a different defect compared to the

phospho-deficient *rps5-T38A* mutation.

Although the loss of Rps5 T38 phosphorylation in the *rps5-T38A* mutation does not lead to a general growth defect under specific conditions – starvation of amino acids (3-AT), inhibition of elongation (cycloheximide), low carbon or ethanol as carbon source – the growth of *rps5-T38A* mutant cells is more severely affected than wild-type cells whereas under rapamycin, inhibiting TOR signaling, the mutant cells grew better (Fig. 2.15). Therefore, the phosphorylation and dephosphorylation of Rps5 T38 is needed for survival under specific conditions.

Concluding, the phosphorylation of Rps5 on T38 is important for efficient 48S initiation complex formation and context dependent start codon selection. Since Rps5 belongs to the conserved family of Rps5/Rps7 proteins and the T38 residue is conserved in higher eukaryotes (Fig. 3.3 B) also the function of this phosphorylation site might be conserved in other organisms.

3.5 Rps12 T23 Phosphorylation Is Important for Scanning Processivity

A second phosphorylation site of a small ribosomal protein, Rps12 T23, functions in canonical translation initiation, specifically Rps12 phosphorylation on T23 is important for initiation complex formation (Fig. 2.21 and Fig. 2.22). However, in contrast to *rps5-T38A* mutation, the *rps12-T23A* mutant ribosomes possess a reduced scanning processivity compared to *RPS12* wild-type ribosomes (Fig. 2.24).

The reduced scanning rate observed in *rps12-T23A* translation active extracts might have two reasons: (i) the ribosomes have a lower scanning speed or (ii) their processivity is reduced due to an increased fall-off of scanning 43S from the mRNA. It is not possible to discriminate between these possibilities based on the used *in vitro* translation assay to measure the scanning activity. However, less processive 43S complexes might be less stable explaining the decrease in 48S levels in *rps12-T23A* cells observed after extract preparation in the *in vivo* assay (Fig. 2.22). In addition, it is generally believed that slowly scanning ribosomes show increased initiation from non-AUG codons which was not observable in

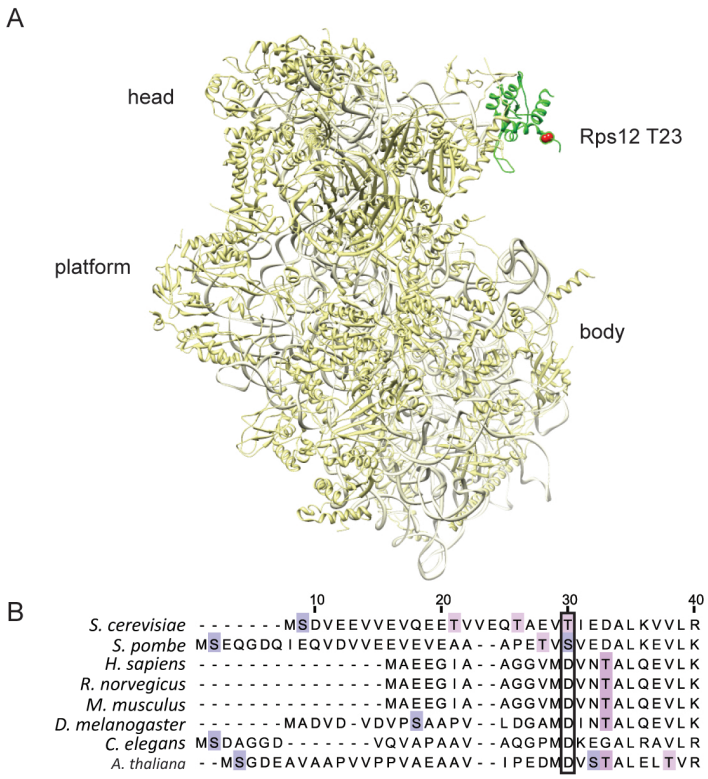

Figure 3.4: Localization of Rps12 T23 on the ribosome and protein sequence conservation of the N-terminal part of Rps12. (A) The phosphorylated amino acid is depicted as red sphere, Rps12 protein in green and all other small ribosomal proteins in yellow and rRNA in gray. The 40S structure was taken from Ben-Shem et al. (2011). (B) Multiple sequence alignment of Rps12 protein sequence (UniProt, www.uniprot.org). Colors used are purple for S and pink for T; light - weakly, dark - highly conserved.

the *rps12-T23A* mutant cells (Fig. 2.25 A), thus corroborating that 43S stability on the mRNA is affected by the *rps12-T23A* mutation.

Several initiation factors have been reported to be crucial for efficient scanning. eIF1 and eIF1A promote the open, scanning competent conformation of the 43S PIC (Passmore et al., 2007) and are important for efficient scanning together with the cap-binding complex eIF4F, which contains the helicase eIF4A and its auxiliary factor eIF4B (Pestova and Kolupaeva, 2002). Two additional helicases with a known and suspected function in translation initiation are Ded1 and Dbp1, respectively (Iost et al., 1999; Jamieson and Beggs, 1991). Interestingly, Ded1 and Dbp1 seem to be more important for scanning processivity than eIF4A and eIF4B as could be demonstrated by Berthelot et al. (2004) using *in vivo* luciferase constructs with different 5' UTR length. The *rps12-T23A* mutation

was found to influence the association and dissociation of several initiation factors to and from the ribosomes (Fig. 2.23). Therefore, Rps12 T23 phosphorylation might either directly function in scanning processivity or via the recruitment of one or more initiation factors.
The *rps12-T23A* mutation does not cause a growth defect under optimal conditions, but there are several conditions that impair growth compared to wild-type: inhibition of elongation (cycloheximide) or TOR signaling (rapamycin), ethanol as carbon source or induction of the unfolded protein response (tunicamycin) (Fig. 2.26). Thus, demonstrating the physiological relevance of the Rps12 T23 phosphorylation.
Interestingly, the residue T23 of Rps12 corresponds to an aspartate (D) in higher eukaryotes, for instance human, mouse, and drosophila (Fig. 3.4 B). This finding suggests that a constitutive phosphorylation of this residue is functional – if the *rps12-T23D* mutation indeed resembles a phosphorylated residue – and that during evolution a reversible phosphorylatable and 'chargeable 'residue was replaced by a residue with an intrinsic negative charge at a physiologic pH.
Taken together, strong evidence is provided that the phosphorylation on T23 of Rps12 functions in canonical translation initiation thus influencing initiation complex formation. Moreover, Rps12, a ribosomal protein about which nothing was known except for its localization in the 40S subunit (Fig. 3.4 A), is the first ribosomal protein important for scanning processivity.

3.6 Conclusion

In this study it could be shown for the first time that two phosphosites on ribosomal proteins of the small subunit are important for translation initiation. Specifically, phosphorylation of Rps5 T38 is involved in context dependent start codon recognition, whereas Rps12 T23 phosphorylation is needed for scanning processivity. In addition, first indications for a role in translation are provided for more phosphorylation sites comparing wild-type and phospho-mutant translation active extracts in cap-dependent and cap-independent translation *in vitro*. However, the detailed step in translation they function in and the underlying molecular mechanism remain to be elucidated.
As ribosomes are phosphorylated on many different sites it will be a challenge to determine

which of these many sites are individually or collectively important for translation and/or other processes such as ribosome biogenesis. It will be fascinating to unravel for each functionally important site their role in translation, their physiological importance, and whether they regulate the expression of specific transcripts.

4 Materials and Methods

4.1 Materials

4.1.1 Consumables and Chemicals

Consumables and chemicals were purchased from the following companies:
Applichem (Darmstadt), Applied Biosciences (Darmstadt), Becton Dickinson (Heidelberg), Beckman Coulter (Krefeld), Biaffin (Kassel), Biomol (Hamburg), Biorad (Munich), Biozym (Hess. Oldendorf), Chemicon (Temecula, Canada), Eppendorf (Hamburg), Fermentas (St. Leon-Rot), Formedium (Norwich, UK), GE Healthcare (Munich), Gilson (Bad Camberg), Invitrogen (Karlsruhe), Kedar (Warsaw, Poland), Macherey&Nagel (Düren), Medac (Hamburg), Medigenomix (Munich), MembraPure (Bodenheim), Merck Biosciences (Darmstadt), Millipore (Molsheim, France), Mobitec (Göttingen), MP Biomedical (Illkirch, France), NEB (Frankfurt), Neolab (Heidelberg), Nunc (Wiesbaden), Peske (Aindling-Arnhofen), Promega (Mannheim), Qiagen (Hilden), Roche (Mannheim), Roth (Karlsruhe), Sarstedt (Nümbrecht), Semadeni (Düsseldorf), Serva (Heidelberg), Sigma (Taufkirchen), Stratagene (Amsterdam, Netherlands), Thermo Scientific (Munich),VWR (Ismaning)

4.1.2 Equipment

Table 4.1: Equipment used in this study.

Name	Supplier
Beckman DU650 spectrophotometer	Beckman Coulter (Krefeld)
L80 and OptimaTM L-90 K ultracentrifuge	Beckman Coulter (Krefeld)

Continued on next page

Table 4.1 (continued)

Name	Supplier
SW32, SW40, Type 45Ti, TLA 110 rotor	Beckman Coulter (Krefeld)
Bioscreen C Analyzer	iLF bioserve (Langenau)
CO8000 Cell Density Meter	WPA (Cambridge, UK)
Dissection microscope manual MSM	Singer (Somerset, UK)
Electrophoresis Power Supply Consort E853	Neolab (Heidelberg)
Heidloph shaker duomax 1030	Neolab (Heidelberg)
Rotator, Vortex Genie2	Neolab (Heidelberg)
Mini-Protean II system	Biorad (Munich)
Gradient machine, Fractionator Foxy Jr., UA-6 UV/Vis Detector	Teledyne ISCO (Lincoln, USA)
Innova 44 shaking incubator	New Brunswick Scientific (Nürtingen)
Liquid scintillation analyzer TriCarb 2810 TR	PerkinElmer (Waltham, USA)
Lumat LB9607, Centro LB 960	Berthold technologies (Bad Wildbad)
Optimax TR developing machine	MS Laborgeräte (Dielheim)
Research Pipettes P2, P20, P200 P1000	Gilson (Bad Camberg)
Rotanda 46R, 460R	Hettich (Tuttlingen)
Sorvall Evolution RC, RC 5B Plus	Thermo Fisher Scientific (Munich)
SLC 6000, SW34 rotor	Thermo Fisher Scientific (Munich)
StepOnePlus™Real Time PCR System	Applied Biosystems (Darmstadt)
T3 Thermocycler	Biometra (Göttingen)
Thermomixer compact, BioPhotometer	Eppendorf (Hamburg)
Eppendorf centrifuge 545D, 541R	Eppendorf (Hamburg)
Universal Analytical Balance	Satorius (Göttingen)

4.1.3 Commercially Available Kits

Table 4.2: Commercially available kits and reagents used in this study.

Name	Supplier
Nucleobond AX PC100	Macherey&Nagel (Düren)
Nucleospin Mini	Macherey&Nagel (Düren)
Nucleospin extract	Macherey&Nagel (Düren)
RNeasy MinElute Clean-Up Kit	Qiagen (Hilden)
AmpliCap™SP6 High Yield Massage Maker Kit	Biozym (Hess. Oldendorf)
AmpliCap-Max™T7 High Yield Massage Maker	Biozym (Hess. Oldendorf)
Dual-Luciferase®Reporter Assay System	Promega (Mannheim)
Power SYBR®Green PCR Master Mix	Applied Biosystems (Darmstadt)
High Capacity cDNA Reverse Transcription Kit	Applied Biosystems (Darmstadt)

4.1.4 Enzymes and Standards

Table 4.3: Enzymes and standards used in this study.

Name	Supplier
DNA Standards, Protein Standards, Restriction Endonucleases, T4 DNA Ligase, Taq Polymerase, DNaseI	Fermentas (St. Leon-Rot)
Lysozyme	VWR (Ismaning)
Protein Phosphatase	NEB (Frankfurt)
RNasin®Plus RNase Inhibitor	Promega (Mannheim)
T3 and T7 RNA Polymerase	Roche (Mannheim)
VentR®DNA polymerase, λ Zymolase 20T	Medac (Hamburg)

4.1.5 Radioactivity

Radioactivity was purchased from Hartmann Analytik (Braunschweig):
α-[32P]-UTP, L-[14C]-phenylalanine, L-[3H]-leucine, L-[35S]-methionine

4.1.6 Antibodies

Table 4.4: Primary and secondary antibodies used in this study.

Antibody	Source	Supplier
α-eIF1 (Sui1)	rabbit	A.G. Hinnebusch
α-eIF1A (Tif11)	rabbit	A.G. Hinnebusch
α-eIF2α (Sui2)	rabbit	T.E. Dever
α-eIF3a (Rpg1)	rabbit	A.G. Hinnebusch
α-eIF3b (Prt1)	rabbit	A.G. Hinnebusch
α-eIF5 (Tif5)	rabbit	A.G. Hinnebusch
α-eIF5B (Fun12)	rabbit	T.E. Dever
α-Rpl6	rabbit	G. Dieci
α-Rps8	rabbit	G. Dieci
α-HA	goat	Roche (Mannheim)
α-Pgk1	mouse	Invitrogen (Karlsruhe)
α-rabbit IgG-HRPO	goat	BioRad (Munich)
α-goat IgG-HRPO	rabbit	Sigma (Taufkirchen)
α-mouse IgG-HRPO	goat	BioRad (Munich)

4.1.7 Buffers, Solutions and Growth Media

Table 4.5: Buffers, solutions and growth media used in this study.

Buffers/Solutions/Media	Components
Coomassie staining	0.25 % (w/v) Coomassie Brilliant Blue R-250; 30 % (v/v) ethanol; 10 % (v/v) acetic acid
Coomassie destaining	30 % (v/v) ethanol; 10 % (v/v) acetic acid
DNA loading dye 6x	40 % (w/v) sucrose; 0.25 % Bromophenol Blue; 0.25 % Xylene cyanol FF
Kinase buffer 5x	500 mM Tris-HCl,pH 7.5; 5 mM $MgCl_2$; 5 mM EGTA

Continued on next page

Table 4.5 (continued)

Buffers/Solutions/Media	Components
KNOP buffer 10x	500 mM Tirs-HCl, pH 9.2; 160 mM $(NH_4)_2SO_4$; 22.5 mM $MgCl_2$
KNOP Polymerase	2 U Taq; 0.56 U Vent
Luria-Bertani Broth (LB)	1 % (w/v) tryptone; 0.5 % (w/v) yeast extract; 0.5 % (w/v) NaCl; (2 % (w/v) agar for plates)
Phosphatase Inhibitors (PhI)	10 mM NaF; 1 mM $NaVO_4$; 5 mM β-glycerophosphate
Phosphate-buffered saline (PBS)	137 mM NaCl; 2,7 mM KCl; 20 mM NaH_2PO_4; 10 mM Na_2HPO_4, pH 7.5
Protease Inhibitors (PI) 100x	28 ng/ml Leupeptin; 137 ng/ml Pepstatin A; 17 ng/ml PMSF; 0.33 mg/ml benzamidine; in 100 % EtOH p.a.
Sample buffer (SB) 4x	0.2 M Tris-HCl, pH 6.8; 40 % (v/v) glycerol; 8 % (w/v) SDS; few grains Bromophenol Blue; 0.1 M DTT
Separation gel buffer 4x	3 M Tris; 0.4 % (w/v) SDS; pH 8.8
Stacking gel buffer 4x	0.5 M Tris; 0.4 % (w/v) SDS; pH 6.8
Solution I	10 mM Tris-HCl, pH 7.5; 1 mM EDTA; 100 mM LiOAc
Solution II	10 mM Tris-HCl, pH 7.5; 1 mM EDTA; 100 mM LiOAc; 40 % (v/v) PEG-4000
Sporulation medium (YPA)	1 % (w/v) yeast extract; 2 % (w/v) peptone; 1 % (w/v) KOAc; (2 % (w/v) agar for plates)
Synthetic complete medium (SC)	0.67 % (w/v) yeast nitrogen base; 0.06 % (w/v) complete synthetic mix of aa; drop out as required; 2 % (w/v) glucose; when required 0.1 % (w/v) 5-FOA was added; (2 % (w/v) agar plates)
TAE 50x	2 M Tris; 100 mM EDTA, pH 8.0; 1M acetic acid
TBE	90 mM Tris-borate; 2 mM EDTA
TE	1 mM EDTA; 10 mM Tris-HCl, pH 8.0
Electrophoresis buffer	25 mM Tris; 0.1 % (w/v) SDS; 0.19 mM glycine

Continued on next page

Table 4.5 (continued)

Buffers/Solutions/Media	Components
Tris-buffered saline (TBS)	137 mM NaCl; 2.7 mM KCl; 12.5 mM Tris-HCl; when required 0.1 % (w/v) Tween-20®was added (TBS-T)
TSNTE buffer	2 % (v/v) Triton X-100; 1 % (v/v) SDS; 100 mM NaCl; 10 mM Tris-HCl, pH 8.0; 1 mM EDTA
Wet blotting buffer	25 mM Tris; 192 mM glycine; 10 % methanol
Yeast full medium (YPD)	2 % (w/v) peptone; 2 % (w/v) glucose; 1 % (w/v) yeast extract; (2 % (w/v) agar for plates)

4.1.8 Oligonucleotides

Oligonucleotides were purchased from Thermo Scientific (Ulm).

Table 4.6: Oligonucleotides used in this study.

Nr.	Name	Sequence
1	5‘NotI Rps5	GGGGCGGCCGCGACCTTTTATACAACAACACCCATATACCC
2	3‘XhoI Rps5	GGGCTCGAGCATGTGTAGATCATTTCAAGGAAACGTTACG
3	Rps5 T38A for	CCAGAAGAAGTCCAACAAGCTCAAGCTGAGATTAAGTTGTTCAAC
4	Rps5 T38A rev	GTTGAACAACTTAATCTCAGCTTGAGCTTGTTGGACTTCTTCTGG
5	Rps5 T21A for	GTTGAAGAATTCGCTCCAGTCGTCTTGGCTACTCC
6	Rps5 T21A rev	GGAGTAGCCAAGACGACTGGAGCGAATTCTTCAAC
7	Rps5 T38D for	CCAGAAGAAGTCCAACAAGCTCAAGATGAGATTAAGTTGTTCAAC
8	Rps5 T38D rev	GTTGAACAACTTAATCTCATCTTGAGCTTGTTGGACTTCTTCTGG
9	5’Pst1 Rps5 3HA	GGGCTGCAGTCTGACACCGAAGCTCCAGTTG
10	5’NotI Rps12	GGGGCGGCCGCCTGCTTCATGTATATACGCACCTCG
11	3’XhoII Rps12	GGGCTCGAGGGCAATGAAACTTCAAATGACAACTTGC
12	Rps12 S2A for	GAGAAGAAAAATGGCTGACGTTGAAGAAGTCGTTGAAGTTC
13	Rps12 S2A rev	GAACTTCAACGACTTCTTCAACGTCAGCCATTTTTCTTCTC
14	Rps12 T19A for	GAAGAAACTGTTGTTGAACAAGCTGCCGAAGTTACTATC

Continued on next page

Table 4.6 (continued)

Nr.	Name	Sequence
15	Rps12 T19A rev	GATAGTAACTTCGGCAGCTTGTTCAACAACAGTTTCTTC
16	Rps12 T23A for	GAACAAACTGCCGAAGTTGCTATCGAAGATGCTTTGAAGGTTG
17	Rps12 T23A rev	CAACCTTCAAAGCATCTTCGATAGCAACTTCGGCAGTTTGTTC
18	S12 T23D for	GAACAAACTGCCGAAGTTGATATCGAAGATGCTTTGAAGGTTG
19	S12 T23D rev	CAACCTTCAAAGCATCTTCGATATCAACTTCGGCAGTTTGTTC
20	5'Pst1 Rps12 3HA	GGGCTGCAGTCTGACGTTGAAGAAGTCGTTGAAG
21	5'18S rRNA	CGGTTTCAAGCCGATGGA
22	3'18S rRNA	AGAACGTCTAAGGGCATCACAGA
23	5'RPL41A	AAGAGAAAGAGACGGAAGGTGAGA
24	3'RPL41A	CAATGACATTACGATACTCTTGAAAGAA
25	5'RPL38	AATTGACCAGAAGAGCTGACGTT
26	3'RPL38	CGGCCTTGTTCAATTTTTTGTT
27	528S rRNA	CCGCCCGTCTTGAAACAC
28	328S rRNA	TTACACCCAAACACTCGCATAGA

4.1.9 Plasmids and Strains

Table 4.7: Plasmids used in this study.

Plasmid	Description / Reference
BSEF-*RPL38*	Britta Coordes (AG Sträßer)
pSP6P	(Vergé et al., 2004)
pWG299	(Gilbert et al., 2017)
pRS315	(Sikorski and Hieter, 1989)
pRS316	(Sikorski and Hieter, 1989)
pBSIIKS(+)	(Alting-Mees and Short, 1989)
pNOP-3HA1L	U. Hardeland
pDB688	(Salas-Marco and Bedwell, 2005)

Continued on next page

Table 4.7 (continued)

Plasmid	Description / Reference
pDB690	(Salas-Marco and Bedwell, 2005)
pDB691	(Salas-Marco and Bedwell, 2005)
pDB720	(Salas-Marco and Bedwell, 2005)
pDB721	(Salas-Marco and Bedwell, 2005)
pDB722	(Salas-Marco and Bedwell, 2005)
pDB723	(Salas-Marco and Bedwell, 2005)
pDB866	(Salas-Marco and Bedwell, 2005)
pDB868	(Salas-Marco and Bedwell, 2005)
pDB869	(Salas-Marco and Bedwell, 2005)
pDB870	(Salas-Marco and Bedwell, 2005)
pYDL-control	(Hager and Dinman, 2003)
pYDL-LA	(Hager and Dinman, 2003)
pYDL-TY1	(Hager and Dinman, 2003)
pYDL-HIV	(Hager and Dinman, 2003)
pYDL-TY3	(Hager and Dinman, 2003)
pPMB24	(Martin-Marcos et al., 2011)
pPMB25	(Martin-Marcos et al., 2011)
pPMB28	(Martin-Marcos et al., 2011)
pRaugFFuug	(Cheung et al., 2007)
pJM48	(Berthelot et al., 2004)
pJM250	(Berthelot et al., 2004)
pJM251	(Berthelot et al., 2004)
RPS5-pRS316	The NotI/XhoI fragment of *RPS5* was inserted into pRS316 using primers 1+2
RPS5-pRS315	The NotI/XhoI fragment of *RPS5* was inserted into pRS315
rps5-T38A-pRS315	Quickchange mutagenesis of *RPS5*-pRS315 using primers 3+4
rps5-T21A-pRS315	Quickchange mutagenesis of *RPS5*-pRS315 using primers 5+6

Continued on next page

Table 4.7 (continued)

Plasmid	Description / Reference
rps5-T38D-pRS315	Quickchange mutagenesis of *rps5-T38A*-pRS315 using primers 7+8
RPS5-pNOP-3HA1L	The PstI/XhoI fragment of *RPS5* was inserted into pNOP-3HA1L using primers 9+2
rps5-T38A-pNOP-3HA1L	The PstI/XhoI fragment of *rps5-T38A* was inserted into pNOP-3HA1L using primers 9+2
rps5-T38D-pNOP-3HA1L	The PstI/XhoI fragment of *rps5-T38D* was inserted into pNOP-3HA1L using primers 9+2
RPS12-pRS316	The NotI/XhoI fragment of *RPS12* was inserted into pRS316 using primers 10+11
RPS12-pRS315	The NotI/XhoI fragment of *RPS12* was inserted into pRS315
rps12-S2A-pRS315	Quickchange mutagenesis of *RPS12*-pRS315 using primers 12+13
rps12-T19A-pRS315	Quickchange mutagenesis of *RPS12*-pRS315 using primers 14+15
rps12-T23A-pRS315	Quickchange mutagenesis of *RPS12*-pRS315 using primers 16+17
rps12-T23D-pRS315	Quickchange mutagenesis of *rps12-T23D*-pRS315 using primers 18+19
RPS12-pNOP-3HA1L	The PstI/XhoI fragment of *RPS12* was inserted into pNOP-3HA1L using primers 20+11
rps12-T23A-pNOP-3HA1L	The PstI/XhoI fragment of *rps12-T23A* was inserted into pNOP-3HA1L using primers 20+11
rps12-T23D-pNOP-3HA1L	The PstI/XhoI fragment of *rps12-T23D* was inserted into pNOP-3HA1L using primers 20+11

Table 4.8: *Saccharomyces cerevisiae* and *Escherichia coli* strains used in this study.

Strain	Genotype	Origin
W303	*Mata/α; ura3-1; trp1-1; his3-11,15; leu2-3,112; ade2-1; can1-100; GAL+*	(Wallis et al., 1989)

Continued on next page

Table 4.8 (continued)

Strain	Genotype	Origin
Δ*lys*	*Mata/α* as W303; Δ*lys::KANMX6*	
RPS5 shuffle	*Mata/α* as W303; *RPS5::KANMX6* (*RPS5*-pRS316)	
RPS12 shuffle	*Mata/α* as W303; *RPS12::KANMX6* (*RPS12*-pRS316)	
DH5α F-	*ϕ*80d*lacZ*ΔM15; Δ(*lacZYA-argF*)U169; it deoR; it recA1; *endA*1; *hsdR*17; (rk^-, mk^+); *phoA*; supE44; λ^-; *thi*-1; *gyrA*96; *relA*1	Stratagene

4.2 Methods

4.2.1 Standard Methods

Cloning procedures were done according to Sambrook, J. and Russell, D. W. (2001) and cover restriction digests, ligations, transformation of vectors in *Escherichia coli*, and separation of DNA in agarose gels. Commercially available kits were used according to manufacturer's instructions. Point mutations were generated by site directed mutagenesis using the Invitrogen protocol (Invitrogen, Karlsruhe). The PCR sample was digested with 10 U DpnI for at least 2 h at 37°C and transformed into *E. coli* DH5α. All plasmids were sequenced by MWG, Eurofins (Munich).

Polymerase Chain Reaction (PCR)

All PCR reactions were done in a 30 µl Phusion Flash®High fidelity PCR reaction, if not indicated differently (see Tab. 4.9) except for amplification of disruption cassettes from genomic DNA, a 100 µl KNOP PCR was used (see Tab. 4.10).

Phenol-Chloroform Extraction of DNA

To purify DNA fragments from plasmids or PCR products one volume of phenol:chloroform: isoamylalcohol (25:24:1) was added and after 10 min centrifugation at 16000 g, the aqueous phase was extracted with an equal volume of chloroform. DNA was precipitated with 1/10

Table 4.9: Phusion Flash®High fidelity PCR reaction and amplification cycle

0.5 µl	template DNA (100-300 ng)	98℃	1 min	
0.25 µl	primer1 (10 pmol/ µl)	98℃	30 s	35
0.25 µl	primer2 (10 pmol/ µl)	55-45℃	30 s	
10 µl	2xPhusion PCR Master Mix	72℃	1 kb/15 s	
ad 20 µl	dd H_2O	72℃	10 min	

Table 4.10: KNOP mix PCR reaction and amplification cycle

1 µl	template DNA (100-300 ng)	94℃	2 min	
0.5 µl	primer 1 (100 pmol/ µl)	94℃	1 min	
0.5 µl	primer 2 (100 pmol/ µl)	55-45℃	0.5 min	35
10 µl	10XKNOP Buffer	68℃	750 bp/ min	
8 µl	dNTPs (25mM each)	68℃	10 min	
2 µl	KNOP Polymerase			
ad 100 µl	dd H_2O			

volume of 3 M NaOAc, pH 5.2 and 2 volumes of 100 % ethanol at -20℃. After washing with 70 % ethanol, the DNA was dried and resuspended in 10 µl TE buffer.

4.2.2 Yeast Specific Methods

Culture of *Saccharomyces cerevisiae*

Yeast strains were cultured in either full media or synthetic complete (SC) medium. The cell density of a yeast culture was determined in a spectrophotometer at a wavelength of 600 nm. One density at 600 nm (1 OD_{600}) corresponds to 2.5×10^7 cells.

Transformation of Yeast Cells

50 ml of a yeast culture were grown to an OD_{600} of 0.5 to 0.8 and harvested by centrifugation (3600 rpm, 3 min). After washing with 10 ml of H_2O and with 500 µl of solution I cells

were resuspended in 250 µl solution I. 1-3 µg DNA and 5 µl of single stranded carrier DNA (DNA of salmon or herring testis, 2 mg/ml) were mixed with 50 µl of cells in solution I and incubated with 300 µl solution II on a turning wheel at rt for 30 min. The samples were heat shocked at 42°C for 10 min, followed by 3 min incubation on ice. 1 ml of H_2O was added, the sample centrifuged, the pellet resuspended in 50 µl H_2O and plated on a selective plate. For genomic integrations, the pellets were resuspended in 1-5 ml YPD and incubated on a turning wheel for 1 h up to over night prior to plating.

Preparation of Genomic DNA

10 ml of an overnight yeast culture with an $OD_{600} > 1$ were harvested by centrifugation (3600 rpm, 3 min) and washed with 10 ml H_2O. The cells were resuspended in 500 µl H_2O and 200 µl TSNTE buffer. For lysis, 300 µl glass beads and 300 µl phenol:chloroform:isoamylalcohol (25:24:1) were added and the sample vortexed for 3 min. After centrifugation (16000 g, 10 min), the aqueous phase was extracted with an equal volume of chloroform. Genomic DNA was precipitated with 1.2 ml of 100 % ethanol at -20°C for at least 10 min. After centrifugation (16000 g, 4°C, 30 min), the pellet was dried and resuspended in 400 µl TE buffer. To remove RNA, the DNA was incubated with 20 µl RNaseA (10 mg/ml) at 37°C for 40 min. The genomic DNA was precipitated by addition of 40 µl 3 M NaOAc, pH 5.2 and 800 µl 100 % ethanol at -20°C for at least 10 min. After centrifugation (16000 g, 4°C, 30 min), the pellet was washed with 80 % ethanol, dried and resuspended in 30 µl TE buffer.

Deletion of Genes

In order to disrupt a gene, the coding sequence of the respective gene has to be replaced by homologous recombination using a construct carrying overlapping regions in the promoter and terminator region of the respective gene, separated by an auxotrophy marker. The *XYZ::KANMX4* disruption cassette was amplified by KNOP PCR from genomic DNA of the corresponding BY deletion strain (euroscarf). The shuffle strain was generated by transformation of the *XYZ::KANMX4* fragment in a diploid W303 strain and selection for *KANMX4*+ transformants. Deletion of *XYZ* was assessed by colony PCR (see 4.2.1) using primers that anneal in the promoter of *XYZ* and in the *KANMX4* gene. Positive

heterozygous transformants were transformed with *XYZ*-pRS316. Cells were sporulated and tetrades dissected.

Mating of Yeast Strains

In order to combine two or more gene deletions, the single deletion strains were mated. For mating, haploid parental strains carrying opposite mating types were mixed onto YPD plates. After several hours, the characteristic diploid cells were selected using a dissection microscope onto YPD plates.

Sporulation and Tetrad Dissection

For sporulating a diploid strain, freshly grown diploid cells were restreaked onto sporulation plates. On these plates, the diploid cells undergo meiosis and the genetic information is divided in four haploid spores, enclosed in a tetrad. Sporulation was monitored on a light microscope. The outer cell wall of the tetrad was destroyed by incubating 1 loop of cells in 10 µl Zymolase 20T. The destruction was stopped by addition of 50 µl of TE buffer, and the spores were dissected using the tetrad microscope. Tetrads with four growing spores were then restreaked onto YPD and the respective selection plates to check for segregation of markers. Double knock out strains were selected by checking for the correct 2:2 auxotrophy marker distribution or by a 1:3 distribution by PCR.

Yeast Whole Cell Extracts (WCE)

Denaturing protein extraction from yeast cells was carried out essentially as described (Knop et al., 1996). Briefly, 5 OD_{600} of cells were resuspended in 500 µl of H_2O, 150 µl of pre-treatment solution (1.85 M NaOH, 7.5 % β-mercaptoethanol) were added and incubated for 20 min on ice. After TCA precipitation the protein pellets were resuspended in 100 µl of 1xSB and 20 µl of 1 M Tris base.

4.2.3 Preparation of Ribosomes

Purification of Ribosomes for Phosphoproteomic Analysis

Yeast cells were grown to an OD_{600} of 0.5-0.7. Cells were harvested (4000 rpm, 4°C, 4 min), resuspended in 5 ml of lysis buffer (20 mM HEPES-KOH, pH 7.5; 75 mM KCl; 2.5 mM $MgCl_2$; 1 mM EGTA; 1 mM DTT; 0.5 mM PMSF) containing a mix of phosphatase inhibitors (PhI) to preserve protein phosphorylation. Cells were lysed by vortexing the cell suspension with two volumes glass beads for 5 min in the cold. After washing the beads once with lysis buffer, cell debris were removed by centrifugation (27000 rpm, SW40 rotor, 4°C, 15 min) and the fatty phase was aspirated. The ribosomes were washed with high salt by adding equal volume of 1 M KCl containing lysis buffer and crude ribosomes were sedimented through a high salt (500 mM KCl) 15 % sucrose cushion (42000 rpm, 45Ti, 4°C, 4 h). The high salt washed ribosomes were resuspended in lysis buffer (phosphatase inhibitor mix containing 200 µM $NaVO_4$) and different ribosomal populations such ribosomal subunits or polysomes were separated on 5-15 % or 10-40 % linear sucrose gradients in lysis buffer by centrifugation (32000 rpm, SW32, 4°C, 2 h). If polysomes should be isolated, 100 mg/l cycloheximide was added 10 min prior to harvesting and in all purification steps present in a final concentration of 100 mg/l. The pooled ribosomal gradient fractions were pelleted by ultracentrifugation (100000 rpm, TLA110, 4°C, 45 min) and washed once with lysis buffer to remove remaining sucrose. Purified ribosomes were resuspended (6 M urea; 2 M thiourea; 10 mM Tris-HCl, pH 8) and protein concentrations were determined using Bradford Assay (BioRad).

Protein samples were digested in-solution with trypsine and Lys-C, and phosphopeptides were enriched by TiO_2 chromatography (Olsen et al., 2006). The resulting phosphopeptide fractions were analyzed by online nanoLC-MS/MS on a high-resolution LTQ-Orbitrap Velos instrument using Higher-energy collisional dissociation (HCD) for high-mass accuracy tandem mass spectrometry (Olsen et al., 2006). Peptides and phosphopeptides were identified by Mascot (www.matrixscience.com).

SILAC - Stable Isotope Labeling with Amino Acids in Cell Culture

The labeling of yeast cells with stable isotopes was adapted from (Gruhler et al., 2005). Two cultures of 500 ml of liquid YNB medium containing 30 mg/ml lysine or [$^{13}C_6$] lysine were inoculated with Δ*lys::KANMX6* cells from a stationary YPD culture (1:10000). Yeasts were grown at 30℃ for 18-20 h until they reached an OD_{600} of 0.5-0.7. To treat the cells with heat shock, 300 ml 80℃ hot YNB complemented with the corresponding lysine were added to one of the cultures and incubated for 10 min at 42℃ while 30℃ warm media was added to the untreated culture and incubated for additional 10 min at 30℃. For glucose deprivation the yeasts were sedimented by centrifugation (4000 rpm, rt, 4 min) and one of the two cultures was resuspended in YNB medium lacking glucose and the other in glucose containing YNB and incubated for further 5 min at 30℃. Cells were harvested (4000 rpm, 4℃, 4 min), resuspended in 5 ml lysis buffer and vortexed with glass beads at 4℃ for 5 min. The lysates were centrifuged (27000 rpm, SW40 rotor, 4℃, 15 min), equal amounts of A_{280} of treated and untreated extracts were combined, diluted 1:1 with lysis buffer containing 1 M KCl and the differently labeled ribosomes were purified as described above (Section 4.2.3). Protein samples were digested in-solution with Lys-C, and processed like above. SILAC pairs were quantified and normalized using the MaxQuant software suite (Cox and Mann, 2008).

4.2.4 Polysome Gradients

Polysome gradients were performed as described in (Rother and Strasser, 2007). Briefly, yeast cells were grown to an OD_{600} of 0.5. Then, 0.1 mg/ml cycloheximide was added and the cells incubated at 30℃ for 10 min before harvesting by centrifugation (3600 rpm, 4℃, 3 min). The cells were resuspended in polysome buffer (20 mM HEPES-KOH, pH 7.5; 75 mM KCl; 2.5 mM $MgCl_2$; 1 mM EGTA; 1 mM DTT; 0.1 mg/ml cycloheximide). Lysis was done by adding 500 µl glass beads and vortexing at 4℃ for 5 min. After removal of the cell debris by centrifugation (16000 g, 5 min), 5 A_{260} were loaded onto a 12 ml 10-40 % linear sucrose gradient for polysome profiles and 5-25 % for separation of initiation complexes, respectively, and centrifuged at 38000 rpm for 2 h using an SW40 Ti rotor. The absorption profile at 254 nm was recorded with a Teledyne ISCO gradient fractionator and,

when needed, 500 µl fractions were taken for subsequent Western blot analysis or RT-PCR analysis (see Section 4.2.5). For Western blot analysis, 300 µl 30 % TCA was added to 300 µl of gradient fractions, the samples were incubated overnight on ice and centrifuged (16000 g, 4℃, 30 min). After washing with cold acetone, the pellets were resuspended in 50 µl 1xSB containing 1 M Tris-Base, denatured and subjected to SDS-PAGE and Western blotting (see Section 4.2.11).

4.2.5 Quantitative Reverse Transcription PCR of Gradient Fractions

Isolation of RNA from Gradient Fractions

To isolate RNA from gradient fractions, RNA of 220 µl fraction were precipitated by addition of 500 µl 100 % EtOH and 1 µl glycogen at -20℃ over night. After centrifugation (16000 g, 4℃, 30 min) the pellet was resuspended in RNA-Buffer (20 mM Tris, 100 mM NaCl, 2.5 mM EDTA, 1 % SDS, pH 7.5) and extracted twice with phenol/chloroform. RNA was precipitated with 500 µl 100 % EtOH and 1 µl glycogen from the aqueous phase. Pellets were washed once with 70 % ethanol, dried for 5 min in the speedvac and redissolved in 50 µl DEPC H_2O.

Quantitative Reverse Transcription PCR

For 1st strand cDNA synthesis the High Capacity cDNA Reverse Transcription Kit (Applied Biosystems) was used according to the manufacturer's instructions except that the reverse transcription (RT) was performed in a total volume of 10 µl. Quantitative PCR (qPCR) was performed using the StepOnePlus™Real Time PCR System (Applied Biosystems). Reaction mixtures (10 µl final volume) contained 2.5 µl of 1:200 dilutions of the individual cDNA samples, 5 pmol forward and reverse primers and Power SYBR®Green PCR Master Mix (Applied Biosystems) as prescribed by the manufacturer. Primers were designed using Primer express 3.0 software and tested for mispriming or formation of primer dimers by melting curve analysis of the individual amplification products. The thermocycling profile included an initial denaturation for 10 min at 95℃, followed by 45 cycles of amplification, comprising denaturation at 95℃ for 15 s and annealing/elongation at 60℃ for 1 min. For melting curve analysis of the amplification products, the temperature was increased in

0.3℃ increments to a final temperature of 95℃ (continuous fluorescence measurement). All reactions were run in triplicates and included negative controls (H_2O and no-RT samples in 1:400 dilution). Relative quantifications were performed by the comparative CT method (Livak and Schmittgen, 2001).

4.2.6 *In Vitro* Transcription

The capped luciferase mRNA was *in vitro* transcribed from pSP6P (Vergé et al., 2004) after its linearization with BsrBI (Fermentas). The *in vitro* transcription was carried out with the AmpliCap SP6 High Yield Message Maker Kit (Biozym) according to the manufacturer's directions. The CrPV IRES plasmid (Gilbert et al., 2017) was linearized with EcI136II before being transcribed with T7 polymerase (NEB). The GpppA cap (KEDAR, Poland) for the IRES construct was added to the reaction together with ATP, CTP and UTP. After 5 min incubation at 37℃, GTP was added and the DNA transcribed for 1 h at 37℃. The template DNA was digested with DNAseI (Fermentas) for 15 min at 37℃. The scanning processivity plasmids (Berthelot et al., 2004) were linearized with AgeI (Fermentas) and *in vitro* transcribed using the AmpliCap-Max T7 High Yield Message Maker Kit (Biozym) according to the manufacturer's instructions. For generating radiolabeled mRNA the BSEF-RPL3 plasmid was linearized with HindIII before being *in vitro* transcribed with T3 polymerase (Roche). m^7GpppG (KEDAR, Poland) together with ATP, CTP and ^{32}P-αUTP were added to the reaction. After 5 min incubation at 37℃, GTP was added and the DNA transcribed at 37℃ for 1 h. The template DNA was digested with DNAseI (Fermentas) for 15 min at 37℃. All mRNAs were purified by using the RNA MinElute Kit according to the manufacturer's directions (Qiagen).

4.2.7 *In Vitro* Translation Assays

Preparation of yeast translation active extracts

In vitro translation active extracts were prepared as described in (Tuite and Plesset, 1986). Briefly, cells were harvested at OD_{600} of 1.0 -1.2 by centrifugation (3000 g, 4℃, 5 min, Sorvall Evolution). After washing with 50 ml H_2O, the cells were weighed and incubated with 40 ml buffer1 (20 mM Tirs-H_2SO_4, pH 9.4; 7.5 mM DTT) on a shaking device at

RT for 10 min. After centrifugation, the pellet was resuspended in 40 ml 1 M sorbitol containing 1 mg zymolyase 20T per g cells for spheroblasting. The reaction was monitored by taking 5 µl of the cell suspension and measuring the OD_{600} when put into 1 ml of H_2O. If after 1 min the OD_{600} of this cell suspension dropped to 50 % of the original value, the cells were pelleted by centrifugation (3000 g, 4°C, 4 min). The pellet was carefully resuspended in YPD additionally containing 1 M sorbitol and incubated with gentle shaking for regeneration for 30 min. After another centrifugation, the cells were resuspended in 2.5 ml translation buffer A (30 mM Hepes-KOH, pH 7.4; 100 mM KOAc; 2 mM DTT) and 5 ml of glass beads added. The cells were lysed by $8x18$ s shaking by hand at 4 °C. The cell lysates were centrifuged (3000 g, 4°C, 2 min) to be separated from the glass beads and transferred to a new tube. After two centrifugation steps (25000 rpm, 10 min and 45000 rpm, 21 min, 4°C, TLA 110 rotor), the lipid layer was removed by aspiration and 2 ml of the supernatant applied onto a PD10 column. The first 1 ml was discarded and the next 2 ml collected, aliquoted and stored in liquid nitrogen.

Determination of Translation Activity of *In Vitro* Transcribed Luciferase mRNA

In vitro translation assays were performed as described in (Altmann and Trachsel, 1997). 1.25 A_{260} of the respective extract were incubated with 1.6 µg of creatin kinase (5 mg/ml (Roche) in 30 mM Hepes-KOH, pH 7.4; 50 % glycerol) in a total volume of 20 µl for 5 min on ice, followed by an incubation with 2mM MgOAc, 76 mM KCl, 0.4 mM GTP, 1 mM ATP, 50 µM of each AA, 12.5 mM creatin phosphate and 4 U RNase inhibitor (RNasin, Promega) in a total volume of 30 µl for 7.5 min, leading to ribosome run-off. 400 ng of *in vitro* transcribed luciferase mRNA (m^7G cap or IRES) were added and *in vitro* translated at 20°C for 30 min. For measurement of luciferase activity, 25 µl of the *in vitro* translation reaction were mixed with 100 µl of 25 mM glycyl-glycine, pH 7.8; 10 mM K_3PO_4, pH 7.8; 12 mM Mg_2SO_4; 3.2 mM EGTA; 2 mM ATP; 1mM DTT and 200M luciferin using a Lumat LB9507 Luminometer (Berthold). The emitted luminescence was detected for 10 s. WT activity was set to 100 % and the activity of the mutant strain calculated accordingly. The results are the mean of two independent experiments for at least three independently prepared extracts.

To determine the scanning processivity, 60 ng of *in vitro* transcribed luciferase mRNA were

added and after 5 min incubation at 20°C a 20 µl sample was measured every minute for 12 min in total to determine a time course. The results are the mean of at least four independently prepared extracts.

Determination of Translation Activity Using Endogenous mRNA

The translation activity was measured by incorporation of [35S]-Met into the nascent polypeptide using endogenous mRNA as template (Altmann and Trachsel, 1997). Translation reactions were assembled as described above except that instead of luciferase mRNA 4 µCi [35S]-Met were added and the reaction was incubated for 30 min at 22°C. 5 µl of the reaction were take at the indicated timepoints and charged met-tRNA were hydrolyzed in the presence of 0.5 M KOH for 30 min at 37°C. After neutralization with glacial acidic, proteins were precipitated in 10 % TCA-50 % EtOH for at least 20 min on ice. Proteins were filtrated on nitrocellulose, washed with 5 % TCA and counted with 3 ml of scintillation cocktail (Roth) using a scintillation counter (Tri-Carb 2810TR, PerkinElmer, Waltham, USA). Results are the mean of three to four independent experiments of independent extracts.

Determination of Elongation Activity and Miscoding Events

Translation elongation can be determined by polyphenylalanine synthesis using poly(U) as mRNA template in the presence of [14C]-F. In parallel, misincorporation of [3H]-L can be measured due to pairing of the UUU codon with the near-cognate UAA or CAA of L-tRNAs. 1.25 A_{260} of extract were incubated with 80 mM spermidine, 2 mM spermine, and 1 µg/ml poly(U) mRNA. The *in vitro* translation reaction was supplemented with 10 U RNase inhibitor, 200 pmol bulk tRNA, 40 pmol F-tRNA, , 150 µg/ml creatin kinase, 360 mM creatin phosphate, 30 mM ATP, and 12 mM GTP. For elongation measurements 2 µl [14C] phenylalanine (specific activity 9,5 dpm/pmol) and for determination of miscoding activity 2 µl [3H]-leucine (specific activity 9,5 dpm/pmol) were added. After 30 min incubation, incorporated radioactivity was measured as described in Section 4.2.7. The result of the negative control (without poly(U) mRNA) was subtracted from the result of the reaction containing poly(U) mRNA. Elongation activity of wt was set to 100 % and the activity of the mutant strain calculated accordingly. Misincorporation was

determined by calculating the ratio of incorporated leucine over phenylalanine, followed by the determination of the percentual increase in misincorporation of the mutant extract in comparison to wt. Results are the mean of at least three independent experiments.

4.2.8 *In Vivo* Translation Activity by Labelling with [35S] Methionine

Cells were grown to mid-log phase. 4 OD_{600} were pelleted and resuspended in 0.2 ml of YPD. Cells were labeled with 10 µCi [35S] methionine for up to 30 min at 30°C. Samples of 30 µl were taken at indicated time points and NaOH and β-mercaptoethanol added to final concentration of 0.5M and 1 %, respectively. Precipitation and Filtration was done as described in Section 4.2.7. Results are the mean of four independent experiments of two independent spores.

4.2.9 *In Vitro* Translation Initiation Assay

Three A_{260} of translation active extract were incubated with 6.25 µg creatin kinase for 5 min on ice, followed by 30 min incubation with 1.25 mM EGTA, 2 mM MgOAc, 76 mM KCl, 0.4 mM GTP, 1 mM ATP, 50 µM of each AA, 12.5 mM creatin phosphate, 1 mM cycloheximide, 8 U RNAse inhibitor, 35 ng of *in vitro* transcribed radioactive mRNA and, where indicated, 1.25 mM GMP-PNP in a total volume of 120 µl at RT. The entire reaction was loaded on a 5-25 % sucrose gradient and centrifuged at 38000 rpm (SW40 Ti rotor) for 2.45 h. 450 µl fractions were taken off and 300 µl of each fraction were counted with 3 ml of scintillation cocktail.

4.2.10 Dual Luciferase Assay

Yeast cells transformed with the corresponding dual luciferase reporters were grown until an OD_{600} of 0.5. Yeast cells of 20 µl, 15 µl, 10 µl and 5 µl aliquots were transferred to black 96-well plates. For measurement of the dual luciferase activity, the Dual-Luciferase®Reporter Assay System (Promega) was used according to the manufacturer's instructions in a Centro LB 960 plate reader (Berthold) with the following

settings: inject 50 µl of passive lysis buffer, shake 2 s, wait 10 s, inject 30 µl solution I, shake 2 s, measure for 8 s, inject 30 µl stop&glow, shake 2 s and measure for 4 s. The results are the mean of at least six independently prepared measurements.

4.2.11 SDS-PAGE and Western Blotting

SDS-PAGE

Sodium dodecylsulfate polyacrylamide gel electrophoresis (SDS-PAGE) was done according to Laemmli (Laemmli, 1970) using the Mini-Protean II system (Biorad). After electrophoresis, separated proteins were either transferred to a membrane (Western blot) or directly stained with Coomassie.

Western Blotting

For blotting, the proteins were transferred onto a PVDF membrane using a wet blotting device. For this, 3 layers of Whatman paper followed by the methanol activated PVDF membrane, the SDS-PAGE gel and another 3 layers of Whatman paper, all presoaked in wet blotting buffer, were assembled in the blotting machine (Biorad). The transfer occurred at 100V for 60-70 min. After transfer, the membrane was blocked with blocking buffer (2 % milk powder and optional 2 % BSA in TBS-T) and incubated with the primary antibody at 4°C overnight. The antibody was removed by washing the membrane with blocking buffer at RT for 45 min. Then, the membrane was incubated with the corresponding secondary antibody at RT for at least 2 h. The immunostained proteins were detected with ECL kit (Applichem). After exposure of the membrane the light sensitive films were developed with a Kodak X omat M35 developing machine.

4.2.12 β-Galactosidase Assay

Yeast cells transformed with the corresponding lacZ-fusion reporters were grown until log phase. Cells were lysed in Z-buffer (60 mM Na_2HPO_4, 40 mM Na_2HPO_4, 10 mM KCl, 1 mM $MgSO_4$, pH 7) by three freeze and thaw cycles. The hydrolysis of Onitrophenylgalactopyranoside (ONPG) was assayed as described (Miller, 1972). Briefly, 10 µl lysate were added to 125 µl Z-Buffer containing 40 mM β-mercaptoethanol and 25 µl

4 mg/ml ONPG in Z-Buffer. Reactions were carried out in triplicates in honeycombe2 plates using a Bioscreen C Analyzer. β-galactosidase activity was calculated from at least four independent experiments.

4.2.13 Yeast Growth Curves

Growth curves under different conditions were monitored using a Bioscreen C Analyzer. 10 µl of stationary phase yeast culture were used to inoculate 300 µl of SDC containing the indicated drugs and conditions in Honeycomb2 plates. Growth curves were measured at 30℃ under continuous shaking for two days. The optical density was measured using an wideband filter of 420-580 nm. All experiments were carried out using two independent spores in triplicates and at least twice at different positions on the Honeycomb2 plates. The observed OD values (OD_{obs}), from which the blank (OD recorded with corresponding medium) value has been subtracted, were corrected for the non-linearity at higher cell densities using the formula $OD_{cor} = OD_{obs} + 0.449(OD_{obs})^2 + 0.191(OD_{obs})^3$. Doubling times were estimated according to Warringer and Blomberg (2003): OD_{cor} values were $\log_{10}$ transformed. A slope was calculated between every third consecutive measurement. The doubling time was calculated as $\log_{10}$ 2 divided by the mean of the slopes during logarithmic growth.

References

Aitken, C. E. and Lorsch, J. R. (2012). A mechanistic overview of translation initiation in eukaryotes. *Nat Struc Mol Biol*, 19(6):568–576.

Algire, M. A., Maag, D., and Lorsch, J. R. (2005). Pi Release from eIF2, Not GTP Hydrolysis, Is the Step Controlled by Start-Site during Eukaryotic Translation Initiation. *Mol Cell*, 20(2):251–262.

Alting-Mees, M. A. and Short, J. M. (1989). pBluescript II:gene mapping vectors. *Nucleic Acids Res*, 17(22):9494.

Altmann, M. and Linder, P. (2010). Power of Yeast for Analysis of Eukaryotic Translation Initiation. *J Biol Chem*, 285(42):31907–31912.

Altmann, M. and Trachsel, H. (1997). Translation Initiation Factor-Dependent Extracts from Yeast Saccharomyces cerevisiae. *Methods*, 11(4):343–352.

Asano, K., Clayton, J., Shalev, A., and Hinnebusch, A. G. (2000). A multifactor complex of eukaryotic initiation factors, eIF1, eIF2, eIF3, eIF5, and initiator tRNAMet is an important translation initiation intermediate in vivo. *Genes Dev*, 14(19):2534–2546.

Avraham, R. and Yarden, Y. (2011). Feedback regulation of EGFR signalling: decision making by early and delayed loops. *Nat Rev Mol Cell Biol*, 12(2):104–117.

Baierlein, C. and Krebber, H. (2010). Translation termination: New factors and insights. *RNA Biol*, 7(5):548–550.

Ballesta, J. P., Rodriguez-Gabriel, M. A., Bou, G., Briones, E., Zambrano, R., and Remacha, M. (1999). Phosphorylation of the yeast ribosomal stalk. Functional effects and enzymes involved in the process. *FEMS Microbiol Rev*, 23(5):537–550.

Becker, T., Franckenberg, S., Wickles, S., Shoemaker, C. J., Anger, A. M., Armache, J. P., Sieber, H., Ungewickell, C., Berninghausen, O., Daberkow, I., Karcher, A., Thomm, M., Hopfner, K. P., Green, R., and Beckmann, R. (2012). Structural basis of highly conserved ribosome recycling in eukaryotes and archaea. *Nature*, 482(7386):501–506.

Beckmann, K., Grskovic, M., Gebauer, F., and Hentze, M. W. (2005). A Dual Inhibitory Mechanism Restricts msl-2 mRNA Translation for Dosage Compensation in Drosophila. *Cell*, 122(4):529–540.

Ben-Shem, A., Garreau de Loubresse, N., Melnikov, S., Jenner, L., Yusupova, G., and Yusupov, M. (2011). The Structure of the Eukaryotic Ribosome at 3.0 Å Resolution. *Science*, 334(6062):1524–1529.

Berthelot, K., Muldoon, M., Rajkowitsch, L., Hughes, J., and McCarthy, J. E. G. (2004). Dynamics and processivity of 40S ribosome scanning on mRNA in yeast. *Mol Microbiol*, 51(4):987–1001.

Black, D. L. (2003). Mechanisms of alternative pre-messenger RNA splicing. *Annu Rev Biochem*, 72(1):291–336.

Bloemink, M. J. and Moore, P. B. (1999). Phosphorylation of Ribosomal Protein L18 Is Required for Its Folding and Binding to 5S rRNA. *Biochemistry*, 38(40):13385–13390.

Bodenmiller, B., Campbell, D., Gerrits, B., Lam, H., Jovanovic, M., Picotti, P., Schlapbach, R., and Aebersold, R. (2008). PhosphoPep – a database of protein phosphorylation sites in model organisms. *Nat Biotech*, 26(12):1339–1340.

Bodenmiller, B., Malmstrom, J., Gerrits, B., Campbell, D., Lam, H., Schmidt, A., Rinner, O., Mueller, L. N., Shannon, P. T., Pedrioli, P. G., Panse, C., Lee, H.-K., Schlapbach, R., and Aebersold, R. (2007). PhosphoPep – a phosphoproteome resource for systems biology research in Drosophila Kc167 cells. *Mol Syst Biol*, 3:1–11.

Campos, F., Corona-Reyes, M., and Zinker, S. (1990). The yeast 5S rRNA binding ribosomal protein YL3 is phosphorylated in vivo. *Biochim Biophys Acta*, 1087(2):142–146.

Castilho-Valavicius, B., Yoon, H., and Donahue, T. F. (1990). Genetic characterization of the Saccharomyces cerevisiae translational initiation suppressors sui1, sui2 and SUI3 and their effects on HIS4 expression. *Genetics*, 124(3):483–95.

Cech, T. R. (2000). The Ribosome Is a Ribozyme. *Science*, 289(5481):878–879.

Chen, M. and Manley, J. L. (2009). Mechanisms of alternative splicing regulation: insights from molecular and genomics approaches. *Nat Rev Mol Cell Biol*, 10(11):741–754.

Cheung, Y.-N., Maag, D., Mitchell, S. F., Fekete, C. A., Algire, M. A., Takacs, J. E., Shirokikh, N., Pestova, T., Lorsch, J. R., and Hinnebusch, A. G. (2007). Dissociation of eIF1 from the 40S ribosomal subunit is a key step in start codon selection in vivo. *Genes Dev*, 21(10):1217–1230.

Choudhary, C. and Mann, M. (2010). Decoding signalling networks by mass spectrometry-based proteomics. *Nat Rev Mol Cell Biol*, 11(6):427–439.

Cohen, P. (2000). The regulation of protein function by multisite phosphorylation – a 25 year update. *Trends in Biochemical Sciences*, 25(12):596–601.

Cox, J. and Mann, M. (2008). MaxQuant enables high peptide identification rates, individualized p.p.b.-range mass accuracies and proteome-wide protein quantification. *Nat Biotech*, 26(12):1367–1372.

Deribe, Y. L., Pawson, T., and Dikic, I. (2010). Post-translational modifications in signal integration. *Nat Struct Mol Biol*, 17(6):666–672.

Dever, T., Dar, A., and Sicheri, F. (2007). *Translational Control in Biology and Medicine*. Cold Spring Harbor Laboratory Press, New York.

Dever, T. E. (2002). Gene-Specific Regulation by General Translation Factors. *Cell*, 108(4):545–556.

Dresios, J., Derkatch, I. L., Liebman, S. W., and Synetos, D. (2000). Yeast Ribosomal Protein L24 Affects the Kinetics of Protein Synthesis and Ribosomal Protein L39 Improves Translational Accuracy, While Mutants Lacking Both Remain Viable. *Biochemistry*, 39(24):7236–7244.

Fekete, C. A., Mitchell, S. F., Cherkasova, V. A., Applefield, D., Algire, M. A., Maag, D., Saini, A. K., Lorsch, J. R., and Hinnebusch, A. G. (2007). N- and C-terminal residues of eIF1A have opposing effects on the fidelity of start codon selection. *EMBO J*, 26(6):1602–1614.

Ficarro, S. B., McCleland, M. L., Stukenberg, P. T., Burke, D. J., Ross, M. M., Shabanowitz, J., Hunt, D. F., and White, F. M. (2003). Phosphoproteome analysis by mass spectrometry and its application to Saccharomyces cerevisiae. *Nat Biotech*, 20(3):301–305.

Fischer, E. H. and Krebs, E. G. (1955). Conversion of phosphorylase B to phosphorylase a in muscle extracts. *J Biol Chem*, 216(1):121–132.

Galkin, O., Bentley, A. A., Gupta, S., Compton, B.-A., Mazumder, B., Kinzy, T. G., Merrick, W. C., Hatzoglou, M., Pestova, T. V., Hellen, C. U., and Komar, A. A. (2007). Roles of the negatively charged N-terminal extension of Saccharomyces cerevisiae ribosomal protein S5 revealed by characterization of a yeast strain containing human ribosomal protein S5. *RNA*, 13(12):2116–2128.

Gebauer, F. and Hentze, M. W. (2004). Molecular mechanisms of translational control. *Nat Rev Mol Cell Biol*, 5(10):827–835.

Gilbert, W. V., Zhou, K., Butler, T. K., and Doudna, J. A. (2017). Cap-Independent Translation Is Required for Starvation-Induced Differentiation in Yeast. *Science*, 317(5842):1224–1227.

Gnad, F., de Godoy, L. M. F., Cox, J., Neuhauser, N., Ren, S., Olsen, J. V., and Mann, M. (2009). High-accuracy identification and bioinformatic analysis of in vivo protein phosphorylation sites in yeast. *Proteomics*, 9(20):4642–4652.

Gnad, F., Ren, S., Cox, J., Olsen, J. V., Macek, B., Oroshi, M., and Mann, M. (2007). PHOSIDA (phosphorylation site database): management, structural and evolutionary investigation, and prediction of phosphosites. *Genome Biol*, 8(11):R250.

Gruhler, A., Olsen, J. V., Mohammed, S., Mortensen, P., Frgeman, N. J., Mann, M., and Jensen, O. N. (2005). Quantitative Phosphoproteomics Applied to the Yeast Pheromone Signaling Pathway. *Mol Cell Proteomics*, 4(3):310–327.

Hager, J. W. and Dinman, J. D. (2003). An in vivo dual-luciferase assay system for studying translational recoding in the yeast Saccharomyces cerevisiae. *RNA*, 9(9):1019–1024.

Hebert, J., Pierre, M., and Loeb, J. E. (1977). Phosphorylation in vitro and in vivo of Ribosomal Proteins from Saccharomyces cerevisiae. *Eur J Biochem*, 72(1):164–174.

Hinnebusch, A. G. (2005). Translation regulation of Gcn4 and the general amino acid control of yeast. *Annu Rev Microbiol*, 59(1):407–450.

Hinnebusch, A. G. (2006). eIF3: a versatile scaffold for translation initiation complexes. *Trends Biochem Sci*, 31(10):553–562.

Hinnebusch, A. G. (2011). Molecular Mechanism of Scanning and Start Codon Selection in Eukaryotes. *Microbiol Mol Biol Rev*, 75(3):434–467.

Huang, H. k., Yoon, H., Hannig, E. M., and Donahue, T. F. (1997). GTP hydrolysis controls stringent selection of the AUG start codon during translation initiation in Saccharomyces cerevisiae. *Genes Dev*, 11(18):2396–2413.

Hunter, T. (2000). Signaling – 2000 and Beyond. *Cell*, 100(1):113–127.

Iost, I., Dreyfus, M., and Linder, P. (1999). Ded1p, a DEAD-box Protein Required for Translation Initiation in Saccharomyces cerevisiae, Is an RNA Helicase. *J Biol Chem*, 274(25):17677–17683.

Ivanov, I. P., Loughran, G., Sachs, M. S., and Atkins, J. F. (2010). Initiation context modulates autoregulation of eukaryotic translation initiation factor 1 (eIF1). *Proc Natl Acad Sci*, 107(42):18056–18060.

Jackson, R. J., Hellen, C. U., and Pestova, T. V. (2010). The mechanism of eukaryotic translation initiation and principles of its regulation. *Nat Rev Mol Cell Biol*, 11(2):113–127.

Jamieson, D. J. and Beggs, J. D. (1991). A suppressor of yeast spp81/ded1 mutations encodes a very similar putative ATP-dependent RNA helicase. *Mol Microbiol*, 5(4):805–812.

Johnson, L. N. and Lewis, R. J. (2001). Structural Basis for Control by Phosphorylation. *Chem Rev*, 101(8):2209–2242.

Johnson, S. and Warner, J. (1987). Phosphorylation of the Saccharomyces cerevisiae equivalent of ribosomal protein S6 has no detectable effect on growth. *Mol Cell Biol*, 7(4):1338–1345.

Jorissen, R., Walker, F., Puoliot, N., Garrett, T., Ward, C., and Burgess, A. (2003). Epidermal growth factor receptor: mechanisms of activation and signalling. *Exp Cell Res*, 284(1):31–53.

Knop, M., Finger, A., Braun, T., Hellmuth, K., and Wolf, D. H. (1996). Der1, a novel protein specifically required for endoplasmtic reticulum degradation in yeast. *EMBO J*, 15(4):753–763.

Kohler, A. and Hurt, E. (2007). Exporting RNA from the nucleus to the cytoplasm. *Nat Rev Mol Cell Biol*, 8(10):761–773.

Kosako, H. and Nagano, K. (2011). Quantitative phosphoproteomics strategies for understanding protein kinase-mediated signal transduction pathways. *Expert Review of Proteomics*, 8(1):81–94.

Kozak, M. (1978). How do eukaryotic ribosomes select initiation regions in messenger RNA? *Cell*, 15(4):1109–1123.

Kozak, M. (1986). Bifunctional messenger RNAs in eukaryotes. *Cell*, 47(4):481–483.

Kramer, G., Boehringer, D., Ban, N., and Bukau, B. (2009). The ribosome as a platform for co-translational processing, folding and targeting of newly synthesized proteins. *Nat Struct Mol Biol*, 16(6):589–597.

Krebs, E. G. and Beavo, J. A. (1979). Phosphorylation-Dephosphorylation of Enzymes. *Annu Rev Biochem*, 48(1):923–959.

Krüger, M., Kratchmarova, I., Blagoev, B., Tseng, Y.-H., Kahn, C. R., and Mann, M. (2008). Dissection of the insulin signaling pathway via quantitative phosphoproteomics. *Proc Natl Acad Sci*, 105(7):2451–2456.

Kruiswijk, T., de Hey, J., and Planta, R. (1978). Modification of yeast ribosomal proteins. Phosphorylation. *Biochem J*, 175(1):213–219.

La Teana, A., Gualerzi, C. O., and Brimacombe, R. (1995). From stand-by to decoding site. Adjustment of the mRNA on the 30S ribosomal subunit under the influence of the initiation factors. *RNA*, 1(8):772–782.

Laemmli, U. (1970). Cleavage of structural proteins during the assembly of the head of bacteriophage T4. *Nature*, 227(5259):680–685.

Leibowitz, M., Barbone, F., and Georgopoulos, D. (1991). In vitro protein synthesis. *Methods Enzym*, 194:536– 545.

Livak, K. J. and Schmittgen, T. D. (2001). Analysis of Relative Gene Expression Data Using Real-Time Quantitative PCR and the $2^{-\Delta\Delta CT}$ Method. *Methods*, 25(4):402–408.

Loewith, R. and Hall, M. N. (2011). Target of Rapamycin (TOR) in Nutrient Signaling and Growth Control. *Genetics*, 189(4):1177–1201.

Lorsch, J. R. and Dever, T. E. (2010). Molecular View of 43 S Complex Formation and Start Site Selection in Eukaryotic Translation Initiation. *J Biol Chem*, 285(28):21203–21207.

Lorsch, J. R. and Herschlag, D. (1999). Kinetic dissection of fundamental processes of eukaryotic translation initiation in vitro. *EMBO J*, 18(23):6705–6717.

Lumsden, T., Bentley, A. A., Beutler, W., Ghosh, A., Galkin, O., and Komar, A. A. (2009). Yeast strains with N-terminally truncated ribosomal protein S5: implications for the evolution, structure and function of the Rps5/Rps7 proteins. *Nucleic Acids Res*, pages 1–12.

Maag, D., Algire, M. A., and Lorsch, J. R. (2006). Communication between Eukaryotic Translation Initiation Factors 5 and 1A within the Ribosomal Pre-initiation Complex Plays a Role in Start Site Selection. *J Mol Biol*, 356(3):724–737.

Maag, D., Fekete, C. A., Gryczynski, Z., and Lorsch, J. R. (2005). A Conformational Change in the Eukaryotic Translation Preinitiation Complex and Release of eIF1 Signal Recognition of the Start Codon. *Mol Cell*, 17(2):265–275.

Macek, B., Mann, M., and Olsen, J. V. (2009). Global and Site-Specific Quantitative Phosphoproteomics: Principles and Applications. *Annu Rev Pharmaco Toxicol*, 49(1):199–221.

Mann, M. and Jensen, O. N. (2003). Proteomic analysis of post-translational modifications. *Nat Biotech*, 21(3):255–261.

Manning, G., Whyte, D. B., Martinez, R., Hunter, T., and Sudarsanam, S. (2002). The Protein Kinase Complement of the Human Genome. *Science*, 298(5600):1912–1934.

Martin, D. E. and Hall, M. N. (2005). The expanding TOR signaling network. *Curr Opin Cell Biol*, 17(2):158–166.

Martin-Marcos, P., Cheung, Y.-N., and Hinnebusch, A. G. (2011). Functional Elements in Initiation Factors 1, 1A, and 2 Discriminate against Poor AUG Context and Non-AUG Start Codons. *Mol Cell Biol*, 31(23):4814–4831.

Melnikov, S., Ben-Shem, A., Garreau de Loubresse, N., Jenner, L., Yusupova, G., and Yusupov, M. (2012). One core, two shells: bacterial and eukaryotic ribosomes. *Nat Struc Mol Biol*, 19(6):560–567.

Meskauskas, A. and Dinman, J. D. (2007). Ribosomal Protein L3: Gatekeeper to the A Site. *Mol Cell*, 25(6):877–888.

Miller, J. H. (1972). *Experiments in Molecular Genetics*. Cold Spring Harbor Laboratory Press, New York.

Miller, J. L., Cimen, H., Koc, H., and Koc, E. C. (2009). Phosphorylated Proteins of the Mammalian Mitochondrial Ribosome: Implications in Protein Synthesis. *Journal of Proteome Research*, 8(10):4789–4798.

Mitchell, S. F. and Lorsch, J. R. (2008). Should I Stay or Should I Go? Eukaryotic Translation Initiation Factors 1 and 1A Control Start Codon Recognition. *J Biol Chem*, 283(41):27345–27349.

Nanda, J. S., Cheung, Y.-N., Takacs, J. E., Martin-Marcos, P., Saini, A. K., Hinnebusch, A. G., and Lorsch, J. R. (2009). eIF1 Controls Multiple Steps in Start Codon Recognition during Eukaryotic Translation Initiation. *J Mol Biol*, 394(2):268–285.

Nita-Lazar, A., Saito-Benz, H., and White, F. M. (2008). Quantitative phosphoproteomics by mass spectrometry: Past, present, and future. *Proteomics*, 8(21):4433–4443.

Olsen, J. V., Blagoev, B., Gnad, F., Macek, B., Kumar, C., Mortensen, P., and Mann, M. (2006). Global, In Vivo, and Site-Specific Phosphorylation Dynamics in Signaling Networks. *Cell*, 127(3):635–648.

Olsen, J. V., Vermeulen, M., Santamaria, A., Kumar, C., Miller, M. L., Jensen, L. J., Gnad, F., Cox, J., Jensen, T. S., Nigg, E. A., Brunak, S., and Mann, M. (2010). Quantitative Phosphoproteomics Reveals Widespread Full Phosphorylation Site Occupancy During Mitosis. *Sci Signal*, 3(104):ra3.

Ong, S.-E., Blagoev, B., Kratchmarova, I., Kristensen, D. B., Steen, H., Pandey, A., and Mann, M. (2002). Stable Isotope Labeling by Amino Acids in Cell Culture, SILAC, as a Simple and Accurate Approach to Expression Proteomics. *Mol Cell Proteomics*, 1(5):376–386.

Ong, S.-E. and Mann, M. (2005). Mass spectrometry-based proteomics turns quantitative. *Nat Chem Biol*, 1(5):252–262.

Passmore, L. A., Schmeing, T. M., Maag, D., Applefield, D. J., Acker, M. G., Algire, M. A., Lorsch, J. R., and Ramakrishnan, V. (2007). The Eukaryotic Translation Initiation Factors eIF1 and eIF1A Induce an Open Conformation of the 40S Ribosome. *Mol Cell*, 26(1):41–50.

Pestova, T. V. and Hellen, C. U. (2003). Translation elongation after assembly of ribosomes on the Cricket paralysis virus internal ribosomal entry site without initiation factors or initiator tRNA. *Genes Dev*, 17(2):181–186.

Pestova, T. V. and Kolupaeva, V. G. (2002). The roles of individual eukaryotic translation initiation factors in ribosomal scanning and initiation codon selection. *Genes Dev*, 16(22):2906–2922.

Pierrat, O., Mikitova, V., Bush, M., Browning, K., and Doonan, J. (2007). Control of protein translation by phosphorylation of the mRNA 5'-cap-binding complex. *Biochem Soc Trans*, 35(6):1634–1637.

Pisarev, A. V., Hellen, C. U., and Pestova, T. V. (2007). Recycling of Eukaryotic Posttermination Ribosomal Complexes. *Cell*, 131(2):286–299.

Pisarev, A. V., Kolupaeva, V. G., Pisareva, V. P., Merrick, W. C., Hellen, C. U., and Pestova, T. V. (2006). Specific functional interactions of nucleotides at key -3 and +4 positions flanking the initiation codon with components of the mammalian 48S translation initiation complex. *Genes Dev*, 20(5):624–636.

Pisarev, A. V., Kolupaeva, V. G., Yusupov, M. M., Hellen, C. U., and Pestova, T. V. (2008). Ribosomal position and contacts of mRNA in eukaryotic translation initiation complexes. *EMBO J*, 27(11):1609–1621.

Pisarev, A. V., Skabkin, M. A., Pisareva, V. P., Skabkina, O. V., Rakotondrafara, A. M., Hentze, M. W., Hellen, C. U., and Pestova, T. V. (2010). The Role of ABCE1 in Eukaryotic Posttermination Ribosomal Recycling. *Mol Cell*, 37(2):196–210.

Proud, C. G. (2007). Signaling to translation: how signal transduction pathways control the protein synthetic machinery. *Biochem J*, 403:217–234.

Rabl, J., Leibundgut, M., Ataide, S. F., Haag, A., and Ban, N. (2011). Crystal Structure of the Eukaryotic 40S Ribosomal Subunit in Complex with Initiation Factor 1. *Science*, 331(6018):730–736.

Ross, P. L., Huang, Y. N., Marchese, J. N., Williamson, B., Parker, K., Hattan, S., Khainovski, N., Pillai, S., Dey, S., Daniels, S., Purkayastha, S., Juhasz, P., Martin, S., Bartlet-Jones, M., He, F., Jacobson, A., and Pappin, D. J. (2004). Multiplexed Protein Quantitation in Saccharomyces cerevisiae Using Amine-reactive Isobaric Tagging Reagents. *Mol Cell Proteomics*, 3(12):1154–1169.

Rother, S. and Strasser, K. (2007). The RNA polymerase II CTD kinase Ctk1 functions in translation elongation. *Genes Dev*, 21(11):1409–1421.

Ruvinsky, I. and Meyuhas, O. (2006). Ribosomal protein S6 phosphorylation: from protein synthesis to cell size. *Trends Biochem Sci*, 31(6):342–348.

Saini, A. K., Nanda, J. S., Lorsch, J. R., and Hinnebusch, A. G. (2010). Regulatory elements in eIF1A control the fidelity of start codon selection by modulating tRNAiMet binding to the ribosome. *Genes Dev*, 24(1):97–110.

Salas-Marco, J. and Bedwell, D. M. (2005). Discrimination Between Defects in Elongation Fidelity and Termination Efficiency Provides Mechanistic Insights into Translational Readthrough. *J Mol Biol*, 348(4):801–815.

Sambrook, J. and Russell, D. W. (2001). *Molecular Cloning: A Laboratory Manual*. Cold Spring Harbor Laboratory Press, New York.

Schäfer, T., Maco, B., Petfalski, E., Tollervey, D., Bttcher, B., Aebi, U., and Hurt, E. (2006). Hrr25-dependent phosphorylation state regulates organization of the pre-40S subunit. *Nature*, 441(7093):651–655.

Shabalina, S. A., Ogurtsov, A. Y., Rogozin, I. B., Koonin, E. V., and Lipman, D. J. (2004). Comparative analysis of orthologous eukaryotic mRNAs: potential hidden functional signals. *Nucleic Acids Res*, 32(5):1774–1782.

Sikorski, R. and Hieter, P. (1989). A system of shuttle vectors and yeast host strains designed for efficient manipulation of DNA in Saccharomyces cerevisiae. *Genetics*, 122(1):19–27.

Sims, R. J. and Reinberg, D. (2008). Is there a code embedded in proteins that is based on post-translational modifications? *Nat Rev Mol Cell Biol*, 9(10):815–820.

Sonenberg, N. and Hinnebusch, A. G. (2007). New Modes of Translational Control in Development, Behavior, and Disease. *Mol Cell*, 28(5):721–729.

Sonenberg, N. and Hinnebusch, A. G. (2009). Regulation of Translation Initiation in Eukaryotes Mechanisms and Biological Targets. *Cell*, 136(4):731–745.

Soung, G. Y., Miller, J. L., Koc, H., and Koc, E. C. (2009). Comprehensive Analysis of Phosphorylated Proteins of Escherichia coli Ribosomes. *J Proteome Res*, 8(7):3390–3402.

Stansfield, I., Jones, K., Herbert, P., Lewendon, A., Shaw, W., and Tuite, M. (1998). Missense translation errors in Saccharomyces cerevisiae. *J Mol Biol*, 282(1):13–24.

Svejstrup, J. Q. (2004). The RNA polymerase II transcription cycle: cycling through chromatin. *Biochim Biophys Acta*, 1677(13):64–73.

Takyar, S., Hickerson, R. P., and Noller, H. F. (2005). mRNA Helicase Activity of the Ribosome. *Cell*, 120(1):49–58.

Tuite, Michael, F. and Plesset, J. (1986). mRNA-dependent yeast cell-free translation systems: theory and practice. *Yeast*, 2:35–52.

Valasek, L., Nielsen, K. H., Zhang, F., Fekete, C. A., and Hinnebusch, A. G. (2004). Interactions of Eukaryotic Translation Initiation Factor 3 (eIF3) Subunit NIP1/c with eIF1 and eIF5 Promote Preinitiation Complex Assembly and Regulate Start Codon Selection. *Molecular and Cellular Biology*, 24(21):9437–9455.

Vergé, V., Vonlanthen, M., Masson, J.-M., Trachsel, H., and Altmann, M. (2004). Localization of a promoter in the putative internal ribosome entry site of the Saccharomyces cerevisiae TIF4631 gene. *RNA*, 10(2):277–286.

Wallis, J. W., Chrebet, G., Brodsky, G., Rolfe, M., and Rothstein, R. (1989). A hyper-recombination mutation in S. cerevisiae identifies a novel eukaryotic topoisomerase. *Cell*, 58(2):409–419.

Walsh, C. T., Garneau-Tsodikova, S., and Gatto, G. J. J. (2006). Protein Posttranslational Modifications: The Chemistry of Proteome Diversifications. *ChemInform*, 37(7):1522–2667.

Walsh, D. A., Perkins, J. P., and Krebs, E. G. (1968). An Adenosine 3',5'-Monophosphate-dependant Protein Kinase from Rabbit Skeletal Muscle. *J Biol Chem*, 243(13):3763–3765.

Warringer, J. and Blomberg, A. (2003). Automated screening in environmental arrays allows analysis of quantitative phenotypic profiles in Saccharomyces cerevisiae. *Yeast*, 20(1):53–67.

Wilson, J. E., Powell, M. J., Hoover, S. E., and Sarnow, P. (2000). Naturally Occurring Dicistronic Cricket Paralysis Virus RNA Is Regulated by Two Internal Ribosome Entry Sites. *Mol Cell Biol*, 20(14):4990–4999.

Wullschleger, S., Loewith, R., and Hall, M. N. (2006). TOR Signaling in Growth and Metabolism. *Cell*, 124(3):471–484.

Abbreviations

3-AT	3-amino-1,2,4-triazole
A	alanine, adenine
aa	amino acid
aa-tRNA	aminoacyl-tRNA
A-site	acceptor site of the ribosomal
ATP	adenosine triphosphate
β-ME	β-mercaptoethanol
bp	basepair
C	cytosine
CDK	cyclin dependent kinase
CH	cyclohximide
CrPV	Cricket Paralysis Virus
D	aspartate
DNA	deoxyribonucleic acid
dNTP	desoxyribonucleosid triphosphate
4E-BP	eIF4E binding protein
ECL	enhanced chemiluminescence
E. coli	*Escherichia coli*
eEF	eukaryotic elongation factor
EGF(R)	epidermal growth factor (receptor)
eIF	eukaryotic initiation factor
ER	endoplasmic reticulum
E-site	exit site of the ribosome
et al.	et alia (and others)
FDR	false discovery rate
FOA	5-fluoorotic acid
G	guanine
Gcn2	general control non derepressable 2
GAP	GTPase activating protein
GTP / GDP	guanosine triphosphate / diphosphate
H	histidine
HRI	Heme-regulated eIF2α kinase
IC	initiation complex
IRES	internal ribosome entry site

LB	Luria-Bertani
LC-MS/MS	liquid chromatography-tandem mass spectrometry
MAPK	mitogen-activated protein kinase
Met	methionine
Met-tRNAi	methionyl initiator tRNA
MFC	multi factor complex
mRNA	messenger ribonucleic acid
mRNP	messenger ribonucleoprotein
(m)TOR	(mammalian) target of rapamycin
nt	nucleotide
OD	optical density
ORF	open reading frame
PAGE	polyacrylamide gel electrophoresis
PCR	polymerase chain reaction
PERK	PKR-like ER-localized eIF2α kinase
pH	potential of hydrogen
PKR	protein kinase R
PI3K	phosphatidylinositol 3-kinase
PIC	pre-initiation complex
P-site	peptidyl site of the ribosome
PTM	posttranslational modification
Q	glutamine
R	arginine
RNA	ribonucleic acid
Rpl	ribosomal protein of the large subunit
Rps	ribosomal protein of the small subunit
RT	room temperature
S	svedberg, serine
SDC	synthetic complete medium
SDS	sodium dodecyl-sulfate
SH2	Src-homology-2
SILAC	Stable Isotope Labelling with Amino Acids in Cell Culture
T	threonine, thymine
TC	ternary complex
TCA	trichloroacidic acid
tRNA	transfer RNA
U	uracil
UPR	unfolded protein response
UTR	untranslated region
WCE	whole cell extracts
wt	wild-type
Y	tyrosine
YPD	yeast extract, peptone, glucose containing medium

Acknowledgement

I would like to thank ...

... first of all, Katja Sträßer for giving me the opportunity to work on this challenging project. I am grateful for her constant support, endless discussions and scientific exchange, for believing in the project and especially for allowing me to work so independently and follow my own ideas.

... the members of my Thesis Advisory Committee: Elena Conti, Roland Beckmann and Daniel Wilson for constructive and fruitful discussions. Especially, I am grateful to Roland Beckmann for his support and for being the second examiner of my thesis.

... the Stiftung Stipendien-Fonds des VCI for granting me one of their Kekulé Ph.D. fellowships and the continuous support during the last years.

... IMPRS-LS for support, scientific exchange, excellent workshops and seminars.

... Our collaborators Jesper Olsen and Matthias Mann for the phosphoprotoemic analysis.

... all the members of the Sträßer lab – present and past. Special thanks to Britta, my translation partner, for introducing me into the wide field of translation, always being willing to help, and your positive view of life! Lina, thank you for endless discussions, the nice atmosphere you created in the outstation and for always being there. Thanks to Connie, Dominik, Anja, Max, Viter, Sittinan, Chiara and Shivendra for being so wonderful colleagues, all the help and the nice working atmosphere. My students Andi and Nadine I would like to thank for giving me the opportunity to teach them and for the great job they did.

... Juliane, I always enjoyed working with you. Thank you for the great time we had together, playing badminton, doing yoga and after-work fitness and especially the lunch breaks. And of course the excellent scientific job you did, without you this would not have been possible!

Besonders danken möchte ich...

... meiner Familie, alte und neue, für ihr Verständnis, ihre Unterstützung und ihre Geduld, mit der sie mich durch die Doktorarbeit begleitet haben. Ganz lieben Dank an meine Eltern für die Unterstützung im letzten Jahr, dass Ihr euch so lieb um Theo kümmert.

... Theo, Du bist das größte Glück für mich!

... Christian für seine grenzenlose Unterstützung und Geduld in guten und in schlechten Tagen. Danke, dass es Dich gibt!

Curriculum Vitae

Katharina Maria Brünger

Birthname	Apfel
Date of Birth	November 16, 1983
Place of Birth	Bad Mergentheim, Germany
Nationality	German

Education

since 06/2008	**Ludwig-Maximilians-Universität Munich**, Germany Ph.D. thesis at the Gene Center, Department of Biochemistry Supervisor: Dr. Katja Sträßer
10/2003 - 03/2008	**Julius-Maximilians-Universität Würzburg**, Germany
07/2008	Diplom, Chemistry
07/2007 - 03/2008	Diploma thesis, Institut für Biochemie, Universität Würzburg Supervisor: Prof. Dr. Utz Fischer
09/1994 - 06/2003	**Abitur**, Martin-Schleyer-Gymnasium Lauda-Königshofen, Germany

Awards and Fellowships

06/2010	**60th Interdisciplinary Meeting of Nobel Laureates** at Lindau, Germany
04/2009 - 06/2012	**Kekulé Fellowship** Fonds der Chemischen Industrie
since 06/2008	**International Max Planck Research School for Life Sciences** (IMPRS-LS)
07/2008	**Matthias Manger Preis** Universität Würzburg (Diplom)
07/2005	**Fakultätspreis** der Fakultät für Chemie und Pharmazie, Universität Würzburg (Vordiplom)

Appendix

Table A.1: Phosphorylation sites in ribosomal protins identified by phosphoproteomics

Protein	Position	pSite Class	Sequence Window	Matching Kinase and binding Motifs	Intensity
YGR214W	219	2	QVAEEATTEEAGE	CK2	4,2E+05
YGR214W	220	2	VAEEATTEEAGEE	FHA KAPP	4,2E+05
YGR214W	103	1	PIAGRFTPGSFTN	Proline-directed, FHA KAPP, PKA	8,8E+05
YGR214W	112	1	SFTNYITRSFKEP		1,1E+06
YGR214W	114	1	TNYITRSFKEPRL	CK2	9,4E+05
YMR230W	98	1	IQERNPSQRPQRR	ATM/ATR, CAMK2, PKC	7,2E+07
YMR230W	48	1	VIKALQSLTSKGY		2,5E+06
YBR048W	2	1	_____MSTELTVQ		3,5E+06
YBR048W	3	3	____MSTELTVQS		3,5E+06
YBR048W	6	1	_MSTELTVQSERA	FHA KAPP, PLK1	3,5E+06
YBR048W	9	1	TELTVQSERAFQK		3,5E+06
YBR048W	44	1	AGLGFKTPKTAIE	Proline-directed, CDK1	1,1E+07
YBR048W	52	1	KTAIEGSYIDKKC	PLK1	6,3E+06
YOR369C	2	1	_____MSDVEEVV	CK2	7,4E+07
YOR369C	19	3	ETVVEQTAEVTIE		7,4E+07
YOR369C	23	1	EQTAEVTIEDALK	FHA1 Rad53p, PLK, PLK1	7,4E+07
YDR064W	12	1	SAGKGISSSAIPY		7,0E+06
YDR064W	13	1	AGKGISSSAIPYS		7,0E+06
YDR064W	14	1	GKGISSSAIPYSR		7,0E+06
YDR064W	19	1	SSAIPYSRNAPAW		7,0E+06
YDR064W	30	1	AWFKLSSESVIEQ		8,5E+06
YDR064W	147	1	YESATASALVN__	CK1	5,8E+05
YCR031C	2	1	_____MSNVVQAR		2,8E+07
YCR031C	11	1	VQARDNSQVFGVA	ATM/ATR, CAMK2	1,8E+07
YCR031C	125	1	TPVPSDSTRKKGG		8,5E+05
YCR031C	126	1	PVPSDSTRKKGGR	CK1	8,5E+05
YJL191W	12	1	VQARDNSQVFGVA	ATM/ATR, CAMK2	2,0E+08
YJL191W	126	1	TPVPSDSTRKKGG		1,3E+07
YJL191W	127	1	PVPSDSTRKKGGR	CK1	1,3E+07
YOL040C	2	1	_____MSQAVNAK	ATM/ATR	3,0E+05
YOL040C	29	1	EKLLEMSTEDFVK	NEK6	1,2E+07
YOL040C	30	1	KLLEMSTEDFVKL		1,8E+06
YDL083C	2	1	_____MSAVPSVQ	GSK3	6,5E+06
YDL083C	6	1	_MSAVPSVQTFGK	CK1	3,7E+07
YDL083C	15	1	TFGKKKSATAVAH		7,6E+05
YDL083C	17	2	GKKKSATAVAHVK	FHA KAPP	2,0E+06
YDL083C	34	1	LIKVNGSPITLVE	Proline-directed	2,3E+06
YDR447C	70	1	GPVRGISFKLQEE	CAMK2	7,4E+06
YDR447C	89	1	QYVPEVSALDLSR		3,4E+07
YDR447C	94	1	VSALDLSRSNGVL	NEK6	3,4E+07
YDR447C	96	1	ALDLSRSNGVLNV	NEK6	1,2E+07
YDR447C	106	1	LNVDNQTSDLVKS	FHA2 Rad53p	1,6E+07
YDR447C	107	1	NVDNQTSDLVKSL		1,2E+07
YDR447C	120	1	GLKLPLSVINVSA	NEK6	1,8E+06
YDR447C	125	1	LSVINVSAQRDRR		9,3E+06
YDR450W	107	1	LANNVESKLRDDL		7,6E+05
YNL302C	5	1	__MAGVSVRDVAA		4,3E+05
YNL302C	117	1	IGIVEISPKGGRR	Proline-directed, CDK1	1,4E+07
YNL302C	139	1	DRIAAQTLEEDE_	CK2	1,1E+06
YLR441C	254	1	KDEVLETV_____		3,9E+05

Table A.1 (continued)

Protein	Position	Class pSite	Sequence Window	Matching Kinase and binding Motifs	Intensity
YML063W	236	1	ALHGEGSGEEKGK	CK2	2,1E+06
YML063W	245	1	EKGKKVSGFKDEV		5,0E+07
YML063W	254	1	KDEVLETV_____		5,0E+07
YGL123W	2	1	_____MSAPEAQQ	CK2	2,3E+06
YGL123W	181	1	GSGIVASPAVKKL	Proline-directed, ERK/MAPK	5,7E+05
YHL015W	38	3	KQLENVSSNIVKN		1,2E+05
YHL015W	39	3	QLENVSSNIVKNA		1,2E+05
YJL136C	84	1	LLKNVWSYSR___		1,3E+08
YJL136C	85	3	LKNVWSYSR____		1,6E+07
YJL136C	86	1	KNVWSYSR_____		1,3E+08
YGR118W	40	2	LGTAFKSSPFGGS	CK1	1,4E+06
YER074W	2	1	_____MSDAVTIR		1,5E+07
YER074W	14	1	RTRKVISNPLLAR		2,9E+07
YER074W	56	1	AEKDAVSVFGFRT		6,0E+06
YLR333C	74	1	RLKIGGSLARIAL		5,9E+06
YLR333C	93	1	GIIKPISKHSKQA	CHK1, PKD	2,8E+05
YGL189C	110	1	NRENKVSPADAAK	Proline-directed	1,3E+06
YER131W	54	1	AAVRDLSEASVYP	CAMK2	3,4E+06
YGL189C	54	1	AAVRDLSEASVYP	CAMK2	1,5E+06
YGL189C	57	2	RDLSEASVYPEYA	CK1, PLK1	1,5E+06
YGL189C	59	2	LSEASVYPEYALP	EGFR	1,5E+06
YHR021C	11	1	QDLLHPTAASEAR	FHA KAPP, NEK6	6,9E+06
YHR021C	14	1	LHPTAASEARKHK		6,9E+06
YOR167C	5	1	__MDNKTPVTLAK	Proline-directed	2,3E+07
YLR264W	3	3	____MDSKTPVTL		5,2E+06
YLR264W	5	1	__MDSKTPVTLAK	Proline-directed	1,5E+07
YLR264W	8	3	DSKTPVTLAKVIK		1,5E+07
YOR167C	19	1	IKVLGRTGSRGGV	NEK6	4,7E+06
YOR167C	37	1	EFLEDTSRTIVRN		3,3E+06
YDL061C	25	1	RQCRVCSSHTGLV	CAMK2	1,5E+05
YNL178W	104	1	AVAQAESMKFKLL		7,1E+04
YNL178W	207	1	ALPDAVTIIEPKE	CK2	5,1E+08
YNL178W	221	1	EPILAPSVKDYRP	NEK6	1,1E+09
YNL178W	231	1	YRPAEETEAQAEP		5,5E+05
YHR203C	120	1	ITDEEASYKLGKV	PLK1	2,0E+05
YHR203C	247	1	GKGIKLSIAEERD	AURORA, CK2	1,8E+06
YJR123W	2	2	_____MSDTEAPV	CK2	5,6E+08
YJR123W	21	2	EVVEEFTPVVLAT	Proline-directed	5,6E+08
YJR123W	38	3	EVQQAQTEIKLFN		1,6E+10
YJR123W	47	1	KLFNKWSFEEVEV	CK2	2,3E+05
YJR123W	206	3	NAAKGSSTSYAIK		2,3E+05
YJR123W	207	2	AAKGSSTSYAIKK	FHA KAPP	2,3E+05
YJR123W	208	2	AKGSSTSYAIKKK	CK1	2,3E+05
YBR181C	15	1	VNGSQKTFEIDDE	CK1, FHA2 Rad53p	2,1E+06
YBR181C	163	1	VIRREVTKGEKTY	CAMK2, CHK1, CK2, PKD	1,3E+07
YBR181C	180	1	KIQRLVTPQRLQR	Proline-directed, CAMK2, CDK1, CDK2, CHK1, PKD	1,0E+06
YBR181C	232	1	IRKRRASSLKA__	CAMK2, PKA, PKA/AKT	2,9E+08
YBR181C	233	1	RKRRASSLKA___	CAMK2	2,9E+08
YOR096W	187	1	IVFEIPSETH___		9,8E+06
YOR096W	189	3	FEIPSETH_____		9,8E+06
YNL096C	30	2	FIDLESSSPELKA	CK2, NEK6	3,3E+04
YNL096C	31	1	IDLESSSPELKAD	Proline-directed, Polo box	3,3E+06
YNL096C	187	1	IVFEIPSQTN___	ATM/ATR	1,3E+07
YNL096C	115	1	VQKRPRSRTLTAV	CAMK2, PKA	1,7E+07
YNL096C	117	1	KRPRSRTLTAVHD	CAMK2, FHA KAPP, PKA/AKT	2,4E+07
YNL096C	119	1	PRSRTLTAVHDKI; PRSRTLTAVHDKV	CAMK2, PKA/AKT	2,4E+07
YOR096W	103	3	RILPKPSRTSRQV		3,6E+05
YOR096W	105	3	LPKPSRTSRQVQK		3,6E+05
YOR096W	106	2	PKPSRTSRQVQKR	CK1, PKA	3,6E+05
YOR096W	115	1	VQKRPRSRTLTAV	CAMK2, PKA	7,5E+06
YOR096W	117	1	KRPRSRTLTAVHD	CAMK2, FHA KAPP, PKA/AKT	1,1E+07
YOR096W	119	1	PRSRTLTAVHDKI; PRSRTLTAVHDKV	CAMK2, PKA/AKT	1,1E+07
YBL072C	45	1	GAKRIHSVRTRGG	CAMK2, PKA, PKC	1,8E+05
YBL072C	132	1	NVKEEETVAKSKN	PLK1	4,9E+04
YBL072C	154	1	ASAKIESSVESQF	CK2, GSK3	2,6E+07

Table A.1 (continued)

Protein	Position	Class pSite	Sequence Window	Matching Kinase and binding Motifs	Intensity
YBL072C	155	2	SAKIESSVESQFS	PLK1	2,6E+06
YBL072C	158	1	IESSVESQFSAGR	ATM/ATR, CK1	2,6E+06
YBL072C	161	1	SVESQFSAGRLYA	CK1	3,9E+06
YPL081W	184	1	ARKAEASGEAADE		4,2E+05
YBR189W	184	1	ARKAEASGEAAEE		4,9E+06
YBR189W	13	2	TYSKTYSTPKRPY	CK1	2,1E+05
YBR189W	14	1	YSKTYSTPKRPYE	Proline-directed, CDK1, CDK2, Polo box	2,1E+05
YBR189W	161	1	HIDFAPTSPFGGA		3,1E+08
YBR189W	162	1	IDFAPTSPFGGAR	Proline-directed, ERK/MAPK, WW GroupIV	4,9E+07
YLR340W	273	3	IENPEKYAAAAPA		4,3E+09
YLR340W	281	2	AAAPAATSAASGD	FHA KAPP	4,3E+09
YLR340W	302	1	AEEEEESDDDMGF		4,3E+09
YDL081C	96	1	EEAKEESDDDMGF		3,5E+08
YDL081C	62	3	DLLVNFSAGAAAP		9,1E+07
YDL130W	58	1	DLKEILSGFHNAG		1,1E+09
YDL130W	73	3	AGAGAASGAAAAG		2,6E+08
YDL130W	96	1	EEAAEESDDDMGF		2,0E+09
YOL039W	43	1	KVSSVLSALEGKS	CK1, CK2	1,2E+07
YOL039W	49	1	SALEGKSVDELIT	CK2	1,1E+08
YOL039W	71	1	PAAGPASAGGAAA		5,2E+08
YOL039W	79	1	GGAAAASGDAAAE		5,2E+08
YOL039W	96	1	EEAAEESDDDMGF		2,3E+09
YDR382W	65	3	GQKKFATVPTGGA		4,3E+09
YDR382W	68	2	KFATVPTGGASSA	FHA KAPP	5,2E+08
YDR382W	72	2	VPTGGASSAAAGA	CK1	5,2E+08
YDR382W	73	3	PTGGASSAAAGAA		5,2E+08
YDR382W	100	1	EEAKEESDDDMGF		3,1E+09
YGL135W	5	2	__MSKITSSQVRE	CK1	3,4E+06
YGL135W	6	1	_MSKITSSQVREH	CHK1, CK1	1,4E+07
YGL135W	7	1	MSKITSSQVREHV	ATM/ATR	1,4E+07
YGL135W	79	1	DVDRAKSCGVDAM	CAMK2, CHK1, PKD	2,1E+07
YGL135W	86	1	CGVDAMSVDDLKK		2,1E+07
YLR075W	205	1	FLSKKGSLENNIR	AURORA, CHK1, CK1, PKD	4,6E+07
YGR085C	44	1	EQLSGQTPVQSKA	Proline-directed, CK1	2,6E+07
YGR085C	161	1	TKEDTVSWFKQKY		2,9E+07
YDR418W	38	1	IGPLGLSPKKVGE	Proline-directed, CDK1, CDK2, NEK6	2,4E+07
YMR142C	144	2	VLSAAATFPIAQP	FHA2 Rad53p	4,9E+07
YMR142C	152	1	PIAQPATDVEARA	CK2	4,9E+07
YMR142C	165	1	VQDNGESAFRTLR		1,7E+07
YHL001W	3	1	____MSTDSIVKA	FHA2 Rad53p	8,8E+05
YHL001W	5	1	__MSTDSIVKASN	CK1	8,8E+05
YLR029C	165	1	REARGLTATGKKS	CAMK2	5,2E+05
YLR029C	167	1	ARGLTATGKKSRG	NEK6	5,2E+05
YLR029C	196	1	TWKRQNTLSLWRY	CAMK2, FHA2 Rad53p, PKA	9,1E+05
YIL133C	163	1	EAKRKVSSAEYYA	CAMK2, CK2, PKA	2,5E+05
YIL133C	180	1	FTKKVASANATAA		7,8E+05
YIL133C	184	1	VASANATAAESDV	CK2	7,8E+05
YIL133C	188	1	NATAAESDVAKQL	CK1	5,8E+05
YNL069C	2	1	_____MSQPVVVI	ATM/ATR	6,7E+06
YNL069C	178	2	AFTKKVSSASAAA	CK1	1,2E+07
YNL069C	179	3	FTKKVSSASAAAS		1,2E+07
YNL069C	181	1	KKVSSASAAASES	CK1, GSK3	1,2E+07
YNL069C	185	1	SASAAASESDVAK	CK1	1,2E+07
YNL069C	187	1	SAAASESDVAKQL		1,2E+07
YJL177W	65	1	PFRRFNSSIGRTA	CAMK2	2,4E+07
YJL177W	66	3	FRRFNSSIGRTAQ		1,1E+07
YJL177W	141	1	RINKYESSPSHIE	CHK1, PKD	5,7E+05
YKL180W	65	1	PFRRFNSSIGRTA	CAMK2	3,5E+07
YKL180W	66	1	FRRFNSSIGRTAQ		3,5E+07
YKL180W	141	1	RINKYESSPSHIE	CHK1, PKD	5,6E+06
YKL180W	142	1	INKYESSPSHIEL	Proline-directed, Polo box	5,6E+06
YKL180W	144	2	KYESSPSHIELVV	CK1, CK2	5,6E+06
YNL301C	63	1	INRPPVSVSRIAR		6,2E+05
YNL301C	65	1	RPPVSVSRIARAL		6,2E+05
YNL301C	167	1	KAPRILSTGRKFE	CAMK2	2,5E+06
YNL301C	168	3	APRILSTGRKFER		2,5E+06
YBL027W	13	1	QKRLAASVVGVGK	NEK6	5,9E+05

Table A.1 (continued)

Protein	Position	Class pSite	Sequence Window	Matching Kinase and binding Motifs	Intensity
YBL027W	29	1	WLDPNETSEIAQA	FHA2 Rad53p	8,4E+07
YBL027W	30	1	LDPNETSEIAQAN		8,4E+07
YBL027W	37	1	EIAQANSRNAIRK		8,4E+07
YBL027W	56	2	IVKKAVTVHSKSR	CHK1, FHA KAPP, PKD	1,4E+06
YBL027W	59	1	KAVTVHSKSRTRA		1,3E+05
YBL027W	91	1	REARLPSQVVWIR	ATM/ATR, CAMK2	2,7E+06
YFR031C-A	95	1	YAGKKASLNVGNV	AURORA	9,5E+05
YFR031C-A	195	1	YRLKRNSWPKTRG	PKA	6,1E+06
YFR031C-A	249	1	TGLLRGSQKTQD_	ATM/ATR, NEK6, PKA	1,5E+07
YMR242C	16	1	IGRRLPTESVPEP	CAMK2	1,4E+07
YMR242C	18	1	RRLPTESVPEPKL	CK2	1,4E+07
YMR242C	60	1	ASGEIVSINQINE		1,2E+06
YMR242C	169	2	FSYKRPSTFY___	PKA	1,1E+06
YMR242C	170	2	SYKRPSTFY____	CAMK2, PKA	1,1E+06
YBR191W	70	1	VYNVTKSSVGVII		1,0E+06
YBR191W	142	1	RESRIVSTEGNVP	CAMK2, CK1	2,9E+07
YBR191W	143	3	ESRIVSTEGNVPQ		2,9E+07
YLR061W	20	2	TFTVDVSSPTENG	CK1	4,8E+06
YLR061W	21	1	FTVDVSSPTENGV	Proline-directed, CK2, ERK/MAPK, Polo box	2,2E+06
YLR061W	23	1	VDVSSPTENGVFD	CK1	4,8E+06
YLR061W	111	1	LAFYQVTPEEDEE	Proline-directed, CK2	9,2E+05
YFL034C-A	21	2	LTVDVSSPTENGV	Proline-directed, CK2, ERK/MAPK, Polo box	1,6E+05
YGL031C	7	1	MKVEIDSFSGAKI		2,2E+07
YGL031C	9	1	VEIDSFSGAKIYP		2,2E+07
YGL031C	83	1	KAQRPITGASLDL	CAMK2, FHA KAPP	1,3E+07
YGL031C	86	1	RPITGASLDLIKE		1,3E+07
YGL031C	95	1	LIKERRSLKPEVR	AURORA, PKA	7,0E+05
YGL031C	153	1	FQKVAATSR____		0,0E+00
YGL031C	154	3	QKVAATSR_____		0,0E+00
YGR148C	26	1	LFVRGDSKIFRFQ	CAMK2	3,4E+06
YGR148C	83	1	KAQRPITGASLDL	CAMK2, FHA KAPP	6,2E+07
YGR148C	86	1	RPITGASLDLIKE		6,2E+07
YGR148C	95	1	LIKERRSLKPEVR	AURORA, PKA	3,6E+07
YGR148C	153	1	FQKVAATSR____		2,2E+06
YGR148C	154	1	QKVAATSR_____		2,2E+06
YGR148C	7	1	MKVEVDSFSGAKI		4,1E+07
YGR148C	9	1	VEVDSFSGAKIYP		4,1E+07
YOL127W	28	3	KALKVRTSATFRL		3,3E+06
YOL127W	29	1	ALKVRTSATFRLP	PKA	2,3E+05
YOL127W	31	2	KVRTSATFRLPKT	FHA2 Rad53p	4,3E+06
YOL127W	69	3	IEQPITSETAMKK		2,3E+06
YOL127W	71	1	QPITSETAMKKVE		2,3E+06
YLR344W	21	1	ARKAYFTAPSSQR	FHA KAPP	4,9E+05
YLR344W	24	3	AYFTAPSSQRRVL		1,7E+06
YLR344W	25	2	YFTAPSSQRRVLL	ATM/ATR, CK1	1,7E+06
YGR034W	24	3	AYFTAPSSERRVL		7,0E+05
YGR034W	25	1	YFTAPSSERRVLL	CK1	1,2E+06
YGR034W	62	1	VLVVRGSKKGQEG	PKA	9,6E+05
YGR034W	72	1	QEGKISSVYRLKF		4,4E+06
YGR034W	94	1	EKVNGASVPINLH		2,1E+05
YHR010W	33	1	KPHDEGSKSHPFG		1,3E+05
YHR010W	94	1	DVEAFKSVVSTET		1,5E+07
YHR010W	97	2	AFKSVVSTETFEQ	CK1	1,5E+07
YHR010W	98	1	FKSVVSTETFEQP		1,5E+07
YHR010W	105	1	ETFEQPSQREEAK	ATM/ATR, CK2	1,5E+07
YDR471W	94	1	DVEAFKSVVSTET		6,3E+06
YDR471W	97	2	AFKSVVSTETFEQ	CK1	6,3E+06
YDR471W	98	3	FKSVVSTETFEQP		6,3E+06
YDR471W	105	1	ETFEQPSQREEAK	ATM/ATR, CK2	6,3E+06
YOR063W	24	1	PRKRAASIRARVK	CAMK2, PKA, PKA/AKT, PKC	5,9E+08
YOR063W	65	1	DLDRPGSKFHKRE	CAMK2, CHK1, CHK1/2, PKD	1,7E+05
YOR063W	101	1	TPRGLRSLTTVWA		1,3E+07
YOR063W	103	1	RGLRSLTTVWAEH	CAMK2	1,3E+07
YOR063W	296	1	DEANGATSFDRTK	FHA1 Rad53p	9,8E+05
YOR063W	297	1	EANGATSFDRTKK		9,8E+05
YOR063W	301	3	ATSFDRTKKTITP		2,2E+07
YOR063W	355	1	KALEEVSLKWIDT	PLK1	1,6E+07

Table A.1 (continued)

Protein	Position	Class pSite	Sequence Window	Matching Kinase and binding Motifs	Intensity
YGL030W	6	1	_MAPVKSQESINQ	ATM/ATR	2,8E+05
YBL092W	40	1	KQKGIDSVVRRRF		6,6E+05
YBL092W	51	1	RFRGNISQPKIGY	ATM/ATR	1,6E+06
YBL092W	67	1	KKTKFLSPSGHKT	Proline-directed, CK1	2,0E+07
YBL092W	69	1	TKFLSPSGHKTFL	NEK6	9,6E+07
YPL143W	15	1	VKGKHLSYQRSKR	GSK3	5,4E+06
YPL143W	97	1	AKTFGASVRIFLY	CK1	2,2E+05
YER056C-A	64	1	RPRQYATVSKTHK		3,9E+05
YER056C-A	66	1	RQYATVSKTHKTV		3,8E+06
YDL136W	19	1	SKEQLASQLVDLK	ATM/ATR	5,6E+06
YDL136W	40	1	QKLSRPSLPKIKT	AURORA, CK1, PKA	3,2E+07
YDL136W	98	1	LTKFEASQVTEKQ	ATM/ATR	0,0E+00
YMR194W	18	3	NKGKKVTSMTPAP		1,7E+05
YMR194W	19	3	KGKKVTSMTPAPK		1,7E+05
YPL249C-A	79	1	AKKRLGSFTRAKA	CAMK2, PKA	4,3E+07
YPL249C-A	81	1	KRLGSFTRAKAKV		3,6E+06
YPL249C-A	21	1	KKVTQMTPAPKIS	Proline-directed	2,3E+05
YPL249C-A	64	1	IDLIRNSGEKRAR	PKA	5,4E+05
YPL249C-A	97	1	NNIIAASRRH___		1,9E+06
YLR185W	80	2	FKNGFQTGSASKA	FHA KAPP	7,1E+05
YLR185W	82	1	NGFQTGSASKASA		7,1E+05
YLR185W	84	1	FQTGSASKASA__	CK1	4,9E+06
YDR500C	80	2	FKNGFQTGSAKAT	FHA KAPP	6,1E+05
YDR500C	82	3	NGFQTGSAKATSA		6,1E+05
YLR185W	5	1	__MGKGTPSFGKR	Proline-directed	5,8E+05
YLR185W	7	1	MGKGTPSFGKRHN		5,8E+05
YBR031W	60	1	EKAGHQTSAESWG	CK2	2,1E+06
YBR031W	61	3	KAGHQTSAESWGT		2,1E+06
YBR031W	282	1	LPSHIISTSDVTR	CK1	2,7E+07
YBR031W	284	1	SHIISTSDVTRII		2,7E+07
YBR031W	287	1	ISTSDVTRIINSS	CK1, FHA2 Rad53p	2,7E+07
YBR031W	293	1	TRIINSSEIQSAI	GSK3	9,4E+06
YBR031W	297	1	NSSEIQSAIRPAG	CK1	9,4E+06
YDR012W	53	1	RQAYAVSEKAGHQ		3,9E+05
YDR012W	60	1	EKAGHQTSAESWG	CK2	1,6E+07
YDR012W	61	1	KAGHQTSAESWGT		1,6E+07
YDR012W	64	1	HQTSAESWGTGRA	CK1	1,6E+07
YDR012W	85	1	GGGTGRSGQGAFG		1,6E+06
YDR012W	270	1	SETVASSKVGYTL	CK1	2,8E+05
YDR012W	278	2	VGYTLPSHIISTS	GSK3	2,8E+07
YDR012W	282	1	LPSHIISTSDVTR	CK1	2,8E+07
YDR012W	283	1	PSHIISTSDVTRI		2,8E+07
YDR012W	284	1	SHIISTSDVTRII		2,8E+07
YDR012W	287	1	ISTSDVTRIINSS	CK1, FHA2 Rad53p	2,8E+07
YDR012W	292	1	VTRIINSSEIQSA		5,6E+06
YDR012W	293	1	TRIINSSEIQSAI	GSK3	5,6E+06
YDR012W	297	1	NSSEIQSAIRPAG	CK1	5,6E+06
YDR012W	306	1	RPAGQATQKRTHV	ATM/ATR	5,6E+06
YPL131W	9	1	FQKDAKSSAYSSR	GSK3	3,4E+06
YPL131W	235	1	DDIDADSLEDIYT		4,0E+07
YML073C	12	1	APKWYPSEDVAAL		8,5E+07
YLR448W	12	1	APKWYPSEDVAAP		2,0E+05
YML073C	88	1	RYVIATSTKVSVE	GSK3	1,0E+05
YML073C	164	1	YLSASFSLKNGDK	CK1	1,5E+05
YGL076C	8	1	AAEKILTPESQLK; STEKILTPESQLK	Proline-directed, FHA KAPP	2,8E+08
YGL076C	11	1	KILTPESQLKKSK; KILTPESQLKKTK	ATM/ATR	2,8E+08
YGL076C	113	1	RLTRINSGTFVKV	CAMK2, CHK1, CHK1/2, CK1, PKD	6,4E+06
YGL076C	228	1	HFIQGGSFGNREE		5,4E+05
YPL198W	8	1	AAEKILTPESQLK; STEKILTPESQLK	Proline-directed, FHA KAPP	1,6E+08
YPL198W	11	1	KILTPESQLKKSK; KILTPESQLKKTK	ATM/ATR	1,6E+08
YPL198W	113	1	RLTRINSGTFVKV	CAMK2, CHK1, CHK1/2, CK1, PKD	2,1E+06
YPL198W	228	1	HFIQGGSFGNREE		5,4E+06
YPL198W	16	1	ESQLKKTKAQQKT	NEK6, NIMA	2,0E+05

Table A.1 (continued)

Protein	Position	Class pSite	Sequence Window	Matching Kinase and binding Motifs	Intensity
YPL198W	115	1	TRINSGTFVKVTK		1,5E+06
YHL033C	29	1	RNPLTHSTPKNFG	NEK6	5,0E+06
YHL033C	30	1	NPLTHSTPKNFGI	Proline-directed, CDK1, Polo box	5,0E+06
YHL033C	216	1	ALAKLVSTIDANF	CHK1, PKD	5,0E+06
YLL045C	126	1	KSKQDASPKPYAV	Proline-directed, CDK1	1,1E+06
YLL045C	130	1	DASPKPYAVKYGL		1,1E+06
YLL045C	216	1	ALAKLVSTIDANF	CHK1, PKD	1,6E+06
YPL237W	112	1	DNVDAESKEGTPS		5,4E+06
YMR309C	93	3	SNKFLKSSNYDSS		3,1E+04
YMR309C	96	2	FLKSSNYDSSDEE	EGFR	3,1E+04
YMR309C	98	1	KSSNYDSSDEESD	CK1, CK2	6,3E+05
YMR309C	99	1	SSNYDSSDEESDE	CK2, GSK3	6,3E+05
YMR309C	103	1	DSSDEESDEEDGK	CK1, CK2	3,1E+04
YEL034W	2	1	_____MSDEEHTF	CK2	9,2E+08
YEL034W	7	1	MSDEEHTFETADA	PLK1	9,2E+08
YEL034W	10	2	EEHTFETADAGSS	FHA KAPP	9,2E+06
YEL034W	15	3	ETADAGSSATYPM		1,0E+09
YEL034W	19	2	AGSSATYPMQCSA	EGFR	9,2E+08
YEL034W	24	3	TYPMQCSALRKNG		1,0E+09
YPR016C	91	1	RNSLPDSVKIQRV	CK1, NEK6	1,0E+05
YPR016C	231	1	QDAQPESISGNLR		2,8E+07
YOR260W	294	1	LKLGPQSMSRQAS		8,3E+06
YOR260W	296	1	LGPQSMSRQASFK	GSK3	1,2E+07
YOL137W	33	2	ELKNLLSSSDSRR	GSK3	1,6E+08
YOL137W	34	2	LKNLLSSSDSRRN	NEK6	1,6E+08
YOL137W	35	2	KNLLSSSDSRRNS	NEK6	1,6E+08
YOL137W	37	2	LLSSSDSRRNSQD	CK1, GSK3	1,6E+08
YOL137W	41	1	SDSRRNSQDEDSL	ATM/ATR, CAMK2, CK1, CK2, PKA	2,8E+07
YCL037C	86	2	WVPIKASITVSGT	AURORA, GSK3	8,5E+08
YCL037C	88	3	PIKASITVSGTKR		8,5E+08
YCL037C	90	2	KASITVSGTKRSG	CK1	8,5E+08
YCL037C	92	2	SITVSGTKRSGSK	FHA KAPP	8,5E+08
YCL037C	95	3	VSGTKRSGSKNGA		8,5E+08
YCL037C	97	2	GTKRSGSKNGASN	CAMK2, PKA	8,5E+08
YHR170W	189	1	AHVDTISISEAKD	CK2	6,7E+04
YHR170W	427	1	HKDIDASLDYNSR	PLK1	1,8E+05
YMR049C	20	2	SKKRAASEESDVE	CAMK2, PKA	3,8E+06
YMR049C	23	1	RAASEESDVEEDE	CK1, CK2	8,1E+07
YMR049C	72	1	KEAQDDSDDDSDA	GSK3	1,2E+06
YMR049C	76	1	DDSDDDSDAELNK	CK1, CK2	1,2E+06
YMR049C	95	2	GDGEEDYDSSEFS	EGFR, SRC	1,0E+07
YMR049C	97	1	GEEDYDSSEFSDD	GSK3	1,0E+07
YMR049C	98	1	EEDYDSSEFSDDT		1,0E+07
YMR049C	101	1	YDSSEFSDDTTSL	CK1	1,0E+07
YMR049C	146	3	INPVYDSDDSDAE		8,3E+07
YMR049C	149	2	VYDSDDSDAETQN	CK1, CK2	8,3E+07
YMR049C	212	1	LDKNSGSSLNLTK		1,3E+06
YMR049C	347	1	PEEYLLSPEEKEA	Proline-directed, CK2	8,0E+06
YNL227C	393	1	DLEKFDSADESVK	CHK1, CK2, GSK3, PKD	6,5E+05
YBR267W	106	1	LENMQKSQEGNTP	ATM/ATR	2,1E+06
YBR267W	111	1	KSQEGNTPDLSKL	Proline-directed, FHA2 Rad53p	2,1E+06
YBR267W	118	1	PDLSKLSLQENEE	AURORA, CK1, CK2	5,3E+05
YBR267W	140	1	EEPEQLTEEEMAE	CK2	1,5E+07
YDR365C	86	1	AENDEDSEVNAKT		4,3E+04
YDR365C	223	1	KKKTDDSDSDMDI		3,5E+06
YDR365C	225	1	KTDDSDSDMDIGI		3,5E+06
YNR054C	47	1	KVEDIESENESDI	CK2, GSK3	5,9E+05
YNR054C	51	1	IESENESDIEEEQ	CK1, CK2	5,9E+05
YPR104C	44	1	KESITNSPTSEVP	Proline-directed, CK1	1,0E+06
YPR104C	47	2	ITNSPTSEVPIET	CK1	1,0E+06
YKL143W	7	1	MSKKFSSKNSQRY		1,2E+05
YDR496C	34	1	PRISIDSSDEESE	CK1, CK2	2,1E+06
YDR496C	35	1	RISIDSSDEESEL	CK1, CK2, GSK3	1,2E+07
YGR245C	278	1	ENFEENSEDEDGF	CK2	1,5E+07
YGR245C	591	1	DVDMEDSDDEKDN	CK2	1,4E+07
YGR245C	603	1	NAKGKESDSDLEL		6,9E+06
YGR245C	605	1	KGKESDSDLELSD	CK2	6,9E+06

Table A.1 (continued)

Protein	Position	Class pSite	Sequence Window	Matching Kinase and binding Motifs	Intensity
YGR245C	610	1	DSDLELSDDDDEK	NEK6	6,9E+06
YOR294W	41	3	DKNDLDSSNARRE		1,6E+05
YOR294W	42	2	KNDLDSSNARREE	NEK6	1,6E+05
YOR294W	169	1	DDKVKGTDNELID	CK2	1,2E+05
YPL012W	1034	3	RKDEEVTTGVSDV		1,5E+06
YPL012W	1035	2	KDEEVTTGVSDVA	FHA KAPP	1,5E+06
YPR143W	69	1	IIDNEQSDAEEDD	CK2	3,5E+06
YPR137W	29	1	TVDEEITDPSSNE	FHA KAPP	5,1E+05
YLR221C	83	1	DIAIEVSDVELTD	CK2	3,3E+06
YLR221C	88	1	VSDVELTDEESKD	CK2	3,3E+06
YLR221C	92	2	ELTDEESKDLKLN	CK1	3,3E+06
YPL217C	478	1	DIDNLPSDEEPYT	CK2	2,1E+07
YPL217C	483	2	PSDEEPYTNDDDV	SRC	2,1E+07
YPL217C	484	2	SDEEPYTNDDDVQ	FHA1 Rad53p	1,3E+04
YPL217C	578	1	DDSKDESDIEEDV	CK1, CK2	1,5E+07
YGR145W	524	2	KRIRALTAAEESD	CAMK2, CK2, PKA/AKT	9,4E+06
YGR145W	529	1	LTAAEESDEERIA	CK2	1,7E+08
YGR145W	555	2	ESDEEESDDETNQ	CK2	3,0E+07
YDR060W	73	1	KLIQGLSDDDDAK		1,3E+07
YDR060W	80	1	DDDDAKSEQEFDA	CK2	2,8E+06
YDR060W	710	1	VDYEYESDAEEEQ	CK2	5,1E+07
YGL111W	257	1	LRFLEPSPGKTEK	Proline-directed, CDK1, CDK2, NEK6	4,6E+04
YLR009W	156	1	ERAESVSEQEESE	CK2	1,2E+07
YLR009W	161	1	VSEQEESEEEEED	CK2	1,2E+07
YLR009W	172	1	EDMEIDSDEEEEE	CK2	1,2E+07
YNL002C	14	1	KAQTLNSNPEILL	CK2	3,1E+05
YNL002C	114	1	NGAEENSVDLEET	PLK1	2,8E+07
YNL002C	120	1	SVDLEETEEEEDD	CK2, NEK6	2,8E+07
YNL002C	278	1	KLNREVSGFGSLN	CAMK2, CHK1, CHK1/2, GSK3, PKD	1,4E+05
YHR064C	477	1	AEEDDESEWSDDE		6,4E+07
YHR064C	480	1	DDESEWSDDEPEV	CK1, CK2	6,4E+07
YMR229C	187	1	EDAEYESSDDEDE		1,7E+05
YMR229C	188	1	DAEYESSDDEDEK	CK2	3,0E+05
YKL172W	104	1	EAQKHMSGDEDES	CK2	9,6E+07
YKL172W	110	1	SGDEDESGDDREE		9,6E+07
YKL172W	177	1	EQDVPLSDVEFDS	CK2	3,6E+07
YKL172W	183	1	SDVEFDSDADVVP		3,6E+07
YGR285C	50	1	LRNHTWSEFERIE	CK2	1,6E+08
YOL041C	181	1	TNPIAETEESGNE	FHA KAPP	3,3E+08
YOL041C	184	1	IAETEESGNEKEE	CK2	3,3E+08
YNL175C	105	1	EESTINTPTGDES	Proline-directed	2,1E+06
YNL175C	107	1	STINTPTGDESGE	CK2	2,1E+06
YER002W	152	1	EIKARDTTEETEV	CK2, PKA	2,3E+05
YER002W	153	2	IKARDTTEETEVV	CAMK2	2,3E+05
YER002W	176	1	VIRKERSQSEREE	ATM/ATR, CHK1, CK2, PKD	4,2E+05
YJL076W	231	1	KIVSNNSDDEDED	CK1, CK2	7,3E+06
YHR052W	11	1	SNSKKSTPVSTPS	Proline-directed, FHA KAPP, Polo box	3,3E+07
YHR052W	14	1	KKSTPVSTPSKEK	CK1	2,1E+07
YHR052W	15	1	KSTPVSTPSKEKK	Proline-directed, CDK1, CDK2, ERK/MAPK, Polo box	4,0E+06
YHR052W	17	1	TPVSTPSKEKKKV	CK1	4,0E+06
YHR052W	357	2	NNAKKRSSSELEK	CK2	0,0E+00
YLR387C	287	1	FTYDDHSISKNLQ	PLK1	4,8E+06
YLR387C	304	1	ITSKLSSVYGAKN	CK1	2,1E+04
YNL124W	255	1	EEEQEFSDDEKEA	CK2	1,2E+07
YLR175W	378	1	GRVNENTPEQWKK	Proline-directed	7,0E+06
YLR175W	398	2	AEQSTSSSQETKE	CK1, CK2	3,3E+07
YLR175W	399	1	EQSTSSSQETKET	ATM/ATR, CK1	3,3E+07
YLR175W	402	2	TSSSQETKETEEE	CK1	3,3E+07
YLR175W	416	1	KKAKEDSLIKEVE	PLK1	2,5E+07
YKL009W	181	2	IKAGKITIDSPYL	AURORA, FHA KAPP	2,8E+07
YKL009W	184	1	GKITIDSPYLVCT	Proline-directed	8,0E+06
YNL308C	174	3	LLNEIKSAFSDEE		4,3E+04
YNL308C	177	2	EIKSAFSDEENEE	CK1, CK2	4,3E+04
YNL308C	184	1	DEENEESSGDEDD		4,3E+04
YNL308C	185	1	EENEESSGDEDDG	CK2	4,3E+04
YNL308C	482	2	QDLKFRYREVSPE	ALK	5,5E+05
YNL308C	486	1	FRYREVSPESFGL	Proline-directed, CAMK2, PKA/AKT	4,0E+06

Table A.1 (continued)

Protein	Position	Class pSite	Sequence Window	Matching Kinase and binding Motifs	Intensity
YLR196W	52	1	EEAEGESGVEDDA	CK2	7,5E+07
YLR196W	105	3	SMFPGLSNDSDVK		3,5E+04
YLR196W	108	2	PGLSNDSDVKFHE	CK1	3,5E+04
YLR196W	131	1	LPNQEDSQEEKQE	ATM/ATR, CK2	2,6E+06
YER036C	43	1	EAAAEESEVDAAA		1,0E+05
YLR106C	3816	3	LDYAAQTLSVISK		5,6E+04
YLR106C	3821	2	QTLSVISKYSATS	CK1	5,6E+04
YLR106C	3823	3	LSVISKYSATSEQ		5,6E+04
YLR106C	3824	2	SVISKYSATSEQQ	CK1	5,6E+04
YLR106C	3826	3	ISKYSATSEQQKI		5,6E+04
YLR106C	3827	2	SKYSATSEQQKIL	CK1	5,6E+04
YLR106C	4353	1	PEEQAMSDEEELK	CK2	4,5E+05
YLR106C	4555	1	DEEEMLSDIDAHD		3,5E+07
YMR290C	12	1	NKRSRDSESTEEP	CK1, PKA	6,2E+05
YMR290C	15	1	SRDSESTEEPVVD	CK1	6,3E+05
YLL008W	208	1	IDEEDDSEEAKAD		3,0E+05
YCR057C	225	1	EFTKRPSDDDDNE	CK1, PKA	1,9E+07
YCR057C	232	1	DDDDNESEDDDKQ		1,9E+07
YCR057C	244	3	QEEVDISKYSWRI		1,8E+07
YCR057C	651	1	DDAGENSDLEDRI	CK2	1,4E+07
YCR057C	888	1	NDVVMESDDEEGW	CK2	5,6E+05
YCR057C	912	1	LSNENDSSDEEEN	CK2	9,9E+07
YCR057C	913	1	SNENDSSDEEENE	CK2	9,9E+07
YAL025C	241	1	EKWLADSDREASS	CK2, NEK6	3,0E+05
YMR014W	257	1	SNIDYDTDDGNEK		6,5E+06
YMR014W	283	2	TQSNKETTSDNED	FHA1 Rad53p	3,9E+07
YMR014W	284	3	QSNKETTSDNEDL		3,9E+07
YMR014W	285	1	SNKETTSDNEDLL	CK2	3,9E+07
YPL093W	469	1	LENEGFYNSDDEE	SRC	4,0E+07
YPL093W	471	1	NEGFYNSDDEEEI	CK2	4,0E+07
YNL224C	217	1	DEEAQQSPDLTKI	Proline-directed	4,6E+06
YDL167C	675	2	PPLSMATKSMKEG	CK1	2,1E+04
YDL167C	677	2	LSMATKSMKEGDG	CK2	2,1E+04
YHR065C	45	1	KEGGSESDSEEDA	CK2	7,5E+04
YNR053C	60	1	NLIRAASFQDSTI	CAMK2, CHK1, CHK1/2, GSK3, PKD	2,9E+07
YNR053C	64	1	AASFQDSTIPDAR	CK1	2,9E+06
YNR053C	85	1	GNTRVISQDALQH	ATM/ATR, CAMK2, CK1	7,1E+06
YIL019W	47	1	EVDTRDSSGDEID	PKA	4,8E+05
YIL019W	48	1	VDTRDSSGDEIDN	CAMK2, CK1, CK2	4,8E+05
YIL019W	55	1	GDEIDNSDHGSDF	GSK3	4,8E+05
YER127W	288	1	KERRVTSFEEDNF	CAMK2, CK2	2,1E+06
YJL109C	385	2	EVRLIITDLIYLS	FHA2 Rad53p, NEK6	7,3E+06
YJL109C	398	2	EILEDKSQLVELF	ATM/ATR	7,3E+06
YJL109C	409	1	LFEYFISINEDLV	CK2	7,3E+06
YLR222C	430	1	FDIYAKYIGHSAA	EGFR	1,8E+06
YLR222C	434	1	AKYIGHSAAVTAV		1,8E+06
YML093W	34	3	NGEFDNSSDNDKR		3,8E+07
YML093W	35	3	GEFDNSSDNDKRH		3,8E+07
YML093W	423	1	RELAAVSSDEDNE	CK2	2,2E+07
YML093W	424	1	ELAAVSSDEDNED		2,2E+07
YML093W	488	1	KMLDRNSDDEEDG	CK2, PKA	3,2E+05
YML093W	498	1	EDGRVQTLSDVEN	CAMK2, FHA1 Rad53p	5,6E+07
YML093W	500	1	GRVQTLSDVENEE	CK2	4,0E+06
YML093W	562	1	DIKLFESDEEETN	CK2, NEK6	7,8E+07
YML093W	640	1	IIVEEESDGEPLQ	CK2	1,4E+06
YML093W	668	1	PWLANESDEEHTV	CK2	1,2E+08
YML093W	673	1	ESDEEHTVKKQSS	PLK1	1,2E+08
YML093W	738	1	VDPYGGSDDEQGD	CK2	7,7E+07
YGR090W	12	3	KRKASETSDQNIV		3,1E+07
YGR090W	13	2	RKASETSDQNIVK	CK1	3,1E+07
YGR090W	60	1	ENDESDTSPESNE	CK2	9,1E+06
YGR090W	10	1	SVKRKASETSDQN	CAMK2, CHK1, PKA, PKD	1,1E+06
YGR090W	58	1	EQENDESDTSPES		5,8E+06
YDR398W	626	2	QDGRLETEQSDGE	CAMK2, FHA KAPP	7,0E+07
YDR398W	629	1	RLETEQSDGEEEA	CK2	3,7E+06
YDR398W	638	1	EEEAGYSDVEME_	CK2	3,7E+06
YGR128C	148	1	TSNDHLSESDIDN		5,6E+06

Table A.1 (continued)

Protein	Position	Class pSite	Sequence Window	Matching Kinase and binding Motifs	Intensity
YGR128C	150	2	NDHLSESDIDNKA	NEK6	5,6E+06
YGR128C	142	2	LEDTTDTSNDHLS	FHA1 Rad53p	4,1E+06
YJR002W	177	1	QDERHSSPDPYGI	Proline-directed, CAMK2, Polo box	5,3E+06
YOL144W	268	1	PMTLNDSDEELLT	CK1, CK2, NEK6	4,7E+05
YOL144W	370	1	FKLIEDSDNDIDH		3,1E+07
YPL226W	120	1	SGTPTPSASTTSL	CK1	1,6E+07
YPL226W	124	3	TPSASTTSLTSLN		1,6E+07
YPL226W	125	2	PSASTTSLTSLNE	CK1	1,6E+07
YPL226W	127	1	ASTTSLTSLNEKL		1,6E+07
YPL226W	1191	1	TPKPVDTDDEED_	CK2	3,4E+07
YOR104W	194	1	ENFEGSSPQPQYD	Proline-directed, Polo box	3,7E+05
YLR342W	269	1	EANPEDTEETLNK		3,6E+06
YOR117W	52	1	SELQRLSHENNVM	PKA	3,4E+06
YHR027C	184	1	SSDGSKSDGSAAT		2,0E+05
YHR027C	187	1	GSKSDGSAATSGF	CK1, GSK3	2,0E+05
YLR421C	132	2	IGVLNNSSESDEE	NEK6	2,0E+08
YLR421C	133	3	GVLNNSSESDEEE		1,9E+07
YLR421C	135	1	LNNSSESDEEESN	CK1, CK2	2,9E+06
YLR421C	153	1	AQDVDVSMQD___	PLK, PLK1	6,4E+05
YDL147W	95	1	LKLSIQYMIQKVM		3,0E+06
YGL009C	494	1	SPKVEVTSEDEKE	FHA1 Rad53p	7,1E+07
YGL009C	495	1	PKVEVTSEDEKEL	CK2	7,1E+07
YGL173C	1500	3	KGEIKPSSGTNST		1,9E+07
YGL173C	1506	1	SSGTNSTECQSPK		6,6E+07
YGL173C	1510	1	NSTECQSPKSQSN	Proline-directed, CDK1, CK1	6,6E+07
YGR240C	179	1	AFLEATSEDEIIS	CK2	1,0E+04
YMR205C	163	1	PEASAESGLSSKV	CK1, GSK3	1,3E+08
YMR205C	166	2	SAESGLSSKVHSY	CK1	1,3E+08
YMR205C	167	1	AESGLSSKVHSYT	CK1, GSK3	1,3E+08
YMR205C	171	1	LSSKVHSYTDLAY	CK1	6,2E+06
YMR205C	173	1	SKVHSYTDLAYRM	FHA KAPP	1,6E+08
YNR016C	1162	1	VSVSDLSYVANSQ	CK1, PLK1	8,8E+06
YNR016C	9	2	EESLFESSPQKME	CK1, NEK6	2,8E+06
YNR016C	10	1	ESLFESSPQKMEY	Proline-directed, CDK1, CDK2, Polo box	2,8E+06
YNR016C	1157	1	GMNRAVSVSDLSY	CAMK2, CHK1	6,5E+07
YIL095W	507	1	PDNINGSKIVRSL		1,5E+06
YCL054W	432	1	KKRMIFTDDELAK	CK2	4,6E+04
YCL054W	505	1	TGFNEGSLEKKEE	PLK1	4,9E+05
YCL054W	529	1	EGVEGDSDDDEAI		1,5E+07
YCL054W	765	1	GLINDDSDKTEKD		4,3E+05
YER122C	281	3	DEFTNSSSSTKIR		2,1E+06
YER122C	282	2	EFTNSSSSTKIRQ	CK1	2,1E+06
YOL086C	2	1	_____MSIPETQK	CK2	1,2E+07
YNL323W	36	1	EEDVDASEFEEDE	CK2	2,6E+07
YLR398C	209	1	GIKPMDSPAENED	Proline-directed, CK2	4,1E+05
YPL195W	918	1	KTKAKNSPEPNEF	Proline-directed	1,0E+07
YPR095C	144	2	PDGERVTLTSSGS	AURORA, FHA KAPP, PKA	1,5E+05
YPR095C	157	2	DNVKRNSKHAPFI	PKA	1,5E+05
YEL022W	284	1	NNEEAISEDDGIE		4,0E+06
YDR465C	181	1	DGQKEESVGSDDD	PLK1	8,4E+07
YDR465C	184	1	KEESVGSDDDATA	CK1	8,4E+07
YLL048C	944	1	ILSRANSSANLAA	CAMK2, CHK1, CHK1/2, CK1, PKD	7,0E+06
YLL048C	954	1	LAAKSSTSLSNLP	FHA KAPP	2,3E+06
YLL048C	955	1	AAKSSTSLSNLPA	CK1	2,3E+06
YPL058C	52	1	QLSRHLSNILSNE	CAMK2, CHK1, CHK1/2, CK1, GSK3, PKD	2,9E+06
YJL033W	692	1	AMEEEISGDEEEG	CK2	4,7E+06
YDL160C	14	1	FNTNNNSNTDLDR	CK1	3,4E+07
YDL160C	16	2	TNNNSNTDLDRDW	FHA1 Rad53p	3,4E+07
YJL050W	34	1	DTNVGDTPDHTQD	Proline-directed	1,5E+07
YJL050W	38	2	GDTPDHTQDKKHG	ATM/ATR	1,5E+07
YBR142W	138	1	SKLTDPSEDVDED		9,6E+03
YBR142W	678	1	LGIDVDSDEDDIS		1,1E+08
YDL084W	13	1	EDLLEYSDNEQEI	CK2, NEK6	6,7E+07
YKL004W	392	1	SRSSATSITSLGV	CK1	1,4E+06
YKL004W	395	1	SATSITSLGVKRA	CK1	1,4E+06
YGR166W	398	1	FSLGAASTTSLVN		5,3E+04
YGR166W	400	3	LGAASTTSLVNSK		5,3E+04

Table A.1 (continued)

Protein	Position	Class pSite	Sequence Window	Matching Kinase and binding Motifs	Intensity
YGR166W	401	1	GAASTTSLVNSKL	CK1, GSK3	5,3E+04
YPR159W	116	1	NNSRAVSTANDNS	CAMK2, CK1	3,5E+05
YPR159W	134	1	HRAIASSPSLNSN	Proline-directed, Polo box	3,5E+06
YPR159W	136	2	AIASSPSLNSNLS	CK1	2,5E+06
YPR159W	139	2	SSPSLNSNLSKND	CK1	2,5E+06
YPR159W	142	1	SLNSNLSKNDILS	CK1	1,0E+06
YGR143W	92	1	YNNDPNSDTSLLA		3,5E+03
YGR143W	95	1	DPNSDTSLLANEK	CK1, PLK1	3,5E+03
YLR399C	270	1	AKGRRSSAQEDAP	CAMK2, CK2, PKA	1,2E+06
YLR399C	615	1	RDASSLSPTSAGS	Proline-directed, CK1	1,6E+05
YOR078W	39	3	KDKEVHSSSDEES		6,1E+04
YOR078W	40	2	DKEVHSSSDEESD	CK2	6,1E+04
YOR078W	45	1	SSSDEESDDDDAP	CK1	4,3E+05
YOR078W	144	1	FDKLDESDENEEA	NEK6	1,2E+07
YFL023W	458	1	KQETTRSVENEVV		3,2E+05
YFL023W	580	1	KILENISDDDYDD		1,8E+07
YCL014W	1075	1	ADVENLSDDDEHR		8,7E+05
YCL014W	1085	1	EHRQNESRVFNDD		8,7E+05
YLR319C	347	1	ASPRRLSSVVTTS	CAMK2, PKA	1,2E+06
YGL203C	660	1	NNRQHDSPNKTVS	Proline-directed, CDK1, CDK2	1,7E+06
YFL034C-B	38	2	IYSSPHSSNSRLS	CK1	1,5E+06
YFL034C-B	39	2	YSSPHSSNSRLSL	CK1	1,5E+06
YFL034C-B	41	2	SPHSSNSRLSLRN	CK1	1,0E+05
YLR413W	652	1	EKAVQESDSTTSR		2,9E+07
YLR413W	654	1	AVQESDSTTSRII		3,2E+06
YLR413W	655	2	VQESDSTTSRIIE	CK1	3,3E+06
YLR413W	656	1	QESDSTTSRIIEE	FHA2 Rad53p	3,2E+06
YLR413W	657	1	ESDSTTSRIIEEH	CK1	3,2E+06
YLR413W	665	1	IIEEHESPIDAEK	Proline-directed	3,0E+07
YLR332W	5	1	__MLSFTTKNSFR	NEK6	0,0E+00
YLR332W	6	1	_MLSFTTKNSFRL	CK1, FHA KAPP	0,0E+00
YNL192W	299	1	GKEELDSVKSGYS		4,3E+04
YNL192W	318	1	YDKDDFSRDDEYD		3,2E+05
YNL192W	328	1	EYDDLNTIDKLQF		3,2E+05
YBR023C	146	3	VDNFEESSTQPIN		8,8E+06
YBR023C	147	1	DNFEESSTQPINK		2,4E+07
YBR023C	148	1	NFEESSTQPINKS	ATM/ATR, FHA2 Rad53p	2,4E+07
YBR023C	538	1	GHKRASTFDLLKK	CAMK2, FHA2 Rad53p, PKA	5,1E+05
YGR202C	59	1	NKDTQLTPRKRRR	Proline-directed, CDK1, CDK2	1,2E+06
YHR090C	188	1	KSVTPVSPSIEKK	Proline-directed, ERK/MAPK, WW GroupIV	2,6E+06
YHR090C	190	3	VTPVSPSIEKKIA		2,6E+06
YMR091C	4	1	___MSDSEGGLAS		1,5E+07
YER164W	36	1	QNYFNDSDDEDDE	CK2	9,3E+05
YHL002W	162	1	STQADNSDDEELQ	CK2	4,4E+06
YPL085W	483	1	KLPWEVSDGEVSS	CK2	6,1E+06
YPL085W	806	1	NKYAPVSPTVQQK	Proline-directed, ERK/MAPK, WW GroupIV	4,0E+06
YPR124W	8	3	EGMNMGSSMNMDA		2,1E+06
YPR124W	9	3	GMNMGSSMNMDAM		2,1E+06
YPR124W	16	3	MNMDAMSSASKTV		2,1E+06
YPR124W	17	3	NMDAMSSASKTVA		2,1E+06
YPR124W	19	2	DAMSSASKTVASS	CK1	2,1E+06
YPR124W	349	1	ESKVAISENNQKK		4,3E+06
YLR429W	460	2	SPSPLKSASSSST	CK1, GSK3	3,5E+08
YLR429W	476	1	VLKEDNSINKLLK	PLK1	3,5E+08
YHR007C	207	3	PEMTIFTASRSLL		7,0E+06
YHR007C	209	3	MTIFTASRSLLGK		7,0E+06
YHR007C	211	2	IFTASRSLLGKEM	CK1	7,0E+06
YIL106W	36	1	NNAGSVSPTKATP	Proline-directed, CDK1, CDK2	3,2E+06
YIL106W	38	1	AGSVSPTKATPHN		1,9E+07
YDR284C	285	1	EELHPLSDEGM__		4,2E+06
YPL265W	12	1	KKMFTSTSPRNSS		9,4E+06
YPL265W	18	2	TSPRNSSSLDSDH	CAMK2, GSK3	2,0E+05
YPL265W	19	3	SPRNSSSLDSDHD		8,5E+03
YPL265W	22	1	NSSSLDSDHDAYY	CK1	2,0E+05
YCR092C	392	2	LVSKLYSHMVEYN	CHK1, CK1, PKD	2,2E+06
YCR092C	798	3	PNMGGKSSYIRQV		1,3E+05
YCR092C	799	3	NMGGKSSYIRQVA		1,3E+05

Table A.1 (continued)

Protein	Position	Class pSite	Sequence Window	Matching Kinase and binding Motifs	Intensity
YCR092C	800	2	MGGKSSYIRQVAL	EGFR	1,3E+05
YCR092C	815	3	IMAQIGSFVPAEE		1,3E+05
YDR097C	166	1	KGKVVDSESDEDE		3,6E+03
YDR097C	168	1	KVVDSESDEDEYL		3,6E+03
YDR097C	201	1	GELAEDSGDDDDL		4,9E+06
YNL102W	31	1	DYEGDESDGDRIY		3,2E+06
YEL055C	789	1	DQLEGLSDDGGDD		1,9E+05
YBR202W	685	2	FSFGQATPRTLLG	Proline-directed, CDK1	8,2E+04
YOL006C	14	1	KVNHELSSDDDDD		2,5E+07
YOL006C	15	1	VNHELSSDDDDDV		2,5E+07
YOL006C	47	1	QDEAEPYDSDEAI	EGFR	2,0E+07
YOL006C	49	1	EAEPYDSDEAISK		2,0E+07
YOL006C	54	3	DSDEAISKISKKK		2,0E+07
YPR190C	392	1	SDNKKRSGSNAAA		3,7E+06
YPR190C	394	1	NKKRSGSNAAASL	CAMK2, PKA	3,7E+06
YPR190C	399	3	GSNAAASLPSKKL		3,7E+06
YDL150W	181	2	DGESEKSSDVDMD	CK1	8,2E+05
YDL150W	182	2	GESEKSSDVDMDD	CK1	8,2E+05
YNL151C	189	1	EDVDDASTGDGAA		7,8E+05
YNL113W	33	1	EQDVDMTGDEEQE	CK2	7,0E+06
YAL023C	34	2	SSSISVSEELSSA	CK1, GSK3	2,0E+04
YAL023C	38	2	SVSEELSSADERD	CK1	2,0E+04
YAL023C	39	1	VSEELSSADERDA	CK2	2,0E+04
YAR028W	176	2	SDSSSNSAEDTQS	CK1	3,0E+05
YAR028W	182	1	SAEDTQSPVSAGK	Proline-directed	3,0E+05
YCR034W	334	1	DLKNVPTPSPSPK	Proline-directed, ERK/MAPK	5,1E+05
YCR034W	336	1	KNVPTPSPSPKPQ	Proline-directed	5,1E+05
YPL046C	21	1	EYEISRSAAMISP		2,3E+08
YPL046C	26	2	RSAAMISPTLKAM	Proline-directed	2,3E+08
YPL046C	28	2	AAMISPTLKAMIE	FHA KAPP	2,3E+08
YLR144C	187	1	KAREFVSSNDIKL		0,0E+00
YDR153C	322	1	KNNNINSNSDDDD		3,1E+07
YDR153C	324	1	NNINSNSDDDDDE		3,1E+07
YGL233W	593	1	NNILVKTMDDIFN	FHA1 Rad53p, NEK6	8,2E+06
YPL231W	50	1	VVEIGPSPTLAGM	Proline-directed	9,1E+06
YPL231W	52	3	EIGPSPTLAGMAQ		1,2E+07
YPL231W	91	1	AKEIYYTPDPSEL	Proline-directed	2,0E+06
YPL231W	95	1	YYTPDPSELAAKE	CK1	2,0E+06
YPL231W	112	1	EEAPAPTPAASAP	Proline-directed, FHA KAPP	7,1E+05
YPL231W	162	1	AHKLKKSLDSIPM	AURORA, NEK6, NIMA	6,8E+04
YPL231W	180	1	DLVGGKSTVQNEI		3,6E+06
YPL231W	576	1	EFEKLYSDLMKFL		5,4E+04
YPL231W	615	1	STKEVASLPNKST		1,9E+05
YPL231W	827	1	QVILPMSPNHGTF	Proline-directed, ERK/MAPK, NEK6, WW GroupIV	4,8E+05
YPL231W	958	1	EVRKAVSIETALE	CHK1, PKD	9,0E+05
YPL231W	977	1	NSADAAYAQVEIQ	ALK	3,4E+04
YPL231W	1073	2	LKGRPYTGWVDSK	CAMK2	4,8E+06
YPL231W	1080	3	GWVDSKTKEPVDD		4,8E+06
YPL231W	1440	1	SSVKYASPNLNMK	Proline-directed	8,6E+05
YPL231W	1479	1	EAEEIPSEDQNEF		1,0E+06
YPL231W	1730	1	KDKKSGSLTFNSK		6,0E+04
YPL231W	1827	1	KSLGVKSLGGGAA		1,1E+05
YKL182W	56	1	ADDEPTTPAELVG	Proline-directed, CK2, ERK/MAPK, WW GroupIV	1,7E+05
YKL182W	449	1	LVKNNVSFNAKDI		5,2E+04
YKL182W	733	1	PIALQWTGGRGGG	NEK6	7,5E+06
YKL182W	1119	2	SQVDSSSVSEDSA	CK2	3,8E+08
YKL182W	1121	1	VDSSSVSEDSAVF	CK1	5,2E+08
YKL182W	1525	1	FLKRNGSTLEQKV	CAMK2, CHK1, CHK1/2, CK2, PKA, PKD	2,9E+05
YLR449W	66	3	ELTRGEYYNQDNN		1,8E+07
YLR449W	80	1	GLEEDESESEQEA	CK2	1,8E+07
YLR449W	82	1	EEDESESEQEADV	CK2	1,8E+07
YPL221W	640	1	KSQEGKSEDNLFG		6,7E+04
YAL053W	688	1	LFDDETSSSSFKQ		3,4E+04
YAL053W	689	1	FDDETSSSSFKQN		3,4E+04
YAL053W	691	1	DETSSSSFKQNSS	CK1	3,4E+04
YDL035C	480	2	NDNSDITSNIKEK	CK1, FHA2 Rad53p	1,7E+06
YDL035C	481	2	DNSDITSNIKEKG	CK1	1,7E+06

Table A.1 (continued)

Protein	Position	Class pSite	Sequence Window	Matching Kinase and binding Motifs	Intensity
YBR018C	273	1	VKEDLASILKQLT		2,9E+04
YCL025C	87	2	DLTSAISPSSRQA	Proline-directed, CK1	4,2E+07
YCL025C	89	1	TSAISPSSRQAQE		4,2E+07
YCL025C	101	1	ELEKNESSDNIGA	CHK1, PKD	3,9E+06
YBR112C	741	1	KKQKLNSPNSNIN	Proline-directed	2,1E+06
YJL031C	44	2	MRDEKIYSIEALK	SRC	3,3E+07
YJL031C	45	3	RDEKIYSIEALKK		3,3E+07
YEL017W	116	1	DDEKPQSGDETSA	CK2	2,1E+05
YGR192C	199	1	DWRGGRTASGNII		9,0E+07
YGR192C	201	1	RGGRTASGNIIPS	CAMK2	9,0E+07
YGR192C	208	1	GNIIPSSTGAAKA		9,0E+07
YGR192C	209	2	NIIPSSTGAAKAV	FHA KAPP	9,0E+07
YHL032C	4	3	___MFPSLFRLVV		1,9E+05
YHL032C	12	3	FRLVVFSKRYIFR		1,9E+05
YDL022W	22	2	NAGRKRSSSSVSL	CAMK2, PKA	3,1E+07
YDL022W	23	2	AGRKRSSSSVSLK	GSK3, PKA	1,7E+06
YDL022W	24	2	GRKRSSSSVSLKA	CAMK2, PKA, PKA/AKT	1,7E+06
YDL022W	27	1	RSSSSVSLKAAEK	CK1	1,1E+07
YOL059W	70	1	DHPIRRSDSAVSI	PKA	2,6E+06
YOL059W	72	1	PIRRSDSAVSIVH	CAMK2, CHK1, PKD	2,6E+06
YER155C	1932	3	YLIQTASSSDLTE		1,1E+06
YER155C	1933	3	LIQTASSSDLTEW		1,1E+06
YER155C	1934	2	IQTASSSDLTEWI	CK1	1,1E+06
YER155C	1937	2	ASSSDLTEWIKMI	CK1, FHA2 Rad53p	1,1E+06
YER155C	1946	2	IKMIKASKRFSFH	GSK3	1,1E+06
YOR070C	25	2	SSSLVTSLMKSWR	CK1, GSK3, NEK6	1,6E+05
YDR389W	16	1	SKIENVSPSKGHV	Proline-directed, CDK1, CDK2	7,9E+05
YDR389W	18	1	IENVSPSKGHVPS		7,9E+05
YDR389W	465	1	LSPISTSIPENSS	CK2	2,5E+06
YFL038C	172	1	ARQIKESMSQQNL		2,3E+06
YFL038C	174	1	QIKESMSQQNLNE	ATM/ATR	2,3E+06
YML001W	17	1	VIILGDSGVGKTS	NEK6	2,6E+06
YML001W	22	1	DSGVGKTSLMHRY		2,6E+06
YML001W	23	1	SGVGKTSLMHRYV	AURORA	2,6E+06
YMR116C	3	1	____MASNEVLVL		2,0E+07
YMR116C	120	1	DIDKKASMIISGS	CHK1, GSK3, PKD	6,6E+05
YMR116C	166	1	EKADDDSVTIISA	PLK1	1,7E+07
YMR116C	168	1	ADDDSVTIISAGN	FHA KAPP	1,7E+07
YLR259C	141	1	MDLRRGSQVAVEK	ATM/ATR, CAMK2, PKA	2,1E+06
YBR169C	363	3	VFGKPLSSTLNQD		2,9E+04
YBR169C	365	2	GKPLSSTLNQDEA	NEK6	2,9E+04
YDL229W	516	1	AVGRLSSEEIEKM	CAMK2, CHK1, PKD	3,5E+05
YJR045C	21	2	SSFRIATRLQSTK	CAMK2	1,5E+07
YJR045C	25	2	IATRLQSTKVQGS	CAMK2, CK1	1,5E+07
YJR045C	26	2	ATRLQSTKVQGSV	NEK6	1,5E+07
YJR045C	40	2	GIDLGTTNSAVAI	FHA KAPP, NEK6	1,5E+07
YJR045C	42	3	DLGTTNSAVAIME		1,5E+07
YGL253W	15	1	PQARKGSMADVPK	CAMK2, PKA	1,5E+07
YMR011W	29	1	IVQKLETDESPIQ	CHK1, FHA KAPP, PKD	4,8E+07
YMR011W	32	1	KLETDESPIQTKS	Proline-directed	4,8E+07
YDR508C	111	2	PISTKDSSSQLDN	CK1	2,0E+07
YDR508C	112	2	ISTKDSSSQLDNE	CK1	2,0E+07
YDR508C	113	1	STKDSSSQLDNEL	ATM/ATR	2,0E+07
YDR508C	123	2	NELNRKSSYITVD	PKA	2,2E+04
YDR508C	124	1	ELNRKSSYITVDG	CAMK2, CHK1, CHK1/2, PKA, PKD	2,2E+04
YDR508C	127	1	RKSSYITVDGIKQ	CK1	2,2E+04
YGR055W	42	1	DADNGASDFEAGQ	CK2	5,5E+05
YGR260W	66	1	EREIMATTTDDDG	FHA1 Rad53p	1,0E+06
YGR260W	67	1	REIMATTTDDDGI	FHA1 Rad53p	1,0E+06
YGR260W	68	1	EIMATTTDDDGIP	FHA1 Rad53p	1,0E+06
YDR225W	129	1	AKATKASQEL___	ATM/ATR	9,6E+05
YBR215W	330	1	SEKAKKSSSASAI	GSK3	2,0E+07
YBR215W	331	1	EKAKKSSSASAIL		2,0E+07
YBR215W	332	1	KAKKSSSASAILP		2,0E+07
YBR215W	334	2	KKSSSASAILPKP	CK1	2,0E+07
YBR215W	342	2	ILPKPTTTKTSKK	CHK1, PKD	2,0E+07
YBR215W	345	3	KPTTTKTSKKAAS		2,0E+07

Table A.1 (continued)

Protein	Position	Class pSite	Sequence Window	Matching Kinase and binding Motifs	Intensity
YBR215W	346	2	PTTTKTSKKAASN	CK1	2,0E+07
YDR168W	14	1	WDKIELSDDSDVE		1,9E+07
YGL133W	332	1	NDSENNSSEEDKK	CK1, CK2	6,8E+05
YGL133W	333	1	DSENNSSEEDKKK		6,8E+05
YBR086C	704	1	DNDTAGSAGKKPL		3,0E+05
YBR086C	726	2	SLVKVPTVGSYGV	CHK1, FHA KAPP, PKD	7,4E+06
YBR086C	729	1	KVPTVGSYGVAGA		2,1E+07
YBR086C	736	2	YGVAGATLPETIP	CK2	2,1E+07
YBR086C	763	2	SIRDAKSSAESSN	CK2, GSK3	5,3E+06
YBR086C	767	1	AKSSAESSNATNN	CK1	5,3E+06
YBR086C	847	1	DNQSKVSVATEQT	AURORA, CK1	1,2E+05
YKL092C	768	1	SKILNLSSTISRP	GSK3, NEK6	2,0E+05
YKL092C	769	1	KILNLSSTISRPK		2,0E+05
YOL081W	927	2	NVNSLNSSPKNLS	CK1	6,0E+05
YOL081W	928	2	VNSLNSSPKNLSS	Proline-directed, CDK1, CK1, NEK6, Polo box	6,0E+05
YOL081W	1018	1	IRTRRYSDESLGK	CAMK2, CK1, PKA, PKA/AKT	2,3E+04
YML123C	321	1	ASTAVESLDNHPP	CK1	2,8E+05
YML123C	578	3	NNDIESSSPSQLQ		5,3E+06
YML123C	579	1	NDIESSSPSQLQH	Proline-directed, Polo box	4,6E+07
YML123C	581	1	IESSSPSQLQHEA	ATM/ATR, CK1	5,3E+06
YLR410W	31	1	SAPSEMSPLFLNK	Proline-directed, CK1	1,3E+05
YLR410W	139	3	DADNINSISKTGS		6,2E+06
YLR410W	141	1	DNINSISKTGSPH	GSK3	6,2E+06
YLR410W	1106	3	FTPVNITSPNLSF		1,9E+07
YLR410W	1107	1	TPVNITSPNLSFQ	Proline-directed, GSK3	1,9E+07
YBR245C	175	1	LLKEEDSDDDESI		1,2E+07
YMR044W	73	1	ARDREQSEEEEDI	CAMK2, CK2, PKA/AKT	1,7E+07
YMR044W	242	1	QQAIDASEEEEEE	CK2	1,4E+05
YDL051W	15	1	EQEKPQSRRNSFA	GSK3	1,9E+06
YDL051W	19	1	PQSRRNSFAVIEF	CAMK2, CK1, PKA	1,6E+07
YFR024C-A	290	1	NSRLAPTNSGGSG	NEK6	5,8E+05
YFR024C-A	292	3	RLAPTNSGGSGGK		5,8E+05
YBR068C	4	1	___MLSSEDFGSS		3,6E+05
YBR068C	9	1	SSEDFGSSGKKET		1,9E+06
YBR068C	16	2	SGKKETSPDSISI	Proline-directed	6,1E+06
YBR068C	21	1	TSPDSISIRSFSA		6,1E+06
YBR068C	75	1	KQINENTSDLEDG	FHA2 Rad53p	4,4E+07
YBR068C	76	1	QINENTSDLEDGV	CK2	6,8E+06
YBR068C	84	1	LEDGVESITSDSK		3,4E+06
YBR068C	86	2	DGVESITSDSKLK	FHA KAPP	6,8E+06
YBR068C	87	1	GVESITSDSKLKK	CK1	3,4E+06
YBR068C	89	1	ESITSDSKLKKSM		4,4E+07
YHR094C	13	2	LISPQKSNSSNSY	CK1	1,7E+06
YHR094C	15	1	SPQKSNSSNSYEL		2,0E+06
YHR094C	16	2	PQKSNSSNSYELE	CK1	1,7E+06
YHR094C	18	2	KSNSSNSYELESG	CK1	1,7E+06
YHR094C	19	2	SNSSNSYELESGR	EGFR	2,0E+06
YHR094C	38	1	PEGKNESFHDNLS		1,0E+07
YHR094C	44	1	SFHDNLSESQVQP		1,0E+07
YHR094C	46	1	HDNLSESQVQPAV	ATM/ATR, NEK6	1,0E+07
YDR345C	23	1	SNADLPSNSSQVM		7,4E+06
YDR345C	25	3	ADLPSNSSQVMNM		7,4E+06
YHR094C	3	1	____MNSTPDLIS		3,7E+07
YHR094C	4	1	___MNSTPDLISP	Proline-directed, FHA2 Rad53p, Polo box	3,7E+07
YNL268W	87	1	TRLQVVSHETDIN		2,5E+05
YNL268W	90	1	QVVSHETDINEDE	CK1	2,5E+05
YKL064W	177	1	VDENSPTDRRQSN		1,7E+05
YKL064W	461	2	IKTHPNSPTPGIK	Proline-directed, CK1, ERK/MAPK, WW GroupIV	8,9E+05
YKL064W	463	1	THPNSPTPGIKAE	Proline-directed, FHA2 Rad53p	8,9E+05
YKL064W	571	3	EKQESATLDHESI		4,8E+05
YKL064W	576	1	ATLDHESISRRKS		4,8E+05
YML115C	21	1	AMDNGLSLPISRN	GSK3	6,4E+06
YML115C	25	1	GLSLPISRNGSSN	CK1, GSK3, NEK6	4,3E+06
YML115C	29	1	PISRNGSSNNIKD	CAMK2, CHK1, CK1, PKD	2,4E+06
YML115C	30	1	ISRNGSSNNIKDK		1,3E+06
YPR079W	279	1	DELHDISPSLNEQ	Proline-directed	8,4E+05
YPR079W	334	2	GGIRLRSSPSASS	CAMK2	3,6E+05

Table A.1 (continued)

Protein	Position	Class pSite	Sequence Window	Matching Kinase and binding Motifs	Intensity
YPR079W	335	2	GIRLRSSPSASSS	Proline-directed, GSK3, NEK6, PKA, Polo box	3,6E+05
YPL057C	349	1	KRLRKDSNTNIVL	CAMK2, PKA, PKA/AKT	1,5E+06
YJL128C	66	2	QRALKRSASVGSN	NEK6, NIMA	8,5E+06
YJL128C	68	1	ALKRSASVGSNQS	CAMK2, CHK1, CHK1/2, PKA, PKD	8,5E+06
YJL128C	71	2	RSASVGSNQSEQD	CK1	8,5E+06
YJL128C	74	2	SVGSNQSEQDKGS	CK1	8,5E+06
YCL061C	19	2	AKKRTTTYKKVAV	CAMK2, PKA	6,7E+06
YCL061C	20	2	KKRTTTYKKVAVP	ALK	6,7E+06
YDR443C	425	1	SNDLENSPLKTEL	Proline-directed, CDK1, CDK2, NEK6	0,0E+00
YOL051W	810	1	TPNTNPSPLKTQT	Proline-directed, CDK1, CDK2	1,0E+06
YBR290W	47	1	GETEIGSDEEDSI	CK1, CK2	5,2E+05
YBR290W	52	2	GSDEEDSIEDEGS	PLK, PLK1	5,2E+05
YDR135C	903	1	GNSDAISLRRASD	CK1	4,8E+06
YDR135C	908	1	ISLRRASDATLGS	CAMK2, PKA	1,5E+06
YDR135C	911	1	RRASDATLGSIDF	CK1, FHA KAPP, PLK1	1,5E+06
YDR135C	914	1	SDATLGSIDFGDD		1,5E+06
YBL091C	35	1	QAKADESDPVESK		1,1E+06
YGL125W	260	1	LVRDIGTNLIVEM	FHA2 Rad53p	3,5E+05
YGL125W	275	1	KLLDSGYVSHLHI	EGFR	3,5E+05
YGL125W	277	1	LDSGYVSHLHIYT	CK1, F box bTrCP	3,5E+05
YGL125W	282	1	VSHLHIYTMNLEK		3,5E+05
YGL125W	283	1	SHLHIYTMNLEKA	FHA2 Rad53p	3,5E+05
YGR076C	67	1	RRMSDVYKLALRY		1,3E+07
YMR302C	477	3	FRNMLTTSLMSIR		1,6E+07
YMR302C	478	2	RNMLTTSLMSIRR	NEK6	1,6E+07
YKR018C	380	1	SSNSEDSEDEEMD	CK1, CK2	6,3E+07
YDR456W	494	2	IKTGCISEEDTSD	CK1	1,4E+07
YDR456W	499	1	ISEEDTSDDEFDI	CK2	1,3E+06
YDR456W	569	1	NETENTSPNPARS	Proline-directed, CK1	1,2E+07
YDR456W	575	3	SPNPARSSMDKRN		1,2E+07
YDR456W	576	2	PNPARSSMDKRNL	PKA	1,2E+07
YBR014C	98	2	NKIMEQSPMIVFS	Proline-directed	1,1E+08
YBR014C	106	3	MIVFSKTGCPYSK		1,1E+08
YPR112C	220	1	LVIENESDDEYSA	CK2	1,3E+06
YJL020C	158	1	RKVPMDSPKLKAR	Proline-directed, CDK1	8,6E+06
YJL020C	620	2	GNVLPVSSPQTRV	NEK6	5,0E+06
YJL020C	621	2	NVLPVSSPQTRVA	Proline-directed, ERK/MAPK, Polo box	5,0E+06
YJL020C	624	2	PVSSPQTRVARNG	CK1, FHA KAPP	5,0E+06
YJL020C	631	1	RVARNGSINSLTK	CAMK2, CHK1, PKD	1,3E+05
YJL020C	634	1	RNGSINSLTKSIS	CK1, GSK3	1,3E+05
YKL129C	776	1	KERRSMSLLGYRA	CAMK2	3,0E+05
YLR138W	447	1	RHLNTITLTKTFT		1,5E+04
YLR138W	449	1	LNTITLTKTFTTH		1,5E+04
YOR025W	380	1	QKDSIGTPPTTPL	Proline-directed, CK1	2,1E+05
YGR197C	42	1	QRFAEGSGHSSDL	GSK3	5,7E+04
YGR197C	45	1	AEGSGHSSDLAKS	CK1	4,1E+04
YGR197C	46	1	EGSGHSSDLAKSL	CK1	4,1E+04
YDR150W	2217	1	KDNDDTSVASSID	GSK3, PLK1	4,9E+06
YDR150W	2220	1	DDTSVASSIDLDH	CK1	4,9E+06
YDR150W	2221	1	DTSVASSIDLDHL	CK1	4,9E+06
YOL123W	2	1	_____MSSDEEDF	CK2	5,1E+07
YOL123W	3	1	____MSSDEEDFN	CK2	5,1E+07
YOL123W	12	1	EDFNDIYGDDKPT		5,1E+07
YOR206W	149	1	PLDGIDSQDEGED	ATM/ATR, CK2	7,7E+07
YOR206W	166	1	SNIEEKSEQMELE		5,1E+05
YOR206W	698	1	LLNSLESDDDNED	CK1	7,0E+06
YOR206W	708	1	NEDVEMSDA____		9,5E+06
YBL079W	397	1	MSIEPAYISRIIG	EGFR	0,0E+00
YLR335W	17	3	QRETYDSNESDDD		1,5E+06
YLR335W	20	1	TYDSNESDDDVTP	CK1	1,5E+06
YLR335W	317	3	PSLEKSSFTFGST		4,2E+05
YLR335W	322	3	SSFTFGSTTIEKK		4,2E+05
YLR335W	323	2	SFTFGSTTIEKKN	CK2	4,2E+05
YLR335W	324	3	FTFGSTTIEKKND		4,2E+05
YMR153W	43	1	EQQKQPTGLLKGL	FHA2 Rad53p	5,7E+05
YGR281W	10	1	TVGDAVSETELEN	CK2	1,5E+07
YGR281W	49	1	SSWDDKSLLPTGE	PLK1	1,1E+07

Table A.1 (continued)

Protein	Position	Class pSite	Sequence Window	Matching Kinase and binding Motifs	Intensity
YJL212C	48	1	EDVNNLTATTDEE		1,4E+06
YJL212C	50	1	VNNLTATTDEEDR	CK2, NEK6	1,4E+06
YJL212C	51	1	NNLTATTDEEDRD	CK2	4,9E+06
YML065W	237	1	TQTAQISDAETRA	CK1, CK2	1,1E+06
YBR060C	213	2	PGKLTLSRNFTPT	NEK6	3,5E+06
YBR060C	217	2	TLSRNFTPTPVPK	Proline-directed, CAMK2, CHK1, CHK1/2, PKD	3,5E+06
YIL147C	833	1	FNKAPGSDDEEGG	CK2	1,4E+07
YHR073W	323	1	QFEDKDTSTLEEN	FHA2 Rad53p	3,1E+04
YHR073W	324	1	FEDKDTSTLEENP	CK2	3,1E+04
YBR233W	51	1	ALKDADSHSDNDH		2,8E+06
YDR264C	51	1	SLKAIRSGNEEES	CK2	4,6E+07
YDR264C	57	1	SGNEEESGNEQVN	CK2	4,6E+07
YKR093W	6	1	_MLNHPSQGSDDA	ATM/ATR	3,9E+07
YKR093W	9	1	NHPSQGSDDAQDE	CK1	3,9E+07
YKR093W	39	1	LKDSYVSDDVANS	CK1	1,0E+07
YKR093W	45	1	SDDVANSTERYNL		1,0E+07
YKR093W	594	3	ILEPMESLRSTTK		7,4E+06
YKR093W	597	2	PMESLRSTTKY__	CK1	8,8E+07
YKR093W	598	2	MESLRSTTKY___	NEK6, PKA	3,1E+07
YKR093W	599	2	ESLRSTTKY____	CAMK2	3,1E+07
YKR093W	601	3	LRSTTKY______		1,2E+06
YLR216C	56	2	KPDVPLSYKGSIF	GSK3	7,3E+06
YPL112C	15	2	IVSGSETPPYSGA	Proline-directed	3,0E+05
YPL112C	190	1	LGKFNKTRKCNFQ		4,7E+05
YPL112C	302	2	AHKDDGSQSPIRK	ATM/ATR	9,8E+05
YPL112C	304	1	KDDGSQSPIRKQL	Proline-directed, CDK1, CDK2	9,8E+05
YGR103W	271	1	ESRQEDSLLKLDP	PLK1	5,7E+05
YGR103W	288	1	EDVKVESLDASTL	GSK3	1,8E+06
YGR103W	292	2	VESLDASTLKSAL	CK1, GSK3, NEK6	1,8E+06
YGR103W	293	2	ESLDASTLKSALN	FHA KAPP	1,8E+06
YGR103W	305	1	NADEANTDETEKE		5,9E+06
YGR103W	308	1	EANTDETEKEEEQ	CK2	5,9E+06
YGR103W	330	1	KEQNEETELDTFE	FHA1 Rad53p	1,4E+06
YGR103W	334	1	EETELDTFEDNNK	FHA1 Rad53p	3,1E+06
YFL026W	354	2	YPRRKETTSDKHS	CAMK2, FHA1 Rad53p, PKA	2,9E+05
YFL026W	355	3	PRRKETTSDKHSE		2,9E+05
YFL026W	356	2	RRKETTSDKHSER	GSK3	2,9E+05
YFL026W	360	1	TTSDKHSERTFVS	CK1	2,1E+04
YFL026W	363	2	DKHSERTFVSETA	CK1, FHA KAPP, PLK1	1,5E+06
YFL026W	366	1	SERTFVSETADDI		2,4E+07
YFL026W	368	2	RTFVSETADDIEK	FHA1 Rad53p	1,5E+06
YFL026W	382	1	QFYQLPTPTSSKN	Proline-directed, FHA KAPP	1,1E+07
YFL026W	385	1	QLPTPTSSKNTRI		1,1E+07
YFL026W	386	1	LPTPTSSKNTRIG	CK1	1,1E+07
YFL026W	398	1	GPFADASYKEGEV	CK2, PLK1	4,8E+06
YFL026W	399	1	PFADASYKEGEVE	SRC	4,8E+06
YFL026W	410	3	VEPVDMYTPDTAA		2,2E+05
YFL026W	411	1	EPVDMYTPDTAAD	Proline-directed	9,9E+06
YMR043W	2	1	_____MSDIEEGT	CK2	8,4E+06
YMR043W	8	1	SDIEEGTPTNNGQ	Proline-directed	1,1E+07
YDL127W	275	1	IKPFNFSKARPVI		0,0E+00
YER059W	312	1	NNENDDSDDENTG	CK2	1,7E+05
YOR281C	35	1	IPERAPSPTAKLE	Proline-directed, CAMK2	3,3E+07
YOR281C	37	2	ERAPSPTAKLEEA	FHA2 Rad53p	3,3E+07
YBR029C	248	1	TKLIEISPKKTLE	Proline-directed, CDK1, CDK2	2,4E+06
YMR105C	111	2	TYEEKCTGGIILT	FHA2 Rad53p	1,7E+06
YMR105C	117	1	TGGIILTASHNPG		1,7E+06
YGL008C	911	1	AAMQRVSTQHEKE	PKA	1,2E+08
YGL008C	912	1	AMQRVSTQHEKET	ATM/ATR, CAMK2, CHK1, CK2	1,2E+08
YOR153W	49	2	IQKLARTLTAQSM	FHA KAPP, NEK6	2,6E+06
YOR153W	51	1	KLARTLTAQSMQN	CAMK2, CHK1, CHK1/2, FHA KAPP, PKD	3,4E+06
YOR153W	54	1	RTLTAQSMQNSTQ	GSK3	3,4E+06
YOR153W	58	1	AQSMQNSTQSAPN	CK1	1,1E+07
YOR153W	59	2	QSMQNSTQSAPNK	ATM/ATR, FHA KAPP	2,6E+06
YOR153W	61	1	MQNSTQSAPNKSD	CK1	1,1E+07
YOR153W	837	2	ENVGERSDLSSDR	GSK3	2,8E+07
YOR153W	840	2	GERSDLSSDRKML	CK1	2,8E+07

Table A.1 (continued)

Protein	Position	Class pSite	Sequence Window	Matching Kinase and binding Motifs	Intensity
YOR153W	841	2	ERSDLSSDRKMLQ	CK1	2,8E+07
YOR153W	849	1	RKMLQESSEEESD	CK2, NEK6	9,1E+06
YOR153W	850	1	KMLQESSEEESDT	CK2, GSK3	9,1E+06
YOR153W	854	1	ESSEEESDTYGEI	CK1	9,1E+06
YLL028W	72	1	RTTTMNSAAESEV	CK1, CK2, GSK3	7,2E+05
YLL028W	76	1	MNSAAESEVNITR	CK1	7,2E+05
YLL028W	89	1	RLTKILTGSVNEP	CHK1, PKD	9,3E+03
YLL028W	91	1	TKILTGSVNEPDR	CK2, NEK6	9,3E+03
YPR156C	132	1	NEDALESDNNEKG		1,8E+07
YOR273C	646	1	DNEDGYSYTEMAT	CK2	2,7E+06
YDL166C	188	1	EYQGPRSDDEDDE	CK2	2,4E+07
YDL166C	196	1	DEDDEDSE_____		2,5E+06
YJR093C	15	1	DKFLYGSDSELAL	CK2, NEK6	4,9E+07
YMR213W	385	1	DFEIVLSEDEKEE	CK2	1,1E+04
YEL040W	360	2	SSTQKSSSSTATS	CK1	5,7E+04
YEL040W	361	3	STQKSSSSTATSS		5,7E+04
YEL040W	362	2	TQKSSSSTATSSS	CK1, GSK3	5,7E+04
YEL040W	363	2	QKSSSSTATSSSK	CK1, FHA KAPP	5,7E+04
YEL040W	366	2	SSSTATSSSKTSS	CK1	5,7E+04
YEL040W	367	2	SSTATSSSKTSSD	CK1, GSK3	5,7E+04
YEL040W	368	2	STATSSSKTSSDH	GSK3	5,7E+04
YEL040W	370	2	ATSSSKTSSDHSS	CK1, FHA1 Rad53p	5,7E+04
YEL040W	375	2	KTSSDHSSSTKKS	CK1	5,7E+04
YER166W	19	2	MSPFEDTFQFEDN	PLK1	2,7E+06
YER166W	26	2	FQFEDNSSNEDTH	CK2	2,7E+06
YER166W	27	3	QFEDNSSNEDTHI		2,7E+06
YER166W	94	1	LNNGSGTFDDVEL	FHA1 Rad53p	1,2E+07
YER166W	104	1	VELDNDSGEPHTN		1,2E+07
YER166W	1483	1	MHGEDGSPSGYQK	Proline-directed	8,7E+06
YER166W	1495	3	KQETWMTSPKETQ		5,2E+06
YER166W	1496	2	QETWMTSPKETQD	Proline-directed, CDK1, CK1, CK2	5,2E+06
YER166W	1506	2	TQDLLQSPQFQQA	Proline-directed, NEK6	4,0E+06
YER166W	1551	2	SVERARTSLDLPG	CAMK2, CHK1, FHA1 Rad53p, PKD	8,0E+05
YER166W	1552	2	VERARTSLDLPGV	AURORA, PKA	8,0E+05
YDR093W	69	1	KPMKDISTPDLSK		4,7E+06
YDR093W	70	1	PMKDISTPDLSKV	Proline-directed, FHA2 Rad53p, Polo box	4,7E+06
YDR093W	85	1	DGIDDYSNDNDIN		2,0E+06
YDR093W	1542	1	ERRDQLSPVTTTN	Proline-directed	3,3E+06
YAL026C	1352	1	SSRDDISFDI___	PLK1	3,7E+03
YIL048W	102	1	MYDNRLSQDDNFK	ATM/ATR, PKA	2,1E+07
YCL024W	296	1	TIKDSKSIKDLPR		8,6E+04
YAL017W	607	2	SLPKMASSPTGSK	CHK1, PKD	1,6E+05
YAL017W	608	2	LPKMASSPTGSKL	Proline-directed, GSK3, Polo box	1,6E+05
YAL017W	612	2	ASSPTGSKLEYSL	CK1, CK2	1,6E+05
YNR047W	300	1	TNTKNLSNLSLNE	CK1	2,0E+06
YNR047W	303	1	KNLSNLSLNEIKE	CK1, CK2	2,0E+06
YNR047W	438	1	ARKTSGSSNINDK		2,8E+05
YDR299W	44	1	NGESDLSDYGNSN	CK1	4,1E+06
YDR299W	91	1	GSRQALYEEVSEN	ALK, EGFR	2,7E+06
YDR299W	95	1	ALYEEVSENEDEE	CK2	2,7E+06
YDR299W	379	1	VDDNENSDDGLDI		6,0E+07
YBL085W	655	1	PLKTSLSPINSKS	Proline-directed, GSK3	8,4E+05
YBL085W	659	1	SLSPINSKSNIAL	CK1	8,4E+05
YER114C	24	1	SRDKDVSDTLSPD	GSK3	9,8E+06
YER114C	28	1	DVSDTLSPDFDSK	Proline-directed, CK1	9,8E+06
YPR171W	462	1	DEIEALSLRNNLK		1,1E+07
YKL179C	364	1	GVNEDDSDNDIRS		6,3E+06
YKL179C	448	3	SPHFNETASMMSG		2,7E+04
YKL179C	450	3	HFNETASMMSGVT		2,7E+04
YKL179C	453	1	ETASMMSGVTRQM	CK1	2,7E+04
YKR071C	206	1	DDLIEDSDDDDFS		3,2E+07
YOR092W	389	1	NLTRIITSDATVS	CAMK2, CHK1, CHK1/2, FHA KAPP, PKD	1,5E+05
YOR092W	395	1	TSDATVSKKDIET		1,5E+05
YMR212C	564	1	SRDNQISTSDLLS		3,1E+05
YMR212C	773	1	EDLHSLSSRGKIF		3,0E+05
YMR221C	269	1	RPQRRKSVLETYV	AURORA, AURORA-A, CAMK2, CK2, PKA	5,9E+06
YDR122W	764	1	AQKFEGSDDDENH		2,2E+07

Table A.1 (continued)

Protein	Position	Class pSite	Sequence Window	Matching Kinase and binding Motifs	Intensity
YNL307C	198	2	HNQPSISYICSRF	GSK3	1,7E+06
YNL307C	199	3	NQPSISYICSRFY		1,7E+06
YNL307C	202	2	SISYICSRFYRAP	CK1	2,6E+07
YKL021C	430	1	ADIGDQSEVESDT	CK2, GSK3	1,9E+07
YKL021C	434	1	DQSEVESDTEELK	CK1, CK2	1,9E+07
YKL021C	436	1	SEVESDTEELKKI	FHA2 Rad53p	1,9E+07
YOL060C	439	2	ESSPLLSPSNSNH	Proline-directed, CK1, GSK3	1,1E+07
YOL060C	441	2	SPLLSPSNSNHPS	NEK6	1,1E+07
YOL060C	443	2	LLSPSNSNHPSEH	CK1, GSK3	1,1E+07
YOL060C	637	1	DWDESKSEYGNEN		4,8E+05
YNL085W	358	1	NKDGKKSNLSSPS	GSK3	1,8E+04
YNL085W	362	2	KKSNLSSPSSASS	Proline-directed, CK1, Polo box	1,8E+04
YNL085W	364	2	SNLSSPSSASSSA	CK1, GSK3	1,8E+04
YDR033W	289	1	PKAPVASPRPAAT	Proline-directed, CDK1, ERK/MAPK	3,5E+07
YDR033W	295	1	SPRPAATPNLSKD	Proline-directed, FHA2 Rad53p	3,5E+07
YDR033W	299	1	AATPNLSKDKKKK	CK1	3,5E+07
YNL156C	81	1	LPRNTVSSNNLER		8,6E+05
YPR075C	285	1	QIAEEESDKEIQD	CK2	1,3E+07
YKL193C	121	1	LTSLDLSFNKIKH	CK1, NEK6, PLK1	5,5E+05
YGL056C	430	1	SSRMANSPVLKSS	Proline-directed	1,1E+06
YLR187W	470	1	MKSPAISSAELFE	CK1, CK2	1,2E+06
YLR187W	471	1	KSPAISSAELFEG		1,2E+06
YLR187W	478	1	AELFEGYDSLPER	ALK, EGFR	1,2E+06
YBL061C	330	1	TRDSRKSVNFLKF	AURORA, CK1, PKA	5,2E+05
YNL243W	294	2	ARTPARTPTPTPP	Proline-directed	1,5E+05
YNL243W	308	1	VAEPAISPRPVSQ	Proline-directed, CDK1	1,5E+05
YDR525W-A	70	2	RYSHLSSSDDNYG	CK1	3,5E+06
YDR525W-A	71	2	YSHLSSSDDNYGS	NEK6	3,5E+06
YDL123W	134	1	KQSLVESPPPYVP	Proline-directed, CK1, ERK/MAPK, NEK6	9,3E+06
YDR011W	10	2	IKSTQDSSHNAVA	CK1	1,0E+06
YDR011W	11	2	KSTQDSSHNAVAR	CK1	1,0E+06
YDR011W	26	1	SASFAASEESFTG	CK1	1,4E+04
YDR011W	29	2	FAASEESFTGITH	CK1, PLK1	1,4E+04
YDR011W	31	3	ASEESFTGITHDK		1,4E+04
YDR011W	80	1	VVSKVESFADALS	CHK1, CK1, PKD	9,1E+06
YDR011W	834	3	AKEQFSSESSGAN		1,7E+05
YDR011W	836	1	EQFSSESSGANDE	CK1	1,7E+05
YER118C	183	2	RRGNRNTTPYQNN	PKA	1,8E+06
YER118C	184	2	RGNRNTTPYQNNV	Proline-directed, CAMK2	1,8E+06
YHR084W	400	1	NKEKLVSPSDPTS	Proline-directed	1,8E+07
YML052W	293	1	FFTIRKSHERPDD	CK1, PKA	4,3E+07
YML052W	301	1	ERPDDVSV_____	PLK1	4,3E+07
YIL047C	859	1	GTFRRRSSVFENI	CAMK2, PKA	2,2E+04
YIL047C	860	1	TFRRRSSVFENIS	AURORA, AURORA-A, CAMK2, CK2, PKA	2,2E+04
YOL109W	40	1	KEQAEASIDNLKN	PLK1	1,9E+08
YER056C	18	1	QDLEKRSPVIGSS	Proline-directed	7,3E+06
YER176W	389	1	KGTSRWTIGSDTE	AURORA, CK1, FHA KAPP, PKA	1,7E+07
YER176W	392	1	SRWTIGSDTESSR	CK2, GSK3	8,0E+05
YLR419W	11	3	TKNNSKSSTPVND		1,9E+06
YNL321W	121	1	NTATPSSPKRMHS	Proline-directed, CDK1, CDK2, ERK/MAPK, Polo box, WW GroupIV	3,3E+06
YGL139W	635	1	KDHDDNSDYESND	CK2, GSK3	3,6E+05
YER178W	309	3	EYETYRYGGHSMS		5,1E+06
YER178W	313	1	YRYGGHSMSDPGT		5,1E+06
YER178W	315	1	YGGHSMSDPGTTY		8,0E+07
YER178W	351	1	IDLGIATEAEVKA	CK2	2,2E+05
YAL038W	130	1	KIMYVDYKNITKV	ALK	4,9E+06
YAL038W	21	2	GSDLRRTSIIGTI	FHA2 Rad53p, NEK6, NIMA, PKA	7,7E+05
YAL038W	22	1	SDLRRTSIIGTIG	AURORA, AURORA-A, CAMK2, PKA	8,0E+06
YNL272C	492	2	RCILHWTHIGIWA	NEK6	1,9E+06
YNL272C	515	1	PLVEDDSDEDQND		2,2E+06
YMR235C	360	1	DFEEVDSEDEEGE	CK2	1,4E+06
YIL063C	179	1	DKDKVHSGSEQLA	CK2	3,7E+06
YIL063C	181	3	DKVHSGSEQLANA		3,7E+06
YOR101W	229	1	TGSSSKSAVNHNG	CK1	2,5E+05
YNL098C	207	1	NSVPRNSGGHRKM	PKA	1,8E+04
YNL098C	214	1	GGHRKMSNAANGK	CAMK2, PKA	2,7E+05

Table A.1 (continued)

Protein	Position	Class pSite	Sequence Window	Matching Kinase and binding Motifs	Intensity
YJL204C	679	2	PPPSRNSPIRDIK	Proline-directed, CDK1, CDK2, CK1, PKA	3,3E+06
YGL097W	135	1	DMDADDSSDDEDG		7,0E+06
YGL097W	136	1	MDADDSSDDEDGD	CK2	7,0E+06
YDR379W	686	1	QKENIATSITVKS		1,1E+04
YDR379W	687	3	KENIATSITVKSP		1,1E+04
YDR379W	689	1	NIATSITVKSPSS	FHA KAPP	1,1E+04
YNL221C	524	1	YKLLTATPNSINK	Proline-directed, FHA KAPP, NEK6	9,2E+05
YNL221C	527	1	LTATPNSINKTTV		9,2E+05
YKR017C	188	3	CCDKKDTETFALE		1,1E+07
YKR017C	190	2	DKKDTETFALECG	FHA2 Rad53p	1,1E+07
YOL145C	1017	1	KKTLSDSDEDDDD	CK1, NEK6	2,9E+04
YOL145C	1046	1	NEFIEDSDEEEAQ	CK2	2,3E+05
YOL145C	1056	1	EAQMSGSEQNKND		2,3E+05
YOR123C	132	1	EDANNFSDQDETT		1,1E+08
YDL189W	148	1	IDGNTRTPNSNLT	Proline-directed, FHA KAPP	5,6E+06
YPL274W	20	3	TKIETESTTIPND		6,1E+05
YPL274W	21	3	KIETESTTIPNDS		6,1E+05
YJL095W	1058	1	ITEGIASPTSPKS	Proline-directed	2,2E+05
YJL095W	1061	1	GIASPTSPKSLDS	Proline-directed, CDK1, CK1, ERK/MAPK, WW GroupIV	2,2E+05
YDR507C	459	3	STIVNQSSPTPAS		3,1E+05
YDR507C	460	2	TIVNQSSPTPASR	Proline-directed, Polo box	3,1E+05
YDR507C	462	1	VNQSSPTPASRNK	Proline-directed, CK1, FHA KAPP	1,5E+07
YDR507C	1004	2	REKNAGSQAKDHS	ATM/ATR	1,0E+10
YDR507C	1010	1	SQAKDHSKDHLKE		1,8E+08
YHL007C	169	1	KLSLTDSTETIEN	CK1, NEK6	9,7E+06
YNL173C	160	1	VVELPDSEDETQQ	CK2, NEK6	6,1E+06
YNL173C	164	1	PDSEDETQQVNKT	ATM/ATR	6,1E+06
YNL173C	306	3	PTGKVATETQTYE		2,4E+06
YNL173C	308	2	GKVATETQTYETK	ATM/ATR	2,4E+06
YFR040W	253	2	KRRKRGSSSFGND	PKA	3,2E+06
YFR040W	254	2	RRKRGSSSFGNDD	CAMK2, PKA, PKA/AKT	3,2E+06
YFR040W	255	3	RKRGSSSFGNDDI		3,2E+06
YDL153C	124	3	NENAWGSTKGEYY		4,3E+05
YDL153C	125	2	ENAWGSTKGEYYG	CK2	4,3E+05
YDL153C	314	2	VNEGDGSESEETA	CK2	2,8E+05
YDL153C	319	1	GSESEETANIEAF	CK1, FHA2 Rad53p	4,6E+06
YDL153C	477	1	DDKDYGSEDEAVS	CK2	1,5E+07
YDL153C	483	3	SEDEAVSRSINTQ		1,5E+07
YOR171C	110	2	TENLSSSSENDDV	NEK6	1,5E+07
YOR171C	111	2	ENLSSSSENDDVE	CK1	1,5E+07
YOR171C	120	1	DDVENHSLSNDKA		1,5E+07
YGL086W	324	1	WEIYNDSDDDDDN		4,3E+06
YML008C	378	1	ETPSQTSQEATQ_	ATM/ATR, CK1	5,9E+04
YLR020C	75	2	SRPLSISSTTPLD	NEK6	2,9E+06
YLR020C	76	2	RPLSISSTTPLDL	CK1	2,9E+06
YCR048W	21	1	KIRRLNSAEANKR	CAMK2, CHK1, PKD	1,7E+06
YNR019W	175	1	NLHHRKSSPDAVD	PKA	4,2E+06
YKR100C	216	1	HNTRQSSNENLIR	CAMK2, CK1	8,1E+06
YKR100C	257	1	FHTRNSSITSVNK	CAMK2, CK1	9,0E+05
YKR100C	273	1	LEDVFATPKSAAQ	Proline-directed, CDK1, FHA KAPP	3,3E+06
YDR310C	623	2	PKPRSASISGISD	CAMK2, PKA/AKT	3,5E+06
YKR092C	301	1	AEETPASSNESTP	CK2, GSK3	1,3E+07
YKR092C	302	1	EETPASSNESTPS	CK1	1,3E+07
YKR092C	305	2	PASSNESTPSASS	CK1	1,3E+07
YKR092C	306	2	ASSNESTPSASSS	Proline-directed, FHA KAPP, Polo box	1,3E+07
YKR092C	312	2	TPSASSSSSANKL	CK1	1,3E+07
YKR092C	313	2	PSASSSSSANKLN	CK1	1,3E+07
YJL176C	210	2	DDQPMISPDNSIF	Proline-directed, GSK3	6,6E+06
YJL176C	214	2	MISPDNSIFGDTK	CK1, PLK1	6,6E+06
YJL176C	229	1	SKQLGNTSSVANT	NEK6	5,7E+06
YJL176C	230	1	KQLGNTSSVANTP		5,7E+06
YJL176C	231	1	QLGNTSSVANTPS		5,7E+06
YJL176C	235	1	TSSVANTPSEIPD	Proline-directed, CK2	5,7E+06
YJL176C	237	1	SVANTPSEIPDAH		5,7E+06
YAL030W	2	3	_____MSSSTPFD		4,1E+07
YAL030W	10	3	STPFDPYALSEHD		8,5E+06
YAL030W	13	1	FDPYALSEHDEER		8,5E+06

Table A.1 (continued)

Protein	Position	Class pSite	Sequence Window	Matching Kinase and binding Motifs	Intensity
YAL030W	39	2	QAEIDDTVGIMRD	FHA2 Rad53p, PLK1	3,2E+06
YOR327C	57	2	ERGERLTSIEDKA	CK2, PKA	3,8E+06
YOR327C	58	1	RGERLTSIEDKAD	CAMK2	2,5E+06
YER093C	10	2	PHSAKQSSPLSSR	CK1, GSK3	5,3E+04
YER093C	14	2	KQSSPLSSRRRSV	CK1	5,3E+04
YGR270W	11	1	LRNRRGSDVEDAS	CAMK2, CK2, PKA, PKA/AKT	1,1E+05
YGR270W	984	1	VLKIKLSGLMDLF		3,9E+07
YGR270W	1142	1	LEAKEQSQENILQ	ATM/ATR	1,2E+07
YDR212W	298	1	GAQVVLTTKGIDD		2,0E+05
YDR212W	299	1	AQVVLTTKGIDDL	FHA2 Rad53p	2,0E+05
YJL008C	218	3	IMGGSLSNSTVIK		6,0E+06
YML062C	264	1	DNIDEDYESDEDE	EGFR, SRC	1,8E+07
YML062C	266	1	IDEDYESDEDEER		1,8E+07
YML010W	36	3	TKDENTSDKDTVD		1,4E+06
YGR116W	155	1	KLEDFFSEDEEEE	CK2	2,0E+07
YPR133C	89	1	HISTDFSDDDLEK	CK1	2,4E+06
YOL148C	438	1	SSSTSNSASNTRN	CK1	9,9E+05
YOL148C	440	2	STSNSASNTRNNS	CK1	9,9E+05
YLR055C	83	1	AARMDKTATPTNE		1,5E+06
YLR055C	85	1	RMDKTATPTNEHQ	Proline-directed, CHK1	1,5E+06
YLR055C	87	3	DKTATPTNEHQHD		1,5E+06
YLR055C	385	1	ADDDMDSLFGDED		1,2E+06
YDR145W	286	2	QNQRKISSSNSTE	CAMK2, GSK3, PKA	1,2E+06
YDR145W	288	3	QRKISSSNSTEIP		1,2E+06
YDR145W	290	2	KISSSNSTEIPSV	CK1	1,2E+06
YDR145W	291	2	ISSSNSTEIPSVT	CK1	1,2E+06
YCR042C	261	1	GQNGEESEKEKED	CK2	7,2E+05
YPL254W	6	1	_MSAIQSPAPKPL	Proline-directed, CK1	5,6E+05
YPL254W	387	1	GDISMSSITKAGE	CK1	1,0E+06
YKL185W	115	2	PEFNKASLSQISF	AURORA	1,2E+07
YKL185W	117	2	FNKASLSQISFTN	ATM/ATR	1,2E+07
YKL185W	120	2	ASLSQISFTNPLN	CK1	1,2E+07
YKL185W	122	2	LSQISFTNPLNYG	FHA2 Rad53p	1,2E+07
YKL185W	129	3	NPLNYGSGLGFSS		1,2E+07
YKL185W	134	2	GSGLGFSSNSQPR	NEK6	1,2E+07
YKL185W	135	3	SGLGFSSNSQPRL		1,2E+07
YKL185W	137	2	LGFSSNSQPRLPL	ATM/ATR, CK1	1,2E+07
YHR099W	172	1	EQGDLDSPKEPQA	Proline-directed, CDK1, CK2	4,5E+07
YHR099W	542	1	KEDINDSPDVEMT	Proline-directed	5,4E+04
YDR098C-B	404	3	ARAHNVSTSNNSP		6,7E+06
YDR098C-B	405	3	RAHNVSTSNNSPS		6,7E+06
YDR098C-B	406	3	AHNVSTSNNSPST		6,7E+06
YDR098C-B	411	3	TSNNSPSTDNDSI		6,7E+06
YDR098C-B	412	2	SNNSPSTDNDSIS	CK1, FHA1 Rad53p	6,7E+06
YDR098C-B	960	1	VLSKAVSPTDSTP	Proline-directed, CHK1, CK1, GSK3, PKD	8,5E+07
YDR098C-B	962	1	SKAVSPTDSTPPS		8,5E+07
YDR098C-B	993	1	EVDPNISESNILP		1,2E+07
YDR098C-B	1055	2	RHSDSYSENETNH	CK1, CK2	4,9E+07
YDR098C-B	1059	3	SYSENETNHTNVP		4,9E+07
YDR098C-B	1062	3	ENETNHTNVPISS		4,9E+07
YDR098C-B	1072	3	ISSTGGTNNKTVP		4,9E+07
YDR098C-B	1081	1	KTVPQISDQETEK	CK2	3,3E+07
YDR098C-B	1093	2	KRIIHRSPSIDAS	Proline-directed	3,6E+07
YDR098C-B	1095	2	IIHRSPSIDASPP	CAMK2, CHK1, GSK3, PKD	3,6E+07
YDR098C-B	1181	1	INSKKRSLEDNET	AURORA, CK1	1,7E+06
YHR214C-B	1089	2	SKDFRHSDSYSDN	GSK3, PKA	1,0E+06
YHR214C-B	1091	3	DFRHSDSYSDNET		1,0E+06
YHR214C-B	1093	2	RHSDSYSDNETNH	CK1, CK2	1,0E+06
YPR158W-B	961	1	VLSKAVSPTDSTP	Proline-directed, CHK1, CK1, GSK3, PKD	1,2E+06
YPR158W-B	965	2	AVSPTDSTPPSTH	CK1, GSK3	1,2E+06
YPR158W-B	994	1	EVDPNISESNILP		1,1E+06
YPR158W-B	996	3	DPNISESNILPSK		1,1E+06
YPR158W-B	1082	1	KTVPQISDQETEK	CK2	1,4E+06
YPR158W-B	1094	2	KRIIHRSPSIDAS	Proline-directed	1,8E+06
YPR158C-D	960	1	VLSKAVSPTDSTP	Proline-directed, CHK1, CK1, GSK3, PKD	5,6E+07
YPR158C-D	962	1	SKAVSPTDSTPPS		5,6E+07
YPR158C-D	964	2	AVSPTDSTPPSTH	CK1, GSK3	7,9E+05

Table A.1 (continued)

Protein	Position	Class pSite	Sequence Window	Matching Kinase and binding Motifs	Intensity
YPR158C-D	993	1	EVDPNISESNILP		4,7E+05
YPR158C-D	1081	1	KTVPQISDQETEK	CK2	1,3E+06
YPR158C-D	1093	2	KRIIHRSPSIDAS	Proline-directed	1,7E+06
YPR158C-D	1095	2	IIHRSPSIDASPP	CAMK2, CHK1, GSK3, PKD	1,7E+06
YPR158C-D	1181	1	INSKKRSLEDNET	AURORA, CK1	1,1E+05
YPR158C-D	1488	2	KLGMENSLTEKIP	CK2, PLK, PLK1	1,9E+05
YPR158C-D	1490	2	GMENSLTEKIPKL	FHA2 Rad53p	1,9E+05
YPR158C-D	404	3	ARAHNVSTSNNSP		4,5E+05
YPR158C-D	405	3	RAHNVSTSNNSPS		4,5E+05
YPR158C-D	406	3	AHNVSTSNNSPST		4,5E+05
YPR158C-D	411	3	TSNNSPSTDNDSI		4,5E+05
YPR158C-D	412	2	SNNSPSTDNDSIS	CK1, FHA1 Rad53p	4,5E+05
YML072C	1350	1	LNSTSVTPRASLD	Proline-directed, CDK1, FHA KAPP	1,9E+06
YML072C	1371	3	SYAPVQSASPVVK		6,2E+05
YML072C	1373	2	APVQSASPVVKPT	Proline-directed	6,2E+05
YML072C	1383	2	KPTDNTSSSSNKK	CK1	6,2E+05
YML072C	1384	3	PTDNTSSSSNKKD		6,2E+05
YML072C	1385	3	TDNTSSSSNKKDT		6,2E+05
YML072C	1386	2	DNTSSSSNKKDTP	CK1	6,2E+05
YML072C	1404	1	GHSRASSFARTLA	CAMK2, CK1	8,9E+05
YBR291C	268	1	KEEGLKTFWKGAT		2,8E+04
YIR026C	202	1	SGSELVSNSGMFK	CK1	2,3E+06
YIR026C	204	3	SELVSNSGMFKDS		1,6E+05
YDR204W	135	2	LENLKQTMLSDSS	FHA KAPP, NEK6	9,5E+04
YDR204W	138	3	LKQTMLSDSSGRR		9,5E+04
YLR167W	86	1	RKKKVYTTPKKIK		4,3E+06
YLR167W	87	1	KKKVYTTPKKIKH	Proline-directed, CDK1, CDK2	4,3E+06
YLR167W	122	2	KLRRECSNPTCGA	CAMK2, CHK1, CHK1/2, PKD	1,9E+05
YLR167W	125	2	RECSNPTCGAGVF	CK1, FHA KAPP	1,9E+05
YDL122W	555	1	EQEFEDSEEEKEY	CK2	3,3E+05
YDL122W	755	1	DLEAIQSNNEEDD	CK2	2,5E+06
YOR124C	907	1	SNDAEVSENEDTT	CK2	1,2E+06
YOR042W	220	1	EQHHEDSEEEDSW	CK2	6,0E+05
YOR042W	407	1	DEFLINSDDEM__	CK2, NEK6	6,1E+07
YBR165W	83	1	CFPINRTVSMTHL		7,4E+07
YBR165W	91	2	SMTHLNYLLLKDL	ALK	7,4E+07
YDR510W	2	1	_____MSDSEVNQ	CK2	8,1E+06
YDR510W	4	1	___MSDSEVNQEA		8,1E+06
YMR067C	388	1	VNTINKSNPQGPS	CK1	3,7E+06
YMR067C	399	3	PSDNATSIKKTLN		3,7E+06
YMR067C	403	1	ATSIKKTLNRVPK	AURORA	3,7E+06
YJL163C	306	2	EKLRSQSGSDDAR	CAMK2, PKA/AKT	1,3E+05
YJL163C	308	2	LRSQSGSDDARNY	CK1	1,3E+05
YMR010W	181	1	IKSLSFTNLLKFS	FHA2 Rad53p, NEK6	1,3E+05
YMR266W	931	1	ANGEFDTASKENN		2,5E+06
YMR266W	933	1	GEFDTASKENNPF		2,5E+06
YAL037W	228	1	LWEFGQTQEILKR	ATM/ATR, FHA2 Rad53p	2,8E+05
YDR089W	668	1	TTDNEESLLLRNS	PLK1	1,4E+06
YDR333C	119	1	AAKDKGSDDDDDD		7,8E+05
YDR384C	7	1	MTSSASSPQDLEK	Proline-directed, CK1, Polo box	2,0E+06
YER134C	151	1	NKEVEKYGVKFVY		0,0E+00
YHR146W	343	1	LVEKRESTEGVLD	CHK1, PKA, PKD	4,4E+07
YHR146W	344	2	VEKRESTEGVLDG	CAMK2, PKA	4,4E+07
YHR149C	135	2	INHLYSSDSQQDF	NEK6	5,5E+06
YHR149C	137	1	HLYSSDSQQDFME	ATM/ATR, CK1	5,5E+06
YHR149C	157	1	SDPFVGSMHSSKY	GSK3	5,1E+03
YHR149C	160	1	FVGSMHSSKYNVR	CK1	1,5E+04
YHR149C	161	1	VGSMHSSKYNVRS	CK1	5,1E+03
YIL091C	155	1	DEKDIDSEDEQDP	CK2	2,7E+07
YKL082C	230	1	DQDEIASDSDMED		7,3E+06
YKL082C	232	1	DEIASDSDMEDID	CK2	7,3E+06
YKL082C	239	1	DMEDIDSDLENNS	CK2	7,3E+06
YKR023W	398	2	NGRREKYVVSMNI	EGFR	7,4E+04
YKR060W	270	1	QKNEDLSDIKL__		4,2E+06
YKR078W	41	1	SVSVSISDDEDSK	CK1, CK2	4,6E+05
YMR192W	17	1	RIEVPRTPHQTQP	Proline-directed, ERK/MAPK, WW GroupIV	4,4E+05
YMR192W	21	1	PRTPHQTQPEKDS	ATM/ATR, CK2	4,4E+05

Table A.1 (continued)

Protein	Position	Class pSite	Sequence Window	Matching Kinase and binding Motifs	Intensity
YMR295C	11	2	RKKSSISNTSDHD	CK1	4,1E+06
YMR295C	13	3	KSSISNTSDHDGA		4,1E+06
YMR295C	14	1	SSISNTSDHDGAN	CK1	4,1E+06
YMR295C	23	1	DGANRASDVKISE	PKA	1,3E+07
YNL050C	25	1	LGEDYDSNSSSKN	GSK3	2,4E+06
YNL050C	28	1	DYDSNSSSKNNSE	CK1	2,4E+06
YNL058C	143	3	RGHHKHSSSLQSN		2,4E+05
YNL058C	144	2	GHHKHSSSLQSNP	GSK3	2,4E+05
YNL058C	148	2	HSSSLQSNPFDIN	CK1	2,4E+05
YNL149C	119	1	QGLDPDSDADIEE		5,2E+07
YNL224C	105	1	PGNRYDSSTDLQA	CAMK2	2,4E+05
YPL146C	31	1	RKNIDLSDVEQYM	CK2	2,9E+07
YPL146C	363	1	EETEILSAIESDS	CK1, CK2, GSK3	5,3E+06
YNL110C	37	3	ALETSSSSSDEED		1,4E+04
YNL110C	38	1	LETSSSSSDEEDE	CK1, CK2	1,1E+05
YNL110C	39	1	ETSSSSSDEEDEK	CK1, CK2	1,1E+05
YNL110C	56	1	IEGLAASDDEQSG	CK2, NEK6	2,1E+08
YNL110C	63	2	DDEQSGTHKIKRL	FHA2 Rad53p	2,1E+08
YDR119W	99	1	GPKIDDSPQDEVN	Proline-directed	2,7E+07
YDR119W	106	1	PQDEVNSIKGKPA		2,3E+07
YBR074W	606	2	VPLLKGSNSMEEG	NEK6	4,9E+05
YBR074W	608	1	LLKGSNSMEEGLS	CK2	7,7E+06
YPR091C	622	1	DNVGNSSDTEDMD	CK2	9,1E+05
YPR091C	640	1	DKKNDDSADERES	CK2	3,0E+06
YCL012C	71	1	RNFDIISENSNDV		9,8E+05
YCL012C	74	2	DIISENSNDVRGG	CK1	9,8E+05
YBL042C	4	1	___MPVSDSGFDN		6,8E+06
YBL042C	38	1	SEMGDATKITSKI		3,5E+06
YBL042C	54	2	VIEKKDTDSENNI	CHK1, CK2, PKD	5,1E+06
YBL042C	56	1	EKKDTDSENNITI		1,6E+07
YKL035W	347	3	IIPNQKTITRDGH		3,1E+05
YJR001W	8	1	PEQEPLSPNGRKR	Proline-directed, ERK/MAPK, WW GroupIV	1,1E+07
YJR001W	77	1	SLRRANSFRNIEL	CAMK2, CHK1, CHK1/2, PKC, PKD	5,3E+06
YJR001W	187	1	TNNDMDSIVVKRV		4,6E+06
YMR054W	223	1	DLTRNQSVEDLSF	CAMK2, CHK1, CHK1/2, CK1, PKD	3,1E+06
YBR127C	501	2	DEEDPDTRSSGKK	FHA KAPP	3,9E+06
YBR127C	503	3	EDPDTRSSGKKKD		3,9E+06
YBR127C	504	2	DPDTRSSGKKKDA	PKA	3,9E+06
YLR148W	907	1	KIDQPISIDETEL	CK2	2,6E+06
YJL154C	853	2	ISDLHITGENNVK	NEK6	4,5E+06
YDR372C	14	1	RVNRADSGDTSSI	CAMK2, CHK1, F box bTrCP, GSK3, PKD	2,0E+06
YDR372C	19	2	DSGDTSSIHSSAN	GSK3	2,8E+05
YNL054W	599	1	SPDKRSSLVSLSK	AURORA, AURORA-A, PKA	4,0E+05
YFL004W	182	3	SNFNTASEPLASA		3,6E+06
YFL004W	187	1	ASEPLASASKFSS		3,6E+06
YFL004W	189	2	EPLASASKFSSIV	GSK3	3,6E+06
YFL004W	193	2	SASKFSSIVSNDI	CK1	2,0E+04
YFL004W	196	1	KFSSIVSNDIDMN	CK1	2,0E+04
YFL004W	615	1	DLEADGSSDEETE	CK2	4,6E+07
YFL004W	616	1	LEADGSSDEETEQ	CK2	4,6E+07
YFL004W	657	1	KLMGVDSEEEEIE	CK2	2,4E+07
YPL019C	592	1	RRLSKISVPDGKT	AURORA, CK1	3,4E+07
YPL019C	621	1	DLEDHESSDEEGT	CK2	2,4E+08
YPL019C	622	1	LEDHESSDEEGTA	CK2	2,4E+08
YPL019C	627	1	SSDEEGTALPKKS		2,4E+08
YBR069C	6	1	_MDDSVSFIAKEA		7,5E+06
YBR069C	13	1	FIAKEASPAQYSH	Proline-directed, CHK1, PKD	2,0E+05
YBR069C	20	2	PAQYSHSLHERTH	CK2	2,0E+05
YDR151C	165	2	ENLQKLSQVDSQS	ATM/ATR, GSK3	8,0E+07
YDR151C	169	2	KLSQVDSQSTGLP	ATM/ATR, CK1	8,0E+07
YDR151C	176	3	QSTGLPYTLPIQK		8,0E+07
YDR151C	177	2	STGLPYTLPIQKT	FHA2 Rad53p, NEK6	8,0E+07

Table A.2: Phosphorylation sites in ribosomal protins that change in response to heat shock (HS) and glucose depletion (Glu).

Gene Name	Position	Av HS/Ctrl	Av Glu/Ctrl	HS/Ctrl 1	HS/Ctrl 2	HS/Ctrl 3	HS/Ctrl 4	Glu/Ctrl 1	Glu/Ctrl 2	Glu/Ctrl 3	Glu/Ctrl 4	Sequence Window
AGP1	2	0,57	1,56			0,33	0,82	1,45	2,06		1,15	_____MSSSKSLY
AGP1	6	0,70	1,56		0,96	0,33	0,82	1,45	2,06		1,15	_MSSSKSLYELKD
AGP1	87	0,45	1,00				0,45		0,87	1,12		DLTSAISPSSRQA
AGP1	89	0,45	1,00				0,45		0,87	1,12		TSAISPSSRQAQE
AGP1	90	0,45	1,00				0,45		0,87	1,12		SAISPSSRQAQEL
AGP1	101	3,14	0,91	3,31	2,97			0,71		1,12		ELEKNESSDNIGA
AKR1	75		1,04								1,04	EEDPLLTRYHTAC
AKR1	77		1,04								1,04	DPLLTRYHTACQR
ALD3	234	0,75		0,88	0,62							VGKALGTHMDIDK
ASC1	108	1,02		1,19	0,86							RFVGHKSDVMSVD
ASC1	135											KTIKVWTIKGQCL
ASC1	166	1,05	0,98	0,97	1,13	0,92	1,18	0,88	1,17	1,16	0,69	EKADDDSVTIISA
ASC1	168	1,06	1,07	0,98	1,12	1,15	0,98	0,94	1,32	0,95	1,07	ADDDSVTIISAGN
BAF1	720											DDEEDLSDENIQP
BAP2	3	2,87		3,32	2,43							____MLSSEDFGS
BAP2	9	2,54		2,70	2,38							SSEDFGSSGKKET
BAP2	10	2,26		2,20	2,33							SEDFGSSGKKETS
BAP2	75	3,34	1,01			3,14	3,54	0,55	1,33	1,04	1,11	KQINENTSDLEDG
BAP2	76	3,34	1,05			3,14	3,54	0,55	1,43	1,04	1,19	QINENTSDLEDGV
BAP2	84	3,34	1,01			3,14	3,54	0,55	1,33	1,04	1,11	LEDGVESITSDSK
BAP2	86	3,34	1,01			3,14	3,54	0,55	1,33	1,04	1,11	DGVESITSDSKLK
BAP2	87	3,34	1,02			3,14	3,54	0,55	1,43	0,98	1,11	GVESITSDSKLKK
BAP2	89	3,34	1,01			3,14	3,54	0,55	1,33	1,04	1,11	ESITSDSKLKKSM
BBC1	103	1,01		1,09	0,92							DLPEPISPETKKE
BEM1	458	0,83	1,31		1,75	0,26	0,47	0,76	1,85			KLNKKLSDLSLSG
BEM1	461	0,83	1,31		1,75	0,26	0,47	0,76	1,85			KKLSDLSLSGSKQ
BEM1	465	0,83	1,31		1,75	0,26	0,47	0,76	1,85			DLSLSGSKQAPAQ
BFR2	41	0,53	1,19		0,03	0,44	1,12	1,07	1,44	1,20	1,04	NEKNGESDLSDYG
BFR2	44	0,54	1,19		0,03	0,44	1,15	1,07	1,44	1,20	1,04	NGESDLSDYGNSN
BFR2	46	0,54	1,19		0,03	0,44	1,13	1,07	1,44	1,20	1,04	ESDLSDYGNSNTE
BFR2	379	0,67	1,24	0,82	0,40	0,40	1,06	1,04	1,50	1,00	1,42	VDDNENSDDGLDI
BMS1	578	0,99	1,30	0,96			1,03	1,52	1,08			DDSKDESDIEEDV
BMS1	1160		3,79						3,79			KEKKKEYFAQNGK
BMS1	1168		3,79						3,79			AQNGKRTTMGGDD
BMS1	1176		3,79						3,79			MGGDDESRPRKMR
BUD21	144	0,96	1,13	0,95	0,47		1,45	1,30		0,97		FDKLDESDENEEA
CBF5	395	0,48	0,58	0,49	0,53		0,43	0,51	0,61		0,61	LDNAEQSTSSSQE
CBF5	396	0,48	0,58	0,49	0,53		0,43	0,51	0,61		0,61	DNAEQSTSSSQET
CBF5	397	0,55	0,58	0,49	0,53		0,62	0,51	0,61		0,61	NAEQSTSSSQETK
CBF5	398	0,54	0,58	0,49	0,53		0,62	0,51	0,61		0,61	AEQSTSSSQETKE
CBF5	399	0,54	0,58	0,49	0,53		0,62	0,51	0,62		0,61	EQSTSSSQETKET
CBF5	402	0,54	0,58	0,49	0,53		0,62	0,51	0,61		0,61	TSSSQETKETEEE
CBF5	405	0,93	1,11				0,93		1,11			SQETKETEEEPKK
CBF5	416	0,19	1,00	0,19						1,00		KKAKEDSLIKEVE
CCT8	537		2,69						2,69			ATEAATTVLSIDQ
CDC37	14	0,40	1,01				0,40	1,01				WDKIELSDDSDVE
CDC37	17	0,40	1,01				0,40	1,01				IELSDDSDVEVHP
CHS3	146	0,89	1,10	0,84	0,94			0,83	1,36			VDNFEESSTQPIN
CHS3	147	0,88	1,10	0,81	0,96			0,83	1,36			DNFEESSTQPINK
CHS3	148	0,89	1,12	0,84	0,94			0,88	1,36			NFEESSTQPINKS
CIC1	10	0,50	1,30	0,06	1,46	0,18	0,31	0,79	1,03	2,63	0,76	KSNSKKSTPVSTP
CIC1	11	0,50	1,30	0,06	1,46	0,18	0,31	0,79	1,03	2,63	0,76	SNSKKSTPVSTPS
CIC1	14	0,47	1,30	0,06	1,33	0,18	0,31	0,79	1,03	2,63	0,76	KKSTPVSTPSKEK
CIC1	15	0,47	1,30	0,06	1,33	0,18	0,31	0,79	1,03	2,63	0,76	KSTPVSTPSKEKK
CIC1	17	0,50	1,30	0,06	1,46	0,18	0,31	0,79	1,03	2,63	0,76	TPVSTPSKEKKKV
CIC1	359	0,20			0,20							AKKRSSSELEKES
CIC1	366	0,14	0,64	0,18	0,11						0,64	ELEKESSESEAVK
COX14	49	1,08	1,59				1,08		1,59			KYEQQVTQQKALE
CTR9	1015	0,86		0,55	0,68	0,92	1,30					AAKKTLSDSDEDD
CTR9	1017	0,86		0,55	0,68	0,92	1,30					KKTLSDSDEDDDD
CUE5	407	1,13	0,80	0,83	1,43			0,80				DEFLINSDDEM__
CWC2	333											GGPLLDYLSSDED
CWC2	336											LLDYLSSDED___

Table A.2 (continued)

Gene Name	Position	Av HS/Ctrl	Av Glu/Ctrl	HS/Ctrl 1	HS/Ctrl 2	HS/Ctrl 3	HS/Ctrl 4	Glu/Ctrl 1	Glu/Ctrl 2	Glu/Ctrl 3	Glu/Ctrl 4	Sequence Window
CYC8	741	1,16		0,88	1,45							KKQKLNSPNSNIN
DCP2	729	1,16		1,16								SSSNVSSSKDLLQ
DCP2	730	1,16		1,16								SSNVSSSKDLLQM
DHH1	10		1,82					1,82				INNNFNTNNNSNT
DHH1	14		1,82					1,82				FNTNNNSNTDLDR
DRS1	18	0,35	1,33				0,35		1,33			DFVPTISDSEDDV
DRS1	20	0,35	1,33				0,35		1,33			VPTISDSEDDVPI
DRS1	29	0,35	1,33				0,35		1,33			DVPILDSSDDEKV
DRS1	30	0,35	1,33				0,35		1,33			VPILDSSDDEKVE
DRS1	208	0,23		0,30	0,16							IDEEDDSEEAKAD
EBP2	104	0,30	1,05			0,23	0,37	1,05	1,05	1,28	0,80	EAQKHMSGDEDES
EBP2	110	0,30	1,05			0,23	0,37	1,05	1,05	1,28	0,80	SGDEDESGDDREE
EBP2	136		0,31							0,31		LEKLAKSDSESED
EBP2	138		0,31							0,31		KLAKSDSESEDDS
EBP2	140		0,31							0,31		AKSDSESEDDSES
EBP2	144		0,31							0,31		SESEDDSESENDS
EBP2	146		0,31							0,31		SEDDSESENDSEE
EBP2	150		0,31							0,31		SESENDSEEDEDV
EBP2	162	0,36	1,02				0,36	0,84	1,13	1,10		VVAKEESEEKEEQ
EBP2	177	0,31	0,97	0,31	0,33	0,23	0,36	0,84	1,13	0,96	0,94	EQDVPLSDVEFDS
EBP2	183	0,31	0,97	0,31	0,33	0,23	0,36	0,84	1,13	0,96	0,94	SDVEFDSDADVVP
ELF1	142											RGALVDSDDE___
ERB1	20	0,29	0,84	0,31	0,25	0,22	0,38	0,75	1,13	0,68	0,82	SKKRAASEESDVE
ERB1	23	0,30	0,86	0,30	0,25	0,22	0,43	0,75	1,20	0,68	0,82	RAASEESDVEEDE
ERB1	62		1,35								1,35	AVEEKESSSDKEA
ERB1	63		1,35								1,35	VEEKESSSDKEAQ
ERB1	64		1,35								1,35	EEKESSSDKEAQD
ERB1	72	0,27	0,68	0,30	0,23		0,28			1,00	0,36	KEAQDDSDDDSDA
ERB1	76	0,27	0,68	0,30	0,23		0,28			1,00	0,36	DDSDDDSDAELNK
ERB1	97	0,33	0,99				0,33		1,14		0,85	GEEDYDSSEFSDD
ERB1	101	0,33	0,99				0,33		1,14		0,85	YDSSEFSDDTTSL
ERB1	212	0,83		1,17	0,48							LDKNSGSSLNLTK
ESF1	364	0,85	0,75				0,85		0,75			DMDFKAYLASDSD
ESF1	367	0,85	0,75				0,85		0,75			FKAYLASDSDESD
ESF1	369	0,85	0,75				0,85		0,75			AYLASDSDESDGQ
ESF1	372	0,85	0,75				0,85		0,75			ASDSDESDGQVDE
ESF2	7	1,19	0,79				1,19		0,79			MSEKVNSDFEDFS
ESF2	13	1,19	0,79				1,19		0,79			SDFEDFSSDEETD
ESF2	14	1,19	0,79				1,19		0,79			DFEDFSSDEETDQ
ESF2	47	1,02					1,02					KVEDIESENESDI
ESF2	51	1,02					1,02					IESENESDIEEEQ
FAS1	55	0,96		0,92	0,99							AADDEPTTPAELV
FAS1	56	0,96		0,92	0,99							ADDEPTTPAELVG
FAS1	1119	0,94	0,86	0,87	1,06		0,89	0,66	1,06			SQVDSSSVSEDSA
FAS1	1121	0,94	0,86	0,87	1,06		0,89	0,66	1,06			VDSSSVSEDSAVF
FAS1	1124	0,95	0,86	0,89	1,06		0,89	0,66	1,06			SSVSEDSAVFKAT
FAS2	226											ALGKQSSSLLSRL
FAS2	227											LGKQSSSLLSRLI
FAS2	230											QSSSLLSRLISSK
FAS2	234											LLSRLISSKMPGG
FAS2	235											LSRLISSKMPGGF
FAS2	615	0,58	1,13	0,52	0,64			0,71		1,56		STKEVASLPNKST
FAS2	958	0,92	0,99	0,92				0,99				EVRKAVSIETALE
FAS2	1440	0,87		0,69	1,04							SSVKYASPNLNMK
FAS2	1728		1,56							1,56		VSKDKKSGSLTFN
FAS2	1732		1,65							1,65		KKSGSLTFNSKNI
FAS2	1735		1,65							1,65		GSLTFNSKNIQSK
FAS2	1827		1,66							1,66		KSLGVKSLGGGAA
FAS2	1870		1,03							1,03		VTDVKVSISHDDL
FAS2	1872		1,03							1,03		DVKVSISHDDLQA
FAS3	2	0,72	0,93	0,60	0,84			1,05		0,81	0,95	_____MSEESLFE
FAS3	5	0,72	0,89	0,60	0,84			0,93		0,81	0,95	__MSEESLFESSP
FAS3	9	0,72	0,89	0,60	0,84			0,93		0,81	0,95	EESLFESSPQKME
FAS3	10	0,78	0,86	0,72	0,84			0,83		0,81	0,95	ESLFESSPQKMEY
FBA1	313	0,97		0,97								KKDYIMSPVGNPE
FKH2	2	8,78	2,89				8,78	1,79	3,99			_____MSSSNFNE

Table A.2 (continued)

Gene Name	Position	Av HS/Ctrl	Av Glu/Ctrl	HS/Ctrl 1	HS/Ctrl 2	HS/Ctrl 3	HS/Ctrl 4	Glu/Ctrl 1	Glu/Ctrl 2	Glu/Ctrl 3	Glu/Ctrl 4	Sequence Window
FKH2	3	8,78	2,89				8,78	1,79	3,99			____MSSSNFNEM
FKH2	4	8,78	2,89				8,78	1,79	3,99			___MSSSNFNEMN
FKH2	17	8,78	2,89				8,78	1,79	3,99			ELNMTQTNYGSTK
FKS1	269	1,86		1,86								EANPEDTEETLNK
FUI1	4	7,22	4,58	11,01	7,27		3,39	4,67	4,49			___MPVSDSGFDN
FUI1	11	5,50	4,58	9,20	3,91		3,39	4,67	4,49			DSGFDNSSKTMKD
FUI1	12	5,50	4,58	9,20	3,91		3,39	4,67	4,49			SGFDNSSKTMKDD
FUI1	54	50,42	2,53	7,20	179,69	6,53	8,28	3,50		1,56		VIEKKDTDSENNI
FUI1	56	50,42	2,53	7,20	179,69	6,53	8,28	3,50		1,56		EKKDTDSENNITI
GCD6	707											QNADEESSSEEE_
GCD6	708											NADEESSSEEE__
GCD6	709											ADEESSSEEE___
GDS1	334	1,31					1,31					NYMDEDTNESMTE
GDS1	337	1,31					1,31					DEDTNESMTEPKK
GDS1	339	1,31					1,31					DTNESMTEPKKTK
GLN4	737		0,07						0,07			EVVYKESVMEHNF
GLN4	750		0,07						0,07			GDVVKNSPWVVDS
GLN4	756		0,07						0,07			SPWVVDSVKNSEF
GNP1	111	5,43	0,87	5,57	7,36	3,31	5,48	0,85	0,89			PISTKDSSSQLDN
GNP1	112	5,43	0,87	5,57	7,36	3,31	5,48	0,85	0,89			ISTKDSSSQLDNE
GNP1	113	5,43	0,87	5,57	7,36	3,31	5,48	0,85	0,89			STKDSSSQLDNEL
GNP1	123	2,36	0,98	3,27	1,54	1,75	2,88	1,00			0,96	NELNRKSSYITVD
GNP1	124	2,36	0,98	3,27	1,54	1,75	2,88	1,00			0,96	ELNRKSSYITVDG
GNP1	127	2,36	0,98	3,27	1,54	1,75	2,88	1,00			0,96	RKSSYITVDGIKQ
GPD1	23	2,17	0,73	0,37	4,19		1,94	0,36	0,97	1,00	0,59	AGRKRSSSSVSLK
GPD1	24	2,17	0,62	0,37	4,19		1,94	0,36	0,97	0,56	0,59	GRKRSSSSVSLKA
GPD1	25	2,17	0,73	0,37	4,19		1,94	0,36	0,97	1,00	0,59	RKRSSSSVSLKAA
GPD1	27	2,18	0,73	0,41	4,19		1,94	0,36	0,97	1,00	0,59	RSSSSVSLKAAEK
HFI1	6	0,76		0,76								_MSAIQSPAPKPL
HFI1	384	0,85	0,90		0,64	0,42	1,49	1,64	0,12	0,67	1,18	DDIGDISMSSITK
HFI1	386	0,85	0,90		0,64	0,42	1,49	1,64	0,12	0,67	1,18	IGDISMSSITKAG
HFI1	387	0,85	0,90		0,64	0,42	1,49	1,64	0,12	0,67	1,18	GDISMSSITKAGE
HFI1	389	0,85	0,90		0,64	0,42	1,49	1,64	0,12	0,67	1,18	ISMSSITKAGEAV
HNM1	18	6,87	3,18		7,11	4,72	8,79		3,18			YMQPDQSSNASMH
HNM1	19	6,87	3,18		7,11	4,72	8,79		3,18			MQPDQSSNASMHK
HNM1	42	7,73		7,73								PLDDMDSKGAVAA
HOM3	332	1,26		0,86	1,66							VAKKGESTPPHPP
HOM3	333	1,26		0,86	1,66							AKKGESTPPHPPE
HPC2	45		0,98					0,94	1,02			NSIKKETGSDSED
HSP26	208	0,01					0,01					KKIEVSSQESWGN
HSP26	211	0,01					0,01					EVSSQESWGN___
HXK2	15	1,00		1,00								PQARKGSMADVPK
HXT1	3	1,56	0,79	1,57	1,80		1,31		0,79			____MNSTPDLIS
HXT1	4	1,54	0,79	1,52	1,80		1,31		0,79			___MNSTPDLISP
HXT1	38	0,77	0,39				0,77	0,26	0,52			PEGKNESFHDNLS
HXT1	44	0,77	0,39				0,77	0,26	0,52			SFHDNLSESQVQP
HXT2	29	1,25	0,71	1,42	1,42		0,89	0,39	0,58	1,35	0,54	IVQKLETDESPIQ
HXT2	32	1,05	0,71	0,86	1,40		0,89	0,39	0,58	1,35	0,54	KLETDESPIQTKS
HYP2	2	0,87	0,85			0,93	0,80	0,77	0,94		0,83	_____MSDEEHTF
HYP2	10	0,87	0,81			0,93	0,80	0,77	0,83		0,83	EEHTFETADAGSS
IWS1	89		0,91					0,91				HISTDFSDDDLEK
KCC4	894	0,57			0,57							KIAASLSDDDLKE
KIC1	2											_____MTTKPQNS
KIC1	3											____MTTKPQNSK
KIC1	8											TTKPQNSKQGLAE
KIC1	266	1,15		1,07	1,24							DPKERLSADDLLK
KRI1	174	0,38	0,42				0,38				0,42	LLNEIKSAFSDEE
KRI1	177	0,38	0,40				0,38				0,40	EIKSAFSDEENEE
KRI1	184	0,38	0,42				0,38				0,42	DEENEESSGDEDD
KRI1	185	0,38	0,42				0,38				0,42	EENEESSGDEDDG
LEU1	494	1,26		0,99	1,53							SPKVEVTSEDEKE
LEU1	495	1,26		0,99	1,53							PKVEVTSEDEKEL
LYS20	395	1,35		1,97	0,72							NFHAEVSTPQVLS
LYS20	396	1,35		1,97	0,72							FHAEVSTPQVLSA
LYS21	409	1,14		1,11	1,17							DFHAELSTPLLKP
LYS21	410	1,14		1,11	1,17							FHAELSTPLLKPV

Table A.2 (continued)

Gene Name	Position	Av HS/Ctrl	Av Glu/Ctrl	HS/Ctrl 1	HS/Ctrl 2	HS/Ctrl 3	HS/Ctrl 4	Glu/Ctrl 1	Glu/Ctrl 2	Glu/Ctrl 3	Glu/Ctrl 4	Sequence Window
MAK11	423	3,09	0,59		7,82	0,44	1,02	0,55	0,43		0,77	KKRDAETADIGDQ
MAK11	430	3,07	0,62		7,82	0,42	0,99	0,55	0,54		0,77	ADIGDQSEVESDT
MAK11	434	3,10	0,66		7,82	0,46	1,02	0,48	0,73		0,77	DQSEVESDTEELK
MAK11	436	3,10	0,58		7,82	0,46	1,02	0,55	0,41		0,77	SEVESDTEELKKI
MAK21	73	0,44	1,05	0,34	0,43	0,32	0,66	0,54	0,88	1,73		KLIQGLSDDDDAK
MAK21	80	0,46	0,78		0,39	0,32	0,66	0,68	0,88			DDDDAKSEQEFDA
MAK21	708		0,67					0,52	0,82			TPVDYEYESDAEE
MAK21	710		0,67					0,52	0,82			VDYEYESDAEEEQ
MAK21	874		0,75					0,75				KKSNKASNFDSDD
MAK21	878		0,75					0,75				KASNFDSDDEMDE
MAK21	1024											QYLDQDSD_____
MAK5	678	0,70	1,07	0,64	0,61	0,62	0,93	0,82	1,43		0,96	LGIDVDSDEDDIS
MCM1	2	0,54		0,48	0,60							_____MSDIEEGT
MDN1	2124	1,01			1,01							SMNMKLSPNATAI
MDN1	2128	1,01			1,01							KLSPNATAIMEGL
MDN1	4353	0,35			0,35							PEEQAMSDEEELK
MDN1	4555		0,66					0,66				DEEEMLSDIDAHD
MEP2	490	0,92	0,45	1,03	0,81						0,45	STPSDASSTKNTD
MEP2	491	0,92	0,45	1,03	0,81						0,45	TPSDASSTKNTDH
MEP2	492	0,92	0,45	1,03	0,81						0,45	PSDASSTKNTDHI
MFT1	264		0,85					0,85				DNIDEDYESDEDE
MFT1	266		0,85					0,85				IDEDYESDEDEER
MHR1	224											TEQTEVSSQ____
MHR1	225											EQTEVSSQ_____
MRD1	264	0,31	0,61		0,31			0,50	0,71			VNDDANSDEKENE
MRT4	181		0,67					0,67				IKAGKITIDSPYL
MRT4	184		0,67					0,67				GKITIDSPYLVCT
MSH6	145		1,07					0,78	1,37			RVNYAESDDDDSD
MSH6	150		1,07					0,78	1,37			ESDDDDSDTTFTA
MSH6	209	4,01	0,98		5,15		2,87	0,84	1,12			DDDDLISLAETTS
MSH6	213	4,01	0,98		5,15		2,87	0,84	1,12			LISLAETTSKKKF
MSH6	214	4,01	0,98		5,15		2,87	0,84	1,12			ISLAETTSKKKFS
MSH6	215	4,01	0,98		5,15		2,87	0,84	1,12			SLAETTSKKKFSY
MUP1	31	1,54	1,84				1,54	1,33	2,36			TTKKEVSNSTVDA
NCL1	667											EKETTESPAETTT
NEW1	107		0,51					0,19	0,83			KSTYKQSAVTPNQ
NEW1	120		0,51					0,19	0,83			SGTPTPSASTTSL
NEW1	124		0,51					0,19	0,83			TPSASTTSLTSLN
NEW1	125		0,51					0,19	0,83			PSASTTSLTSLNE
NEW1	127		0,51					0,19	0,83			ASTTSLTSLNEKL
NEW1	128		0,51					0,19	0,83			STTSLTSLNEKLS
NEW1	1191	1,27	0,66	1,19	0,92	1,01	1,97	0,34	0,51	0,94	0,86	TPKPVDTDDEED_
NOC2	70		0,62					0,62				EVFKDMSVETFFE
NOC2	97	0,40					0,40					KTTKEQSDEDSSS
NOC2	101	0,40					0,40					EQSDEDSSSSEEE
NOC2	102	0,40					0,40					QSDEDSSSSEEEE
NOC2	103	0,40					0,40					SDEDSSSSEEEED
NOC2	104	0,40					0,40					DEDSSSSEEEEDM
NOC2	149	0,45	1,10				0,45		1,10			PLDGIDSQDEGED
NOC2	160	0,45	1,10				0,45		1,10			EDAERNSNIEEKS
NOC2	166	0,55	0,99	0,55						0,99		SNIEEKSEQMELE
NOC2	695											EAKLLNSLESDDD
NOC2	698											LLNSLESDDDNED
NOC2	708											NEDVEMSDA____
NOG1	352		13,37					13,37				NKLKSQSRINNVL
NOP12	70	0,23		0,23								ASKPDVSDEQTEE
NOP12	175	0,56	0,80	0,54	0,60	0,39	0,72	0,79	0,90	0,63	0,90	FKKLFGTNPIAET
NOP12	184	0,56	0,80	0,54	0,57	0,39	0,75	0,79	0,90	0,63	0,90	IAETEESGNEKEE
NOP12	192		0,71						0,71			NEKEEESSKKSDN
NOP12	193		0,71						0,71			EKEEESSKKSDNN
NOP13	2	0,32		0,32								_____MSETELSK
NOP13	105	0,90	1,18		0,71	0,81	1,18	1,34	1,24		0,97	EESTINTPTGDES
NOP7	288	0,28		0,34	0,23							EDVKVESLDASTL
NOP7	292	0,45		0,53	0,36							VESLDASTLKSAL
NOP7	308	0,59		0,68	0,51							EANTDETEKEEEQ
NOP7	334	0,34	0,80		0,24		0,44	0,65	0,94			EETELDTFEDNNK

Table A.2 (continued)

Gene Name	Position	Av HS/Ctrl	Av Glu/Ctrl	HS/Ctrl 1	HS/Ctrl 2	HS/Ctrl 3	HS/Ctrl 4	Glu/Ctrl 1	Glu/Ctrl 2	Glu/Ctrl 3	Glu/Ctrl 4	Sequence Window
NOP8	234	0,27	0,70			0,16	0,38				0,70	CSGEMDSDENMSE
NOP8	239	0,27	0,70			0,16	0,38				0,70	DSDENMSEEEKEK
NOP8	268	0,23		0,22	0,23							PMTLNDSDEELLT
NOP8	370	0,21	1,33	0,22	0,20	0,21		0,70		1,97		FKLIEDSDNDIDH
NPL6	2	0,71	0,92	0,42	0,49	0,36	1,58	0,57	1,60	0,61	0,91	_____MSDSEGGL
NPL6	4	0,71	0,92	0,42	0,49	0,36	1,58	0,57	1,60	0,61	0,91	___MSDSEGGLAS
PFK1	895	1,62			1,62							NKKNEASPNTDAK
PFK2	163	5,42	5,83	0,26	18,31	1,14	1,99	9,68	8,86	0,73	4,06	PEASAESGLSSKV
PFK2	166	5,50	5,83	0,56	18,31	1,14	1,99	9,68	8,86	0,73	4,06	SAESGLSSKVHSY
PFK2	167	5,40	6,32	0,15	18,31	1,14	1,99	9,68	8,86	2,68	4,06	AESGLSSKVHSYT
PFK2	171	1,18		1,33	1,02							LSSKVHSYTDLAY
PHO84	316	1,42	1,28				1,42	1,21	1,36			NGLERASTAVESL
PHO84	317	1,42	1,28				1,42	1,21	1,36			GLERASTAVESLD
PHO84	321	1,42	1,28				1,42	1,21	1,36			ASTAVESLDNHPP
PHO84	577											KNNDIESSSPSQL
PHO84	578											NNDIESSSPSQLQ
PHO84	579											NDIESSSPSQLQH
PHO84	581											IESSSPSQLQHEA
POP1	524	1,88		1,71	2,04							YKLLTATPNSINK
POP1	527	1,88		1,71	2,04							LTATPNSINKTTV
PRP20	135	0,76	0,76			0,56	0,95	0,66	0,86		0,77	DMDADDSSDDEDG
PRP20	136	0,76	0,76			0,56	0,95	0,66	0,86		0,77	MDADDSSDDEDGD
PRP20	149	0,76	0,76			0,56	0,96	0,66	0,83		0,77	LNELESTPAKIPR
PTR2	6	1,71		1,71								_MLNHPSQGSDDA
PTR2	9	2,41		2,41								NHPSQGSDDAQDE
PTR2	594	1,68	1,33			1,30	2,07	0,94	1,72			ILEPMESLRSTTK
PTR2	597	1,73	1,36			1,30	2,15	1,00	1,72			PMESLRSTTKY__
PTR2	598	1,73	1,36			1,30	2,15	1,00	1,72			MESLRSTTKY___
PTR2	599	1,68	1,36			1,30	2,07	1,00	1,72			ESLRSTTKY____
PTR2	601	1,73	1,37			1,30	2,15	1,01	1,72			LRSTTKY______
PUF6	31	0,84	1,03				0,84	0,77	1,29			AKKPRISIDSSDE
PUF6	34	0,84	1,03				0,84	0,77	1,29			PRISIDSSDEESE
PUF6	35	0,84	1,03				0,84	0,77	1,29			RISIDSSDEESEL
PUP2	251											EKEAAESPEEADV
PWP1	44	0,58	1,00	0,57	0,67	0,49	0,58	0,93	1,23	1,12	0,72	LDDAKATLEEAEG
PWP1	52	0,58	1,00	0,57	0,67	0,49	0,58	0,93	1,23	1,12	0,72	EEAEGESGVEDDA
PWP1	131		0,67					0,67				LPNQEDSQEEKQE
PWP2	232	0,75	0,85		0,41	0,53	1,30	0,82	0,92		0,82	DDDDNESEDDDKQ
PWP2	907	1,75	0,85	0,62	4,85	0,51	1,02	0,83	0,89	0,60	1,07	DNKLPLSNENDSS
PWP2	912	1,76	0,90	0,66	4,85	0,51	1,02	0,83	0,96	0,75	1,07	LSNENDSSDEEEN
PWP2	913	1,76	0,90	0,66	4,85	0,51	1,02	0,83	0,96	0,75	1,07	SNENDSSDEEENE
PYK1	257	0,85		0,85								DEILKVTDGVMVA
RCN2	160	0,39		0,39								DKSSLESPTMLKL
RCO1	683											ENPENQSE_____
REI1	106	1,04		1,44	0,64							LENMQKSQEGNTP
REI1	111	0,58		0,53	0,64							KSQEGNTPDLSKL
REI1	118	3,33		3,51	3,15							PDLSKLSLQENEE
RLP24	154	0,55	0,87				0,55	0,75	1,09	0,77	0,86	EQERAESVSEQEE
RLP24	156	0,41	0,86				0,41	0,92	1,09	0,68	0,76	ERAESVSEQEESE
RLP24	161	0,30	0,89				0,30	1,05	1,06	0,68	0,76	VSEQEESEEEEED
RLP24	172	0,30	0,89				0,30	1,05	1,06	0,68	0,76	EDMEIDSDEEEEE
RLP7	120		0,75								0,75	SVDLEETEEEEDD
RNR2	15	0,74		0,74								AAADALSDLEIKD
RPA34	8	1,27	1,01				1,27	0,80	1,22			SKLSKDYVSDSDS
RPA34	10	1,27	1,01				1,27	0,80	1,22			LSKDYVSDSDSDD
RPA34	12	1,27	1,01				1,27	0,80	1,22			KDYVSDSDSDDEV
RPA34	14	1,27	1,01				1,27	0,80	1,22			YVSDSDSDDEVIS
RPC19	33		1,12						1,12			EQDVDMTGDEEQE
RPC31	189	0,90		0,80	1,00							EDVDDASTGDGAA
RPC31	190	0,99		0,80	1,18							DVDDASTGDGAAK
RPL11B	44	1,14		1,11	1,16							EQLSGQTPVQSKA
RPL11B	161	1,00	1,13	0,91	0,96	1,17	0,96	1,08	1,22	1,09		TKEDTVSWFKQKY
RPL12A	38	1,91	0,83	1,89	1,94					0,90	0,77	IGPLGLSPKKVGE
RPL14B	3	1,09		0,94	1,19	1,08	1,15					____MSTDSIVKA
RPL14B	5	1,10		0,98	1,19	1,08	1,15					__MSTDSIVKASN
RPL16A	2	0,91		0,91								_____MSVEPVVV

Table A.2 (continued)

Gene Name	Position	Av HS/Ctrl	Av Glu/Ctrl	HS/Ctrl 1	HS/Ctrl 2	HS/Ctrl 3	HS/Ctrl 4	Glu/Ctrl 1	Glu/Ctrl 2	Glu/Ctrl 3	Glu/Ctrl 4	Sequence Window
RPL16A	188	1,07	1,12	1,00	1,14					1,12		NATAAESDVAKQL
RPL16B	2	1,07	1,18	1,03	1,11		1,05	1,09	1,36	1,10	1,18	_____MSQPVVVI
RPL16B	181	1,10	1,24	1,00	1,27		1,02	0,99	1,71	1,08	1,20	KKVSSASAAASES
RPL16B	185	1,08	1,25	1,01	1,27		0,96	1,02	1,71	1,08	1,20	SASAAASESDVAK
RPL16B	187	1,10	1,23	0,96	1,27		1,08	0,95	1,71	1,06	1,20	SAAASESDVAKQL
RPL19A	59		1,10								1,10	KAVTVHSKSRTRA
RPL1A	79		1,13					1,21			1,06	DVDRAKSCGVDAM
RPL1A	86		1,12					1,18			1,06	CGVDAMSVDDLKK
RPL20A	169											FSYKRPSTFY___
RPL21A	70		1,16					1,00	1,31	1,18		VYNVTKSSVGVII
RPL22B	111											LVFYQVTPEDADE
RPL24A	7	1,08	1,01	1,03	1,19		1,04	0,90	1,18	0,86	1,10	MKVEIDSFSGAKI
RPL24A	9	0,95	1,23	0,94	0,87		1,04	1,22	1,18	1,44	1,09	VEIDSFSGAKIYP
RPL24A	86	0,59	1,15	0,82	0,50	0,51	0,53	1,31	1,38	1,19	0,74	RPITGASLDLIKE
RPL24A	153											FQKVAATSR____
RPL24A	154											QKVAATSR_____
RPL24B	7	1,06	1,12	1,01	1,23	0,94	1,03	1,11	1,29	1,04	1,05	MKVEVDSFSGAKI
RPL24B	9	1,06	1,13	1,01	1,23	0,94	1,03	1,11	1,34	1,04	1,05	VEVDSFSGAKIYP
RPL24B	130											KAEKAKSAGVQGS
RPL24B	136											SAGVQGSKVSKQQ
RPL26B	74		0,92								0,92	GKISSVYRLKFAV
RPL27A	33		1,58					1,58				KPHDEGSKSHPFG
RPL27A	97	1,06	1,30	1,05	1,06				1,30			AFKSVVSTETFEQ
RPL27A	98	1,08	1,30	1,10	1,06				1,30			FKSVVSTETFEQP
RPL27A	100	1,06	1,30	1,05	1,06				1,30			SVVSTETFEQPSQ
RPL27A	105	0,97	1,30	1,00	0,95				1,30			ETFEQPSQREEAK
RPL2A	195		1,02					1,02				YRLKRNSWPKTRG
RPL3	187	1,25			1,25							IQLNGGSISEKVD
RPL3	296	1,08	1,04	1,01	1,14			1,04				DEANGATSFDRTK
RPL3	297	1,08	1,04	1,01	1,14			1,04				EANGATSFDRTKK
RPL3	301	1,08	1,04	1,01	1,14			1,04				ATSFDRTKKTITP
RPL3	355	1,08	1,04	0,97	1,19			1,06	1,15	1,06	0,86	KALEEVSLKWIDT
RPL30	6	0,99	0,93	0,96	1,03						0,93	_MAPVKSQESINQ
RPL31A	100											EPVLVASAKGLQT
RPL32	67	1,08	1,00	1,16	0,99					1,00		KKTKFLSPSGHKT
RPL37A	80	0,99	0,99	0,99						1,02	0,97	FKNGFQTGSASKA
RPL37A	82	0,99	0,99	0,99						1,02	0,97	NGFQTGSASKASA
RPL37A	84	0,99	0,99	0,99						1,02	0,97	FQTGSASKASA__
RPL37B	7											MGKGTPSFGKRHN
RPL37B	80		0,79								0,79	FKNGFQTGSAKAT
RPL37B	82		0,79								0,79	NGFQTGSAKATSA
RPL4A	158	0,87			0,87							VSTDLESIQKTKE
RPL4A	269		1,48					1,48				GSETVASSKVGYT
RPL4A	270		1,48					1,48				SETVASSKVGYTL
RPL6A	12	1,43	1,05	1,48	1,39			1,03	1,17		0,96	APKWYPSEDVAAL
RPL7A	8	1,18	1,18	1,22	1,43	1,13	0,94	0,73	1,37	0,92	1,69	AAEKILTPESQLK, STEKILTPESQLK
RPL7A	11	1,00	1,18	1,20	0,74	1,13	0,94	0,73	1,37	0,92	1,69	KILTPESQLKKSK, KILTPESQLKKTK
RPL8A	126	2,52		0,27	4,77							KSKQDASPKPYAV
RPL8A	216	1,03	1,04	1,11	0,94			1,04				ALAKLVSTIDANF
RPN1	19	0,88		0,88								DEQSQISPEKQTP
RPN1	178	1,14	1,08				1,14				1,08	DAEDETSSDGSKS
RPN1	184	1,22	0,99		1,25		1,20	0,53	1,22		1,22	SSDGSKSDGSAAT
RPN1	187	1,22	0,99		1,25		1,20	0,53	1,22		1,22	GSKSDGSAATSGF
RPN1	196	1,21	0,99		1,25		1,17	0,53	1,22		1,22	TSGFEFSKEDTLR
RPN13	132	0,94	1,14	0,71	1,04	0,63	1,37	0,51	1,40	1,53	1,13	IGVLNNSSESDEE
RPN13	135	0,97	1,10	0,71	1,20	0,63	1,35	0,51	1,40	1,36	1,13	LNNSSESDEEESN
RPN13	153											AQDVDVSMQD___
RPN3	512											DLMDDMSDISDLD
RPN3	515											DDMSDISDLDDLG
RPP0	273											IENPEKYAAAAPA
RPP0	281											AAAPAATSAASGD
RPP0	282											AAPAATSAASGDA
RPP0	302											AEEEEESDDDMGF
RPP1A	62	1,27		1,58	0,96							DLLVNFSAGAAAP

Table A.2 (continued)

Gene Name	Position	Av HS/Ctrl	Av Glu/Ctrl	HS/Ctrl 1	HS/Ctrl 2	HS/Ctrl 3	HS/Ctrl 4	Glu/Ctrl 1	Glu/Ctrl 2	Glu/Ctrl 3	Glu/Ctrl 4	Sequence Window
RPP1A	96	1,15	1,01	1,58	0,96	0,99	1,09	1,05	0,98	0,96	1,04	EEAKEESDDDMGF
RPP1B	58	0,98	0,99			0,91	1,06	0,86	1,08	0,97	1,05	DLKEILSGFHNAG
RPP1B	73	0,98	0,87			0,91	1,06	0,86	1,08	0,97	0,57	AGAGAASGAAAAG
RPP1B	96	0,99	0,96			0,91	1,06	0,86	1,08	0,94	0,96	EEAAEESDDDMGF
RPP2A	43	1,22	1,03	1,18			1,26	1,04	1,17		0,89	KVSSVLSALEGKS
RPP2A	49	1,22	1,08	1,14	1,28	0,94	1,51	0,93	1,21	1,13	1,04	SALEGKSVDELIT
RPP2A	71	1,15	0,98	1,24	1,38	0,90	1,07	0,93	1,08	0,93	0,97	PAAGPASAGGAAA
RPP2A	79	1,15	0,98	1,24	1,38	0,90	1,09	0,93	1,03	0,97	0,97	GGAAAASGDAAAE
RPP2A	96	0,99	0,96			0,90	1,09	0,90	1,03	0,98	0,94	EEAAEESDDDMGF
RPP2B	65	1,07	1,22	1,06	1,19	0,98	1,05	0,86	1,01	0,80	2,21	GQKKFATVPTGGA
RPP2B	68	1,07	1,22	1,06	1,19	0,98	1,05	0,86	1,01	0,80	2,21	KFATVPTGGASSA
RPP2B	72	1,07	1,22	1,06	1,19	0,98	1,05	0,86	1,01	0,80	2,21	VPTGGASSAAAGA
RPP2B	73	1,07	1,22	1,06	1,19	0,98	1,05	0,86	1,01	0,80	2,21	PTGGASSAAAGAA
RPP2B	100	1,05	1,05			0,99	1,11	1,07	1,05	0,99	1,07	EEAKEESDDDMGF
RPS10B	48	0,91		0,91	0,90							VIKALQSLTSKGY
RPS10B	50	0,91		0,91	0,90							KALQSLTSKGYVK
RPS11A	2	1,09	0,95	1,09	1,09			0,92	1,00		0,91	_____MSTELTVQ
RPS11A	3	1,05	0,95	1,02	1,09			0,92	1,00		0,91	____MSTELTVQS
RPS11A	9	1,01	0,95	0,96	1,05			0,92	1,00		0,91	TELTVQSERAFQK
RPS12	2	1,05	1,07	1,07	1,07	1,04	1,02	1,05	0,96	1,15	1,11	_____MSDVEEVV
RPS13	30	0,93		0,93								AWFKLSSESVIEQ
RPS13	143											PNWKYESATASAL
RPS13	145											WKYESATASALVN
RPS13	147											YESATASALVN__
RPS15	2		1,48							1,69	1,28	_____MSQAVNAK
RPS15	29	1,13	1,05	1,13	1,13			1,09	1,00			EKLLEMSTEDFVK
RPS15	30	1,13	1,05	1,13	1,13			1,09	1,00			KLLEMSTEDFVKL
RPS16A	2	1,01	1,01	1,01						1,01		_____MSAVPSVQ
RPS16A	15		1,40							1,11	1,69	TFGKKKSATAVAH
RPS16A	37	0,72		0,72								VNGSPITLVEPEI
RPS17B	96	0,97			0,97							ALDLSRSNGVLNV
RPS18A	107		1,08					0,88	1,28			LANNVESKLRDDL
RPS19B	117	1,11	0,96	0,97	1,08		1,29	0,96		0,85	1,07	IGIVEISPKGGRR
RPS1A	254											KDEVLETV_____
RPS1B	254		1,29					1,29				KDEVLETV_____
RPS2	2	1,48	0,98	2,24	1,37	1,06	1,25	0,99		0,93	1,03	_____MSAPEAQQ
RPS20	2		1,37					0,94	1,80			_____MSDFQKEK
RPS20	38	1,05			1,05							KQLENVSSNIVKN
RPS20	39	1,05			1,05							QLENVSSNIVKNA
RPS21B	84											LLKNVWSYSR___
RPS21B	86											KNVWSYSR_____
RPS25A	107											YTRATASE_____
RPS25B	107											YTRAAASE_____
RPS28A	5	0,74	1,00	0,31	1,17			0,92		1,03	1,05	__MDNKTPVTLAK
RPS28B	3	2,45	0,97	0,25	4,64			0,97				____MDSKTPVTL
RPS28B	5	1,06	0,99	0,96	1,17			0,97		1,01		__MDSKTPVTLAK
RPS3	207	1,27	1,17	1,16		1,21	1,43	1,10	1,40	0,52	1,68	ALPDAVTIIEPKE
RPS3	221	1,22	1,17	1,02	1,23	1,21	1,43	1,03	1,40	0,83	1,41	EPILAPSVKDYRP
RPS3	231											YRPAEETEAQAEP
RPS5	2	1,01	0,97	1,01	1,00			1,03	0,84		1,04	_____MSDTEAPV
RPS5	21	1,04	0,97	1,01	1,08			1,03	0,84		1,04	EVVEEFTPVVLAT
RPS5	27	1,01	0,97	1,01	1,00			1,03	0,84		1,04	TPVVLATPIPEEV
RPS5	38	1,01	0,97	1,01	1,01			1,03	0,84		1,04	EVQQAQTEIKLFN
RPS6A	232	0,32	0,33	0,17	0,20	0,23	0,67	0,35	0,36	0,36	0,25	IRKRRASSLKA__
RPS6A	233	0,32	0,33	0,17	0,20	0,23	0,67	0,35	0,36	0,36	0,25	RKRRASSLKA___
RPS7A	187											IVFEIPSETH___
RPS7A	189											FEIPSETH_____
RPS7B	10	1,63	1,20				1,63	1,01	1,36		1,22	VQSKILSQAPSEL
RPS7B	14	1,63	1,20				1,63	1,01	1,36		1,22	ILSQAPSELELQV
RPS7B	31	0,99	0,87	0,87	1,10			0,87				IDLESSSPELKAD
RPS7B	187											IVFEIPSQTN___
RPS7B	189											FEIPSQTN_____
RPS9A	184											ARKAEASGEAADE
RPS9B	184											ARKAEASGEAAEE
RRP14	219	0,23	0,62				0,23	0,59	0,65			KRKRLESEQEQDQ
RRP14	230	0,26	0,62				0,26	0,59	0,65			DQDEIASDSDMED

Table A.2 (continued)

Gene Name	Position	Av HS/Ctrl	Av Glu/Ctrl	HS/Ctrl 1	HS/Ctrl 2	HS/Ctrl 3	HS/Ctrl 4	Glu/Ctrl 1	Glu/Ctrl 2	Glu/Ctrl 3	Glu/Ctrl 4	Sequence Window
RRP14	232	0,26	0,62				0,26	0,59	0,65			DEIASDSDMEDID
RRP14	239	0,23	0,62				0,23	0,59	0,65			DMEDIDSDLENNS
RRP14	245	0,23	0,62				0,23	0,59	0,65			SDLENNSKKRFKK
RRP15	69	0,43	0,48			0,30	0,57	0,52	0,44			IIDNEQSDAEEDD
RRP5	187	0,53	1,21		0,53			1,13	2,00	0,65	1,07	EDAEYESSDDEDE
RRP5	188	0,53	1,21		0,53			1,13	2,00	0,65	1,07	DAEYESSDDEDEK
RSN1	933	0,98			0,98							GEFDTASKENNPF
SAC3	1167	1,43		1,43								HSSQFKTPLASRL
SAC3	1176	1,43		1,43								ASRLNTSGSSTSP
SAC3	1178	1,43		1,43								RLNTSGSSTSPPL
SAC3	1179	1,43		1,43								LNTSGSSTSPPLP
SAC3	1180	1,43		1,43								NTSGSSTSPPLPS
SAC3	1186	1,43		1,43								TSPPLPSHLAMKF
SAS10	314		2,01						2,01			VNEGDGSESEETA
SAS10	316		2,01						2,01			EGDGSESEETANI
SAS10	319		2,01						2,01			GSESEETANIEAF
SAS10	533											ELAENVSGDGKRA
SDA1	591	0,05	0,86	0,04	0,04	0,03	0,10	0,63	1,21	0,95	0,65	DVDMEDSDDEKDN
SDA1	603	0,08	0,82	0,02	0,20	0,03	0,07		1,09	0,29	1,09	NAKGKESDSDLEL
SDA1	605	0,09	0,82	0,02	0,20	0,03	0,09		1,09	0,29	1,09	KGKESDSDLELSD
SDA1	610	0,09	0,82	0,02	0,20	0,03	0,09		1,09	0,29	1,09	DSDLELSDDDDEK
SEC4	10	0,24	0,83	0,22	0,22		0,29		1,14	0,69	0,66	LRTVSASSGNGKS
SEC4	11	0,24	0,83	0,22	0,22		0,29		1,14	0,69	0,66	RTVSASSGNGKSY
SKG1	276	0,67	1,56		0,58		0,75	1,53	1,58			VFATPKSAAQSQL
SKG1	280	0,67	1,56		0,58		0,75	1,53	1,58			PKSAAQSQLPNTF
SMC1	261	1,04		0,96	1,12							KLSALNSEISSLK
SMX3	2		0,85						0,85			_____MSESSDIS
SMX3	4		0,85						0,85			___MSESSDISAM
SMX3	5		0,85						0,85			__MSESSDISAMQ
SNU114	85	1,56	1,24				1,56		1,24			ETKNTQSPQTPLV
SNU114	88	1,56	1,24				1,56		1,24			NTQSPQTPLVEPV
SPB1	529	0,34	0,66				0,34	0,45	1,08	0,52	0,57	EGVEGDSDDDEAI
SPB1	799	0,88					0,88					VTLVVASGRNKGL
SPS1	282	0,99	1,14			0,99				1,14		TITNLKSDVDLIK
SPT8	385	1,00	1,20			0,48	1,52	1,29	1,10			ADDDMDSLFGDED
SRO9	422											QETKEDSAPVAAG
SSD1	491	1,47		1,47								NDSDSLSSPTKSG
SSD1	492	1,47		1,47								DSDSLSSPTKSGV
SSZ1	477	0,56	0,69			0,69	0,43	0,61	0,83		0,62	AEEDDESEWSDDE
SSZ1	480	0,56	0,69			0,69	0,43	0,61	0,83		0,62	DDESEWSDDEPEV
STE2	382	0,94	1,02			0,44	1,45	0,95	1,45	1,03	0,67	QFYQLPTPTSSKN
STE2	384	0,91	1,02			0,44	1,37	1,01	1,36	1,03	0,67	YQLPTPTSSKNTR
STE2	385	0,87	1,04			0,44	1,30	0,99	1,45	1,03	0,68	QLPTPTSSKNTRI
STE2	386	0,87	1,04			0,44	1,30	0,99	1,45	1,03	0,67	LPTPTSSKNTRIG
STE2	411	0,79	1,03			0,63	0,94	1,03				EPVDMYTPDTAAD
STE2	414	0,79	1,03			0,63	0,94	1,03				DMYTPDTAADEEA
STE20	169	0,77	0,92				0,77		0,92			KLSLTDSTETIEN
STE20	172	0,77	0,92				0,77		0,92			LTDSTETIENNAT
STE20	492	0,34			0,24		0,44					SAPIIKSPVMNSA
STE20	502	0,34			0,24		0,44					NSAANVSPLKQTH
STE6	623	0,47	1,15				0,47	1,35	1,48	0,90	0,88	TETEEKSIHTVES
STE6	626	0,47	1,15				0,47	1,35	1,48	0,90	0,88	EEKSIHTVESFNS
STE6	629	0,47	1,15				0,47	1,35	1,48	0,90	0,88	SIHTVESFNSQLE
STE6	632	0,47	1,15				0,47	1,35	1,48	0,90	0,88	TVESFNSQLETPK
STF2	69	3,62			3,62							KKDRRGSNLQSHE
SUB1	119		0,69					0,69				KMVRLLSDDEYED
SUB1	123		0,69					0,69				LLSDDEYEDDNNN
SUB2	13		0,87					0,65	1,24	0,73		EDLLEYSDNEQEI
SUI3	112	1,15	0,48	1,11	1,19			0,36	0,60			DNVDAESKEGTPS
SUR1	349	0,88	0,49	1,07		0,69		0,49				KRLRKDSNTNIVL
SUR1	351	0,88	0,49	1,07		0,69		0,49				LRKDSNTNIVLLK
SUR1	381											YSLGNNSS_____
SUR7	293											FFTIRKSHERPDD
SUR7	301											ERPDDVSV_____
SWI3	229	2,17	1,40		1,11		3,22		1,40			SKQLGNTSSVANT
SWI3	231	2,17	1,40		1,11		3,22		1,40			QLGNTSSVANTPS

Table A.2 (continued)

Gene Name	Position	Av HS/Ctrl	Av Glu/Ctrl	HS/Ctrl 1	HS/Ctrl 2	HS/Ctrl 3	HS/Ctrl 4	Glu/Ctrl 1	Glu/Ctrl 2	Glu/Ctrl 3	Glu/Ctrl 4	Sequence Window
SWI3	235	2,17	1,40		1,11		3,22		1,40			TSSVANTPSEIPD
TAF12	286	0,81		0,73	0,90							QNQRKISSSNSTE
TAF12	288	0,76		0,73	0,78							QRKISSSNSTEIP
TAF12	290	0,76		0,73	0,78							KISSSNSTEIPSV
TAF12	291	0,76		0,73	0,78							ISSSNSTEIPSVT
TAL1	148		0,36						0,36			LIKIASTWEGIQA
TGL1	538		2,00					2,00				QLDANSSTTALDA
TGL1	539		2,00					2,00				LDANSSTTALDAL
TIF1	2	1,17		0,89	1,46							_____MSEGITDI
TIF4632	913											MNNDGDSD_____
TOF1	1232											KSRVVLSQGDSDD
TOF1	1236											VLSQGDSDD____
TOP1	14	0,84	0,87			0,73	0,94	0,70	1,05			KVNHELSSDDDDD
TOP1	15	0,84	0,87			0,73	0,94	0,70	1,05			VNHELSSDDDDDV
TOP1	24	0,84	0,87			0,73	0,94	0,70	1,05			DDDVPLSQTLKKR
TOP2	1314	1,17		1,17								ATSKENTPEQDDV
TPO5	569	0,75	1,30	0,71	0,78				1,30			ESVENNSEEGFIK
TPS2	888	2,04		0,25	3,84							AYVMKRSASYTGA
TPS2	890	2,04		0,25	3,84							VMKRSASYTGAKV
TRA1	172		1,03					0,80	1,26			EQGDLDSPKEPQA
TRA1	542		0,61					0,61				KEDINDSPDVEMT
TRA1	2442											MTILDNSLERDIK
TRX2	11	0,11			0,11							LKSASEYDSALAS
TRX2	13	0,11			0,11							SASEYDSALASGD
TY1B-PR2	1082	0,30			0,30							KTVPQISDQETEK
TY1B-PR2	1086	0,30			0,30							QISDQETEKRIIH
UBI1	86	1,07	0,96	1,02	1,13					0,97	0,95	RKKKVYTTPKKIK
UBI1	87	1,07	0,96	1,02	1,13					0,97	0,95	KKKVYTTPKKIKH
UBP1	530	0,86					0,86					KAAQQDSSEDENI
UBP1	531	0,86					0,86					AAQQDSSEDENIG
UBP1	618	1,23		0,92	1,53							KRIIEHSDVENEN
UBP1	755	1,09			1,09							DLEAIQSNNEEDD
UFD1	354	1,16		0,89	1,43							KSKAPKSPEVIEI
URA6	90											LLRNAISDNVKAN
UTP14	423	0,49	1,25			0,35	0,63	1,13	1,37			RELAAVSSDEDNE
UTP14	424	0,49	1,25			0,35	0,63	1,13	1,37			ELAAVSSDEDNED
UTP14	488	0,48	1,10			0,32	0,63	1,11	1,20		1,00	KMLDRNSDDEEDG
UTP14	498	0,48	1,10			0,32	0,63	1,11	1,20		1,00	EDGRVQTLSDVEN
UTP14	500	0,48	1,10			0,32	0,63	1,11	1,20		1,00	GRVQTLSDVENEE
UTP14	562		1,06					1,07	1,06			DIKLFESDEEETN
UTP14	668	0,31	1,59		0,31			1,48	1,70			PWLANESDEEHTV
UTP14	673	0,31	1,59		0,31			1,48	1,70			ESDEEHTVKKQSS
UTP14	738		1,18					1,07	1,18		1,29	VDPYGGSDDEQGD
UTP22	3	7,30		7,30								____MATSVKRKA
UTP22	4	7,30		7,30								___MATSVKRKAS
UTP22	10	3,88		7,30	0,46							SVKRKASETSDQN
UTP22	13	3,85		7,30	0,39							RKASETSDQNIVK
UTP5	626											QDGRLETEQSDGE
UTP5	629											RLETEQSDGEEEA
UTP5	637											GEEEAGYSDVEME
UTP5	638											EEEAGYSDVEME_
UTP8	148	0,68	0,76	0,97	0,39			0,76				TSNDHLSESDIDN
UTP8	150	0,68	0,76	0,97	0,39			0,76				NDHLSESDIDNKA
VAN1	21	0,39	2,59			0,39		3,68	1,42		2,68	AMDNGLSLPISRN
VAN1	25	0,39	2,62			0,39		3,68	1,49		2,68	GLSLPISRNGSSN
VAN1	29	0,39	2,72			0,39		4,06	1,42		2,68	PISRNGSSNNIKD
VAN1	30	0,39	2,72			0,39		4,06	1,42		2,68	ISRNGSSNNIKDK
VTC3	621		0,85					0,83	0,87			DLEDHESSDEEGT
VTC3	622		0,85					0,83	0,87			LEDHESSDEEGTA
YAP1	528	0,86		0,86								KKAANMSDDESSL
YBL047C	1340	1,60		0,58	2,63							NRGVATTPKSLAV
YBT1	936		1,27						1,27			EDELVKSSILSRA
YBT1	940		1,27						1,27			VKSSILSRANSSA
YBT1	952	1,51	2,42		1,68		1,35	3,22	2,21		1,85	ANLAAKSSTSLSN
YBT1	954	1,51	2,42		1,68		1,35	3,22	2,21		1,85	LAAKSSTSLSNLP
YBT1	955	1,51	2,42		1,68		1,35	3,22	2,21		1,85	AAKSSTSLSNLPA

Table A.2 (continued)

Gene Name	Position	Av HS/Ctrl	Av Glu/Ctrl	HS/Ctrl 1	HS/Ctrl 2	HS/Ctrl 3	HS/Ctrl 4	Glu/Ctrl 1	Glu/Ctrl 2	Glu/Ctrl 3	Glu/Ctrl 4	Sequence Window
YDL109C	269	11,55					11,55					DSVGKISFIGHSL
YDL109C	274	11,55					11,55					ISFIGHSLGGLTQ
YDL109C	279	11,55					11,55					HSLGGLTQTFAIC
YDL109C	281	11,55					11,55					LGGLTQTFAICYI
YDL109C	286	11,55					11,55					QTFAICYIKTKYP
YDL109C	289	11,55					11,55					AICYIKTKYPYFF
YDL109C	291	11,55					11,55					CYIKTKYPYFFKK
YDL109C	293	11,55					11,55					IKTKYPYFFKKVE
YDR119W	106	0,79		0,60	0,99							PQDEVNSIKGKPA
YEF3	1015	1,03		1,03								KKKKKLSSAELRK
YEF3	1039	1,06	1,44			0,91	1,20	1,33	1,32	0,84	2,27	LGDAYVSSDEEF_
YEF3	1040	1,06	1,44			0,91	1,20	1,33	1,32	0,84	2,27	GDAYVSSDEEF__
YGL039W	2		0,44						0,44			_____MTTEKTVV
YGL039W	3		0,44						0,44			____MTTEKTVVF
YGL039W	6		0,44						0,44			_MTTEKTVVFVSG
YGL039W	11		0,44						0,44			KTVVFVSGATGFI
YGL039W	14		0,44						0,44			VFVSGATGFIALH
YGR130C	247	0,72		0,72								EDKVSESTSIGKG
YGR130C	248	0,72		0,72								DKVSESTSIGKGT
YGR130C	249	0,72		0,72								KVSESTSIGKGTA
YHR146W	343	1,06		0,83	1,29							LVEKRESTEGVLD
YHR146W	344	1,06		0,83	1,29							VEKRESTEGVLDG
YIL091C	155		0,24					0,24				DEKDIDSEDEQDP
YIL127C	197											LAPVGLSDEEDSS
YIL127C	202											LSDEEDSSEED__
YIL127C	203											SDEEDSSEED___
YJL123C	340	1,32		0,71	1,94							DRSSISSNSNKIS
YKR018C	380	1,29	0,64			1,09	1,48	0,64				SSNSEDSEDEEMD
YKT6	20											EKALELSEVKDLS
YKU80	3	0,75					0,75					____MSSESTTFI
YKU80	5	0,75					0,75					__MSSESTTFIVD
YKU80	6	0,75					0,75					_MSSESTTFIVDV
YKU80	7	0,75					0,75					MSSESTTFIVDVS
YKU80	13	0,75					0,75					TFIVDVSPSMMKN
YKU80	15	0,75					0,75					IVDVSPSMMKNNN
YKU80	23	0,75					0,75					MKNNNVSKSMAYL
YLR413W	652	2,46	2,75			3,87	1,04	1,14	6,17		0,95	EKAVQESDSTTSR
YLR413W	654	2,63	2,75			4,22	1,04	1,14	6,17		0,95	AVQESDSTTSRII
YLR413W	655	2,30	2,75			3,55	1,04	1,14	6,17		0,95	VQESDSTTSRIIE
YLR413W	656	2,30	2,75			3,55	1,04	1,14	6,17		0,95	QESDSTTSRIIEE
YLR413W	657	2,46	2,75			3,87	1,04	1,14	6,17		0,95	ESDSTTSRIIEEH
YMR086W	874		2,03						2,03			VVSPGVSSPNHTT
YMR086W	875		2,03						2,03			VSPGVSSPNHTTT
YMR086W	879		2,03						2,03			VSSPNHTTTDPAI
YMR086W	880		2,03						2,03			SSPNHTTTDPAIT
YMR086W	881		2,03						2,03			SPNHTTTDPAITS
YMR086W	887		2,03						2,03			TDPAITSKKVDKK
YMR209C	3	0,86	0,95			0,98	0,74	0,95	0,95			____MVSSLASNI
YMR209C	4	0,86	0,95			0,98	0,74	0,95	0,95			___MVSSLASNII
YMR209C	19	0,86	0,95			0,98	0,74	0,95	0,95			LVVVLMTLLRQNK
YMR295C	14	1,01		1,01								SSISNTSDHDGAN
YNL050C	23	0,46	0,65			0,32	0,60	0,66	0,69		0,61	EGLGEDYDSNSSS
YNL050C	25	0,46	0,66			0,32	0,59	0,68	0,70		0,61	LGEDYDSNSSSKN
YNL050C	27	0,46	0,66			0,32	0,60	0,66	0,69		0,61	EDYDSNSSSKNNS
YNL050C	28	0,46	0,66			0,32	0,60	0,66	0,69		0,61	DYDSNSSSKNNSE
YNL050C	29	0,46	0,66			0,32	0,60	0,66	0,69		0,61	YDSNSSSKNNSEH
YNL058C	145	0,47	0,55				0,47		0,55			HHKHSSSLQSNPF
YNL058C	148	0,47	0,55				0,47		0,55			HSSSLQSNPFDIN
YNL058C	277	1,34	1,16				1,34		1,16			HKRNQSSLGLIPV
YNL058C	285	2,30	1,16				2,30		1,16			GLIPVASATSNTS
YNL058C	287	1,75	1,16				1,75		1,16			IPVASATSNTSSP
YNL058C	290	1,75	1,16				1,75		1,16			ASATSNTSSPKKA
YNL058C	292	1,75	1,16				1,75		1,16			ATSNTSSPKKAHK
YNL110C	34	0,01	0,62		0,01		0,02		0,61		0,63	EELALETSSSSSD
YNL110C	35	0,01	0,62		0,01		0,02		0,61		0,63	ELALETSSSSSDE
YNL110C	36	0,01	0,62		0,01		0,02		0,61		0,63	LALETSSSSSDEE

Table A.2 (continued)

Gene Name	Position	Av HS/Ctrl	Av Glu/Ctrl	HS/Ctrl 1	HS/Ctrl 2	HS/Ctrl 3	HS/Ctrl 4	Glu/Ctrl 1	Glu/Ctrl 2	Glu/Ctrl 3	Glu/Ctrl 4	Sequence Window
YNL110C	37	0,01	0,62		0,01		0,02		0,61		0,63	ALETSSSSSDEED
YNL110C	38	0,01	0,62		0,01		0,02		0,61		0,63	LETSSSSSDEEDE
YNL110C	39	0,01	0,62		0,01		0,02		0,61		0,63	ETSSSSSDEEDEK
YNL110C	56	0,17	0,56	0,17	0,12	0,16	0,23	0,61	0,61	0,51	0,53	IEGLAASDDEQSG
YNL110C	61	0,17	0,56	0,17	0,12	0,16	0,21	0,61	0,61	0,51	0,53	ASDDEQSGTHKIK
YNL110C	63	0,17	0,56	0,17	0,12	0,16	0,21	0,61	0,61	0,51	0,53	DDEQSGTHKIKRL
YNL149C	119											QGLDPDSDADIEE
YOR287C	41	0,72			0,70	0,78	0,69					EIDEQESSDDELK
YOR287C	42	0,72			0,70	0,78	0,69					IDEQESSDDELKT
YPL146C	31	0,20	0,33	0,22	0,11	0,16	0,30	0,30	0,42	0,31	0,29	RKNIDLSDVEQYM
YPL146C	363	0,28	0,57	0,28	0,18		0,38	0,47	0,67			EETEILSAIESDS
YPL146C	367	0,28	0,57	0,28	0,17		0,38	0,47	0,67			ILSAIESDSNKVK
YRB1	60	1,47			1,47							GDDAPESPDIHFE
YRB2	179	0,86		0,86								DKDKVHSGSEQLA
YRB2	181	0,86		0,86								DKVHSGSEQLANA
YVH1	212		4,26								4,26	MFKDSESSQDLDK
YVH1	213		4,26								4,26	FKDSESSQDLDKL
ZEO1	25	1,11		0,82	1,40							LEETKESLQNKGQ
ZEO1	40	1,25		0,84	1,66							KEQAEASIDNLKN
ZEO1	49	1,37		0,78	1,96							NLKNEATPEAEQV